Genotypic and phenotypic resistance profiles of HIV-1 infected patients failing salvage antiretroviral therapy.

Ashlyn Samantha Christal Davis
706769

A dissertation submitted to the Faculty of Health Sciences,
University of the Witwatersrand, Johannesburg,
in fulfilment of the requirements for
the Degree of Master of Science in Medicine.

May 2020

Declaration

I, Ashlyn Samantha Christal Davis declare that this dissertation is my own, unaided work. It is being submitted for the degree of Master of Science in Medicine at the University of the Witwatersrand, Johannesburg.
It has not been submitted before for any degree or examination at this or any other University.

Ashlyn Samantha Christal Davis

20/11/2020

Date

Dedication

Commit to the Lord whatever you do, and He will establish your plans.
Proverbs 16:3 NIV

This dissertation is dedicated to:

God, thank you for being my light in times of joy and darkness, for teaching me lessons and allowing me to lean on you for everything I needed.

Dad, you are a reminder of why I decided to obtain this degree. Hard work, perseverance and never looking back.

Mom, my hope in turmoil, the one who speaks sense when sense seemed lost. You are my pillar, and my drive to be better, and do better.

Ashleigh, the laughter of my soul. My tear catcher. You know you are like mom, but you bring a different atmosphere to my vulnerability. Thank you, sister.

Skyler, my breath of fresh air (breaks). These were needed. You were needed, your presence, your smile and cartoons were needed to get through these two years.

Gregory, my clarity. You remind me to be kind to myself. Thank you for the element of art, and freedom.

You have made the journey worthwhile!

Presentations arising from this study

1. A.S.C. Davis, M.A. Papathanasopoulos and A.E. Basson. Genotypic and phenotypic resistance profiles of HIV-1 infected patients failing salvage therapy. November 2019. Molecular Bioscience Research Thrust, postgraduate research day, Witwatersrand University, Johannesburg, South Africa. Poster presentation.

Abstract

Antiretroviral drug resistance is a major concern for HIV-1 patients failing third line regimens or salvage therapy. Currently, South African patients who fail third line antiretroviral therapy (ART) have no further antiretroviral drug options or resistance test recommendations, therefore remain on heavily compromised regimens and will likely develop AIDS and die. A phenotypic susceptibility assay that could determine which antiretroviral drugs may still be effective against HIV-1 from these patients would be a valuable tool in their successful long-term treatment success. Thus, the overall aim of this study was to establish a locally relevant *in vitro* phenotypic susceptibility assay to allow for the phenotypic profiling of HIV-1 from South African HIV-1 positive patients failing a third-line regimen. Viral RNA was extracted from six South African HIV-1 positive patients failing a third-line regimen, and the approximately 4.5 kb *gag-pol* regions were successfully RT-PCR amplified and sequenced using a newly established protocol. Nucleotide sequences were submitted to the Stanford University HIV drug resistance database to describe any known antiretroviral drug resistance mutations present, and manually aligned to look at mutations in the Gag cleavage sites and PTAP insertions. Overall, all six patients were infected with HIV-1 subtype C, with a complex mixture of known drug resistance mutations to the various ARV drug classes, in line with their current (and previous) drug regimen. Looking at the Gag cleavage sites, CA/P2 showed no changes, whereas various mutations were detected in MA/CA, P2/NC, NC/P1 and P1/P6. Intact PTAP motifs were observed in all six patient samples, and virus from two patients had an additional full or partial PTAP motif. An *in vitro* phenotypic inhibition assay was successfully set up using the wild-type HIV-1 subtype B pNL4.3.Luc.R-E- and its performance and robustness was tested against a panel of ARV drugs. IC_{50} values against pNL4.3.Luc.R-E- were obtained for one protease inhibitor, six reverse transcriptase inhibitors and two integrase inhibitors. The next step was to create patient derived *gag-pol* pseudoviruses/expression vectors for substitution of pNL4-3.Luc.R-.E- in these assays. Within the time constraints of the study, multiple attempts using Gibson assembly and traditional restriction/ligation cloning of *gag-pol* into the pNL4-3.Luc.-R.-E backbone (and a psPAX2 backbone) were unsuccessful. Overall, genotypic sequence analysis of the *Gag-pol* confirmed that the known HIV-1 drug resistance profiles from each of the six patients used in this study were unique, justifying future phenotypic testing, and compensatory mutations in Gag may contribute to overall resistance. Future optimization of the protocols described here to successfully create a locally relevant HIV-1 subtype C *in vitro* phenotypic susceptibility assay for use by patients failing third line ART is critical.

Acknowledgements

First and foremost, I would like to forward my gratitude to the HIV Pathogenesis Research Unit for the opportunity to join your team and be part of ground-breaking research.

I would like to specifically thank:

Professor Maria Papathanasopoulos, for her clarity and the peace she brought to every situation, as well as the direction through the degree. Thank you for guiding me and allowing for growth in all aspects of the project. I appreciate your style of leadership.

Doctor Adriaan Basson, for the challenges, questions, trials and allowing me to conquer through the project. Your guidance throughout has brought much needed reflection and I am appreciative thereof. I have grown as a scientist under your wing.

Simone, Nelia, Katherine and Melanie, ladies thank you for the constant support and assistance, you have all truly been a shoulder and an ear throughout this time. I appreciate your patience with me too.

The HPRU team thank you for the support, chats and laughter. You have been a critical part in developing the type of scientist I am pushing toward being. Each of you have taught me valuable lessons throughout these two years, and I will cherish them all.

Table of Content

Genotypic and phenotypic resistance profiles of HIV-1 infected patients failing salvage antiretroviral therapy. i
Declaration ii
Dedication iii
Presentations arising from this study iv
Abstract v
Acknowledgements vi
Table of Content vii
List of abbreviations x
List of symbols xiii
List amino acids xiv
List of Figures xv
Chapter 1 xv
Chapter 2 xv
Chapter 3 xvi
List of Tables xviii
Chapter 1 xviii
Chapter 2 xviii
Chapter 3 xviii
Chapter 1: Introduction 19
1.1. A Brief Historical Overview of HIV and AIDS 20
1.2. The Impact and Statistics of the HIV pandemic 21
1.2.1. Global Impact 21
1.2.2. Local Impact 22
1.3. Virus Characteristics 22
1.3.1. HIV types, subtypes and recombinant forms 22
1.3.2. Viral genome and structure 23
1.3.3. Viral Replication 24
1.3.3.1. Host Factors supporting viral replication 28
1.4. Host response to viral infection 31
1.4.1. Immunological response to infection 31
1.4.2. Immune evasion 33
1.4.3. Host factors restricting viral replication 34
1.5. Clinical monitoring of disease progression and viral replication 34
1.6. Treatment and prevention strategies 36
1.6.1. Antiretroviral drug classes and targets 38
1.6.1.1. Entry inhibitors (EIs) 39

1.6.1.2. Reverse transcriptase inhibitors 41
1.6.1.3. Protease inhibitors (PIs) 44
1.6.1.4. Integrase strand transfer inhibitors (INSTIs) 45
1.6.2. Antiretroviral Drug Resistance 46
1.6.2.1 The development of antiretroviral drug resistance 47
1.6.2.2. Mechanism of antiretroviral drug resistance for each drug class 48
1.6.2.3. Methodological detection of antiretroviral drug resistance 53
1.6.3. ART regimens in the South African public sector 60
1.6.4. Antiretroviral drug resistance testing guidelines in South Africa 62
1.7 Study Rationale 63
Chapter 2: Materials and Methods 65
2.1. Reagents used in the study 66
2.1.1. Clinical patient samples 66
2.1.2. Recombinant Plasmids 66
2.1.3. Antiretroviral (ARV) drugs 67
2.1.4. Mammalian cell lines 67
2.2. Genotypic resistance testing of patient samples 69
2.2.1. RNA extraction from patient plasma 69
2.2.2. RT-PCR Amplification of HIV-1 *gag-pol* 69
2.2.2.1. Primer design 69
2.2.2.2. One-step RT-PCR 69
2.2.2.3. Nested PCR 71
2.2.2.4. Silica membrane-based purification of PCR products 72
2.2.3. Population-based Sanger Sequencing 72
2.2.3.1. Cycle sequencing 72
2.2.3.2. Phylogenetic tree analysis and genotypic drug resistance interpretation 73
2.3. Setting up *in vitro* phenotypic inhibition testing assays 74
2.3.1. Antiretroviral drug preparation 74
2.3.2. Gag-PR *in vitro* phenotypic inhibition assay 74
2.3.3. RT-IN *in vitro* phenotypic inhibition assay 78
2.4. Construction of patient-derived HIV-1 subtype C expression vectors for use in the Gag-PR and RT-IN *in vitro* phenotypic inhibition assays 79
2.4.1. Construction through Gibson assembly 79
2.4.1.1. Preparation of the psPAX2 and pNL4-3.Luc.R-E- vector backbones 79
2.4.1.2. Preparation of the pMJ4 and patient derived *gag-pol* inserts 80
2.4.1.3. Gel extraction-based purification of PCR products 81
2.4.1.4. Gibson Assembly reaction 82
2.4.1.5. Validation of recombinant clones 83
2.4.2. Construction through traditional restriction enzyme/ligation 85

2.4.2.1. Preparation of the vector backbone 86
2.4.2.2. Preparation of pMJ4 and patient derived *gag-pol* inserts 87
2.4.2.3. Restriction enzyme/ligation reactions 87
Chapter 3: Results 89
3.1. Genotypic resistance testing of HIV-1 positive patient samples 90
3.1.1. Demographic and clinical profiles of South African patients failing third-line ARV treatment 90
3.1.2. RT-PCR and nested PCR of HIV-1 *gag-pol* 90
3.1.3. Population-based Sanger sequence analysis 92
3.1.4. Genotypic drug resistance interpretation 92
3.2. Setting up the *in vitro* phenotypic inhibition assays 97
3.2.1. Gag-Pro *in vitro* phenotypic assay 97
3.2.2. RT-IN *in vitro* phenotypic assay 99
3.2.2.1 Pseudovirus production and titration for RT and IN phenotypic assay 99
3.2.2.2. RT and IN Phenotypic assay 99
3.3. Constructing patient derived HIV-1 subtype C *gag-pol* expression vectors 102
3.3.1. Construction through Gibson assembly 103
3.3.1.1. Preparation of the psPAX2 vector backbone 103
3.3.1.2. Preparation of the pNL4-3.Luc.R-E- vector backbone 104
3.3.1.3. Preparation of pMJ4/patient *gag-pol* inserts 105
3.3.1.4. Gibson Assembly reaction 106
3.3.1.5 Validation of Clones by restriction enzyme digest and Sequence analysis 107
3.3.1.6. *In vitro* performance of patient derived pseudoviruses 110
3.3.2. Construction through traditional restriction enzyme digest/ligation 111
3.3.2.1. Preparation of vector backbone and pMJ4 *gag-pol* inserts 113
3.3.2.2. Restriction enzyme/ligation reactions 114
Chapter 4: Discussion 116
References: 128
Appendix A 146
Appendix B 147
Appendix C 154
..... 154
Appendix D 155

List of abbreviations

Abbreviations/acronyms	Description
3' H	3' hydrogen group
3' OH	3' hydroxyl group
3TC	Lamivudine
6HB	Six Helical Bundle
ABC	Abacavir
ADAR1	Adenosine deaminase acting on RNA 1
ADCC	Antibody-dependent cell mediated cytotoxicity
AIDS	Acquired Immunodeficiency Syndrome
APV	Fosamprenavir
APC	Antigen presenting cells
APOBEC3G	Apolipoprotein B mRNA editing enzyme, catalytic polypeptide -like-3G
ART	Antiretroviral therapy
AS-PCR	Allele specific polymerase chain reaction
ATV/r	Atazanavir ritonavir boosted
AZT	Zidovudine
BIC	Bictegravir
bNAbs	Broadly neutralizing antibodies
bp	Base pair
CA	Capsid protein
cART	Combination antiretroviral therapy/treatment
C/EBPs	CCAAT-enhancer-binding proteins
CCR5	C-C chemokine
CD4	Cluster of differentiation 4
CD8	Cluster of differentiation 8
CDC	Centres for Disease Control and Prevention
CDK9	Cyclin dependent kinase 9
cDNA	Complementary deoxyribonucleic acid
CPSF6	The cleavage and polyadenylation specificity factor subunit 6
CRF	Circulating Recombinant Form
CTL	Cytotoxic T lymphocyte
CXCR4	C-X-C chemokine receptor 4
CypA	Cyclophilin A
d4T	Stavudine
dATP	Deoxyadenine triphosphate
DC-SIGN	Dendritic Cell Specific Intracellular Adhesion Molecule 3
ddATP	Dideoxyadenosine triphosphate
ddC	Zalcitabine
ddCTP	Dideoxycytosine triphosphate
ddGTP	Dideoxyguanosine triphosphate
ddI	Didanosine
ddTTP	Dideoxythymidine triphosphate
DEPC	Diethyl pyrocarbonate
dH_2O	Distilled water
dCTP	Deoxycytosine triphosphate
dGTP	Deoxyguanosine triphosphate
DMEM	Dulbecco's modified eagle medium

DNA	Deoxyribonucleic acid
dNTP	Deoxyribonucleotide triphosphate
DOR	Doravirine
DRMs	Drug resistance mutations
DRV	Darunavir
dsRNA	Double stranded ribonucleic acid
DTG	Dolutegravir
dTTP	Deoxythymidine triphosphate
EFV	Efavirenz
Env	Envelope glycoprotein
env	Envelope glycoprotein gene
ESCRT	Endosomal sorting complexes required for transport
ETR	Etravirine
EVG	Elvitegravir
FDA	Food and Drug Administration
FI	Fusion inhibitors
FTC	Emtricitabine
Gemin2	Interacting protein 2
Gp120	Glycoprotein 120
Gp41	Glycoprotein 41
HAART	Highly active antiretroviral therapy/ treatment
HDAC1	Histone Deacetylase
HIV	Human Immunodeficiency Virus
HIVDR	Human Immunodeficiency Virus drug resistance
HLA class I & II	Human Leukocyte Antigen class I & II
HR1/2	Heptad repeat region 1/ 2
HR-C	Carboxy-Terminal Helical Region
HR-N	Amino Terminal Helical Region
HTLV	Human T cell leukemia virus
IDV	Indinavir
IFNs	Interferons
IL	Interleukin
IN	Integrase
INIs	Integrase inhibitors
INSTIs	Integrase strand transfer inhibitors
LMIC	Low middle-income countries
LPV	Lopinavir
LTRs	Long Terminal Repeats
MA	Matrix protein
mRNA	Messenger RNA
MVC	Maraviroc
MX2	Myxovirus resistance 2
NAb	Neutralizing antibody
NDOH	National Department of Health
Nef	Negative factor protein
NFV	Nelfinavir
NGS	Next generation sequencing
NK	Natural killer
NKR	Natural killer receptors
NNRTIs	Non-nucleoside reverse transcriptase inhibitors

NPC	Nuclear Pore Complexes
NRTIs	Nucleotide/nucleoside reverse transcriptase inhibitors
NVP	Nevirapine
OLA	Oligonucleotide ligation assay
PBMC	Peripheral blood mononuclear cells
PBS	Phosphate-buffered saline
PCR	Polymerase chain reaction
PEP	Post exposure prophylaxis
PEPFAR	The Presidents Emergency Plan for AIDS Relief
PIs	Protease inhibitors
PIC	Pre-integration complex
PMTCT	Prevention of mother to child transmission
Ppt	Polypurine tract site
PR	Protease
PRRs	Pattern recognition receptors
PrEP	Pre-exposure prophylaxis
RAL	Raltegravir
RNA	Ribonucleic acid
RNase H	Ribonuclease H
RPV	Rilpivirine
RT	Reverse transcriptase
RTI	Reverse transcriptase inhibitor
RT-PCR	Reverse transcriptase polymerase chain reaction
RTV or /r	Ritonavir
RTV	Resistance test vectors
SA	South Africa
SAP18	Sin3A-associated protein
SGS	Second generation sequencing
SIV	Simian Immunodeficiency Virus
SMRT	Single molecule real time
SQV	Saquinavir
ssRNA	Single stranded ribonucleic acid
T-20	Enfuvirtide
TAMS	Thymidine analog mutations
TB	Tuberculosis
TDF	Tenofovir disoproxil fumarate
TLART	Third line antiretroviral treatment/therapy
TLRs	Toll-like receptors
TNF α	Tumour necrosis factor α
TPV	Tipranivir
TRIM5α	Tripartite motif 5α
TSG101	Tumour susceptibility gene 101
tRNA	Transfer ribonucleic acid
VL	Viral load
WHO	World Health Organisation
ZMW	Zero mode waveguide

List of symbols

Symbol	Units of measurement
µM	micromolar
mM	millimolar
M	molar
ml	millilitre
g/L	grams per litre
°C	degrees Celsius
ng	nanograms
g/mol	grams per mole
bp	base pairs
Kb	kilobase
RLU	relative light units
pH	potential of hydrogen
%	percentage
mg/ml	milligram per millilitre
µL	microlitre
U/ µL	units per microlitre
µg	microgram
Rpm	revolutions per minute
× *g*	relative centrifugal force
cm^2	centimeters squared
°	degrees
µg/ml	microgram per millilitre

List amino acids

One letter abbreviation	Amino acid
A	Alanine
R	Arginine
N	Asparagine
D	Aspartic acid
C	Cysteine
Q	Glutamine
E	Glutamic acid
G	Glycine
H	Histidine
I	Isoleucine
L	Leucine
K	Lysine
M	Methionine
F	Phenylalanine
S	Serine
T	Threonine
W	Tryptophan
Y	Tyrosine
V	Valine

List of Figures

Chapter 1

Figure 1.1: Lentivirus lineage indicating the relationship between Pol sequences derived from mammalian lentiviruses. Copied from [8].

Figure 1.2: The approximately 9.8kb HIV-1 genome indicating the structural genes, regulatory genes and accessory genes important for virus production. Copied from [22].

Figure 1.3: Labelled schematic of the HIV-1 viral particle. Copied from [17].

Figure 1.4: Overview of HIV-1 attachment to the host CD4 membrane that induces a conformational change allowing fusion peptide exposure for the viral membrane and host membrane fusion. Copied from [27].

Figure 1.5: Brief overview of the HIV-1 replication cycle including the different stages that are targeted by the different antiretroviral drug classes. Copied from [47].

Figure 1.6: HIV-1 infection results in a characteristic cytokine storm during the acute phase of infection, with an increase of different cytokines and chemokines in the plasma being detected. The two cytokine waves are respectively from the IL-15(Interleukin-15) and IFN-α (Interferon- α). Copied from [76].

Figure 1.7: HIV-1 disease progression to AIDS in an untreated individual (a) and the impact of antiretroviral drug treatment on viral loads and CD4+T cell counts, with no progression to AIDS (b) Copied from [102].

Figure 1.8: The biochemical structure of nucleoside/tide reverse transcriptase inhibitors and the phosphorylation that takes place within the host after administration. Copied from [140].

Figure 1.9: The biochemical structure of non-nucleotide reverse transcriptase (RT) inhibitors and the binding to the active site of RT. Copied from [140].

Figure 1.10: HIV-1 Integrase inhibitors displayed in the active site of the integrase enzyme. Copied from [140].

Figure 1.11: The 2015 South African National antiretroviral regimen guidelines for adults and adolescents. Copied from [246].

Figure 1.12: The 2019 updated South African National antiretroviral regimen guidelines antiretroviral first line therapy for children, adolescent and adults Copied from [247].

Figure 1.13: Third-line antiretroviral therapy (ART) drugs chosen for HIV-1 positive South African patients failing a second line regimen, according to the Stanford drug resistance scores. Copied from [116].

Chapter 2

Figure 2.1: Schematic representation of the 96 well plate layout for the Gag-PR inhibition assay, indicating the triplicate plate set up of the PR inhibitor tested.

Figure 2.2: Schematic representation of the 96 well plate layout for the RT-IN inhibition assay, indicating the duplicate plate set up of the RT and IN inhibitors tested.

Chapter 3

Figure 3.1: Agarose gel electrophoresis of one step RT-PCR (A) and nested (B and C) *gag-pol* products from the six HIV-1 positive patient plasma samples.

Figure 3.2: A neighbour-joining phylogenetic tree illustrating the association between the six HIV-1 positive patient derived *gag-pol* sequences and HIV-1 subtype C reference sequences.

Figure 3.3: Prevalence of antiretroviral (ARV) drug mutations present in patient samples that cause failure to therapy.

Figure 3.4: Sequencing alignments of the HXB2 p1/p6 region to HIV-1 from patients 1 - 6, with the PTAP regions highlighted in the bold block.

Figure 3.5: Phenotypic inhibition curve of pNL4-3.Luc.R-E- to darunavir (DRV).

Figure 3.6: Titration of the pNL4-3.Luc.R-E- pseudovirus in HEK293T cells.

Figure 3.7: Phenotypic inhibition of pNL4-3.Luc.R-E- to (A) lamivudine (3TC), (B) stavudine (d4T), (C) zidovudine (AZT), (D) emtricitabine (FTC), (E) etravirine (ETR), (F) tenofovir disoproxil fumarate (TDF).

Figure 3.8: Phenotypic inhibition curves of pNL4-3.Luc.R-E- to (A) raltegravir (RAL) and (B) dolutegravir (DTG).

Figure 3.9: Agarose gel electrophoresis of psPAX2 vector backbone PCR performed with CloneAmp™ HiFi PCR Premix at 66°C (A), or at gradient temperatures, 72°C-54°C (B).

Figure 3.10: Agarose gel electrophoresis of pNL4-3.Luc.R-E- vector backbone PCR performed with CloneAmp™ HiFi PCR Premix at 66°C (A) and at gradient temperatures 61°C to 66°C (B).

Figure 3.11: Agarose gel electrophoresis of pMJ4 *gag-pol* insert PCR performed with the CloneAmp™ HiFi PCR Premix at 65°C (A) and at gradient temperatures 54°C to 65°C (B).

Figure 3.12: Endonuclease restriction of recombinant psPAX2 clones potentially containing the MJ4 gag-pol insert.

Figure 3.13: A neighbour-joining phylogenetic tree illustrating the association between clones A-G and HIV-1 group M reference subtype sequences.

Figure 3.14: Endonuclease restriction of recombinant pNL3-4.Luc.R-E- clones potentially containing the MJ4 *gag-pol* insert.

Figure 3.15: A neighbour-joining phylogenetic tree illustrating the association between clones 1-20 and HIV-1 group M reference subtypes.

Figure 3.16: The plate layout of the titrations completed with positive clones formed from pNL4-3.Luc.R-E- and pMJ4 (top).

Figure 3.17: Silent mutator software indicating the targeted region and the unique restriction site on the (A) pMJ4 reference plasmid at the 5' gag start site (MGARA); (B) pMJ4 reference plasmid at the Integrase 3' end

(MENRW); and (C) the targeted 5' *gag-pol* region and (D) 3' targeted *gag-pol* region and the unique restriction site for the pNL4-3.Luc.R-E- reference plasmid.

Figure 3.18: Agarose gel electrophoresis of the pNL4-3.Luc.R-E- vector backbone amplicon with CloneAmp™ HiFi PCR Premix (A) and the Expand™ Long Template PCR System (B), and the pMJ4 *gag-pol* insert PCR with a primer annealing temperature of 60°C (C).

Figure 3.19: Endonuclease restriction of PCR products with SacII and NruI for (A) *gag-pol* pMJ4 and (B) pNL3-4. Luc.R-E- vector backbone.

Figure 3.20: Ligation reaction of the restricted pNL4-3.Luc.R-E- backbone and pMJ4 gag-pol insert.

List of Tables

Chapter 1

Table 1.1: The antiretroviral drugs approved by the Food and Drug Administration for use in antiretroviral therapy.

Chapter 2

Table 2.1: Antiretroviral drugs for use in the *in vitro* phenotypic inhibition assays, and selected to reflect third-line failure patients' regimen and the available treatment guidelines for third-line therapy in South Africa.

Table 2.2: Primer sequences used in the amplification of HIV-1 *gag-pol* from patient samples.

Table 2.3: HIV-1 subtype C specific sequencing primers for the HIV-1 *gag-pol* gene.

Table 2.4: Primers used for the amplification of the psPAX2 and pNL4-3.Luc.R-E- backbone and for adding appropriate overlaps (highlighted in red) to the pMJ4/patient samples *gag-pol* inserts for Gibson assembly cloning.

Table 2.5: Description of sequencing primers used for validation of recombinant clones.

Table 2.6: Primers used to introduce the restriction enzyme sites *Nru*I and *Sac*II into the *gag-pol* or pMJ4 insert, and the pNL4-3.Luc.R-E- vector backbone.

Chapter 3

Table 3.1: Demographic data and clinical characteristics of the six HIV-1 positive South African patients failing third-line antiretroviral treatment (ART) whose samples were used in this study. The information was provided by the National Health Laboratory Services (NHLS).

Table 3.2: Concentration of the nested PCR *gag-pol* amplicons from the six HIV-1 positive patient plasma samples, subsequently used for Sanger sequencing.

Table 3.3: Major and minor/accessory mutations associated with resistance to antiretroviral drugs for each viral enzyme from the six HIV-1 positive South African patient samples.

Table 3.4: Phenotypic resistance and resistance scores for HIV-1 virus from the six South African patient samples obtained from the Stanford University HIV-1 Drug Resistance Database version 8.9-1.

Table 3.7: Alignment of the HIV-1 $PR55^{gag}$ polyprotein P2/NC, NC/P1 and P1/P6 cleavage sites from the six HIV-1 positive South African patient samples with HXB2 and HIV-1 consensus C sequences.

Chapter 1: Introduction

1.1. A Brief Historical Overview of HIV and AIDS

The initial reports of Acquired Immunodeficiency Syndrome (AIDS) emerged in the United States in 1981, recognized as clusters of unusual disease presentations in young homosexual men, thus the disease was firstly termed Gay Related Immune Deficiency. Within a few years, in 1983 the research groups of Gallo and Barre-Sinoussi isolated the causative agent of AIDS as a retrovirus, with Gallo calling it Human T cell leukaemia virus III (HTLV-III) [1], whereas Barre-Sinoussi named it lymphadenopathy associated virus [2, 3]. Throughout this time, similar clinical pictures of acquired immunodeficiency were observed in injection drug users, infants, and in selected blood transfusion recipients in various regions of the world, confirming various routes of transmission of the virus.

In 1986, the virus that caused AIDS was officially called Human Immunodeficiency Virus (HIV; later HIV type 1, HIV-1), and a virus that is morphologically associated but antigenically divergent was found as the source of AIDS in Western Africa [4]. The new virus termed virus HIV-2 (Human Immunodeficiency Virus type 2) was however closely associated to a simian virus that caused immunodeficiency in captive macaques native to Africa [5, 6]. Simian immunodeficiency viruses (SIVs) are non-pathogenic in their natural hosts (African green monkeys, sooty mangabeys, mandrills, chimpanzees and others). It became evident that HIV infection is a zoonotic disease, where phylogenetic analysis showed that HIV-1 infection was caused from chimpanzee (SIV_{cpz})-to-human transmission, and HIV-2 infection from sooty mangabey (SIV_{sm})-to-human transmission (Figure 1.1). Since the disease was first discovered the reasons for its sudden development, epidemic spread and distinctive pathogenicity has been an intense subject of study [7].

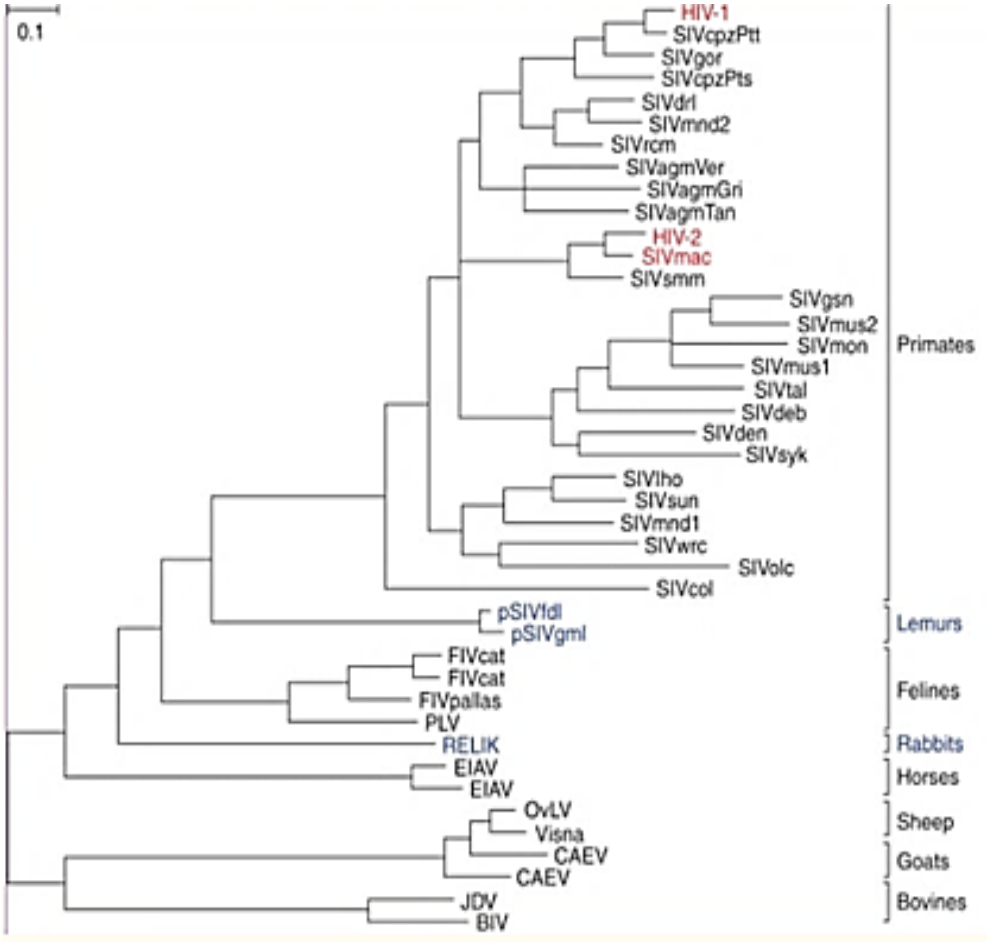

Figure 1.1: Lentivirus lineage indicating the relationship between Pol sequences derived from mammalian lentiviruses. The host species are shown on the right. Exogenous viruses (black), HIV-1 and HIV-2 (red) and endogenous viruses (purple). Copied from [8].

1.2. The Impact and Statistics of the HIV pandemic

1.2.1. Global Impact

HIV infection is the cause of AIDS, which has infected approximately 74.9 million people since the disease was described in 1981, with 32 million of the infected individuals having died from AIDS related illnesses since the start of the pandemic. In 2018, there were 37.9 million individuals living with HIV/AIDS worldwide [9]. An estimated 1.7 million new infections occurred during the year 2018; estimated to be 5000 new infections per day on a global analysis. The global AIDS related deaths have decreased to 770 000 people in 2018 from 1.4 million in 2010 [10]. The vast majority affected by HIV/AIDS live in low-to-middle-income countries (LMIC), who suffer from additional communicable illnesses, food uncertainty and issues that decline the economy. Africa has had the greatest prevalence of infected persons, with an estimated 19.6 million people living

with the virus in Southern and Eastern Africa, and roughly 6.1 million in Western and Central Africa [9, 10].

1.2.2. Local Impact

South Africa (SA) had approximately 7.7 million people living with HIV in 2018 [11]. In 2017 there were 270 000 new infections and 110 000 patients who died of AIDS related illnesses. Despite having the highest HIV new infections, mortalities and people living with HIV, South Africa has the largest antiretroviral program, with approximately 62% of people on antiretroviral therapy (ART). These efforts have mainly been funded by SA's domestic resources and The Presidents Emergency Plan for AIDS Relief (PEPFAR) [12] which have successfully increased life expectancy in this population group.

1.3. Virus Characteristics

1.3.1. HIV types, subtypes and recombinant forms

HIV is genetically associated to the *Lentivirus* genus of the *Retroviridae* family and subfamily *Orthoretrovirinae* [13]. Retroviruses cause a continuing course of disease that includes a stage of clinical latency, consistent replication and participation of the central nervous system. The virus is categorized into two types, HIV-1 and HIV-2. HIV-1 is accountable for most infections worldwide and HIV-2 infections are generally limited to Western Africa. Both these virus types cause AIDS, however, HIV-2 is shown to be less virulent than HIV-1 and the progression of AIDS is prolonged [14, 15]. The type 1 virus is subdivided into groups namely Major (M), Outlier (O) and Non-M/Non-O (N) and group P [16]. Group M is further categorized into 9 subtypes/clades: A, B, C, D, F, G, H, J and K, has broadened with geographic distribution in the global pandemic [16, 17]. Group O represents 5% of west and central African country infections whereas group N and P, rarely recognized in areas such as Gabon, Cameroon and neighbouring countries [18].

There have been several cases reported on recombinant HIV which are sourced from variegated subtypes and are named circulating recombinant forms (CRFs). The recombinant forms originate from the infection of a target cell with two HIV subtypes that exchange genetic sequences in unselected positions resulting in new hybrid mosaic viruses. Some of these have been transmitted and successfully established infections globally, for example CRF02_AG, a mixture of subtypes A and G, is prevalent in west and west -central Africa [19, 20]. There are currently 102 circulating CRFs described from HIV-1 group M, and one CRF from HIV-2 (https://www.hiv.lanl.gov/content/sequence/HIV/CRFs/CRFs.html; accessed February, 2020).

1.3.2. Viral genome and structure

The retroviral genome is made of two identical single-stranded RNA molecules with an approximate length of 9.8 kilobases (kb) (Figure 1.2). The two molecules end (5' and 3' ends) with long terminal repeats (LTRs) encoding for the transcriptional promoters. The three genomic reading frames encode structural (*gag*, *pol*, *env*), regulatory (*tat* and *rev*) and accessory (*vif*, *nef*, *vpr*, *vpu*) proteins required to form a mature, infectious viral particle, seen in Figure 1.2 [21, 22].

The structural Gag (p55) protein is processed to form the matrix (p17), capsid (p24), nucleocapsid (p7) and smaller proteins (p6, p1 and p2). The viral specific *pol* encodes for the enzymes, protease (PR, p12), reverse transcriptase (RT, p51) and RNase H (p15) and integrase (IN, p31), that are needed for viral replication. The *env* encodes for the viral envelope glycoprotein (Env) gp160, cleaved into subunits gp120 and gp41.

The HIV-1 particle is encapsulated by a host derived lipoprotein rich membrane that contains non-covalently bound viral envelope glycoprotein (Env) heterodimer complexes, formulated from trimers of gp120 (glycoprotein 120) on the exterior surface and gp41(glycoprotein 41) spanning the transmembrane (Figure 1.3) [21]. The virus incorporates certain host proteins in its membrane during viral budding such as the Human leukocyte antigen (HLA class I & II) which assists adhesion to host cell targets. The intracellular adhesion molecule I also assists adhesion to target cells.

The matrix protein (MA, p17), a structural protein, involved in the early stages of virus replication, RNA directing to the plasma membrane, incorporation of viral Env into virions and, virus particle assembly. The capsid (CA, p24) houses the two RNA (ribonucleic acid) copies, nucleoprotein and the three functional enzymes, RT, IN and PR. The remainder of the proteins namely accessory and regulatory plays supportive and modulating roles during viral replication (Figure 1.2, Figure 1.3).

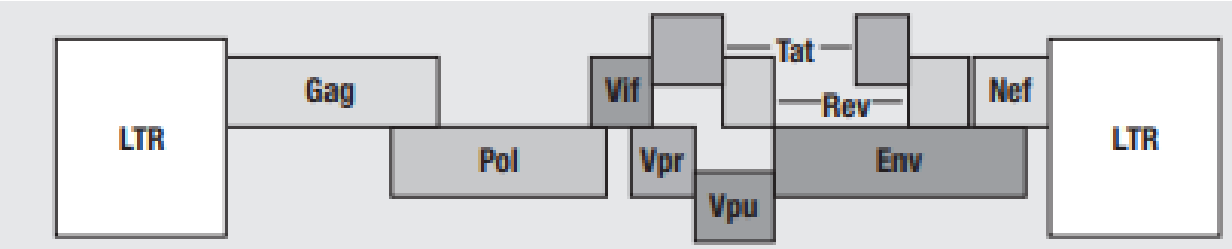

Figure 1.2: The approximately 9.8kb HIV-1 genome indicating the structural genes, regulatory genes and accessory genes important for virus production. Copied from [22].

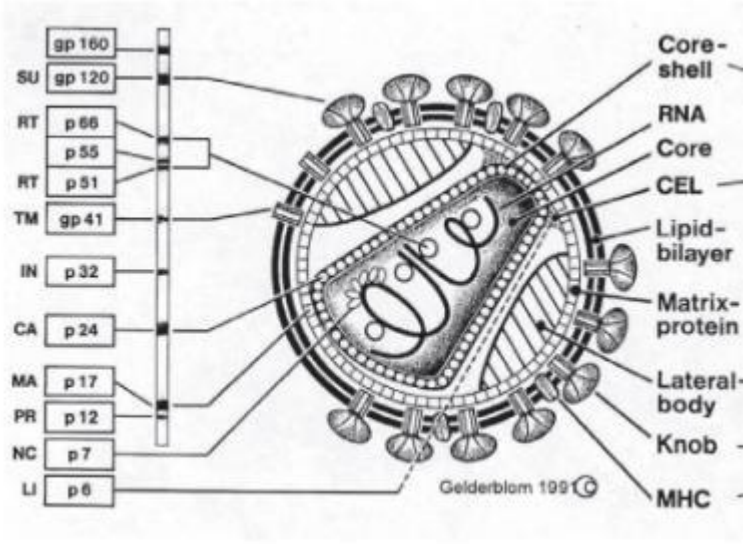

Figure 1.3: Labelled schematic of the HIV-1 viral particle. Copied from [17].

1.3.3. Viral Replication

HIV routinely makes use of a complex sequence of stages to transport its genome into the cytoplasm of the host cell to produce progeny virions, whilst concurrently escaping the host immune response. Hence, a thorough understanding of the lifecycle assists in creating and developing novel and effective preventative and therapeutic strategies.

During viral binding and entry, the virus adheres to the host cell which is mediated by protein-protein interactions, viral Env or host cell membrane proteins (Figure 1.4). Nonspecific attachment with Env occurs when binding to cell heparan sulfate proteoglycans that are negatively charged [23] or binding can be more specific i.e. Env to α4β7 integrin [24] and pattern recognition receptors [25]. These factors bring the virus into proximity to the host cell which increases the efficiency of infection [26].

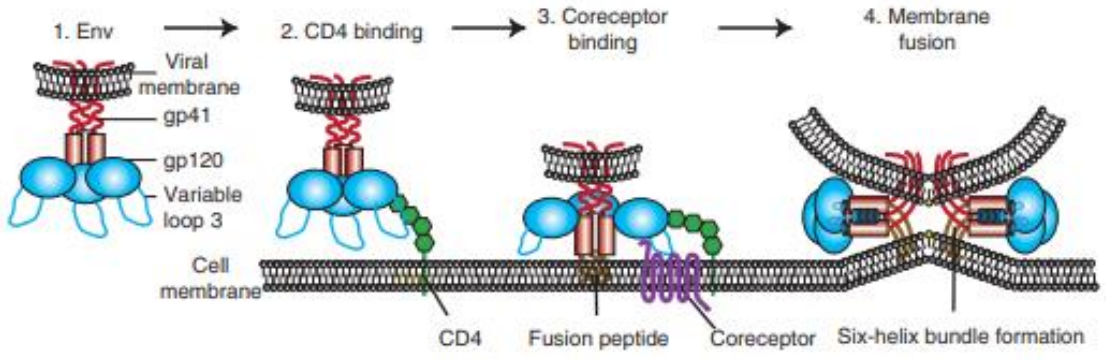

Figure 1.4: Overview of HIV-1 attachment to the host CD4 membrane that induces a conformational change allowing fusion peptide exposure for the viral membrane and host membrane fusion. Copied from [27].

Viral entry is the second step to the virus's journey. Receptors play a critical role in tropism determination and the virus's ability to weaken the host's immune system. Infection entails binding of the gp120 subunit of Env to its main receptor, the host protein cluster of differentiation 4 (CD4) [28]. Env as mentioned previously is a glycosylated trimer of heterodimeric forms of gp120 and gp41 [29]. CD4 is required by HIV-1 isolates for robust infections. Other cells that are commonly infected by HIV are monocytes, macrophages and dendritic cells which express lower levels of CD4 [30]. CD4 + T cells also express varying levels of chemokine receptors CCR5 (C-C chemokine receptor 5) and CXCR4 (C-X-C chemokine receptor 4). CCR5 is expressed on memory CD4+ T cell subsets as well as CD8 (cluster of differentiation 8) + T cells and CXCR4 is expressed on both memory and naïve CD4+ T cell subsets [21]. Both chemokine receptors form part of the family of the heterodimeric G protein coupled receptor. They can be recognised by the 7 membrane spanning domains specifically the three intracellular and three extracellular loops including a cytoplasmic tail, and most commonly the extracellular amino terminal domain (Figure 1.4) [27]. HIV-1 isolates that bind to CCR5 are termed R5- tropic and viruses that bind to CXCR4 are termed X4 tropic. [31]. Viruses that utilise both co-receptors are termed dual tropic. [32] The detection of viral tropism is a crucial step, since it has implications in HIV entry therapy and progression of AIDS.

Once the gp120 is bound to CD4, changes of the V1/V2 and V3 loops occur. In addition to the binding, a bridging sheet is formed [33]. These two changes are important for the next step in entry, namely co-receptor engagement [27]. Co-receptor binding to CCR5 or CXCR4 is assumed activate the fusion of the Env membrane [34]. Finally, the fusion is mediated by Env through co-

receptor binding that exposes the gp41 hydrophobic fusion peptide allowing for penetration of the host cell membrane [35]. Tethering of the viral and host membrane allows the fusion peptide, of each gp41in the trimer, to fold at a pivot region where the amino terminal (HR-N) and the carboxy-terminal (HR-C) helical regions, from each gp41 subunit, are brought together to form a six helical bundle (6HB) [36]. The 6HB drives the opposing membranes into apposition which results in the fusion pore formation [37].

Subsequently the virus enters the host cell cytosol by using the host cell's endocytic machinery [38]. Once the endosome has taken up the capsid, the phagosome pH alters which induces the capsid contents to be released into the cytoplasm, Figure 1.5 [39]. Whilst in the cytoplasm, HIV reverse transcription catalysed by the viral reverse transcriptase, a multifunctional enzyme [40] is activated. The activation initiates the RT functions, DNA (deoxyribonucleic acid) polymerase and ribonuclease hybrid (RNase H) activity. Reverse transcriptase requires the host tRNA (transfer Ribonucleic acid) primer that binds to the primer binding site located near the 5' end of the viral genome [41]. The positive strand is synthesized to a minus strand of DNA initiated by the tRNA primer. Once the double strand composed of RNA/DNA is formed the RNase H begins the degradation of the HIV RNA positive strand, except the polypurine tract site (ppt) near the 3' end of viral RNA. The ppt site is unaffected by the activity of the RNase H, due to its use in the second DNA positive strand synthesis. The polymerase active site is used in the production of the complementary strand of DNA to form the double helix DNA molecule [42].

The newly synthesized complementary deoxyribonucleic acid (cDNA) remains attached to proteins from both the virus and host, forming the Pre-integration complex (PIC), a high molecular weight nucleoprotein complex. At this stage, the 3' processing is performed where two nucleotides are cleaved from each 3' end of the blunt ended linear viral cDNA, this procedure terminates with the CA 3' sequence, an endo-nucleolytic processing step that occurs in the cytoplasm. The PIC is translocated to the nucleus through nuclear pore complexes (NPC). The NPC's are specific channels of nuclear membrane made up of nucleophorins. The PIC enters the channel through an active mechanism with the assistance of host nuclear import machinery [43].

Integration of the viral cDNA into a host cell chromosome is the most vital stage in the HIV-1 replication cycle [44]. Integration is facilitated by the viral integrase protein. Genetic studies have defined that integration coding regions and the Long Terminal Repeats (LTRs) of the viral DNA are essential for this replication stage [45]. DNA strand transfer occurs when the 3' ends attack the two phosphodiester bonds located on the opposite strands of the host DNA across the major

groove. In the integration intermediate the 3’ ends of the viral DNA are bound to the genome. The nucleotide overhangs at the 5’ ends and the single strand gaps are repaired by host enzymes to complete the integration stage (Figure 1.5). The integration process and the expression of the provirus require an activated target cell.

Upon activation of the target cell, the transcription to messenger RNA (mRNA) with the proviral DNA occurs and results in early production of regulatory HIV-1 proteins i.e. Tat and Rev. The Tat protein binds to the Transactivation Response Element site located at the start of the HIV-1 RNA in the nucleus resulting in transcription and the formation of longer RNA transcripts. The Rev protein assists transcription of longer RNA transcripts and the expression of the enzymatic and structural genes. This protein also hinders the synthesis of regulatory proteins, that endorses the mature viral particle formation. The viral mRNA coding for the longer fragments migrate into the cytoplasm. In the cytoplasm from the transcript, structural viral proteins are produced. The products encoded by *env* form the glycoprotein spikes of the viral envelope whereas the *gag* and *pol* encoded products form the nucleus of the maturing HIV particle.

The viral protease cleaves the Gag and Pol proteins (p24, p17, p9 and p7 Gag final products and the RT, RNase H, PR and IN Pol proteins) derived from a large precursor molecule, because this step is necessary for the formation of mature (infectious) HIV-1 particles [17].

All the components necessary for infectivity are packaged in the mature virion [46]. New viral particle formation is a process that includes the incorporation of two copied positive viral RNA strands, cellular $tRNA^{Lys3}$ molecule for priming of the cDNA synthesis, the viral Env, partially cleaved Gag polyprotein and the fully cleaved Pol to viral enzymes into an immature particle at the surface of the infected cell [46]. The Gag-Pro-Pol polyprotein mediates assembly of the virion including plasma membrane binding to allow protein-protein interactions, for the formation of spherical particles. The latter shape populates the Env trimers and packaging the genomic RNA through interactions with the RNA packaging sequence. The result is host budded new immature viral particles, facilitated by the endosomal sorting complexes required for transport (ESCRT) machinery, taking part of the host membrane with them. During the budding stage, the viral Env trimers are embedded in the host derived membranes which incorporates numerous host cell proteins supplemented with membrane constituents - phospholipids and cholesterol [21]. Following budding, the Gag is fully cleaved by the viral PR, allowing for the formation of a mature virion capable of a new round of infection.

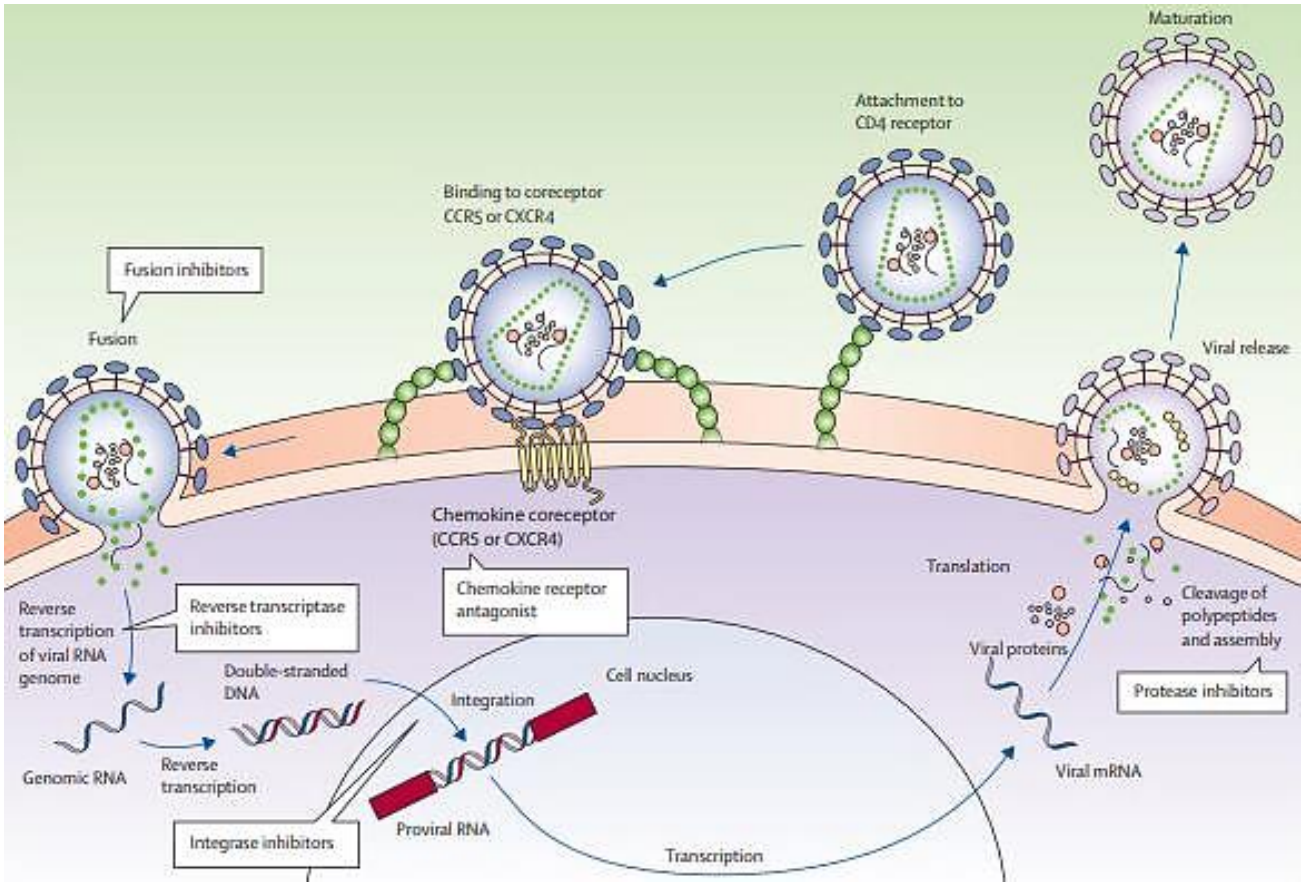

Figure 1.5: Brief overview of the HIV-1 replication cycle including the different stages that are targeted by the different antiretroviral drug classes. Copied from [47].

1.3.3.1. Host Factors supporting viral replication

HIV-1 utilizes both its viral proteins and host factors during viral replication. The viral proteins utilise host cells and regulate their cellular processes. During each replication stage there are several host proteins, whose primary function is redirected to assist HIV-1 in efficient replication. This begins as early as the attachment stage and continues until the release of viral particles.

Binding and entry of virus

The CD4 conserved cellular receptor found on the CD4 + T cells binds the gp120 trimer and causes conformational changes. The chemokine co-receptors, CCR5 and CXCR4, facilitate movement of phagocytic cells as well as T cells to areas of inflammation [48]. The co-receptors conform differently on diverse cell types, ultimately inducing HIV infection support. The surface exposed domains of the chemokine receptors are responsible for the gp120 binding that further results in a cellular kinase called Focal adhesion kinase that engages with CCR5. The affinity of all the proteins affects the strength of signal transduction likely associated with post fusion success events

within the virus [49]. The co-receptor is a critical component of the host and pathogen attachment due to evidence indicating that even without the CD4 presence the co-receptor is vital in both CD4-dependent and CD4-independent infection [50]. The conformational changes that occur post CD4 binding enable gp120 to bind a co-receptor, CCR5 or CXCR4, resulting in gp41 structural changes. This procedure is followed by cell membrane fusion and entering the cell's cytoplasm by the virion's core. When inside a cell, the virus is protected from the neutralizing ability of antibodies, nonetheless, is vulnerable to the response of CD8+ T cells/ cytotoxic T lymphocytes (CTLs) specific to HIV.

Since the expression of CD4 is not identical in all hematopoietic cells, the cells that express a barely detectable level of CD4 are also susceptible to HIV infection. The susceptibility indicates the presence of other cell surface receptors on the host cell that HIV-1 may utilise. The sugar groups of sugar on the viral and the host cell surface i.e. Mannose-specific macrophage endocytosis receptor, facilitate interactions between host and virus resulting in infection assistance. [51]. Other than sugars, dendritic cell surface protein DC-SIGN, glycolipids such as galactocerebroside and galactosulfatide expressed on glia and neurons in the brain, as well as epithelial cell lines and most notably macrophages assist during HIV-1 infection [52].

Uncoating and Reverse transcription of viral genome

Cyclophilin A, a peptidyl-prolyl isomerase directly interacts with the virus capsid and regulates viral infectivity. Viral capsid uncoating involves cyclophilin A (CypA) through stabilizing or destabilizing effects as well as enhancing the anit-HIV-1 infection of human cells [53, 54]. The cleavage and polyadenylation specificity factor subunit 6 (CPSF6) mediate the capsid particle transportation toward the nucleus where it associates to the transportin 3 (TNPO3) [55]. Capsid stability and trafficking are a significant step for efficient replication.

During reverse transcription the first host factor association is the cellular $tRNA^{Lys3}$ bound to aminoacyl- $tRNA^{Lys3}$, synthetase (LysRS) [56]. This cellular factor mimics a primer that binds to the primer binding site [57] on the HIV-1 mRNA during the generation of a reverse transcribed transcript. Another host factor that supports reverse transcription is phosphodiesterase 8A (PDE8A). Its role is to mediate DNA synthesis. PDE8A was associated with HIV-1 replication that occurs in prime macrophages [58] identified in two RNAi studies with a nucleotide polymorph was seen in the protein.

Transportation and Integration of viral DNA

Proviral DNA is brought in by nuclear importins such as transportin 3 (TNPO3), Ran binding protein 2 /Nucleoporin 358 (RanBP2/Nup358), nucleoporin153, importin-7 and transportins [59]. These proteins are localised by nuclear localization signal on the IN. In dividing and non-dividing cells, Importin-α3 interacts with IN and is critical for nuclear import and replication [60]. Moreover, protein factors like the high mobility group protein (I/Y) and the lens epithelium-derived growth factor (LEDGF/p75) governs integration site selection and supports proviral DNA into the host chromatin [61].

Cellular factors that bind to the integrase enzyme and affect reverse transcription were recognised but their function is not understood. The known proteins are integrase interactor 1 [62] sin3A-associated protein (SAP18), histone deacetylase (HDAC1) [63] and survival motor neuron-interacting protein 2 (Gemin2) [64].

The protein INI1 is a component of the SWI/SNF chromatin remodelling complex from the host cell. INI1 links with viral reverse transcription complex/PIC (RTC/PIC) to stimulate IN activity additionally involved in reverse transcription regulation [65]. Like INI1, the Sin3a-HDAC1 complex includes Sin3a, Sap18, Sap30 and HDAC1 [63]. HDAC1 is a prerequisite for reverse transcriptase initiation. Another protein that binds IN is

Gemin2 required for early reverse transcription products or the integration of viral DNA, this proposes the association with RTC/PIC [64]. However, the mechanism by which it affects RT and IN is poorly understood.

Transcription, translation of provirus and budding

This process is mediated by a range of host factors namely nuclear factor kappa-light-chain-enhancer of activated B cells, nuclear factor of activated T cells, CCAAT-enhancer-binding proteins (C/EBPs) and specificity protein 1*. The positive transcription elongation factor b that is made of cyclin dependent kinase 9 (CDK9) and Cyclin T1 is recruited by the viral Tat protein for transactivation of transcription. The mRNA is spliced and translated with the use of host cellular machinery to viral proteins. Adenosine deaminase acting on RNA1 (ADAR1), a host factor, has been implicated in regulation of these post transcriptional events [66]. It is reported to inhibit protein kinase RNA activated Ppt resulting in the eukaryotic translation initiation factor 2a being phosphorylated which is crucial for translation [67]. During late replication the new virions are assembled and use the host membrane to bud, taking host membrane constituents too. The host

proteins ESCRT family, tumour susceptibility gene 101 and ALG-2- interacting protein X are mandatory for effective budding from the host membrane.

1.4. Host response to viral infection

During a viral infection the immune system guards the host by attempting to decrease the effects the viral pathogen may have, or even eliminate the pathogen completely. However, it is widely known that the host immune system responds ineffectively to HIV-1 infection. The viral infection stimulates, according to the host, a strong innate immune activation trailed by the expansion on adaptive immune activation.

1.4.1. Immunological response to infection

Innate immune responses toward HIV infection

The innate system is the primary line of protection constituting of cells that function through identification and response to infections using pattern recognition receptors (PRRs) [68]. The PRRs include Toll-like receptors (TLRs) that detect double stranded (dsRNA) and single stranded (ssRNA) ribonucleic acid, and proteins that appear in viral infections [69, 70] this is supported by a report that observed multiple TLR7/8 ligands encoded by HIV-1 ssRNA used to facilitate *in vitro* activation of the immune system [71]. The early increase in cytokines and chemokines i.e. IFNα production, CXC-chemokine ligand 10 (CXCL10) and interleukin 15 (IL-15) trailed by secondary tumour necrosis factor α (TNFα), interferon γ (IFN γ), interleukin 18 (IL-18) and IL-10 and IL-22 secretion, clearly seen in Figure 1.6, is stimulated by the rise in viral load and accompanied by virus-specific adaptive immune responses [72]. The antiviral effects that are released by the cytokines and chemokines range from inhibit HIV replication in severe combined immunodeficient mice reconstituted with human lymphocytes [73]. Natural killer cells and Natural Killer T cells are activated during acute HIV infection, prior to the viremia peak [74], NK cells multiply and have enhanced activity [74]. These cells control HIV replication by lysing of infected cells and cytokine and chemokine production [75].

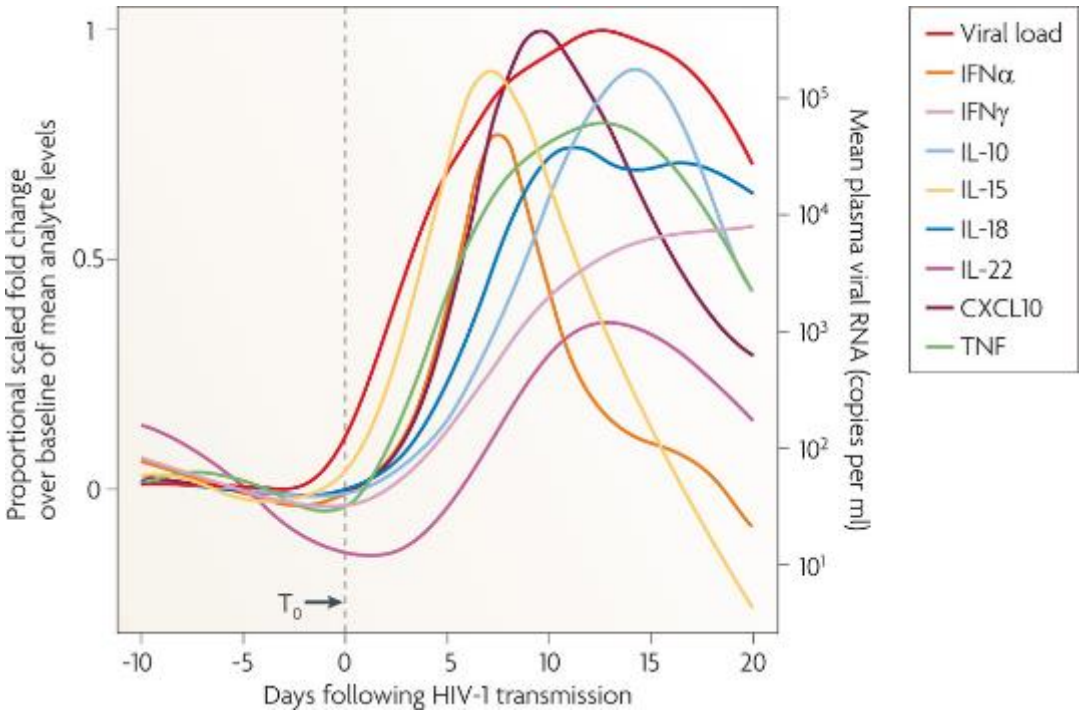

Figure 1.6: HIV-1 infection results in a characteristic cytokine storm during the acute phase of infection, with an increase of different cytokines and chemokines in the plasma being detected. The two cytokine waves are respectively from the IL-15(Interleukin-15) and IFN-α (Interferon- α). Copied from [76].

Adaptive immune responses to HIV infection

The primary adaptive immune response is the increase in CD8+ T cells [77], accountable for regulating viral replication, resulting in the decline in viremia to a viral set point. The CD8+ cytotoxic T lymphocyte (CTL) has a more focused response namely targeting a certain number of epitopes on the virus. In the chronic stage of infection, the response does expand due to mutations that develop and the increase in viral quasispecies. Furthermore, the hosts CD4+ T cells regulate immunological processes by stimulating other lymphocytes to secrete cytokines, that aid B cell maturation, stimulate antibody generation and activation of macrophages and CD8+ T cells [78]. The CD4+T cell responses become less potent because they are the most targeted cell population which supports claims of their significant decline of CD4 +T cells. The depletion ultimately influences the immune dysfunction that is observed throughout the progression toward AIDS [79].

The most ideal adaptive immune response is categorised with the use of B cell produced antibodies that target the viral antigens presented by the antigen presenting cells. The antibodies would ideally respond by neutralization of the pathogen, activation of other defence cells, differing between individuals [80]. Unfortunately, in the natural course of infection binding/non-neutralizing antibodies develop as early as a week or two post infection from plasma cells [81] and are

unsuccessful at neutralizing the virus a seeing as irrelevant and linear epitopes are targeted. Three months' post infection a neutralizing antibody (NAb) response specifically directed against Env emerges [82]. The NAb may neutralize the variable loop regions on Env inhibiting entry of the virus but this response is confined and selects the most common mutants that are directed toward viral escape [83]. Apart from neutralising, antibodies target HIV-1 through mediated effector functions i.e. agglutination, activation of the complement system and antibody-dependent cell mediated cytotoxicity (ADCC) [84]. When the antibody binds to the pathogen, the response may be deemed ineffective through agglutination, which mark and destroy clumps. The complement system recruit's components which result in it being marked for ingestion through phagocytosis or cell lysis. Lastly, during ADCC, the effector cell of the immune system (NK cells) actively lyse the infected target cells, mostly initiated by the recognition of the antigens coated on the cell surface [85].

1.4.2. Immune evasion

HIV-1 has evolved to overcome the strategies used by the host response mechanisms specifically by counteracting and subverting through various immune effector functions [86].

Innate immunity evasion

The viral negative factor protein (Nef) downregulates the ligand expression for the NK receptors (NKRs) [87] leading to a reduction in the NK-cell mediated anti-HIV activity. HIV-1 enhances its coverage by combining CD55, CD59 and CD46 receptors on its membrane to resist complement facilitated lysis [88]. Lastly, immune evasion occurs through avoiding immune interaction by modifying its pathogen associated molecular patterns by altering or concealing its nucleic acids in the viral capsid to impersonate cellular proteins [89].

Adaptive immunity evasion

HIV-1's genetic variability is a major factor in host immune evasion, due to the HIV reverse transcriptase lack of proofreading ability which is accountable for the demonstrated high mutation rate in HIV-1 [90]. Partnered with the virus's mutation rate is the time taken by the host to produce antibodies against HIV. The rapid mutation rate of the virus means that autologous antibodies cannot neutralize circulating virus at the point in time when they emerge. This tactic enables HIV to successfully evade antibody responses. The second mechanism is by Env glycosylation, this amendment masks vital epitopes [91]. Furthermore, several neutralizing antibodies that target the regions on Env are only momentarily exposed at the time of viral entry [33]. HIV-1 also avoids

CTL interaction by latency and is repressed in two regions namely: resting T lymphocytes and the glial cells in the central nervous system [92].

1.4.3. Host factors restricting viral replication

As mentioned above, HIV-1 has established interactions with host cellular factors that support its replication in the host, similarly it has also developed replication restriction factors [93].

Protein factors tripartite motif 5 α was identified as a retroviral restriction factor in [94] that is induced by both type I and type II IFN [95] and interacts with the incoming viral capsid to prevent uncoating. A second factor was identified that expresses intrinsic immunity against retroviral infections, apolipoprotein B mRNA editing enzyme catalytic polypeptide-like proteins. These Specifically acts on ssDNA or RNA substrates and their main function is to induce changes in the nucleotide sequences through cytidine deamination, which converts cytidine to uridine or deoxycytidines to deoxyuridines.

The Tripartite motif-containing protein 22 is induced by IFN's and used by the host to inhibit viral transcription of the provirus though promoting HIV latency [96]. Similarly, another transcriptional level restriction factor namely dual specificity tyrosine-phosphorylation regulated kinase 1a limits the nuclear localization of the Nuclear factor of activating T cells, as well as latency regulation. The translational based restriction protein Schlafen11 is induced by IFN-β [97] and is reported to selectively suppress viral protein expression. This is completed through utilizing the unique HIV-1 codon by limiting tRNAs required by the virus for protein synthesis, while expression for host cellular protein synthesis is unaffected [98]. Lastly, Tetherin/BST-2, an integral membrane protein that forms parallel disulfide bond homodimers allowing virion bridging prevents viral particles from being released, by trapping the budding virions at the surface of infected cells [99, 100].

1.5. Clinical monitoring of disease progression and viral replication

Many of the determinants in disease progression demonstrate an existing relationship amongst HIV-1 RNA levels (viral load), CD4+T cell count and the rapidity of disease progression to AIDS. An understanding of predictive determinants is critical to lead patient treatment and management. The monitoring of disease progression and viral replication can be determined through the detection of several markers related to host and virus (e.g. viral load-virus and CD4 counts-host; Figure 1.7) [101].

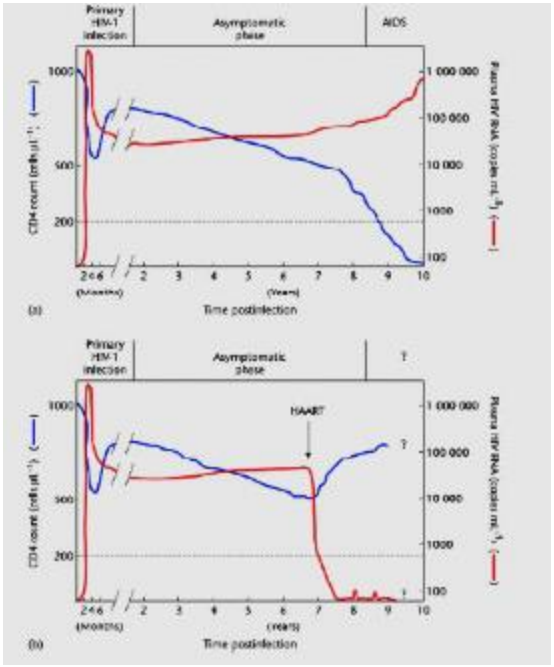

Figure 1.7: HIV-1 disease progression to AIDS in an untreated individual (a) and the impact of antiretroviral drug treatment on viral loads and CD4+T cell counts, with no progression to AIDS (b) Copied from [102].

In the absence of treatment, variable virus progression rates between individuals have been well recognized and classified as rapid, intermediate and late progressors. The individuals that progress rapidly are approximately 10-15% of the infected individuals and have a faster CD4+T cell reduction and an increase in the incidence of AIDS related illness events within a limited amount of years infected with HIV-1. An approximate 70-80% of infected patients are categorized as typical progressors in which HIV-1 RNA rises and CD4+ T cells decline gradually during the chronic/asymptomatic phase, resulting in AIDS related illnesses generally within 6-10 years of acquiring HIV. The slow or long term non-progressors persist without significant CD4+T cell count or HIV-1 RNA changes for well over 10 years. [103]. Lastly, elite controllers (<1%) maintain stable, undetectable viral loads (VL) for over 5 years. In all instances, once an individual has progressed to AIDS (cluster of opportunistic infections), they will die within two years of the diagnosis if they are not initiated on antiretroviral therapy (ART).

Immunological factors

The CD4+T cell count is the most substantial clinical disease progression and survival predictor. In the early days of the pandemic, the US Department of Health and Human services treatment guidelines recommend starting therapy be based on CD4+T cell count. In particular, in resources limited settings the threshold for ART initiation was at 200 cells/mm^3 compared to 350 cells/mm^3

in resource rich settings [104]. Subsequently, most countries, including South Africa now implement a test-and-treat strategy, regardless of patient CD4+ T cell count (which is generally performed at time of diagnosis/baseline).

Once a person is initiated on ART, the standard method of HIV testing is routine VL monitoring. People living with HIV on ART have better health outcomes with routine VL monitoring than people who are monitored from CD4 testing only, also seen by the low loss to follow-up rates and death [105]. Moreover, VL monitoring promotes motivation to stay in care and adhere to ART, since VL testing is more sensitive than CD4 testing and detects early virological treatment failure [106].

Additionally, VL testing prevents unnecessary switching of a patients to the more expensive second- or third-line treatments. A study from African countries reported that most patients who were advised to switch to a second-line regimen, based solely on clinical or CD4 monitoring were unnecessarily changed [107]. A second study conducted by Medicines San Frontiers found that only 30% of patients assumed to be failing treatment had an elevated VL, meaning that 70% might have been changed to a second-line treatment pointlessly if VL was not used to confirm virological treatment failure [108].

1.6. Treatment and prevention strategies

Approaches implemented to avoid HIV-1 infection include a variety of biomedical and community interventions [109]. The available biomedical avoidance approaches include male circumcision, reported to decrease the risk of HIV-1 attainment in heterosexual men by 48-61% [110]. Antiretroviral drug-based approaches include use of (1) pre-exposure prophylaxis (PrEP), (2) post-exposure prophylaxis (PEP) and (3) prevention of mother-to-child transmission (PMTCT) [111].

PrEP is prescribed when the risk of becoming exposed to HIV is extremely high i.e. sex workers and drug users [112]. This preventative approach was demonstrated as effective in multiple randomized, placebo-controlled, double-blinded clinical trials (RCTs). The United States Food and Drug Administration (FDA) approved tenofovir disoproxil fumarate (TDF) and emtricitabine (FTC) for oral PrEP use, in addition the US Centers for Disease Control and Prevention (CDC) and the World Health Organization (WHO) have released guidelines recommendations that include oral PrEP usage to individuals at higher risks of HIV infection [113]. Furthermore, open-

label extensions of PrEP RCTs and projects are ongoing in several countries to assess execution issues [114].

When someone may have been exposed to HIV infection, an immediate precaution (within 72 hours of exposure) is to take PEP as an emergency short course (28 days) of ART. PEP is not meant for regular use by people who may be exposed to HIV frequently. It is not intended to replace regular use of other HIV prevention methods, like consistent condom use during sex or PrEP [115]. According to Moorhouse et al, patients exposed to HIV-1 are recommended ART in PEP with a combination of TDF, lamivudine (3TC)/ (FTC) as the active backbone and raltegravir (RAL) as the third drug ART for PEP, however, in pregnancy atazanavir (ATV/r) is preferred [116].

PMTCT is ART specifically used to reduce mother-to-child transmission. Thus far there has been significant improvements regarding antiretroviral choice and accessibility of the PMTCT program [117]. A third of children born to mothers living with HIV will obtain HIV infection without preventive measures. A further 14% of children who breastfeed for approximately two years will obtain the infection during breastfeeding, accounting for 40–64% of children who are HIV-positive. The transmission risk is higher if the mother obtains HIV during pregnancy or breastfeeding, since VL tends to be higher during the acute stages of infection. During model conditions, prevention programs can decrease MTCT rates to between 1 - 2%, and this has become standard of care in all countries for eligible women.

The social preventative strategies include (i) education, clear communication about information regarding various HIV related topics, for example, safe sexual behaviour and practices, condom usage, sexually transmitted infections, and ending gender-based violence, (ii) programs that inform drug users of safe injection sites and needle exchange projects (iii) social marketing in terms of improving healthcare services and accessibility to ART, and (iv) changing public health policies [111]. A few examples of the social preventative strategies include large-scale programmes that attained high coverage and assessable effects on patient attitudes, the use of condoms and increase of HIV testing services. An example thereof is the South African LoveLife multi-media campaign that occurred in 2017, with a coverage of 300,000 youth, a second example is Zimbabwe's national behaviour change project that is inclusive of the Sista2sista campaign that speaks to the limitations young women face in accessing sexual health services [118].

The currently available treatment for patients infected with HIV-1 includes combination ART (cART), also known as highly active antiretroviral therapy (HAART). The drug therapies have

been available and used for suppressing HIV since the 1990's (as monotherapy), but novel drug discovery and treatment optimization strategies have transformed HIV-1 infection from a progressive disease with a fatal outcome into a chronic but manageable disease [47].

1.6.1. Antiretroviral drug classes and targets

During the early years of the pandemic, the management of HIV-1 mainly entailed treatment against AIDS-related illnesses and common opportunistic pathogens. HIV-1 infection treatment restructured in the mid-1990s due to the advances in inhibitor development targeting RT, that were administered as monotherapy [119]. However, treatment failure due to the development of antiretroviral drug resistance was common [119]. PR inhibitor discovery revolutionized ART, and strategies incorporating a combination/cocktail of two drug classes termed HAART or cART became widely available in 1996. The cART dramatically suppressed HIV-1 replication and reduced plasma VL below the limit of detection hence, the initiation of cART was pivotal in the morbidity and mortality reduction related to HIV-1 infection and AIDS (Figure 1.7) [120]. This also resulted in a boost of the patient's immune system [121], clinically measured using the increased circulating CD4+ T-lymphocytes. Notably, the use of more than one antiretroviral agent targeted toward two or more molecular targets is a fundamental baseline for the prevention of antiretroviral drug resistance.

Currently, the FDA has approved HIV-1 ARV drugs that have been categorized into one of four drug classes, based on the targets within the HIV-1 replication life cycle. These include the entry inhibitors (EI), reverse transcriptase inhibitors: nucleoside/tide reverse transcriptase inhibitors (NRTIs) and non-NRTIs (NNRTIs)), protease inhibitors (PIs), and integrase strand transfer inhibitors (INSTIs), listed in Table 1.1.

Table 1.1: The antiretroviral drugs approved by the Food and Drug Administration for use in antiretroviral therapy.

Drug class	Drug class abbreviation	Antiretroviral generic name	Abbreviation	Brand name
Fusion Inhibitor	EI	Enfuvirtide	ENF/T-20	Fuzeon
Co-receptor antagonist	EI	Maraviroc	MVC	Selzentry/Cesentri
Pharmacologic enhancers	Drug boosters	Ritonavir	RTV or /r	Norvir
		Cobicistat	CBS or /c	Tybost
Nucleotide/nucleoside reverse transcriptase inhibitors	NRTI	Abacavir	ABC	Ziagen
		Didanosine	ddI	Videx
		Emtricitabine	FTC	Emtriva
		Lamivudine	3TC	Epivir
		Stavudine	d4T	Zerit
		Tenofovir disoproxil fumarate	TDF	Viread
		Tenofovir alafenamide	TAF	Vemlidy
		Zidovudine	AZT	Retrovir
Non-nucleoside reverse transcriptase inhibitors	NNRTI	Delavirdine	DLV	Rescripor
		Doravirine	DOR	Pifeltro
		Efavirenz	EFV	Sustiva
		Etravirine	ETR	Intelence
		Nevirapine	NVP	Viramune
		Rilpivirine	RPV	Edurant
Protease inhibitors	PI	Atazanavir	ATV	Reyataz
		Darunavir	DRV	Prezista
		Fosamprenavir	FPV	Lexiva
		Indinavir	IDV	Crixivan
		Lopinavir	LPV	Kaletra
		Ritonavir	RTV	Norvir
		Saquinavir	SQV	Invirase, Fortovase
		Tipranavir	TPV	Aptivus
Integrase inhibitor	INSTI	Bictegravir	BIC	Biktarvy
		Dolutegravir	DTG	Tivicay
		Elvitegravir	EVG	Vitekta
		Raltegravir	RAL	Isentress

1.6.1.1. Entry inhibitors (EIs)

EIs are a class of anti-HIV drugs that function by blocking the virus' ability to infect the target cell. FDA approved inhibitors function by attaching to the CCR5 co-receptors on the cell surface, or target the gp41 fusion peptide.

1.6.1.1.1. Co-receptor antagonists

CCR5 antagonists bind the hydrophobic pockets in the transmembrane helices of the host co-receptor CCR5 [122]. These pockets do not overlap with the CCR5 agonists or HIV-1 Env binding sites. As an alternative, drug binding stabilizes and induces receptor conformations that are not recognised; hence the inhibitors are considered allosteric inhibitors. Maraviroc (MVC) was FDA approved in 2007 [123]. MVC binds to the CCR5 hydrophobic transmembrane pocket. Once bound, it adjusts the second extracellular loop conformation of the receptor and thwarts interaction of gp120 and the V3 stem loop [122]. MVC is only effective against CCR5-tropic viruses, so viruses from patients initiating MVC must be genotyped/phenotyped to ensure the absence of CXCR4-tropic HIV-1. Interestingly, CCR5 utilizing viruses resistant to MVC appear to use the CCR5 co-receptor differently, and resistance has not been associated with mutations in gp120. CXCR4 serves as a co-receptor for HIV-1 however, antagonist development attempts (e.g., AMD3100) have failed during clinical studies [124].

1.6.1.1.2. Fusion Inhibitors

Fusion inhibitors were premeditated based on the detection of two structurally identical domains present on the gp41 protein that interacts to promote fusion. It was discovered that imitating one of these domains using a similar structured protein can impede the binding of the viral proteins. Alpha-helical peptides similar to the gp41 leucine zipper domain demonstrated substantial antiviral activity toward the virus, all dependent on the ordered structure solution [125]. Based on this reason, the design of the inhibitors produced a helical molecule (T-20, enfuvirtide) with effective *in vivo* antiviral activity [126]. T-20, a 36 conserved amino acid artificial C-peptide resembles to the structure of the C helix heptad repeat region 2 (HR2) from gp41, approved in 2003 by the FDA. The function of the T-20 mimics the activity of HR2 binding to HR1 after gp120 has bound to the CD4 receptor. This blocks all subsequent gp41 conformational changes required for membrane fusion [127].

Resistance to enfuvirtide is mapped by mutations in the gp41amino-terminal HR region [128], specifically at amino acid sites G36, I37, V38A, V38, N42, N42 and N43 [129]. Mutations conferring resistance to T-20 results in decreased replication capacity as a direct result. Presumably, since mutations reduce efficiency of bundle formation it is observed that fusion rates decrease [130]. A benefit of these mutations is that cross resistance cannot be conferred to other entry inhibitors [131], however, do sensitize HIV-1 to neutralization by means of monoclonal

antibodies targeting the gp41 domain due to the exposure of fusion intermediates [130]. Adaptation to T-20 has resulted, hence these adapted viruses need enfuvirtide for fusion [132].

1.6.1.2. Reverse transcriptase inhibitors

The inhibitors in this class target the viral RT and prevent the alteration of viral RNA to cDNA.

1.6.1.2.1. Nucleoside/Nucleotide reverse transcriptase inhibitors (NRTIs)

The nucleoside compounds are inactive enzyme substrate precursors. However, upon administration as a prodrug, they require phosphorylation [133] by cellular kinases to mimic the dNTP substrates used during the synthesis of proviral cDNA (Figure 1.8). The moiety on the NRTI halts the formation of a 3'-5' phosphodiester bond between the NRTIs and incoming 5' -nucleoside triphosphates due to the lack of a 3'-hydroxyl group at the sugar (2'-deoxyribosyl). Ultimately, resulting in the growing viral DNA chain being terminated. Consequently, NRTIs are responsible for blocking of HIV-1 replication at the third step in the life cycle [134]. Viral DNA chain termination could occur while the RNAis being changed to DNA or DNA is synthesised from DNA, inhibiting the generation of either the (-) or (+) strand of the HIV-1 proviral DNA [135].

NRTIs were the first drug class developed and approved by the FDA [136]. The initial inhibitor in this class was azidothymidine (AZT, zidovudine) [137]. The synthesis of AZT occurred in 1964 and was tested as an experimental cell cytotoxin. In 1985, clinical trials demonstrated that AZT inhibits the infectious and cytopathic properties of HIV-1 [137]. Clinical studies confirmed a substantial reduction in drug efficacy in HIV-1-infected patients receiving AZT monotherapy, which attributed to the emergence of drug resistant virus [138].

TDF is hydrolysed to tenofovir which is phosphorylated to tenofovir diphosphate; hence it is reported as a pre-phosphorylated nucleotide RT inhibitor [139]. Similarly, to the previously explained nucleoside inhibitors, nucleotide analogues terminate growing DNA strands, which hinders the viral activity of RT by challenging the natural substrate adenine [140]. Since TDF is pre-phosphorylated it can work immediately upon entry.

There are currently a number of FDA-approved NRTIs: abacavir (ABC, Ziagen), didanosine (ddI, Videx), FTC (Emtriva), 3TC (Epivir), stavudine (d4T, Zerit), zalcitabine (ddC, Hivid) and AZT (Retrovir), and TDF (Viread) (Table 1.1 and Figure 1.8). The structure of TDF has a phosphate group attached, Figure 1.8, to it giving this drug an advantage for therapy compared to nucleoside inhibitors.

Each nucleoside analogue specifically competes with a cellular deoxynucleotide triphosphate (dNTP): AZT, and d4T competes with deoxythymidine triphosphate (dTTP); FTC and 3TC competes with deoxycytosine triphosphate (dCTP); ddI and TDF competes with deoxyadenine triphosphate (dATP) and lastly ABC competes with deoxyguanosine triphosphate (dGTP) [141]. Most NRTIs are considerably stable in the cell, enbling long-term viral suppression [142].

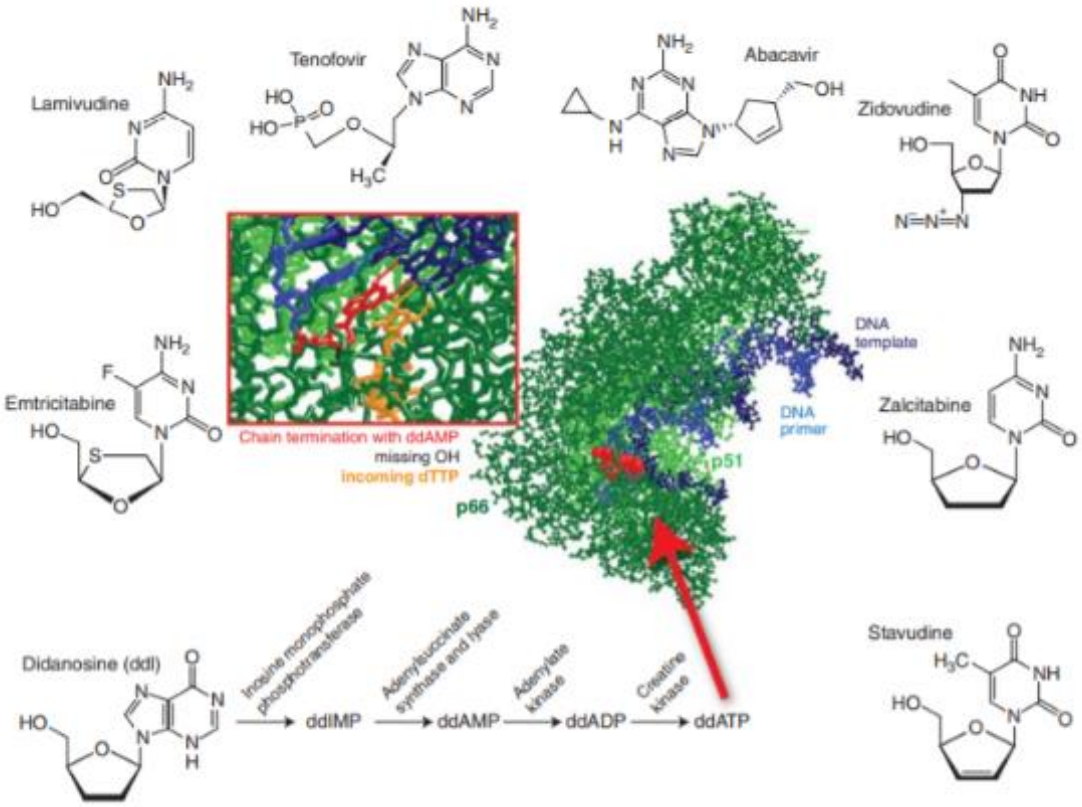

Figure 1.8: The biochemical structure of nucleoside/tide reverse transcriptase inhibitors and the phosphorylation that takes place within the host after administration. Copied from [140].

Designing and synthesizing next generation nucleoside/nucleotide analogues are an objective of many researchers that are developing anti-HIV-1 drugs. New nucleoside analogues are required, since HIV-1 is highly variable through point mutations that confer drug resistance to the virus [138]. Importantly, viral strains develop antiretroviral drug resistance to all the NRTIs [143]. For example, M184V is demonstrated to confer 3TC and FTC high level resistance, but results in impaired viral fitness, and hypersensitization to several other NRTIs.

1.6.1.2.2. Non-nucleoside reverse transcriptase inhibitors (NNRTIs)

NNRTIs are ARVs that do not compete with substrates of HIV-1 RT. These inhibitors bind directly to the hydrophobic pocket of RT that is reported [144]. Binding of NNRTIs alter the three-dimensional conformation of the active site and decreases the activity of the polymerase [145]. The NNRTI-binding site contains hydrophobic i.e. Y181, Y188 and hydrophilic i.e. K103 residues of the p66 subunit and of the p51 subunit (E138) [146]. These non-competitive drugs lack prevention of RT in other lentiviruses i.e. as HIV-2 [144]. The hydrophobicity characteristics of NNRTIs allow entry into the cell with no further processing required [147]. There are currently five approved NNRTIs: efavirenz (EFV), nevirapine (NVP), etravirine (ETR), rilpivirine (RPV) and doravirine (DOR) (Table 1.1).

Nevirapine was the first drug approved in 1996 [148]. Currently, NVP is rarely used since it is responsible for inferior clinical effectiveness and problematic toxicities that include rash, Stevens-Johnson syndrome and hepatic necrosis [149]; hence efavirenz is used and recommended more often for therapy. The chemical structure of NNRTIs is diverse (Figure 1.9), but their effect on the enzyme is comparable. NNRTIs were understood to bind only to the RT substrate complex [150] and was later clarified to bind irrespective of substrate binding. It was further demonstrated that NNRTIs displayed increased affinity to the enzyme once the substrate was bound [151]. Therefore, it is suggested that NNRTIs do not inhibit substrate binding to the active site; however, could potentially promote it [152]. This characteristic aid the combination of NNRTIs with NRTIs. NNRTIs were also identified with a capability to inhibit RNase H activity of RT [153]. Resistance to all the NNRTIs has also been reported, for example, K103N, which reduces susceptibility to NVP and EFV.

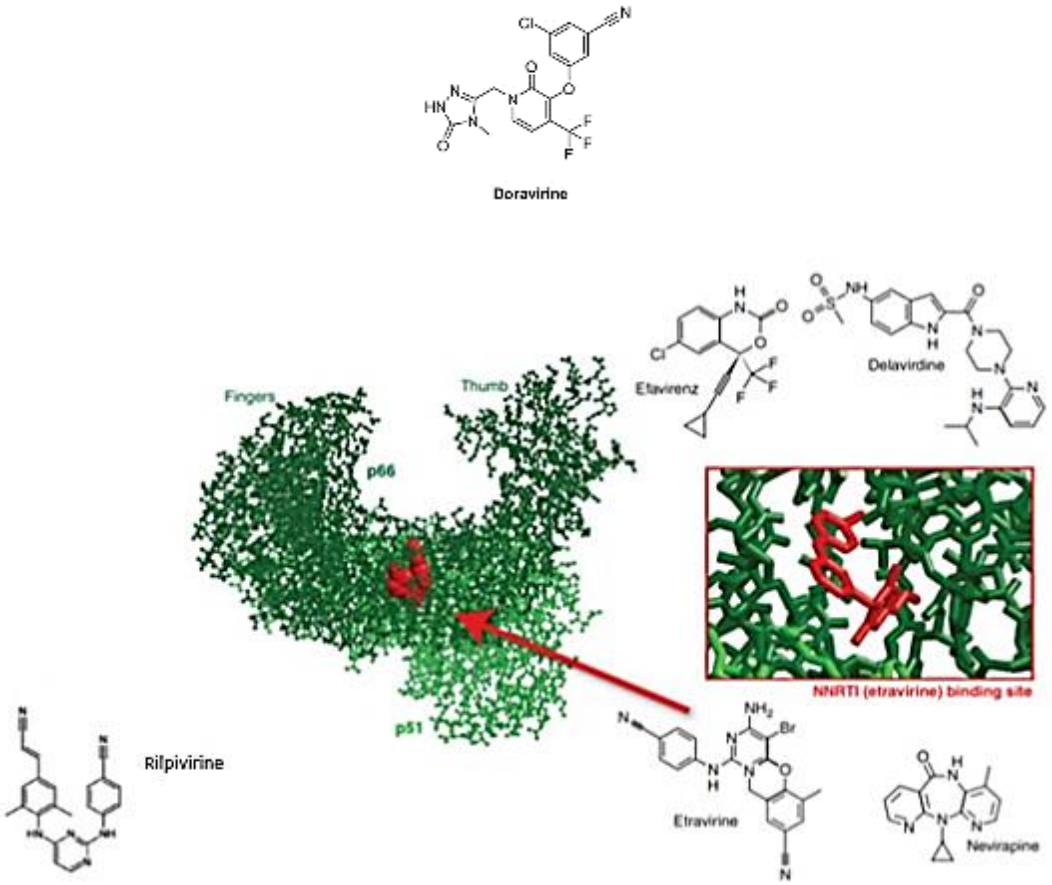

Figure 1.9: The biochemical structure of non-nucleotide reverse transcriptase (RT) inhibitors and the binding to the active site of RT. Copied from [140].

1.6.1.3. Protease inhibitors (PIs)

The viral protease is essential in the formation of virion maturation stages [154] i.e. cleavage of viral *gag* and *gag-pol* polyprotein precursors, it is therefore the second crucial inhibitor. The inhibitors were designed as peptidomimetic molecules that bind to the proteolytic cleavage site. The inhibitors are not cleaved due to the differences seen in the natural substrate peptide bonds and the inhibitor hydroxyethylene bonds. Upon binding to the active site, competition occurs between the inhibitor and the natural substrate of protease once the inhibitor binds enzymatic cleavage is hindered resulting in reduced processing [155].

The first drug to be developed and approved in this class of inhibitors was saquinavir [156]. There are currently nine inhibitors in this class: fos/amprenavir (APV, Agenerase), atazanavir ATZ

(Reyataz), darunavir (DRV, Prezista), indinof theavir (IDV, Crixivan), lopinavir (LPV), nelfinavir (NFV, Viracept), saquinavir (SQV, Invirase), ritonavir (RTV, Norvir), and tipranavir (TPV, Aptivus) (Table 1.1).

By reason of its crucial role in the replication cycle and small magnitude (11 kDa), resistance to this class of inhibitors was initially expected to be sporadic. However, due to the genes boundless flexibility of polymorphisms detected in 49 codons and more than 20 substitutions are linked to resistance [157]. Amino acid residue replacement induces resistance to protease inhibitors whereas natural substrates continue to interact with the drug-resistant protease [158]. The change of natural substrate affinity decreases the efficiency of protease; therefore, drug-resistant viral forms are subject to mutations that compensate the enzyme's efficiency and does not directly affect resistance to an inhibitor [159]. Similarly, to RT inhibitors resistance to all the above-mentioned PIs has been reported. For example, I47A confers high level resistance to LPV.

1.6.1.4. Integrase strand transfer inhibitors (INSTIs)

Integrase is an HIV-1 enzyme that has been currently targeted for HIV-1 drug development, Figure 1.10 [160]. Integrase catalyzes the 3'- processing end of reverse transcribed viral RNA and transfers the cDNA strands into the host chromosome. The approved integrase inhibitors mark the strand transfer reaction and are therefore named INSTIs [160]. The dynamic development of integrase inhibitors began in the year 2000 when diketone organic acids were revealed to impede the integration and viral replication in cell culture, specifically, the step of proviral DNA integration into host cellular genomic DNA [161]. This was the initial indicator that integrase inhibitors were potential antiviral drugs. This class of ARVs bind to two elements of the virus, the integrase enzyme as well as the substrate, the viral DNA which support its function.

The mechanism of action for INSTIs begin with (1) binding to the viral elements: integrase and the viral DNA and (2) with the two magnesium ion cofactors present in the active site and the viral DNA. Consequently, INSTIs are structured to have two indispensable components also known as the metal-binding pharmacophore, that function by sequestering magnesium, and a hydrophobic group that binds to viral and host DNA in addition to IN [162].

The first FDA approved integrase inhibitor was RAL (Isentress, MK-0518; approved in 2007, Figure 1.10). RAL demonstrated a very high efficiency and quickly became one of the most used drugs [163]. Additional drugs from this group include elvitegravir (EVG), dolutegravir (DTG) and Bictegravir (BIC). Recent co-crystallization of the integrase-DNA complex and bound RAL and/or EVG has confirmed the biochemical mechanism as well as provided structural origin for

dissecting the inimitable breadth of the observed antiviral activity for INSTIs [164]. The general make-up and amino acids in the active site are highly conserved, however, these resistance causing mutations are mapped within the IN active site particularly at residues that manage the magnesium cofactors [164]. Antiretroviral drug resistance to INSTIs has been widely reported i.e. N155H confers high level resistance to first generation INSTIs, RAL and EVG. Interestingly, DTG has the highest genetic barrier to drug resistance development compared to all available antiretroviral drugs.

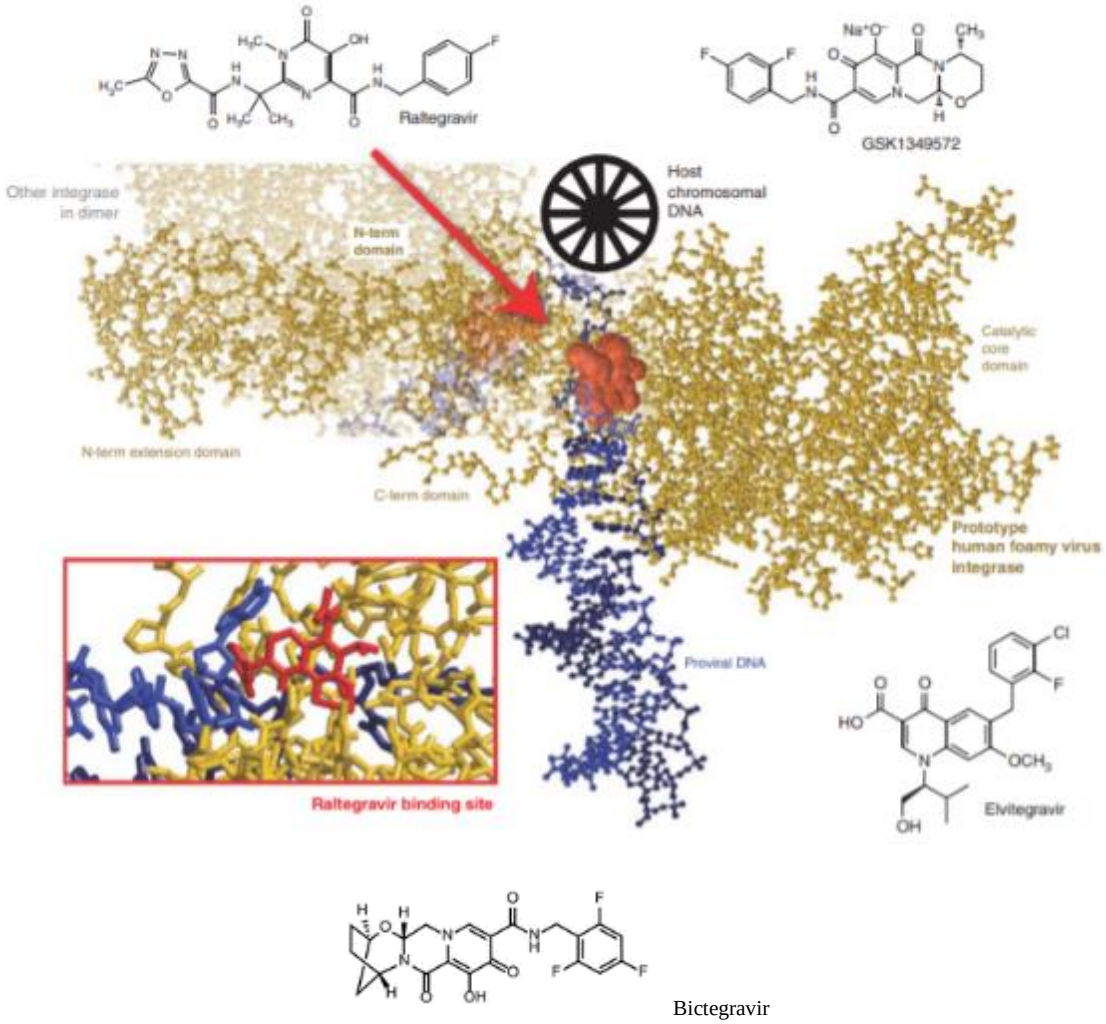

Figure 1.10: HIV-1 Integrase inhibitors displayed in the active site of the integrase enzyme. Copied from [140].

1.6.2. Antiretroviral Drug Resistance

The combinatorial use of antiretroviral drugs was confirmed as the most effective toward regulating the advancement of HIV disease progression and extending survival [165]. However,

these advantages have conceded to the inevitable emergence of drug resistance, the virus' ability to replicate in the presence of ARVs leading to drug resistant mutations (DRMs) [166]. Single mutations rarely cause complete, high level resistance [158].

Several other factors contribute to drug resistance development during ART. The factors range from poor treatment adherence in certain cases which could mean anything from not taking ARV's at all to missing certain doses [167]. Poor adsorption into the bloodstream results in low drug levels being available and therefore allows for HIV replication and accumulation of drug resistance mutations, or the ARVs could be expelled from the gut too quickly due to side effects such as diarrhoea [168]. Pharmacokinetics and pharmacogenetics, mainly focused on how the drug is absorbed into cells, distributed, broken down and removed, in the context of each patient impacts on optimal drug levels. Moreover, drug-drug interactions could also cause a breakdown in the ARV leading to low levels in the blood allowing for HIV replication and the accumulation of DRMs over time [169].

1.6.2.1 The development of antiretroviral drug resistance

Antiretroviral drug resistance is either acquired, generally following pressure exerted by ART, or transmitted from a treatment-experienced individual as well as through minority resistant variants.

In acquired drug resistance there are important concepts that require thorough understanding. Firstly, the high infection levels for viral production and cell turnover. In untreated patients the total amount of infected lymphoid tissue is estimated at 10^7 -10^8 cells [170]. During the chronic stage of infection, the target cells become relatively stable due to the infection and clearance of newly infected cells. The half-life of the newly infected cells is about 2-3 days which means regulation of this state requires cells to be infected at an extremely high rate [171]. At this rate of infection and turnover the second avenue results in rapid replication rate of HIV-1. The population of viruses in a patient are extremely heterogenous due to the high error rate of HIV RT [158], introducing at least one mutation per genome per transcription cycle. The increased infection rate in combination with the increased mutation rate ensures a diverse viral quasispecies. The mutations therefore do in certain cases confer a selective advantage to the virus by decreasing susceptibility to ARVs leading to the 'Darwinian selection process', which is fully dependent on the degree of selective advantage conferred by the mutation(s), mutant prevalence in the population and the level of ARV. The use of cART could potentially halt the selection advantage for reasons such as multiple mechanisms being required for all the drugs in a regimen to develop resistance and

multiple drugs that suppress viral replication more effectively than single ARV agents [172]. The second is through drug selective pressure. In the presence of the latter and the virus's high replication rate the occurrence of drug resistance is inevitable [173]. The mutations that occur due to the drug selection pressure caused by drug-drug interactions or suboptimal adherence reduce susceptibility to ARVs and since the virus continues to replicate in the presence of ARVs, the emergence of additional resistance mutations is inevitable. This ultimately leads to multi-drug resistant virus. Activated latent virus could potentially result in the resistant viruses appearing and replicating causing resistance or enhancing cross resistance to the ARV regimen the patients are currently on.

Transmitted drug resistance occurs when infection is caused by a virus bearing drug resistance mutations [174]. Most transmitted drug resistant viruses return to wild type over several years because of the decrease in viral fitness, or remain present as minority variants [175].

Minority drug-resistant variants may be present in patients on ART, and due to their low frequency levels, they may not be detected or quantified using conventional methods i.e. genotypic drug resistance and phenotypic susceptibility testing. However, recent interest in minority variants was driven by the development of sensitive assays that detect, quantify and characterize the low abundant variants in the genetically diverse HIV population within infected patients [176]. The scientific significance of low frequency variants of HIV-1 **is** indicated in classes such as NNRTI after single dose exposure to NVP, secondly prior to initiation of NNRTI first line therapy and lastly CXCR4 variants prior to CCR5 antagonist treatment. The impact on other drug classes are reported as controversial due to the limitations e.g. small sample groups [177]. Therefore, it is suggested that no significant impact of the presence of minority variants is reported on therapy used in second- and third-line therapy.

1.6.2.2. Mechanism of antiretroviral drug resistance for each drug class

A great deal of research has been placed in understanding and identifying the mechanisms through which mutations associated with drug resistance confer resistance.

Cross resistance occurs when a drug in a specific class is used by a patient and targets specific amino acids within the active site of the enzyme, and a drug in the same class, however, the patient has not been exposed to cannot use due to structural similarity and since the drug targets the exact same resistant amino acids, resulting from resistance mutations selected using a structurally similar drug. Cross-resistance is restricted to ARVs within the same drug class [178]. During early evolution of resistance to either RT or PR inhibitors, viruses may have had low levels of cross-

resistance to other drugs within the class [179]. Nonetheless, this could potentially be the pre-existing framework for higher-level cross-resistance to develop with additional mutation in these two enzymes. Thus, infected patients that acquire strains that have low levels of cross-resistance should perhaps be genotypically tested so that the switch to alternative drug substitutes that bind to or select for different residues [180].

1.6.2.2.1. Co-receptor antagonists

Maraviroc resistance is dissimilar to other ARV classes, mainly through the resistance mechanism which include (1) tropism switching, the initial use of CCR5 and a later switch to CXCR4, (2) Env having an increased affinity for the co receptor [181]. Tropism switching has been identified and studied by the therapeutic industry seeing as it is a major limitation for this drug class as. Although the tropism switching is rare, it naturally leads to earlier disease progression. Thus, if a patient is on CCR5 antagonist and the selection of CXCR4 tropic virus occurs, this would negatively impact the patient's progression to chronic infection and AIDS.

CCR5 inhibitors were previously used for drug resistance selection in peripheral blood mononuclear cell cultures (PBMC), that express both CCR5 and CXCR4 and other potential chemokine receptors that assist in infection [181, 182]. Experiments have reported that resistant viruses require CCR5 for entry [183]. Moreover, further assessments of viral tropism in patients who failed MVC therapy during clinical trials proposed that a change occurred when pre-existing X4 viruses were detected in the patient quasispecies before therapy initiation [184].

1.6.2.2.2. Fusion Inhibitor resistance

T-20 resistance occur due to mutations situated within the gp41 HR1 domain [128]. Amino acid changes on the exterior surface of HR1 and even intracellular gp120 alterations are associated to substantial differences to viral susceptibility to T-20 [185]. These mutations describe the wide array of susceptibility to enfuvirtide among HIV-strains [185] and the probable evolutionary contribution of acquired drug resistance to T-20.

1.6.2.2.3. NRTI resistance

In drug resistance to NRTIs, two mechanisms are in play during the reverse transcriptase process, namely the impairment of analogue inclusion into the DNA or the excision of the incorporated analogue from the prematurely terminated DNA chain [186].

Single mutations or a collection of mutations initiate resistance by weakening the ability of RT to incorporate an inhibitor. The most common mutations are M184V, K65R and TAMS (Thymidine analogue mutations). The methionine 184 (M184) is located at the active site of RT and is replaced by valine (M184V) which has a different side chain, characterized as aliphatic and hydrophobic. This change restricts the positioning of 3TC triphosphate [187]. The M184V mutation confers a high level of resistance against lamivudine. When used as a single ARV, resistant strains overtake the wild type virus during a limited time period and when used in sub-optimally suppressive HAART, M184V almost always emerges first. This is however, not supported in patients who are on fully suppressive HAART [188].

The K65R is a signature mutation seen in patients who fail nucleotide or/and nucleoside analogues, particularly in treatment combinations containing tenofovir or abacavir [189]. This mutation is observed to have an association with HIV-1 subtype C at a double frequency rate [190]. The wide variation is potentially due to the different standards of care, with slower switching after virological failure allowing for drug mutation accumulation [190].

The most common mutations present during the excision of the nucleoside inhibitors from the terminated DNA chain are TAMS, that are frequently selected for after failure of combinations that include zidovudine and stavudine but are able to endorse resistance to almost all nucleoside and nucleotide inhibitors including tenofovir [191]. The development of these mutations can vary and occur gradually. Resistance occurs when they promote ATP or pyrophosphate-mediated excision of inhibitors from the 3' end of the terminated DNA strand [192]. The ATP and pyrophosphates in the lymphocytes do not participate in the DNA polymerization reaction, however, can abolish the phosphodiester bond linking the inhibitor and DNA further resulting in the removal of the inhibitor. The only disadvantage of this process is that it can be decreased in the presence of other mutations i.e. M184V reduces the selection of TAMS by the thymine analogues and increases lingering activity of some nucleoside analogues despite the presence of TAMS [193].

1.6.2.2.4. NNRTI resistance

NNRTI's have a bind to the hydrophobic pocket situated nearby the catalytic site of the RT. The enzymes flexibility is mostly affected after binding of the inhibitor and prevents the ability of synthesizing DNA [194]. NNRTIs main restriction is the low genetic barrier to resistance that it possesses [195]. This ultimately means that a single mutation is able to confer high level resistance

or cross resistance. The NNRTIs select for mutations located in the hydrophobic site and result in reduced drug affinity to the binding pocket [196]. Studies have reported that resistance also develops when NNRTIs are prescribed to patients as monotherapy or during incomplete viral suppression, which further signifies that resistance is triggered by drug selected pre-existing mutant virus populations within a patient [197], lingering from previous treatment or treatment-naïve mutations.

1.6.2.2.5. Protease Inhibitor resistance

The protease constitutes a symmetric substrate-binding site at the centre of the protein [175]. This enzyme digests polyproteins at crucial sites, allowing the release of viral proteins necessary for infectious viral particles assembly. Without efficient protease, virions are produced, but are deemed non-infectious, immature virus particles. PI's are chemical structures used to impersonate viral peptides recognized and cleaved by protease [175]. The chemical inhibitors exhibit a durable affinity for the protease active site and impede the functionality of this crucial enzyme in a highly discriminatory manner.

PI resistance development is reported to be a stepwise process [198]. Protease inhibitor resistance results from amino acid substitutions that occur within the binding domain or distant sites [199]. The modified sites cause decreased affinity both directly and indirectly through altering the contact between the inhibitors and the enzyme. Some mutations are selected for through exposure of protease inhibitors because of their chemical structure. An overlap between protease mutation combinations in HIV strains and the development of protease resistance has been noticed. The mutation combinations explain the wide cross-resistance within this drug class [200].

In addition, the mutations in the protease gene, mutations have been reported within the Gag cleavage sites that are associated with enzyme substrate synergy to overcome protease inhibitors [201]. This occurs through the facilitation of cleavage under sub optimal active enzyme due to low replicative capacity or through improving the capability of resistant protease to interact with the substrate. Therefore, as reported by Francois Clavel and Fabrizio Mammano in 2010 [202], the role of Gag cleavage site mutations can essentially be related to viral replicative capacity or fitness.

The pathways for drug resistance selection can generally be explained through acquiring resistance mutations within the protease gene, selecting compensatory protease mutations for enzymatic repair (the virus adapting to the mutated substrate-binding cleft of the mutant enzyme) [203] and viral fitness rescue as well as through the selection of major cleavage site mutations within Gag that result in restorative Gag-pol processing and an increase in HIV-1 protease production [199].

HIV-1 Gag protein consists of 4 domains matrix p17, capsid p24, nucleocapsid p9 and p6 including 2 spacer peptides, SP1 and SP2. These proteins form the part of the structural components of the virus with the matrix facilitating nuclear transport of the viral genome due to recognition of a karyophilic signal on the matrix which ultimately allows infection of nondividing cells. The capsid located beside the matrix gene forms the core of viral particles. This protein has been shown to associate with cyclophilin A resulting in the incorporation into HIV-1 particles. The capsid is followed by the spacer protein 1, as well as the nucleocapsid responsible for recognising the packaging signal of HIV. The spacer protein 2 follows on with the p6 protein thereafter which is important for mediating the interaction between p55 Gag and the accessory protein Vpr resulting in the incorporation of Vpr into the virion.

Mutations in these regions have been previously detected however, present day studies have identified insertions, TGNS, SQVN, AQQA, SRPE, APP, and/or PTAPPA, near the Gag cleavage sites. Seeing as only a limited amount of studies have been evaluated for variation in Gag and the Gag cleavage sites in Subtype C, this study aims to distinguish differences between wild type and patients. The most variable cleavage site according to literature is the p2/NC followed by p1/p6, NC/p1, CA/p2 and lastly MA/CA which is the most conserved [281]. During protease exposure, the cleavage sites MA/CA at codon 128, NC/p1 at codons 431, 436 and 437 and lastly p1/p6 at codons 449, 452 and 453 have been reported the most frequently in vitro and in vivo.

1.6.2.2.6. Integrase inhibitor resistance

INSTI resistance mutations are mapped within the IN active site near residues D64, D116 and E152, that manage the essential magnesium cofactors [204]. Consequently, these mutations obtain fatal effects on the function of integrase and viral replicative fitness [205]. During clinical studies, raltegravir resistance was reported to be linked to three autonomous pathways or sets of mutations within the gene, demarcated by signature mutations at positions Y143, N155, or Q148 [206]. These initial mutations are partnered with particular secondary mutations i.e. for N155H - E92Q, V151L, T97A, G163R, and L74M, whereas for Q148(K/R/H)-G140S/A and E138K are common. Cross resistance among the INSTIs class, irrespective of the mutation combination sets are observed [205]. Although cross resistance is widespread within the INSTI class, different ARVs appear to select different resistance mutation patterns [207].

The resistance profile of DTG was characterized extensively (reviewed in [208, 209]. DTG has a greater barrier to resistance development compared to the initial INSTIs, RAL and EVG and is

reported to have a lengthier binding half-life to the viral enzyme, maintaining function contrary to most INSTI resistant variants [210]. DTG is therefore, categorized by the potency retention against resistant mutants selected by RAL and EVG [211]. Patients who are advised to continue on failing regimens that contain RAL or EVG may accumulate additional mutations, similar to PI and RTI's, and acquire reduce drug susceptibility even to the most potent ARV, DTG. Two clinical studies, VIKING-2 and VIKING-3, have further delved into in treatment-experienced patients on RAL- or EVG-resistant HIV-1 and established reduced efficacy to DTG. DTG is reported to select for the first-generation INSTI resistance mutations and that resistance to this compound is derived from the R263K DTG specific mutations. Particularly, the R263K substitution results in low level DTG resistance, however, is responsible for the viral fitness decrease which is yet to be compensated by secondary mutations. Other deleterious mutations consist of G118R and H51Y that also reduce the emergence of resistance against reverse transcriptase inhibitors during *in vitro* experiments [212].

The FDA approved BIC in 2018 for use in adults, and in 2019 for use in paediatric patients. Resistance mutations were seen in BIC *in vitro* studies, but clinical studies have produced no indication of emergent, therapeutically significant resistance to the inhibitor. Resistance linked to previous INSTI exposure could potentially affect the efficacy of BIC since, brief structural similarities are identified, but this has yet to be evaluated in clinical studies. Several more BIC *in vitro* studies, have selected for mutations R263K and M50I [213]. These studies suggest that BIC may preserve activity in a resistance mutation setting, previously selected by selected by either RAL or EVG, but to date there have been no clinical studies of BIC in persons with pre-existing integrase inhibitor-associated mutations. Reports indicate that BIC has sustained inhibition against the single mutants at important first-generation mutation sites: E92, Y143, Q148, N155, and R263, like DTG [211]. Recent studies reported that BIC exhibited negligible cross-resistance (1- to 2-fold) to a single HIV-1 mutant variant resistant to RAL and EVG and intermediate cross-resistance (2- to 9-fold) to double HIV-1 mutant variants highly resistant to RAL and EVG [214].

1.6.2.3. Methodological detection of antiretroviral drug resistance

When an increase in VL is detected despite therapy use, it is reported that antiretroviral treatment is changed [215], since cross-resistance in each class of ARVs is frequent. Treatment changes should presumptively not be constructed on the postulation that HIV will remain susceptible to drugs within a previously received class. For alternative treatment selection, assessing patient HIV susceptibility to single antiretroviral drugs should be performed, also known as resistance testing.

Drug resistance testing is a route to aid physicians during treatment modifications, since it is allied with improved treatment outcomes but regrettably, not cost effective in LMIC settings [215, 216]. There are currently two methods for detection of drug resistance mutations: genotypic and phenotypic resistance testing, both containing their own unique set of advantages and disadvantages. Considering standard genotypic assays, the technique uses HIV sequences to identify drug resistance mutations and algorithms to infer drug responses. Antiretroviral resistance is linked to sequence changes within the genes targeted by ARVs [217]. The genes are amplified from extracted HIV RNA through reverse transcriptase polymerase chain reaction (RT-PCR) and sequenced by an automated Sanger sequencing instrument. Phenotypic susceptibility assessments measure the ability of a virus (primary, lab-adapted or pseudovirus) to multiply in different ARV concentrations *in vitro*. This method utilises plasmids, patient HIV sequences or a combination of the two through cloning to produce proteins for inhibition testing against approved ARVs.

The limitations of both assessments include the low-quality assurance for assays, the relatively high cost and insensitivity to minority variants [218]. The latter restriction is of more importance to the current genotypic routine resistance testing, the inability of the automated population-based Sanger sequencer to reproducibly detect low frequency drug resistant variants especially when the patient has low VL [157]. The detection limit of minority variants is currently 20% for Sanger sequencing, and evidence proposes that the existence of minority drug resistant variants negatively affects treatment success [218]. The critical threshold at which these rare variants become clinically pertinent remains to be defined. Nevertheless, if resistant variants are available at 1-2% of the viral population it could have a significant effect on treatment outcome over time. The solution to the above predicament would be to develop a more meticulous PCR method that leads to less non-specific banding patterns as well as an increased yield before purification and sequencing systems that increase the threshold at which detection is possible. Several methods have been carefully designed to solve non-specificity and increase sequencing detection limits, nevertheless, one resolved issue always brings light to another. A list of alternatives and their shortages are listed below.

1.6.2.3.1. Allele specific PCR (AS-PCR)

According to research AS-PCR coupled with real time PCR assays would be a more cost saving drug resistance test alternative [218] and reported to be more sensitive but restricted to the number of mutations that can be sampled simultaneously, consequently limiting mutation linkage studies. In the AS-PCR protocol two reactions are completed for each variant by utilising similar primers

on one end, and on the other end a different primer that mainly corresponds to the original or mutant sequence. The main downfall is the increased PCR reactions where incorrect bases can be inserted [219]. Through the standard PCR protocol, the polymerase encounters a prime based genomic region which continues to complement the single stranded genomic region. Nevertheless, if the 3' end of the primer is unattached to the single stranded genomic region the extension would be inefficient. Therefore, with AS-PCR, the inability of the polymerase to extend the primer with 3' unbounded areas where incorrect bases can be discriminated between a native nucleotide and a drug resistance mutation can be determined [218].

1.6.2.3.2. Oligonucleotide ligation assay (OLA)

The OLA method differentiates between the wild-type and mutant alleles using two 20 oligomer DNA probes. The one probe is affixed to a biotin molecule and the other to a hapten molecule that corresponds to either the wild-type or the mutant allele [220]. Both probes are designed to be the perfect complement and positioned adjacent to each other for successful results. Mismatches at the site of ligation or mispriming would prevent ligation insomuch that a mutant-specific hapten-appended probe could not be ligated to the biotin probe when both are hybridized to a wild-type template. The hybridization stringency confers allelic specificity to the oligonucleotide ligation assay. The biotin ligated probe moieties are captured on a streptavidin coated well and the hapten is recognized using an enzyme conjugated antibody. The hapten identifies the template allele as either mutant or wild type [221]. OLA is restricted to the number of mutations assayed in parallel and therefore restricts mutation linkage studies.

1.6.2.3.3. Population based Sanger sequencing

The DNA sequencing technique developed by Frederick Sanger in 1975 forms the foundation of automated 'cycle' sequencing reactions. Sanger sequencing requires a DNA polymerase enzyme, primers (short single stranded DNA pieces that bind to the template DNA and functions to initiate the polymerase), nucleotides (dATP, dTTP, dGTP, dCTP) as well as the template DNA. However, the reaction requires a unique reagent namely dideoxy- or chain terminating versions of the 4 nucleotides (ddATP, ddTTP, ddGTP, ddCTP) each labelled with a different colour dye/ radioactively labelled [222]. The difference between the dNTP and the ddNTP is the lack of a hydroxyl group on the 3' carbon of the ribose sugar ring that terminates the growing chain compared to the regular 3' hydroxyl group that acts as a linkage for the 5' end of an incoming nucleotide. Currently, Sanger-based cycle-sequencing is performed using nucleotides labelled with fluorophores [222]. These sequences contain different DNA lengths ending with each of the

nucleotides; the end of the fragments is labelled with dyes that indicate the final dNTP. The fragments are then run through a thin, long tube that constitutes of gel matrix capillary electrophoresis. As each fragment crosses the end of the tube the laser detects the dye linked to the specific dNTP. The recorded data displays a series of peaks (fluorescently labelled dideoxy-) measured by fluorescence intensity, the peaks are read on the chromatogram [223].The most limiting aspects of this sequencing technique is the size/length of the PCR amplicons produced [224] as well as it being less likely to determine low level minority variants seeing as the level of detection is at 20%.

1.6.2.3.4. Second generation sequencing

Commercial second-generation sequencing (SGS) was developed in 2005, in response to the first-generation automated Sanger sequencing limitations [225]. To address the low throughput and high costing, SGS was a response design to increase the sequencing of many DNA fragments simultaneously. A popular example thereof is the next generation sequencing (NGS) Illumina sequencing technology.

The library preparation for the Illumina platform is prepared through dividing genomic DNA or cDNA samples and joining specialized adapters to both ends on the fragmented sample strand. A substitute process called "tagmentation" combines the dividing and joining reactions into a single step. The fragments that are joined to adaptors are further processed through amplification and purified through gel extraction. Cluster generation is performed by immobilising the gel purified adapter ligated fragments are on a flow cell surface, proposed to display the DNA in a way that enables the polymerase to access while also certifying high stability of the surface bound template.

The sequencing by synthesis technology makes use of four fluorescently labelled nucleotides to sequence the surface bound template in parallel. During the sequence cycles, a single labelled dNTP is added to the growing chain. The label on the nucleotide aids as a terminator for polymerization, after a single dNTP incorporation the fluorescence is captured for identification purposes and followed by enzymatic cleavage to allow for binding of the next nucleotide. The presence of all four reversible terminator nucleotides allows room for natural competition which decreases incorporation bias. The signal intensity measurements are what is used for base calling during each cycle. This technology, therefore, decreases raw error rates. This process results in correct base-by-base calling that has eliminated sequence-context specific errors which allow for vigorous base calling across the genome, including repetitive regions in the sequence and

homopolymers. The advantages of using the Illumina sequencing technology includes the high throughput results, low cost per Gb data and high accuracy however, their technology retains disadvantages with short reading lengths and overall high instrumental costs [226].

1.6.2.3.5. Third generation sequencing (TGS)

Stephen Quakes' laboratory developed the first single molecule sequencing technology that was commercialized by Helicos Bioscience [227]. The real time element was hypothesized to this technology by Steve Turner and Jonas Korlach at Cornell University in the 1990's [228]. This technology was then referred to as Single Molecule Real Time (SMRT) Sequencing that has incorporated photonics and biochemistry fields and the development of a zero-mode waveguide (ZMW) technology [229].

The library preparation consists of joining hairpin adaptors to the targeted double stranded DNA ends, called a SMRTbell, altered to a closed single stranded circular DNA. [230]. The SMRTbell molecule is added to a chip, SMRT cell [231], and disseminates into a sequencing 'well' also known as a ZMW. In every ZMW, polymerase is restrained to the bottom and binds to the adaptors consequently initiating replication. When a base is held by the polymerase, a light pulse distinguishes the fluorescently labelled bases, since the four fluorescent-labelled nucleotides produce diverse emission ranges when incorporated and begins recording when a base is gripped by the polymerase. The advantage of this technology begins with the polymerase processivity generating highly accurate reads of up to 2000 nucleotides. Secondly, the technology involves numerous sample preparations steps and negligible sequencing reagent quantities and the run time is short, between 30–60 minutes.

The downfall of technology occurs with the polymerase restrictive factor: when the high strength imagining lasers damages the polymerase and therefore leads to decreased activity. The challenge brought about by the prompt run time is that the imaging technology that captures the real time insertion of bases are not able to detect nucleotide incorporation at the naturally fast paced polymerase speed i.e. approximately 100 nucleotides per second. With a restricted throughput, approximately 40–90 megabases of sequence per run, analysis of species with medium- large-sized genomes are deemed a challenge. Another limiting factor is the error rates percentages of 15–20% [232].

As a result of the rapid and high-throughput genotypic assays, recognition of specific point mutations on complete DNA sequences are being performed [233, 234]. However, the rapid

increasing reports of HIV-1 drug resistance mutations and diversity of each HIV-1 sequence provide technical difficulties for point mutation detection assays. Despite the availability of PR, IN and RT sequences, the distinct mutation patterns within these enzymes as well as the complexity of the crosstalk between mutations in the environment have made it challenging to predict the actual drug resistance within an individual. A second resistance monitoring *in vitro* technique was designed to cover the aspect of mutation interactions within patient viruses, namely the phenotypic susceptibility assessment [235].

1.6.2.3.6. Phenotypic susceptibility assessment

Phenotypic susceptibility assays quantitate the drug inhibition of the virus by determining the concentration of drug that inhibits viruses as well as determining the inhibitory concentration of a drug that reduces HIV-1 replication by 50% (IC_{50}) in *in vitro* tissue culture. There are several ways to detect the phenotypic susceptibility of viral strains within patients by either using patient peripheral blood mononuclear cells (PBMCs) or through resistance test vectors [236].

The first method cultivates HIV-1 isolates in patient PBMCs with negative donor PBMCs to produce a virus stock [237]. The virus stock is titrated to establish the virus infectivity of the stock, through a standardized inoculum to infect cell cultures with different concentrations of an ARV, as well as calculating IC_{50} to measure the infection rate through HIV-1 p24 antigen levels. The p24 antigen levels demonstrate viral capsid protein in culture. This assay is deemed reproducible however; it includes several limitations, the first being that it is time consuming. The assay takes a minimum of 6 weeks from specimen collection to the data generation stage. Secondly, the assay is labour intensive. Additionally, *in vitro* selective pressure could be imposed, since the stock generation takes time, which might benefit certain virus isolates and not all from the heterogenous virus population. This method determines the susceptibility of virus existing in a patient's infected PBMC and can therefore not be used to detect the virus present in patient plasma levels. Several studies have determined the assay insignificant because of the latter [238, 239]. Both Young et al and Bacheler et al [240, 241] have demonstrated that despite the limitation's, studies have displayed agreement with the plasma HIV-RNA and viruses cultured from PBMCs.

The second type of phenotypic drug susceptibility assay is reliable [235], accurate [242], and reproducible [243]. This single round assay is reliant on virus particles produced in transfectable human embryonic kidney (HEK) cell line 293T as well as infection of the same cell line. In these

assays 2 plasmids are transfected into the HEK 293T cells one containing the HIV-1 genome with the envelope gene deleted and replaced by a reporter gene and the other plasmid containing an envelope gene. The cultured supernatants containing the pseudovirus are collected and used to infect a new culture of HEK 293T cells in the presence of an increasing drug concentration. In most cases the patient derived HIV genome portions (*gag* only, *pol* only) are incorporated in the parent vector to test the susceptibility to single ARVs. The phenotypic assay is intentionally designed to analyse HAART experienced patients' complicated genome. The ARV concentrations produce dose responses from which dose response curves can be generated. From these curves the IC_{50} can be obtained and are normally compared to the wild type virus under the exact same conditions, these results could potentially assist in the management of treatment and improve long-term HIV replication suppression [235].

The results are intended to aid physicians, by giving them the accurate responses of mutations in combination and to select optimal treatment regimens/more efficacious therapy for treatment failures prior or drug-naive patients infected with drug-resistant virus. In accumulation to the latter, the assay is used to assess new drugs and support drug development against resistant yet active (high replicative capacity) viruses [235]. Assay restrictions include the absence of quality assurance testing as well as high costing for resistance testing, and lastly the low sensitivity of the assays to detect minority viral quasispecies. These viral variants form less than <20% of the circulating strains within a patient's virus population and cannot be detected by the current standardised available assays. This leads to the recurrence of wild type virus in plasma halting of drugs that select drug resistant populations [244].

Alternatively, the luciferase reporter gene can be exchanged with green fluorescent protein gene and the use of HIV-1 CXCR4 or CCR5 tropic envelope. The virus production would be similar however, infection is completed in primary $CD4^+$ T cells with an advantage of measuring the drug inhibition by entry inhibitors, instead of transfecting HEK 293T cell lines with CD4 and the CXCR4 and CCR5 co receptor genes that allow HIV-1 envelope mediated entry. Another aspect that is different is the measurement of the green fluorescent protein which is quantitated through flow cytometry. This detects individual infection events however; the most limiting aspect of this particular assay are the number of cells infected.

The phenotypic assay employed in this study is well-established in our laboratory and has been utilized extensively for *in vitro* drug susceptibility testing of FDA approved and novel drugs against both wild-type and drug resistant HIV-1. In addition, a similar assay (PhenoSense) is employed by Monogram Biosciences (CA, USA) for commercial phenotypic drug resistance

testing of clinical specimens. We therefore argue that our chosen phenotypic assay is more than sufficient and appropriate of use in this study. Furthermore, certain elements of the assay differ dramatically from the Petropoulos paper in terms of the vector and insert used. Two different backbones (psPAX2, pNL4.3.Luc.R-E-) were used in conjunction with full (not partial) HIV-1 gag-pol (4,5kb). Others have used the Petropoulos assay specifically for gag only, PR only, RT only, gag-PR or PR-RT only and INT only. However, in our endeavour to include full *gag-pol* we aimed at reducing the number of constructs required to screen all available classes of approved ARVs. It would also allow us to assess the impact of viral genome-associated drug resistance mutations, located in different parts of HIV-1 *gag-pol*, on phenotypic drug susceptibility. The latter is a novel approach in HIV-1 drug resistance testing.

Forthcoming clinical studies established that despite this plasma reversion, the commencement on the failing ARV agents is related to drug failure, and the virus present at failure originates from previously latent resistant virus [245]. Hence why, resistance testing is important when performed while virological failure is being experienced or within 4 weeks of ceasing therapy since, resistant viruses may remain in the plasma of patients longer to provide useful information to guide future treatment options.

1.6.3. ART regimens in the South African public sector

ART eligibility has changed over time in South Africa, to implementation of test-and-treat strategies where the government sector now administers therapy to all patients infected with HIV-1 regardless of age, CD4 count or VL [246, 247]. Before ART initiation patients are clinically assessed. This assessment includes everything from respiratory/neurological or abdominal danger signs, nutritional assessment, tuberculosis (TB) screening, meningitis screening, mental health or substance abuse screening, major non-communicable diseases screening, pregnancy and lastly screening for other sexually transmitted infections. The laboratory baseline tests include HIV status, CD4 count/%, Creatinine and estimated glomerular filtration rate, haemoglobin, screening for TB, cervical cancer, and hepatitis B antigen, and together with a thorough history and clinical examination are used to determine the patient's clinical stage, according to the WHO [246]. Counselling on antiretroviral drug administration as well as adherence counselling is required. Poor adherence is not only seen as the largest factor leading to the emergence of drug resistance, but also a major determinant in virological failure, disease progression, mortality and health care costs.

The 2015 SA national ART guidelines, Figure 1.11 were updated in 2019, mainly to incorporate INSTs (i.e. DTG) into the first-line regimens of children, adolescents and adults (Figure 1.12) [247].

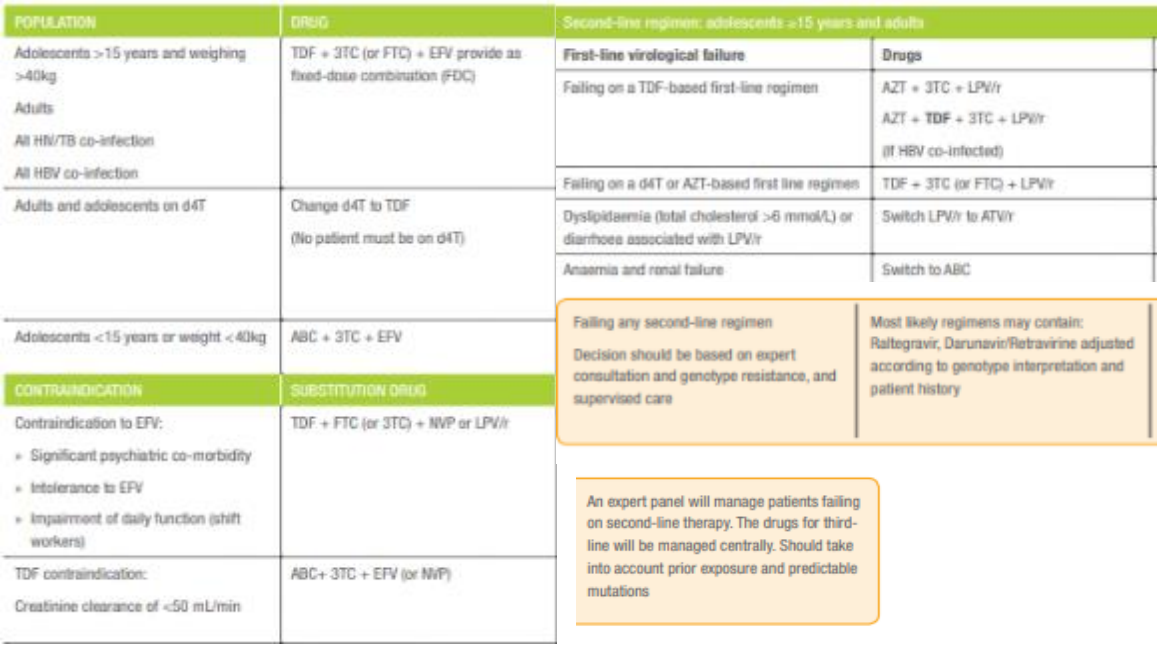

Figure 1.11: The 2015 South African National antiretroviral regimen guidelines for adults and adolescents. Copied from [246].

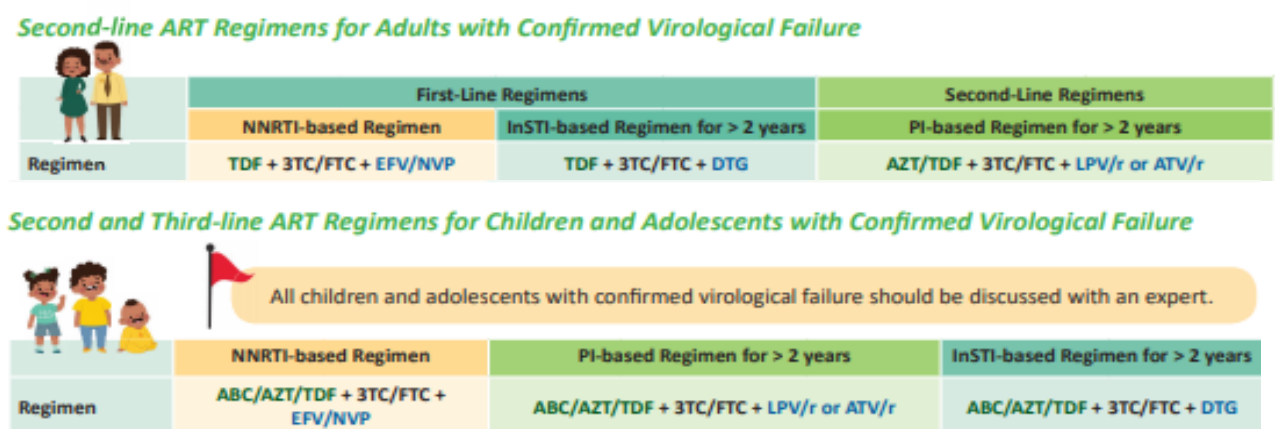

Figure 1.12: The 2019 updated South African National antiretroviral regimen guidelines antiretroviral first line therapy for children, adolescent and adults Copied from [247].

South African HIV-1 positive patients starting ART are initiated on the most appropriate first line regimen. Following virological failure, and if treatment intensification fails, then patients are moved to a second line regimen. When patients fail second line therapy, genotypic testing is performed to detect the mutation profile, and the third-line committee will make an informed

decision based on the patient's genotypic profile (Figure 1.13). Once a genotypic resistance test is performed, the Stanford drug resistance scores govern which combination of ARVs are most fitting for the patients third-line regimen.

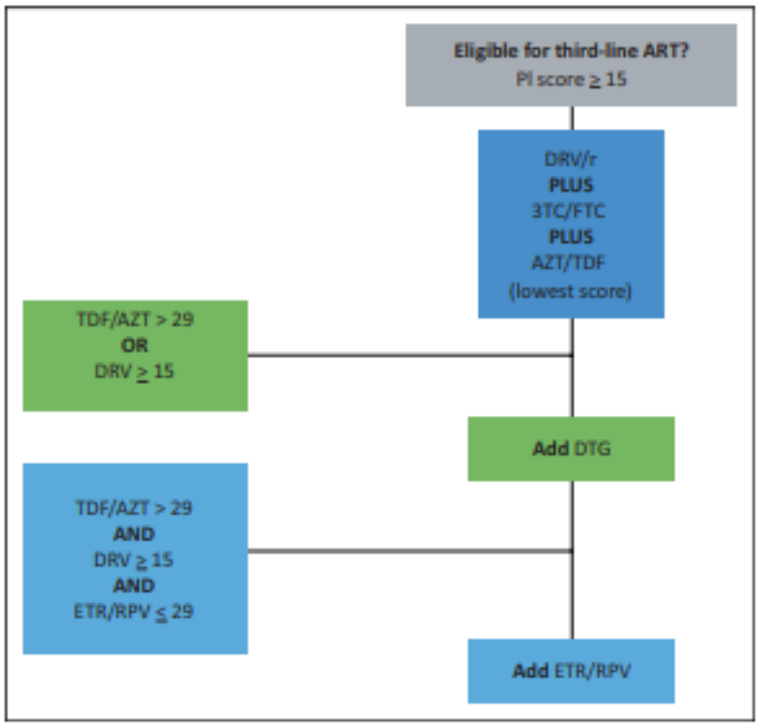

Figure 1.13: Third-line antiretroviral therapy (ART) drugs chosen for HIV-1 positive South African patients failing a second line regimen, according to the Stanford drug resistance scores. Copied from [116].

Once patients fail the third-line salvage therapy, the National Department of Health (NDOH) in South Africa have no further recommendations for these patients in terms of resistance testing or drug options available [151, 152]. The patients remain on a failing third-line therapy and are assumed to have accumulated mutations that are shown to have deleterious effects [248] specifically in HIV-1 subtype C.

1.6.4. Antiretroviral drug resistance testing guidelines in South Africa

Antiretroviral drug resistance can be abated through continuous medication supply, scientifically prescribed practices, adherence support, consistent VL monitoring, and quick responses to confirmed virological failure with timeous changes of ART [249]. The National Department of Health has developed guidelines for HIV resistance testing that deliberate both the international

best practices and the financial constraints SA come across. These guidelines are founded on the levels of resistance in the community as reported in the 2012 WHO HIV drug resistance report [250]. America and Britain's resistance testing guidelines [251, 252], although ideal, are not affordable, nor applicable in most Southern African situations.

In South Africa, the NDOH recommended drug resistance testing once an adult patient has failed the PI-second line therapy [246, 247]. However, although this is true for the update ART guidelines state that resistance testing for adults and adolescents failing a DTG-based second-line regimen and who meet the definition on of confirmed virological failure may be authorized by an expert on a case-by-case basis. Resistance testing for clients failing a DTG-containing first-line regimen is not indicated. Only resistance testing at failure on a PI-based regimen is required [246, 247].

1.7 Study Rationale

Information on antiretroviral drug resistance mutations responsible for failure of third-line treatment in South African patients is scarce. There are currently an estimated 2800 patients on third line antiretroviral treatment/therapy (TLART). In 2018 a total of 1606 patient were switched to a TLART regimen including 1084 on an INSTI based regimen, 650 on DTG and 434 on RAL. The treatment options available for these patients are limited, and if they fail this salvage therapy, the National Department of Health has no further recommendations or suggestions [253]. A phenotypic susceptibility assay that could determine which antiretroviral drugs may still be effective against HIV-1 from these patients would be a valuable tool in their successful long-term treatment success.

Thus, the overall aim of this study was to establish a locally relevant *in vitro* phenotypic susceptibility assay to allow for the phenotypic profiling of HIV-1 from South African HIV-1 positive patients failing a third-line regimen. To achieve the aim, the following objectives were undertaken (Appendix A):

1. To genotypically characterize HIV-1 *gag-pol* from South African HIV-1 positive patients failing a third-line regimen.
2. To establish an *in vitro* phenotypic susceptibility assay and test the susceptibility of pNL4-3.Luc.R-E- against a range of NRTI, NNRTI, PI and INSTIs.

3. To clone the genotypically characterized HIV-1 *gag-pol* sequences from the South African patients into pNL4-3.Luc.R-E-, to establish a locally relevant, HIV-1 subtype C specific *in vitro* phenotypic susceptibility assay.

Chapter 2: Materials and Methods

2.1. Reagents used in the study

2.1.1. Clinical patient samples

Plasma samples from HIV-1 infected patients failing third-line combined antiretroviral therapy (cART), submitted to the National Health Laboratory Services (NHLS) for routine genotypic resistance testing, were used in this study. Samples (n=6) were included from patients with VL > 1,000 RNA copies/ml, and who received a PI and/or INSTI containing third-line regimen. Non-related HIV-1 positive patient plasma samples were obtained from the NHLS for optimisation of the RT-PCR protocol and used as a positive control. The study obtained ethical clearance from the Human Research Ethics Committee (HREC) at the University of the Witwatersrand (Protocol Reference Number: M180658, see Appendix B1).

2.1.2. Recombinant Plasmids

The following recombinant plasmids were obtained through the NIH AIDS Research and Reference Reagent Program, Division of AIDS, NIAID, NIH: psPAX2 (Cat# 11348) from Dr. Didier Trono (unpublished), HIV-1 pNL4-3 ΔEnv Vpr Luciferase Reporter Vector (pNL4-3.Luc.R-E-; Cat# 3418) from Dr. Nathaniel Landau [254, 255, 256], HIV-1 MJ4 Infectious Molecular Clone, Genbank number AF321523,(pMJ4; Cat# 6439) from Thumbi Ndung'u, Boris Renjifo and Max Essex [257], and pHEF-VSVG (Cat# 4693) from Dr. Lung-Ji Chang [258].

The pCSFLW reporter construct was available in the HIV Pathogenesis Research Unit, and obtained from Nigel Temperton (University College London, London, United Kingdom) through Deenan Pillay (Health Protection Agency, London, United Kingdom).

The psPAX2 HIV-1 packaging construct, (10,703 bp) encodes for the HIV-1 group M subtype B *gag-pol* (insert size 4,300 bp). This construct contains an ampicillin resistant gene and is competent for one round of replication. This packaging construct was available and small in size which would potentially be easier to produce more of. The pCSFLW reporter construct is derived from pHR-SIN-CSGW, that expresses firefly (*Photinus pyralis*) luciferase under the Spleen Focus Forming Virus promoter [259, 260]. The 5,471 bp envelope expression plasmid, pHEF-VSVG, encodes for the vesicular stomatitis virus G (VSVG) envelope glycoprotein, that allows for broad cell tropism [261, 262]. Co-transfection of cell lines with psPAX2, pCSFLW and pHEF-VSV-G generates infectious pseudoviruses capable of a single round of infection (See Appendix B Figure:4, 5 and 6 for the plasmid map of psPAX2, pHEF-VSVG and PCSFLW, respectively).

The HIV-1 pNL4-3 ΔEnv Vpr Luciferase Reporter Vector (16,396 bp) encodes for HIV-1 group M subtype B *gag-pol* (approximately 4,300 bp) and contains an ampicillin resistance gene. This construct is competent for one round of replication and in comparison, to psPAX2 contains the firefly luciferase reporter gene which decreases the number of vectors that need to be incorporated in the transfection. However, it requires co-transfection with an envelope expression vector (e.g. pHEF-VSVG) to generate infectious virus and is larger in size which could potentially lead to difficulty in amplification. The firefly luciferase is inserted into the pNL4-3 *nef*, which creates a frameshift in the genes 5' *env* and *vpr*, resulting in protein deficiency [254, 255, 256].

HIV-1 MJ4 is a full length infectious molecular clone (IMC) sized at 12,833 bp that encodes for HIV-1 M subtype C *gag-pol, at* approximately 4,314 bp. The IMC contains an ampicillin resistant gene and originates from Botswana, Southern Africa [257].

2.1.3. Antiretroviral (ARV) drugs

The ARV drugs listed in Table 2.1 were obtained through the NIH AIDS Research and Reference Reagent Program, Division of AIDS, NIAID, NIH, with the exception of DTG which was obtained from MedChem Express, USA as well as ETR and DRV from Janssen Pharmaceutica, Beerse, Belgium and RAL from Merck & Co., New Jersey, USA. The ARV drugs were resuspended to the required concentration, for use in the *in vitro* phenotypic inhibition assays.

2.1.4. Mammalian cell lines

The human embryonic kidney (HEK293T) mammalian cell line was available in the HIV Pathogenesis Research Unit and used in transfection experiments to create pseudoviruses and in *in vitro* phenotypic inhibition assays.

HEK293T cells were maintained in complete DMEM medium consisting of Dulbecco's Modified Eagle Medium (DMEM) with 4,5 g/L glucose, 1% sodium pyruvate and 1% UltraGlutamine™ I (Lonza, Rockland Maine, USA) supplemented with 10% heat-inactivated foetal bovine serum (FBS) (Sigma-Aldrich (Pty) Ltd, St Louis, MO, USA), 2.5 ml of 10 mg/ml Gentamicin (Gibco, Life Technologies, Carlsbad, CA, USA) as antibiotic and 12.5 ml of 1 M HEPES (Gibco, Life Technologies, Carlsbad, CA, USA) to maintain physiological pH. The cells were maintained at 37°C using a humidified, water jacketed incubator (Thermo Fisher Scientific, Waltham, MA, USA) in an environment with 5% CO_2 (Medical CO_2, Afrox, Selby South Africa).

Cells were sub-cultured tri-weekly when the confluency is between 60-90% were reached. Briefly, the cells were rinsed with Dulbecco's 1x Phosphate Buffered Saline (PBS) (Sigma Aldrich St

Louis, MO, USA) and trypsinized for approximately 3-5 minutes at room temperature in the BioFlow-II (Labotec, Midrand South Africa) using 0.2% TrypLE (Gibco, Life Technologies, Carlsbad, CA, USA). Trypsinization was halted with the addition of 3 ml of complete DMEM. The cells were resuspended and mixed thoroughly to disperse cell clumps. Cells were counted by staining a 10 µl cell suspension with 90 µl of 0.4% trypan blue solution (Sigma-Aldrich, St. Louis, MO, USA). Viable cells were then enumerated by automated cell counting on the Countess II FL cell counter (Life Technologies, Carlsbad, CA, USA), as per manufacturer's instructions. Cells were seeded at approximately 8×10^5 cells/ml in 10 ml of complete DMEM in T75 culture flasks (Thermo Fischer Scientific Waltham, MA, USA) and placed in the incubator.

Table 2.1: Antiretroviral drugs for use in the *in vitro* phenotypic inhibition assays, and selected to reflect third-line failure patients' regimen and the available treatment guidelines for third-line therapy in South Africa.

Drug class	Antiretroviral drug name (abbreviation)	Molecular Weight (g/mol)	Antiretroviral drug contributors	Resuspension solution	ARV working stock (mM)	Working ARV Stock (µM)	Highest final concentration (µM)
NRTIs	Zidovudine (AZT)	367.0	NIAID, DAIDS	DMSO	10	12.0	6.0
	Lamivudine (3TC)	229.3	NIAID, DAIDS	DMSO		120.0	60.0
	Emtricitabine (FTC)	247.2	NIAID, DAIDS	DMSO		300.0	150.0
	Tenofovir Disoproxil Fumarate (TDF)	635.5	NIAID, DAIDS	dH_2O		4.0	2.0
	Stavudine (d4T)	224.2	NIAID, DAIDS	DMSO		200.0	100.0
NNRTIs	Etravirine (ETR)	435.3	Janssen Pharmaceutica,	DMSO		0.2	0.1
PIs	Darunavir (DRV)	547.7	Janssen Pharmaceutica,	DMSO		0.4	0.2
INSTIs	Raltegravir (RAL)	482.5	Merck & Co.	DMSO		2.0	1.0
	Dolutegravir	419.4	MedChemExpress, USA	DMSO		0.2	0.1

ARV: Antiretroviral; NRTIs: nucleot(s)ide reverse transcriptase inhibitors; NNRTIs: non-nucleoside reverse transcriptase inhibitors; PIs: protease inhibitors; INSTIs: integrase strand transfer inhibitors; dH_2O: distilled water; DMSO: dimethyl sulfoxide; NIAID, DAIDS: National Institute of Allergy and Infectious diseases Division of Acquired Immunodeficiency Syndrome.

2.2. Genotypic resistance testing of patient samples

The HIV-1 *gag-pol* region from the six patient plasma samples was converted to cDNA and amplified through reverse transcription polymerase chain reaction (RT-PCR) and sequenced to identify known ARV drug resistance mutations.

2.2.1. RNA extraction from patient plasma

Viral RNA was extracted from 500 µl patient plasma with the automated NucliSENS easyMAG system (bioMérieux Inc., Belgium), as per manufacturer's instructions. Samples were lysed through the addition of 2 ml lysis buffer and incubated at room temperature for 10 minutes. After the addition of 50 µl of NucliSENS® easyMAG® magnetic silica beads, the automated extraction process commenced. Total viral RNA was eluted in 25 ul elution buffer and used immediately for RT-PCR or stored at -80°C until required.

2.2.2. RT-PCR Amplification of HIV-1 *gag-pol*

2.2.2.1. Primer design

Primers were designed using Los Alamos National Laboratory software: the Quick Align tool to align primers to the HXB2 reference sequence, as well as the HIV-1 subtypes, (https://www.hiv.lanl.gov/content/sequence/HIV/mainpage.html), to amplify a 4,316 bp fragment encompassing the 5'-3' *gag* region including the *gag-pol* cleavage sites and full length *pol* (Table 2.2) and the subtype C changes seen in Appendix B (Figure B7 and B8). All primers were manufactured by Integrated DNA Technologies™ (IDT™ Coralville, Iowa, USA). **Since the amplification od full HIV-1 *gag-pol* is not typically performed for genotypic resistance testing and is seldom published in the literature, custom primers had to be designed for this purpose. Additional custom primers had to be designed for cloning of gag-pol into the HIV-1 expression vectors using the Gibson Assembly cloning strategy.**

2.2.2.2. One-step RT-PCR

The RT-PCR was optimised using extracted viral RNA from the positive control plasma samples, and tested across a range of three annealing temperatures**:** 50°C, 53°C and 56°C. The annealing of

50°C was subsequently chosen as the most suitable temperature, and used in the one-step RT-PCR assay.

The viral RNA was converted to cDNA through RT-PCR with the use of the PrimeScript™ One Step RT-PCR Kit Ver.2 (Takara Bio, Mountain View, CA, USA). A master mix was prepared by combining 4.5 µl RNase-free dH_2O, 12.5 µl 1-step reaction buffer (2 ×) and 1.0 µl PrimeScript 1-Step Enzyme Mix per reaction, in a 1.5 ml microfuge tube. For each reaction, 5 µl of extracted viral RNA and 1 µl of each primer GP_1ST_FWD and GP_1ST_REV in (Table 2.2) at 10 µM were combined in a 200 µl PCR tube and incubated for 5 minutes at 65°C to denature the RNA. The tubes were immediately placed on ice afterwards. For the RT-PCR, 18 µl of master mix was combined with each of the denatured RNA samples.

Reactions were performed under the following conditions on the BIORAD C1000 Touch™ Thermal Cycler (BioRad, California USA): reverse transcription at 50°C for 30 minutes; heat-inactivation at 94°C for 2 minutes; denaturation at 95°C for 3 minutes; followed by 30 cycles of denaturation at 98°C for 10 seconds, annealing at 50°C for 1 minute 30 seconds, and extension at 72°C for 5 minutes. The reaction was concluded with a final extension at 72°C for 10 minutes, and a holding temperature of 12°C. The amplified product was immediately used or stored at -80°C until further use.

Table 2.2: Primer sequences used in the amplification of HIV-1 *gag-pol* from patient samples.

Description	Name	Sequence (5'-3')	HXB2 position (5'-3')	Gene related position
RT-PCR Forward primer	GP_1ST_FWD	ATG GGT GCG AGA GC	790-803	Gag 1-14 P17 1-14
RT-PCR Reverse primer	GP_1ST_REV	ATT CCA TGT TCT AAT CYT CAG CC	5084-5106	Pol 3000-3012 IN 855-867 Vif 44-66
Nested Forward primer	GP_2ND_FWD	ATG GGT GCG AGA GCG TC	790-806	Gag 1-17 P17 1-17
Nested Reverse primer	GP_2ND_REV	CCT GCC ATC TGT TTT CCA TAA TCC YTA	5033-5056	Pol 2949-2975 IN 804-830

				Vif 1-19

RT-PCR: reverse transcriptase polymerase chain reaction; GP: *gag-pol*; FWD: forward; REV: reverse.

2.2.2.3. Nested PCR

The optimization of the annealing temperature to be used in the nested PCR reaction investigated the use of either a single annealing temperature (66°C) and a touchdown protocol with several, decreasing annealing temperatures (68°C, 66°C, 64°C and 62°C).

Amplicons from section 2.2.2.2 were further amplified using the Expand High Fidelity PCR System (Roche, Basel, Switzerland). A master mix was prepared by combining 17.25 µl DEPC-treated dH_2O (Ambion™, Thermo Fisher, Waltham, MA, USA), 2.5 µl Expand High Fidelity Buffer (1 ×), 0.75 µl Expand High Fidelity Enzyme mix (3.5 U/ µl) and 0.5 µl dNTP mix (10 mM) (KAPA Biosystems, Roche, Basel, Switzerland) (10mM) per reaction in a 1.5 ml microfuge tube. For each reaction, 2.5 µl of RT-PCR reaction and 0.75 µl of each primer GP_2ND_FWD and GP_2ND_REV (Table 2.2) at 10 µM were combined in a 200 µl PCR tube. Following the addition of 21 µl master mix to each tube, the reactions were performed under the following conditions on the BIORAD C1000 Touch™ Thermal Cycler (BioRad, California USA): initial denaturation at 94°C for 2 minutes; denaturation at 94°C for 15 seconds; 30 cycles of denaturation at 94°C for 15 seconds, annealing at 68°C (3 cycles) 66°C (3 cycles) 64°C (3 cycles) 62°C (21 cycles) for 1 minute and 30 seconds, extension at 68°C for 5 minutes and a final extension at 68°C for 5 minutes. The reaction was concluded with a final extension at 68°C for 7 minutes, and a holding temperature of 4°C.

The outcome of PCR reactions (RT-PCR and Nested PCR) was assessed by agarose gel electrophoresis. A 1% agarose gel was prepared by dissolving 1g of SeaKem® LE Agarose (Lonza, Rockland Maine, USA) in 100 ml of Tris/Acetic acid/EDTA buffer (TAE) (Thermo Fischer Scientific Waltham, MA, USA) by heating in a microwave. Ethidium bromide (BioRad, California USA) was added to 0.5 µg/ml final concentration. Once cooled, the solution was poured into the casting tray of the horizontal electrophoresis casting system (Cleaver Scientific Ltd, Warwickshire United Kingdom) and the comb was applied to the cast. The solidified agarose gel was transferred to the horizontal electrophoresis tank containing TAE buffer (pH 8.3). For each sample, 5 µl of PCR reaction was combined with 5 µl of 6 × Orange DNA Loading dye (Thermo Fisher Scientific, Waltham, MA, USA) and applied to a well in the agarose gel. The Quick Load® Purple 1 kb DNA Ladder (New England Biolabs, Ipswich, Massachusetts) was included. Electrophoresis commenced at 80 Volts for an average of 90 minutes. The agarose gel was

visualized on the White/2UV™ Transilluminator (Thermo Fischer Scientific Waltham, MA, USA) and imaged on the Gel Doc System (BioRad, California USA). PCR reactions were assessed for the presence of an approximately 4,314 bp amplicon, with reference to the molecular weight marker.

2.2.2.4. Silica membrane-based purification of PCR products

For the purification of *gag-pol* amplicons, the QIAquick® PCR Purification Kit (Qiagen, Maryland, USA) was used. PCR reactions were combined with Buffer PB in a 5:1 (volume/volume) ratio. If the mixture remained yellow no extra solution was added, however, if the mixture changed to violet, 10 µl of 3 M sodium acetate pH 4.3 was added to decrease the pH. The sample was mixed thoroughly and applied to the QIAquick column for centrifugation at 13,000 rpm for 1 minute using the Eppendorf Centrifuge 5415R microcentrifuge, (Merck Millipore, Darmstadt, Germany). The flow-through was discarded and followed by a column wash with 750 µl of Buffer PE, at 13,000 rpm for 1 minute. The flow-through was discarded and followed by a second centrifugation step for 1 minute at 13,000 rpm to remove residual wash buffer. The QIAquick column was placed in a clean 1.5 ml microcentrifuge tube. Elution buffer to the volume of 50 µl was added to the silica membrane of the column. The column was incubated for 1 minute at room temperature before centrifugation at 13,000 rpm for 1 minute. The eluate was collected, and the concentration of the purified amplicons was quantified on the NanoDrop 1,000 Spectrophotometer system (Thermo Fischer Scientific Waltham, MA, USA), blanked against elution buffer. The eluted DNA was stored at -20°C until required.

2.2.3. Population-based Sanger Sequencing

2.2.3.1. Cycle sequencing

Population-based Sanger sequencing was performed using the primers shown in Table 2.3. A sequencing master mix was prepared by combining 1 µl Big Dye® Terminator v3.1 cycle sequencing RR-100 enzyme (Thermo Fischer Scientific Waltham, MA, USA), 2 µl of the Big Dye® Terminator v1.1 and v3.1 ×5 Sequencing buffer (Thermo Fischer Scientific Waltham, MA, USA), and 4.5 µl DEPC-treated dH_2O (Ambion™, Thermo Fisher, Waltham, MA, USA) per reaction, in a 1.5 ml microcentrifuge tube.

In a MicroAmp® Optical 96-well reaction plate (Applied Biosystems, Foster City, USA), 7.5 µl of master mix was combined with 1 µl amplicon DNA (±100 ng)), and 1.5 µl of sequencing primer (3.2 µM; Table 2.3). Reactions were performed under the following conditions on the GeneAmp® PCR System 2700 (Applied Biosystems, Foster City, USA): initial denaturation at 96°C for 1

minute; denaturation at 96°C for 10 seconds; of denaturation at 94°C for 15 seconds, annealing at 50°C for 5 seconds, extension at 60°C for 4 minutes for 26 cycles and a holding temperature of 4°C.

Sequencing products were purified through DNA precipitation. A fresh solution of sodium acetate (NaAc) and ethanol (EtOH) was prepared by adding 80 µl of 3 M NaAc (pH 4.6) to 2 ml EtOH. To the 96-well reaction plate containing the sequencing reactions, 50 µl of the EtOH/NaAc solution was added and mixed, followed by centrifugation at 2 000 x *g* for 30 minutes on the Eppendorf 5810R Centrifuge (with rotor A-4-81) (Merck, Kenilworth, USA). The 96-well reaction plate was then inverted on paper towel in the rotor and centrifuged for 1 minute at 30 x *g* to remove the solution from the pellet. Rinsing of the pellet in the 96-well reaction plate was performed with 100 µl of cold 70% EtOH without resuspension. The 96-well reaction plate was centrifuged for 5 minutes at 2000 x *g*, thereafter, inverted in paper towel and followed by an additional centrifugation step for 1 minute at 30 x *g*. The 96-well reaction plate was incubated at 95°C for 2 minutes without closing the wells using the Applied Biosystems GeneAmp® PCR System 2700 (Applied Biosystems, Foster City, USA) to dry the DNA pellet. Ten microlitres of HiDi™ Formamide (Life Technologies, Carlsbad, USA) was added to each well containing the dried pellets and incubated at 65°C for 5 minutes to resuspend the pellet, and briefly vortexed. The reaction plate was placed in the automated ABI PRISM® 3730 Genetic Analyzer (Applied Biosystems, HITACHI, Foster City, USA) for sequence analysis.

2.2.3.2. Phylogenetic tree analysis and genotypic drug resistance interpretation

The nucleotide sequence reads obtained from the genetic analyser were assembled and manually edited using Sequencher v5.1 software (Genecodes Corporation, Ann Arbor, USA) or Geneious v10.1.3 software (Auckland New Zealand). Ambiguous bases were trimmed from the sequence reads and the reads assembled using the Dirty Data algorithm in Sequencher and the minimum match percentage and overlap were 65% and 20 bases respectively.

Sequences were also checked for complete, bi-directional coverage (sense and antisense sequence) from at least one primer sequence in each direction over the entire region analysed. In the case of ambiguous bases, the sequences were evaluated to confirm the presence of sequencing artefact or true mixtures. Once manual editing was completed, the consensus sequences were exported in fasta format and submitted to the Stanford HIV Drug Resistance database version 8.9-1 (http://hivbd.standford.edu) [263] for identifying genotypic drug resistance mutations in the PR,

RT and IN regions. The 2019 Updated IAS-USA Drug resistance mutations list was used to associate drug resistance mutations with the relevant ARVs and the ARVs, for further analysis and interpretation [264].

For the analysis of HIV-1 *gag*, the individual patient *gag* consensus sequences were aligned to the HXB2 and the HIV-1 subtype C control (i.e. pMJ4) *gag* region and manually analysed with Geneious v10.1.3 (Auckland New Zealand). Positions scrutinized for the mutations, insertions or deletions within the *gag* sites were MA/CA, CA/P2, p2/NC, NC/p1 and p1/p6. Confirmation of PTAP insertion was also determined through manual editing.

A multiple alignment of the *gag-pol* contigs with reference sequences from HIV-1 subtypes A to K (http://hiv-web.lanl.gov), as well as selected HIV-1 subtype C sequences in Africa from 2017 (http://hiv-web.lanl.gov), were generated using the Molecular Evolutionary Genetics Analysis software (MEGA, version 7.0.26; Pen N State University, USA) [265]. The generated alignments were used to construct Neighbor-Joining phylogenetic trees to verify subtype clustering and the absence of cross-contamination between samples.

2.3. Setting up *in vitro* phenotypic inhibition testing assays

The *in vitro* phenotypic inhibition assay was set up using the wild-type HIV-1 subtype B pNL4.3.Luc.R-E- and tested against the panel of ARV drugs targeting PR, RT and IN**.** The phenotypic inhibition assay required validation before using patient-derived pseudoviruses seeing as only a limited amount of sample volume was available. Since pNL4.3.Luc.R-E- was available and did not require any modification, this construct was used for validation. All incubation steps were carried out at 37°C using a humidified, water jacketed incubator (Thermo Fisher Scientific, Waltham, MA, USA) in an environment with 5% CO_2 (Medical CO_2, Afrox, Selby South Africa).

2.3.1. Antiretroviral drug preparation

The antiretroviral drugs were dissolved at 20 mg/ml in DMSO or dH_2O, and further diluted to a 10 mM ARV stock in the same solvent. The stocks were aliquoted and stored at -80°C.The ARV working stocks were prepared in complete DMEM media. The ARVs were prepared as described in Table 2.1 for the drug inhibitory assessment.

2.3.2. Gag-PR *in vitro* phenotypic inhibition assay

HIV-1 pseudoviruses were produced by co-transfection of HEK293T cells with the HIV-1 Luciferase reporter vector (pNL4-3.Luc.R-E-) and the pHEF-VSVG encoding the vesicular

stomatitis virus G (VSVG) that expresses the envelope for the pseudovirus. The transfected cells were subsequently used in the Gag-PR inhibition assay. Briefly, 293T cells were trypsinized and enumerated as described previously in section 2.1.4. Cells were seeded at 1.4×10^7 cells in 10 ml of complete DMEM in an 8.8 cm^2 Nunclon Delta cell culture dish (Thermo Fisher Scientific Waltham, MA, USA). The culture dish was incubated for 5 hours, to allow for cell attachment to occur. The transfection mix was prepared in a sterilised 1.5 ml microcentrifuge tube (Axygen, Union City, CA, USA) by adding 5 µg of pNL4-3.Luc.R-E- and 5 µg of pHEF-VSVG to 150 µl of Opti-MEM®I (1×) (Gibco® Life Technologies, Carlsbad, CA, USA).

Table 2.3: HIV-1 subtype C specific sequencing primers for the HIV-1 *gag-pol* gene.

Description	Name	Sequence (5' – 3')	HXB2 position	HXB2 gene related position
Gag Primer	GagA	AAATCTCTAGGAGTGGCGCCCGAACAG	623 - 649	LTR5 623 - 634
Gag Primer	GagB	GTCTTCTAATACTGTATCATCTGCTCC	2331-2357	Pol 247 -273 PR 79 - 105
Gag Primer	GagC	GCGGAGGCTAGAAGGAGAGAGATGG	769-793	NCR 135 - 155 Gag 1 - 4
Gag Primer	GagD	GAGAGCCTCCCTTGTCTGGC	5453-5473	Vif 413 - 433
Gag Primer	Gag1F	GGCTTTTAGCCCAGAGG	1275-1291	Gag 486 - 502
Gag Primer	Gag1R	AAGCTTGCTTCTCTGCATCATTATG	1914-1938	Gag 1125 - 1149
Gag Primer	Gag2F	GGATGACAGATACCTTG	1736-1752	Gag 947 - 963
Gag Primer	Gag2R	GCCTCTTCATTGATGGTATC	1396-1415	Gag 607 - 626
Pol Primer	PolA	CTAGCCAGAAATTGCAGAGCCCCTAGG	1990-2016	Gag 1201 - 1227
Pol Primer	PolB	CTCTTGGATGTCTACTTTCATAATGATG	5164-5191	Vif 124 -151
Pol Primer	PolC	GAAGGACACCAAATGAAAGACTGTAC	2044-2069	Gag 1255 - 1280
Pol Primer	PolD	GCTCTTCTTGAAACATACATATGGTGC	5118-5144	Gag 78 - 104
Pol Primer	Pol1F	GGTACAGTATTAGTAGGGCC	2469-2488	Pol 385 - 404 PR 217 - 236
Pol Primer	Pol2F	CACCAGGGATTAGATATC	2965-2982	Pol 881 - 898

				RT 416 - 433
Pol Primer	Pol3F	AAGAACCAGTGCATGGAG	3481-3498	Pol 1397 - 1414 RT 932 - 949
Pol Primer	Pol4F	GTGAATCAGAGTTGGTC	4087-4103	Pol 2003 - 2019
Pol Primer	Pol5F	AGATGGCCAGTCAAAG	4548-4563	Pol 2464 - 2479 Integrase 319 - 334

Primers were manufactured by Integrated DNA Technologies (Coralville, Iowa, USA).

Transfection grade Linear Polyethylenimine Hydrochloride at 1 mg/ml (PEI^{max}) (Polysciences Inc, Warrington, PA, USA) was added to the meniscus of the transfection mixture in a ratio of 3 µg of PEI^{max}: 1µg of DNA. The transfection reaction was incubated for 15 minutes in the BioFlow-II (Labotec, Midrand, South Africa), allowing the polymer to form micelles that coat the plasmid DNA for cell uptake. The transfection mix was added dropwise to the cells in the transfection dish, which was then incubated for a further 18 hours.

Before the transfected HEK293T cells were harvested, they were assessed to ensure they were healthy and approximately 70% confluent. The supernatant was discarded and 2ml of PBS (Sigma Aldrich St Louis, MO, USA) was used to wash the transfected cells and discarded. One millilitre of TrypLE (Gibco, Life Technologies, Carlsbad, CA, USA) was added to the transfected cells to dislodge them from the plate. Complete DMEM, 10 ml, was added to the dislodged cells and mixed well to remove cell clumps, and additional complete DMEM was added to achieve a cell suspension concentration of 2.7×10^{5} cells/ml.

For the Gag-PR *in vitro* phenotypic inhibition assay, Nunc™Edge 2.0 96-well plates (Thermo Fisher Scientific, Waltham, MA, USA) were prepared by adding 2 ml of PBS (Sigma Adlrich St Louis, MO, USA) to each quadrant of the plate frames, and 200 µl of PBS into each of wells in rows A and H (Figure 2.1). The assay allows for the testing of two PR inhibitors, but for the purposes of this study, only DRV was tested. One hundred and fifty microlitres of DRV working stock (0.4 µM) was added to the wells in column 1B to 1D (assay performed in triplicate). One hundred microliters of complete DMEM (Sigma-Aldrich (Pty) Ltd, St Louis, MO, USA) was added to the remaining wells of the plate. A three-fold serial dilution of DRV was prepared by transferring 50 µl of DRV working stock in series to adjacent wells across the plate. Wells in column 12 did not received drug but contained complete medium only. To the prepared plate, 100

µl of the above transfected cells in suspension were added to each well and incubated at 37°C for 24 hrs.

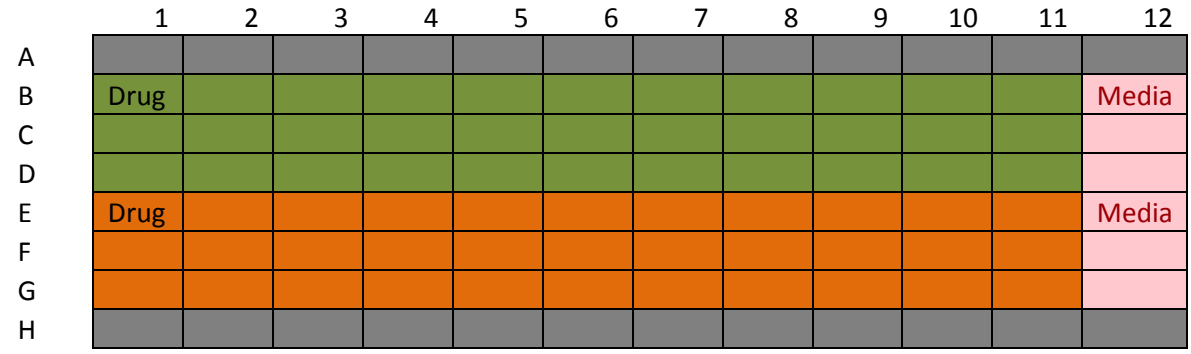

Figure 2.1: Schematic representation of the 96 well plate layout for the Gag-PR inhibition assay, indicating the triplicate plate set up of the PR inhibitor tested.

As a transfection control, an indicator plate was set up by adding 75 µl of HEK293T cells (2.7 x 10^5 cells/ml) to all the wells of a new Nunc™Edge 2.0 96-well plate. From the phenotypic assay plate, 25 µl of supernatant was transferred to the corresponding wells of the indicator plate. After thorough mixing, the indicator plate was incubated at 37°C for 48 hours.

For both the test and indicator plates, the expression of the luciferase reporter gene in the cells were measured using the BrightGlo™ Luciferase Substrate (Promega, Madison, USA). For this, 100 µl of the substrate was added to each well and incubated for 2 minutes at room temperature in the dark. The contents of each well was mixed properly and transferred to the wells of a FiltrEX 3510 Solid White 96-well Filter plate (Thermo Fisher Scientific, Waltham, MA, USA) for the quantification of bioluminescence on the GloMax Explorer (Promega,Madison, USA) in relative light units (RLUs).

The data analysis was performed with Microsoft Office Excel (version 1908, 2016, Microsoft Excel, Albuquerque, New Mexico, United States) to determine the average of viral activity, relative to the media control. A scatter plot was generated by plotting the log of 10 ARV concentrations and the average viral activity. From the data the IC_{50}, the ARV concentration at which 50% of the viral activity is inhibited, was calculated using the forecasted formula from: FORECAST (0.5, known_y's, known_x's), known y values are the drug dilutions and the known x values are the average relative light units (RLU).

2.3.3. RT-IN *in vitro* phenotypic inhibition assay

Transfection was performed as previously described in section 2.3.2, with the exception that transfected cells were incubated for 48 hours before harvesting the supernatant containing pseudoviruses. The supernatant was filter-sterilised through a sterile 0.45 µm Acrodisc® syringe filter with Supor® Membrane, (Paul Corporation, Vorna Valley, Midrand, South Africa). Subsequently, pseudoviruses were aliquot PIoted and stored at -80°C before titration was performed in HEK293T cells. For this, a stored aliquot of pseudovirus was removed from -80°C and allowed to thaw to room temperature. Two-fold serial dilutions were prepared in triplicate in Nunc™Edge 2.0 96-well plates (Thermo Fisher Scientific, Waltham, MA, USA) by serially diluting 50 µl of neat pseudovirus into 50 µl of complete DMEM. HEK293T cells were harvested and enumerated according to the above section 2.3.2. Cells were resuspended at 4 x 10^5 cells/ml in complete DMEM, after which 50 µl of the cells was added to each well. The plate was incubated for 48 hours. The expression of the luciferase reporter gene in the cells was measured using the BrightGlo™ Luciferase Substrate (Promega, Madison, USA) as described in section 2.3.2. A pseudoviral dilution that would provide a bioluminescence reading of 1 x 10^6 RLU in the absence of drug was chosen for the RT-IN *in vitro* phenotypic inhibition assay.

For the RT-IN *in vitro* phenotypic inhibition assay three ARVs were assessed per Nunc™Edge 2.0 96-well plate (Thermo Fisher Scientific, Waltham, MA, USA) which were prepared by adding 2 ml of PBS (Sigma Adlrich St Louis, MO, USA) to each quadrant of the plate frames, and 200 µl of PBS into wells in rows A and H, to minimize evaporation from the inner wells of the plate (Figure 2.2). Seventy-five microlitres of ARV working stock was added to the wells in columns B1 and C1 (assay performed in duplicate). Fifty microlitres of complete DMEM (Sigma-Aldrich (Pty) Ltd, St Louis, MO, USA) was added to the remaining wells of the plate. A three-fold serial dilution of ARV was prepared by transferring 25 µl of ARV working stock in series to adjacent wells across the plate. The wells in column 12 did not received drug but contained complete medium only. Cells were harvested as describe in section 2.3.2, and resuspended to a final concentration of 4 × 10^5 cells/ml in complete DMEM. Pseudovirus (50 µl; to a standardized input of 1 ×10^6 relative light units) was added to each of the wells, and the plates were incubated for 48 hours. The expression of the luciferase reporter gene in the cells was assessed, and data analysis was performed with Microsoft Office Excel as described in section 2.3.2.

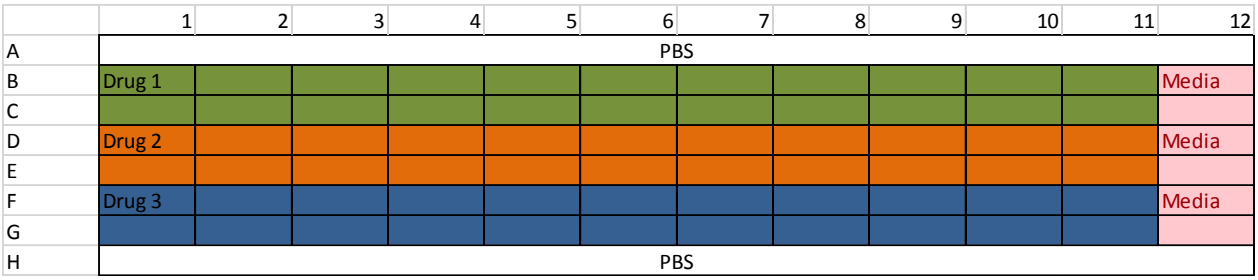

Figure 2.2: Schematic representation of the 96 well plate layout for the RT-IN inhibition assay, indicating the duplicate plate set up of the RT and IN inhibitors tested.

2.4. Construction of patient-derived HIV-1 subtype C expression vectors for use in the Gag-PR and RT-IN *in vitro* phenotypic inhibition assays

Following the successful set up of *in vitro* phenotypic inhibition assays to test RT, PR and IN inhibitors, the *gag-pol* amplicons from the pMJ4 plasmid and the six patient samples were used to construct patient-derived HIV-1 subtype C resistance expression vectors in either the psPAX2 and/or pNL4.3.Luc.R-E- HIV-1 expression vectors. Two approaches were followed for the cloning, namely Gibson assembly and traditional restriction enzyme/ligation.

2.4.1. Construction through Gibson assembly

Gibson assembly relies on user-defined overlapping ends that are incorporated into the fragments to allow the joining of adjacent DNA fragments. The insert and the vector backbone 5' and 3' ends have identical overlapping regions for Gibson Assembly preparation purposes.

The nested *gag-pol* products were subjected to an additional *gag-pol* PCR to introduce 5'- and -3' overlap sequences that correspond to the 5'- and -3' ends of the psPAX2 and/or pNL4-3.Luc.R-E- vectors. Construction was attempted using two different kits: the Infusion® HD Cloning Kit (Takara Mountain View, CA, USA) for cloning into psPAX2 and pNL4-3.Luc.R-E- and the Gibson Assembly® Cloning Kit (New BioLabs Inc Ipswich, MA, USA) for cloning into pNL4-3.Luc.R-E-.

2.4.1.1. Preparation of the psPAX2 and pNL4-3.Luc.R-E- vector backbones

The amplification of the approximately 6.3 kb psPAX2 backbone was optimised using gradient temperatures ranging from 54°C to 72°C, using the appropriate primers for cloning as indicated in Table 2.4 for psPAX2. Similarly, the amplification of the approximately 12 kb pNL4-3.Luc.R-E-

backbone was optimised with gradient temperatures in the range of 54°C to 64°C, using the appropriate primers for cloning as indicated in Table 2.4 for pNL4-3.Luc.R-E-.

A PCR master mix was prepared by combining 6.25 µl DEPC-treated dH2O (Ambion™, Thermo Fisher, Waltham, MA, USA), 12.5 µl CloneAmp™ HiFi PCR Premix (Takara Bio, Mountain View, CA, USA) (1×) and 0.625 µl of the relevant forward and reverse primer (at 10 mM; Table 2.4), in a 1.5 ml microfuge tube. For each reaction, 20 µl of master mix was combined with 5 µl (10 ng) of the relevant backbone plasmid.

Reactions were performed under the following conditions on the BIORAD C1000 Touch™ Thermal Cycler (BioRad, California, USA): initial denaturation at 95°C for 3 minutes; 30 cycles of denaturation at 98°C for 10 seconds, annealing at 65°C for 1 minute (psPAX2) and annealing at 66°C (pNL4-3.Luc.R-E-), extension at 72°C for 1 minute and 30 seconds. The reaction was concluded with a holding temperature of 4°C. Amplicons were run on a 1% agarose gel and visualized on the White/2UV™ Transilluminator (Thermo Fischer Scientific Waltham, MA, USA) and imaged on the Gel Doc System (BioRad, California, USA). The correct product was assessed at positions 6,363 bp for psPAX2 or 12,082 bp for pNL4-3.Luc.R-E- with reference to the molecular weight marker (O'Gene™ 1kb DNA Ladder, Thermo Fisher Scientific, Waltham, MA, USA).

2.4.1.2. Preparation of the pMJ4 and patient derived *gag-pol* inserts

The *gag-pol* region from pMJ4 was PCR amplified with the CloneAmp™ HiFi PCR Premix (Takara Bio, Mountain View, CA, USA) using 6.25 µl DEPC-treated dH2O (Ambion™, Thermo Fisher, Waltham, MA, USA), 12.5 µl CloneAmp™ HiFi PCR Premix (Takara Bio, Mountain View, CA, USA) (1×) and 0.625 µl of the relevant forward and reverse primer (at 10 mM; Table 2.4), in a 1.5 ml microfuge tube. For each reaction, 20 µl of master mix was combined with 5 µl (10 ng) of the relevant insert pMJ4/patient derived *gag-pol*.

The reaction was performed under the following conditions on the BIORAD C1000 Touch™ Thermal Cycler (BioRad, California, USA): initial denaturation at 95°C for 3 minutes; 30 cycles of denaturation at 98°C for 10 seconds, annealing at 65°C for 30 seconds and extension at 72°C for 1 minute. The reaction was concluded with a holding temperature of 4°C. Amplicons were run on a 1% agarose gel and visualized on the White/2UV™ Transilluminator (Thermo Fischer Scientific Waltham, MA, USA) and imaged on the Gel Doc System (BioRad, California, USA). The correct product was assessed at positions 4,314 bp for pMJ4 with reference to the molecular weight marker (O'Gene™ 1kb DNA Ladder, Thermo Fisher Scientific, Waltham, MA, USA).

Table 2.4: Primers used for the amplification of the psPAX2 and pNL4-3.Luc.R-E- backbone and for adding appropriate overlaps (highlighted in red) to the pMJ4/patient samples *gag-pol* inserts for Gibson assembly cloning.

Description	Name	Sequence (5'-3')	Area amplified	HXB2 position (5'-3')
psPAX2 Forward primer	psPAX2F	CTCTCACCAGTCGCCGCC	Vector	5738 – 5759
psPAX2 Reverse primer	psPAX2R	AACACATGGAATTCTGCAACA ACTG	Vector	733-750
pNL4-3 FWD primer	pNL4-3.Luc.R-.E-Fwd	CACACCGTTCATCTGTCCTAC TCCTAATT	Vector	7702-7730
pNL4-3 REV primer	pNL4-3.Luc.R-.E-Rev	TTAATACCGACGCTCTCGCAC CCAT	Vector	790-814
pMJ4fwd primer	pMJ4Fwd	*GGCGACTGGTGAGAGATGGG TGCGAGAGCGTCA	Gag-pol	774-807
pMJ4rev primer	pMJ4Rev	**AGAATTCCATGTGTTRATCY TCATCCTGTCTACCTGCCA	Gag-pol	5071-5109

*Regions that overlap with 5' *gag* . **Regions that overlap with 3' *pol*. Fwd: forward; Rev: reverse.

2.4.1.3. Gel extraction-based purification of PCR products

To prevent the cloning of non-specific insert amplicons into the backbone vectors, agarose gel extraction was performed on the insert fragment (4,314 bp) and the vector backbone for psPAX2 (6,363 bp) and pNL4-3.Luc.R-E- (12,082 bp) using the QIAEX II® Gel Extraction Kit (Qiagen, Maryland, USA).

The specific bands were excised from the agarose gel using a scalpel and placed in respective pre-weighed 2 ml microcentrifuge tubes. The microcentrifuge tubes containing the gel slices were weighed and frozen at -70°C for 30 minutes. Buffer QX1 (300 µl per 100 mg of gel) was added and the gel slices were melted for 10 minutes at 50ºC in a water bath (GLS Aqua 12 Plus, Keison Products, Essex, United Kingdom). When melted, QIAEX II beads were added according to manufacturer's instructions (10 µl for ≤ 2 µg DNA, 30 µl for 2-10 µg DNA). The mixture was placed in a Hula Mixer® Sample Mixer (Life Technologies, Carlsbad, USA) at room temperature for 10 minutes, shaking at 30 rpm for 10 seconds, reciprocated at 15º for 10 seconds and vibrated at 5º for 5 seconds. The samples were centrifuged in the Eppendorf Centrifuge 5415R (Merck

Millipore, Darmstadt, Germany) for 1 minute at 13,000 rpm. The supernatant was discarded, and the pellet resuspended in 500 µl of QX1 buffer. The mixture was centrifuged for 1 minute at 13,000 rpm and the supernatant was discarded. The DNA pellet was washed with 500 µl buffer PE and resuspended twice and air dried for 15-20 minutes. Resuspension of the pellet in 40 µl of warm elution buffer was performed. The microcentrifuge tube was centrifuged for 1 minute at 13,000 rpm followed by the supernatant being transferred to a clean 1.5 ml microcentrifuge tube to collect the DNA. The eluted DNA was quantified with the NanoDrop 1,000 Spectrophotometer system (Thermo Fisher Scientific Waltham, MA, USA), blanked against elution buffer, and stored at -20°C until required.

2.4.1.4. Gibson Assembly reaction

With the use of the In-fusion® HD Cloning Kit (Takara Bio, Mountain View, CA, USA), the linearized and purified vector backbone (100 ng) and *gag-pol* (132 ng) amplicons were combined at a ratio of 1:1 with 2 µl 5× In-Fusion HD Enzyme Premix and 10 µl dH_2O. The reaction was placed in the BIORAD C1000 Touch™ Thermal Cycler (BioRad, USA) for 15 minutes at 50°C.

Approximately 5 µl of the total 232 ng of the In-fusion® HD Cloning Kit product was added to 100 µl thawed chemically competent Stellar™ E. coli cells (Takara Bio, Mountain View, CA, USA). The mixture was placed on ice for 30 minutes followed by heat shock at 42˚C for 45 seconds. The mixture was immediately placed back on ice for 1-2 minutes. Four hundred microliters of warm Super Optimal broth with Catabolite repression (SOC) (Takara Bio, Mountain View, CA, USA) was added. The transformed bacteria were incubated at 37˚C for an hour with shaking at 200 rpm. The bacterial culture was centrifuged for 5 minutes at 6,000 rpm and 400 µl of supernatant was discarded. The bacterial cells were resuspended in the remaining 100 µl of supernatant and plated on carbenicillin-containing (100 µg/ml) Lysogeny Broth (LB) agar plates. The LB agar plates were incubated at 37˚C overnight. The following day, ±4 colonies were selected and inoculated in 4 ml of LB medium containing 100 µg/ml carbenicillin. The inoculated cultures were incubated at 37˚C overnight with shaking at 200 rpm in a Labcon Shaking incubator (Model FSIM-SPC**,** CC Imelmann (Pty) Ltd, Robertsham, Johannesburg, Gauteng).

With the use of the Gibson Assembly® Master Mix (New BioLabs, Inc., Ipswich, MA, USA), linearized and purified pNL4-3.Luc.R-E- vector (75 ng) and *gag-pol* (150 ng) inserts were combined at a ratio of 1:2, denatured for 5 minutes at 60°C and immediately placed on ice for 2-3 minutes. Ten microFORECASTlitres of Gibson Assembly® Master Mix (2×) was added and the reaction was placed in the C1000 Touch™ Thermal Cycler for 15 minutes at 50°C. A similar

transformation protocol was followed for Gibson Assembly® Master Mix products as described above, however NEB® Stable Competent E. coli (New BioLabs Inc Ipswich, MA, USA) (high efficiency) and stable outgrowth medium (New BioLabs Inc Ipswich, MA, USA, #B9035) were used.

2.4.1.5. Validation of recombinant clones

Overnight cultures from presumptive positive colonies were centrifuged at 13,000 rpm for 3 minutes at 25˚C in a Centrifuge 5424 R (Eppendorf Merck, Kenilworth, USA). Plasmid DNA was extracted with the QIAprep Spin Miniprep Kit (Qiagen, Maryland, USA) following the manufacturer's instructions. Briefly, the bacterial pellet was resuspended in 250 µl resuspension buffer, followed by the addition of 250 µl lysis buffer. The solution was inverted several times and incubated for 5 minutes at room temperature. The lysis reaction was neutralised with 350 µl N3 Buffer, followed by thorough inversion and incubation for 5 minutes on ice. The mixture was centrifuged at 13,000 rpm for 10 minutes at 25˚C in the Centrifuge 5424 R (Eppendorf, Merck, Kenilworth, USA). The supernatant was transferred to a QIAprep spin column and centrifuged for 1 minute at 13,000 rpm. The flow-through was discarded. Five hundred microlitres of Buffer PB was added to the spin column and centrifuged at 13,000 rpm for 1 minute. After the flow-through was discarded, the spin column was washed with 750 µl of Buffer PE, at 13,000 rpm for 1 minute and the flow-through discarded. The spin column was centrifuged for 1 minute at 13,000 rpm to remove residual wash buffer. The QIAprep column was placed in a clean 1.5 ml microcentrifuge tube and 40 µl of elution buffer was added before incubation for 1 minute. The column was centrifuged at 13,000 rpm for a minute at 25˚C. Quantification of the eluate containing the extracted plasmid DNA was performed as previously described in section 2.2.2.4.

2.4.1.5.1. Restriction enzyme digest analysis of recombinant clones

The purified recombinant plasmids were screened for identity and size. Single restriction enzyme digests of the extracted, purified and quantified plasmid DNA were performed with *Nhe*I and *Pvu*I (10 U/µl; Thermo Fischer Scientific Waltham, MA, USA) for the psPAX2 recombinant plasmids. Five hundred nanograms of plasmid DNA was added to 5 units of *Nhe*I or *Pvu*I in buffer Tango (for *Nhe*I) and buffer R (for *Pvu*I). The reactions were mixed gently, centrifuged and incubated in the thermal cycler at 37°C for 1 hour. A similar restriction enzyme digestion protocol was repeated for clones selected with the pNL4-3.Luc.R-E- backbone, however, the enzyme used was *Bam*HI (10 U/µl, with Buffer Unique Buffer (10 × Buffer BamHI); Thermo Fischer Scientific Waltham, MA, USA). Restriction enzyme digests were visualized on a 1% agarose gel, and sized relative to

the Quick-Load® 1kb Extended DNA Ladder (New England Biolab, Ipswich, MA) molecular weight marker.

2.4.1.5.2. Nucleotide sequence analysis

Sanger sequencing was performed to confirm the identity of the *gag-pol* insert, as well as uninterrupted open reading frames. Sanger sequencing was performed using the primers in Table 2.5, as described in Section 2.2.3.

Table 2.5: Description of sequencing primers used for validation of recombinant clones.

Description	Name	Sequence (5' – 3')	HXB2 position	HXB2 gene related position
RT Primer	BF	AAA CAA TGG CCA TTG ACA GA	2613 - 2632	Pol 529 - 548 RT 64 - 83
RT primer	BRRTR	GGT GAT CCT TTC CAT CC	3003-3019	Pol 919 - 935 RT 454 - 470
PR primer	ProtF	CTT CAG AAC AGA CCA GAG C	2134-2152	Gag 1345 - 1363 Pol 50 - 68
PR primer	ProtR	CTC TTC TGT TAA CGG CCA TTG	2616-2636	Pol 532 - 552 RT 67 - 87

Primers were manufactured by Integrated DNA Technologies (Coralville, Iowa, USA).

2.4.1.5.3. Characterization of the ability of the patient derived recombinant plasmids to generate functional pseudoviruses

The ability of the recombinant plasmids to generate functional pseudoviruses following transfections of HEK293T cells was evaluated as described previously in section 2.3.3., with the following exceptions: HEK293T cells were seeded at 4×10^6 cells in 4 ml of complete DMEM in a 4.4 cm^2 Nunclon Delta Surface transfection dishes (Thermo Fisher Scientific Waltham, MA, USA); for the psPAX2-based clone transfections, recombinant plasmid DNA (400 ng), pHEF-

VSVG (400 ng), and pCSFLW (600 ng) in 100 µl OptiMEM (Gibco® Life Technologies, Carlsbad, CA, USA), 4.2 µl of 1 mg/ml PEI^{max} (Polysciences Inc, Warrington, PA, USA) was added to the meniscus of the transfection mixture; for the pNL4-3.Luc.R-E- based clone transfections, recombinant plasmid DNA (400 ng) and pHEF-VSVG (400 ng) in 100 µl OptiMEM (Gibco® Life Technologies, Carlsbad, CA, USA), 4.2 µl of 1 mg/ml PEI^{max} (Polysciences Inc, Warrington, PA, USA) was added to the meniscus of the transfection mixture.

The transfection reactions were incubated for 15 minutes in the BioFlow-II (Labotec, Midrand, South Africa), allowing the polymer to form micelles that coat the plasmid DNA for cell uptake. The transfection mix was added dropwise to the cells in the transfection dish, which was then incubated for 48 hours. Supernatants were harvested as described previously (section 2.3.3), with an additional spinning step at 2,500 rpm for 10 minutes after the removal of the supernatant from the transfection dish. The pseudoviruses were used immediately or stored at -80°C when required.

The pseudovirus (PSV) titration was performed as previously described in section 2.3.3. The difference included the addition of 50 µl thawed PSV, 50 µl of media and 50 µl of 4×10^{5} cells/ml and incubated for 48 hours thereafter, the expression of luciferase reporter gene in the cells were assessed as previously described (section 2.3.3).

2.4.2. Construction through traditional restriction enzyme/ligation

Since the objective was to create HIV-1 subtype C specific reagents that can be used in *in vitro* phenotypic inhibition assays, the selection of restriction enzyme sites not likely to be present in the regions of circulating HIV-1 subtype C was important. Restriction sites were selected in order to utilise them during cloning using the traditional method. This would require techniques that can detect circulating subtype C's and detecting whether these have the selected restriction sites. If the sites were present the cloning would be deemed unsuccessful since the genome would be restricted incorrectly therefore leading to inefficient ligation or no ligation. HIV-1 subtype C *gag-pol* reference sequences (n=2,000) were downloaded from the Los Alamos National Laboratory website (https://www.hiv.lanl.gov/content/sequence/HIV/mainpage.html), and all naturally occurring restriction enzyme sites were identified using Geneious version 10.1.3 (Auckland New Zealand). The sequences were then analysed on Silent Mutator, an *in-silico* mutagenesis online tool incorporated in molbiotools (info@molbiotools.com). Silent Mutator assists with the introduction of new restriction sites without changing the encoded amino acid sequence. Subsequently, primers were designed to introduce two novel restriction sites (*Nru*I and *Sac*II),

neither of which were observed in HIV-1 subtype C *gag-pol*, pMJ4 or the pNL4-3.Luc.R-.E- backbone (Table 2.6).

The traditional cloning strategy made use of the identified *Nru*I and *Sac*II endonucleases in conjunction with the Quick Ligation Kit (New BioLabs Inc Ipswich, MA, USA) for ligation of the *gag-pol inserts* into pNL4-3 Luc.R-E-.

Table 2.6: Primers used to introduce the restriction enzyme sites *Nru*I and *Sac*II into the *gag-pol* or pMJ4 insert, and the pNL4-3.Luc.R-E- vector backbone.

Description	Name of primer	Sequence (5'-3')	HXB2 position (5'-3')
Vector NruI Forward primer	pNL4-3_Fwd_NruI	GTG TCG CGA GTA GAC AGG ATG AGG ATT AAC	5071-5097
Vector SacII Reverse primer	pNL4-3_Rev_SacII	TCC CCC GCG GAG TAC CGA CGC TCT CGC	796-819
Forward SacII adaptor primer	Gp_2nd_Fwd_SacII	AAT ACT CCG CGG GGR AAA ATT AGA TAM ATG GGA AAR	810-842
Reverse NruI adaptor primer	Gp_2nd_Rev_NruI	GTC TAC TCG CGA CAC AAT CAG CAC CTG CC	5054-5079

Primers were manufactured by Integrated DNA Technologies (Coralville, Iowa, USA). The underlined nucleotides indicate the position of the restriction site. Gp: *gag-pol* ; Fwd: forward; Rev: reverse.

2.4.2.1. Preparation of the vector backbone

The PCR reaction to amplify the approximately 12 kb pNL4-3.Luc.R-E- vector backbone was optimised using CloneAmp™ HiFi PCR Premix (Takara Bio, Mountain View, CA, USA) at gradient temperatures and Expand™ Long Template PCR System using all three buffers within the kit.

Overall, pNL4-3.Luc.R-E- was successfully amplified using the CloneAmp™ HiFi PCR Premix (Takara Bio, Mountain View, CA, USA). A PCR reaction mix was prepared by combining 6.25 µl DEPC-treated dH2O (Ambion™, Thermo Fisher, Waltham, MA, USA), 12.5 µl CloneAmp™ HiFi PCR Premix (Takara Bio, Mountain View, CA, USA) (1×) and 0.625 µl of each primer, pNL4-3_Rev_SacII and pNL4-3_Fwd_NruI (10 µM) (Table 2.7). For each reaction, 20 µl of master mix was combined with 5 µl (10 ng) of pNL4-3.Luc.R-E- plasmid DNA.

Reactions were performed under the following conditions on the BIORAD C1000 Touch™ Thermal Cycler: initial denaturation at 95°C for 3 minutes; 30 cycles of denaturation at 98°C for

10 seconds, annealing at 68°C (pNL4-3.Luc.R-E-) for 1 minute and 30 seconds, extension at 72°C for 13 minutes.. The reaction was concluded with a final extension at 72°C for 7 minutes, and a holding temperature of 4°C. Amplicons were assessed by agarose gel electrophoresis and PCR products were purified as previously described (section 2.2.2.4.).

2.4.2.2. Preparation of pMJ4 and patient derived *gag-pol* inserts

The nested *gag-pol* products were subjected to an additional *gag-pol* PCR to introduce restriction sites at the 5' and 3' ends of amplicons using the Expand High Fidelity PCR System (Roche, Basel, Switzerland). A PCR reaction mix was prepared by combining 17.25 µl DEPC-treated dH_2O (Ambion™, Thermo Fisher, Waltham, MA, USA), 2.5 µl Expand High Fidelity Buffer (1 X), 0.75 µl Expand High Fidelity Enzyme mix (3.5 U/ µl) and 0.5 µl dNTP mix (10 mM; KAPA Biosystems, Roche, Basel, Switzerland), 2.5 µl of the *gag-pol* amplicon and 0.75 µl of each primer Gp_2nd_Fwd_SacII and Gp_2nd_Rev_NruI at 10 µM (Table 2.6) in a 200 µl PCR tube.

The reactions were performed under the following conditions on the BIORAD C1000 Touch™ Thermal Cycler (BioRad, California USA): initial denaturation at 94°C for 2 minutes; denaturation at 94°C for 15 seconds; 30 cycles of denaturation at 94°C for 15 seconds, annealing at 60°C for 1 minute and 30 seconds, extension at 68°C for 5 minutes and a final extension at 68°C for 7 minutes. The reaction was concluded with a holding temperature of 4°C. The amplification product was analysed as previously described (Section 2.2.2.3. and 2.2.2.4.).

2.4.2.3. Restriction enzyme/ligation reactions

The amplified pNL4-3.Luc.R-E- vector was treated with the *Dpn*I restriction enzyme (New BioLabs, Ipswich, Massachusetts, USA) in order to remove original intact plasmid template DNA that may have remained in the reaction. The reaction was prepared by combining 2 µl of CutSmart® Buffer (New BioLabs, Ipswich, Massachusetts, USA), 2 µl of *Dpn*I restriction enzyme, 1 µl of dH_2O added and 20 µl (2 µg) of purified vector backbone DNA. The reaction was incubated at 37°C on the C1000™ Thermal cycler for 60 minutes and heat-inactivated at 80°C for 20 minutes. Purification was performed as described in Section 2.2.2.4.

The *Dpn*I treated and purified pNL4-3.Luc.R-E- vector backbone and *gag-pol* amplicons were double-digested with *Nru*I and *Sac*II (10,000 units/ml). The reaction contained 2 µl of each restriction enzyme, 2 µg of DNA (vector backbone or *gag-pol*), 4 µl of CutSmart® Buffer (New BioLabs, Ipswich, Massachusetts, USA) and dH_2O to a total volume of 40 µl. The reaction was incubated at 37°C for 2 hours and the *Sac*II was then heat-inactivated at 65°C for 20 minutes.

To prevent self-ligation, the pNL4-3.Luc.R-E- vector was dephosphorylated using the NEB Antarctic Phosphatase kit (New BioLabs, Ipswich, Massachusetts, USA). The *Nru*I/*Sac*II-double-digested pNL4-3.Luc.R-E- vector (2 µg) was combined with 4 µl of Antarctic Phosphatase Reaction Buffer (10×), 5 units of Antarctic Phosphatase enzyme and dH_2O to 50 µl. The reaction was mixed and incubated at 37°C for 60 minutes and heat-inactivated at 80°C for 20 minutes. Purification and quantification of the reaction was performed as described in Section 2.2.2.4.

The Quick Ligation Kit (New BioLabs, Ipswich, Massachusetts, USA) components were combined as follows in a 200 µl microcentrifuge tube: 1 µl Quick Ligase, 10 µl Quick Ligase Reaction Buffer (2×), pNL4-3.Luc.R-E- vector DNA (50 ng with a copy number of 3.77×10^{9} number of copies), *gag-pol* insert DNA (37.5 ng 7.72×10^{9} number of copies) and nuclease free dH_2O to 20 µl. The reaction was mixed gently and incubated at room temperature (25°C) for 5 minutes. The cloning reaction was analysed on a 1% agarose gel. Bacterial transformation, plasmid DNA extraction and validation of clones were performed as previously described in Section 2.4.1.5**.**

Chapter 3: Results

3.1. Genotypic resistance testing of HIV-1 positive patient samples

3.1.1. Demographic and clinical profiles of South African patients failing third-line ARV treatment

A summary of the demographic data and clinical characteristics of the six HIV-1 positive South African patients failing third-line antiretroviral treatment, whose plasma samples were used in this study are presented in Table 3.1. All patients had detectable viral loads, correlating to virological failure. All six patients (n=6/6, 100%) had been administered DRV/r as a PI and 3 patients (n=3/6, 50%) were on an INSTI. Hence, it can be distinguished that patients exposed to INSTI were on an integrase based third-line regimen and patients only on a PI based regimen were on a PI based third-line regimen.

Table 3.1: Demographic data and clinical characteristics of the six HIV-1 positive South African patients failing third-line antiretroviral treatment (ART) whose samples were used in this study. The information was provided by the National Health Laboratory Services (NHLS).

Patient number	Age (years)	Province	*HIV VL (RNA copies/ml)	ART Regimen type	Current ART regimen**	Previous ART**
1	53	Eastern Cape	2,628	Protease Inhibitor	AZT, 3TC, DRV/r	AZT-3TC-SQV/r-LPV/r
2	51	Kwa Zulu-Natal	27,500	Integrase Inhibitor	3TC, DRV/r, RAL	AZT, 3TC, TDF, EFV, LPV/r
3	45	Gauteng	29,400	Integrase Inhibitor	TDF, 3TC, DRV/r, DTG	TDF, 3TC, AZT, DDI, d4T, 3TC, NVP, LPV/r, DRV/r
4	7	Gauteng	2,190	Protease Inhibitor	d4T, 3TC, DRV/r	ABC,3TC, LPV/r
5	45	Gauteng	13,000	Integrase Inhibitor	TDF, FTC, DRV/r, RAL	d4T, 3TC, TDF, AZT, EFV, ETR, LPV/r, ATV/r, RAL
6	53	Gauteng	143,000	Protease Inhibitor	TDF-FTC-DRV/r	N/A

*HIV VL: HIV Viral Load; **For a description of all the antiretroviral drug abbreviations, refer to Table 1.1 in Chapter 1: Introduction.

3.1.2. RT-PCR and nested PCR of HIV-1 *gag-pol*

The first round RT-PCR and nested PCR primers were designed to bind to the 5' *gag* site and the 3' *vif* start site (integrase end), and optimised amplification protocols were successfully established

(Figure 3.1). The one step RT-PCR reaction resulted in several nonspecific products (Figure 3.1A), which was expected since the first round is completed at a low annealing temperature, but amplicons at the expected size (4,3 kb) were not visible. Nested PCR amplification products following optimization of the annealing temperatures, either through the use of a single annealing temperature (66°C; Figure 3.1B) and a touchdown protocol with several, decreasing annealing temperatures (68°C, 66°C, 64°C and 62°C; Figure 3.1C), were visible at approximately 4,3 kb for all 6 patient samples. The nested PCR amplicons were purified, quantified (Table 3.2) and used for population-based sequencing.

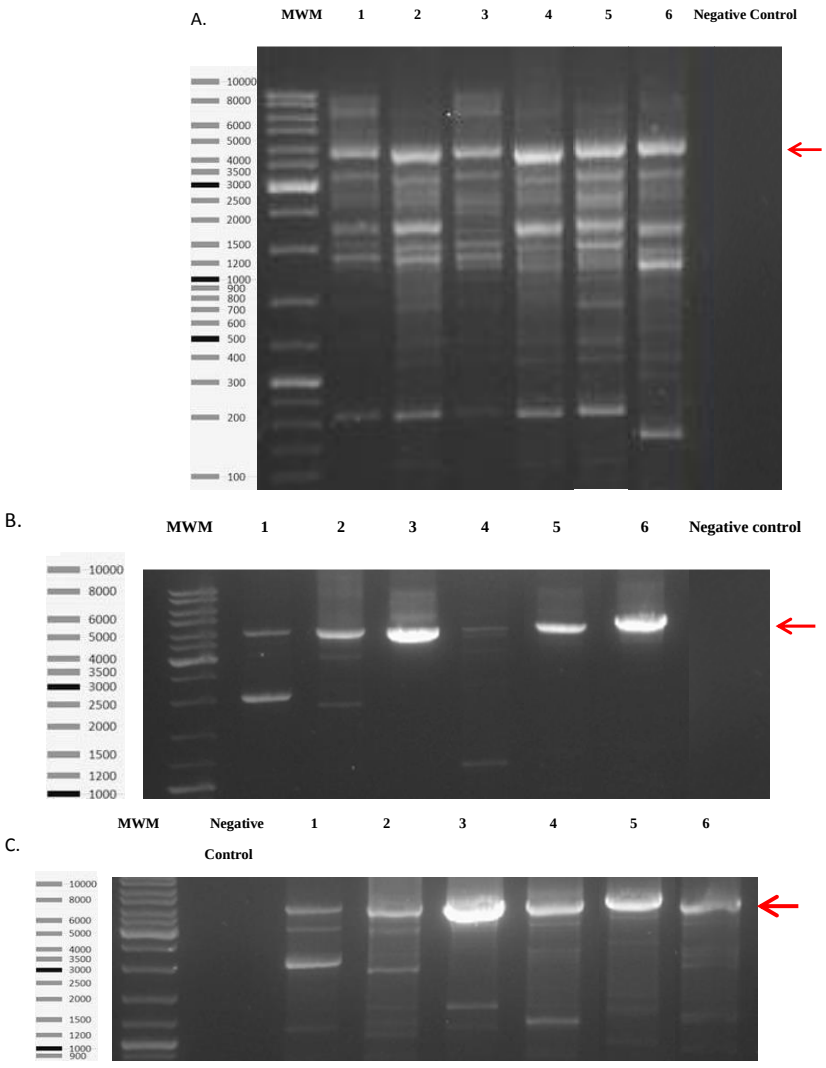

Figure 3.1: Agarose gel electrophoresis of one step RT-PCR (A) and nested (B and C) *gag-pol* products from the six HIV-1 positive patient plasma samples. The nested PCR products were analysed after using a single annealing temperature (B) or using touchdown temperatures (C). Lanes 1 to 6 represent the different patient samples. The negative control lane confirmed there was no cross contamination. The O' Gene Ruler DNA ladder (Thermo Fisher Scientific, Waltham, MA, USA) molecular weight marker (in base pairs; MWM) is indicated on the left. The red arrow on the right points to the expected fragment size.

Table 3.2: Concentration of the nested PCR *gag-pol* amplicons from the six HIV-1 positive patient plasma samples, subsequently used for Sanger sequencing.

Sample number	Nested PCR product concentration (ng/µl)
1	62
2	107
3	118
4	72
5	110
6	116

3.1.3. Population-based Sanger sequence analysis

Aligned nucleotide sequences obtained from Sanger sequencing were used to construct a neighbour joining phylogenetic tree (Figure 3.2, and Appendix C1), and confirmed that the six patient samples used in this study clustered with the HIV-1 group M subtype C reference sequences, and were unique, that is, there was no cross contamination. Thus, the six South African patients were infected with HIV-1 subtype C.

3.1.4. Genotypic drug resistance interpretation

The *gag-pol* nucleotide sequences were submitted to the Stanford HIV Drug Resistance database version 8.9-1 (http://hivbd.standford.edu) [263] and the ARV drug resistance mutation profiles were identified (Table 3.3). The clinical significance, as determined by the calculated resistance scores and predicted phenotypic responses is shown in Table 3.4. The major, minor or accessory mutations were classified according to the 2019 Updated IAS-USA Drug resistance mutations list [264].

Overall, all six patients harboured virus with known drug resistance mutations to the various ARV drug classes, in line with their current drug regimen (Table 3.3). The mutation profiles were different for each patient sample, and all had major NRTI mutations. While all were on a third line regimen that contained a PI, only patients 1, 3 and 4 harboured viruses with major mutations against PI's. HIV-1 from one of the three patients on an INSTI based regimen, patient 5, had the N155H major resistance mutation. Patient 4 was not on an INSTI based regimen, yet sequence analysis detected the presence of the N155H and T97A major and accessory mutations, respectively, hence potential transmission of drug resistant virus containing INSTI mutations [266]. The combination of mutations seen in the *protease, reverse transcriptase* and/or *integrase* accounts for varying levels of phenotypic resistance to at least two of the four ARV drug classes

(Table 3.4), which correlate with virological failure. Interestingly, HIV-1 from patient 5 remained susceptible to PIs, and patients 1, 3 and 6 to NNRTIs and INSTIs.

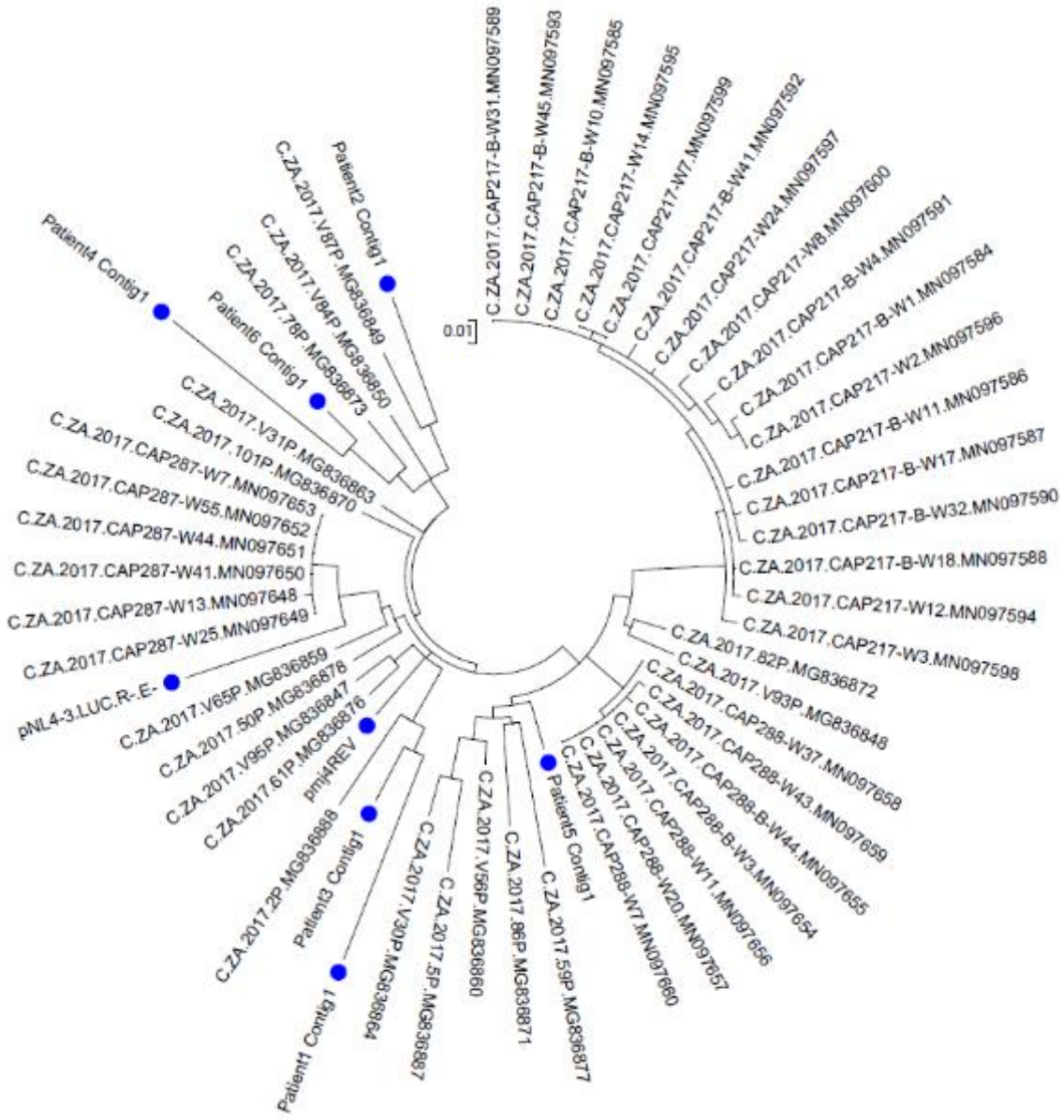

Figure 3.2: A neighbour-joining phylogenetic tree illustrating the association between the six HIV-1 positive patient derived *gag-pol* sequences and HIV-1 subtype C reference sequences. The phylogenetic tree analysis based on the neighbour joining method was performed on aligned *protease* nucleotide sequences from the six patients and Subtype C reference sequences from 2017, obtained from the Los Alamos National Laboratory and third line failure patient sequences [267], and evolutionary distances conducted with MEGA7 were computed using the Maximum Composite Likelihood method [268, 269].

Table 3.3: Major and minor/accessory mutations associated with resistance to antiretroviral drugs for each viral enzyme from the six HIV-1 positive South African patient samples. The bolded mutations were selected by the patient's current third-line antiretroviral drug therapy regimen.

Patient sample number	*Previous ART exposure	*Current ART regimen	PR mutations		NRTI mutations		NNRTI mutations	IN mutations	
			Major	Accessory	Major	Minor		Major	Accessory
1	AZT-3TC-SQV/r-LPV/r	AZT, 3TC, DRV/r	**I47V, I50V, 154L,** Q58E, V82A	L10R, K20R, **L33F,** M36I, M46I, D60E, L63P, H69K, A71V, **L89V,** I93L	**M184V**	A62V	None	None	None
2	AZT, 3TC, TDF, EFV, LPV/r	3TC, DRV/r, RAL	I54V, V82A	L10F, M36I, M46I, L63P, H69K, G73A/S, I93L	**M184V**	None	L100I, K103N**,** Y188F P225H	None	E157Q
3	TDF, 3TC, AZT, DDI, d4T, 3TC, NVP, LPV/r, DRV/r	TDF, 3TC, DRV/r, DTG	**I54L, I84V**	K20T, M36I, H69K, A71V, **T74P,** L89M, I93L	**K65R, M184V**	None	None	None	None
4	ABC,3TC, LPV/r	d4T, 3TC, DRV/r	**I50V,** I54V	K20R, L33I, M36I, M46L, I62V, L63P, A71V, G73S, **T74P,** V82I, **L89V**, L90M, I93L	**M41L, D67N, K70R, F77L, M184V, T215Y, K219Q**	None	A98G, K103N, Y181C	N155H	T97A
5	d4T, 3TC, TDF, AZT, EFV, ETR, LPV/r, ATV/r, RAL	TDF, FTC, DRV/r, RAL	None	L10I, M36I, I93L	**M41L, D67N, V75I, M 184V, L 210W, T215Y**	None	L100I, K103N	**N155H**	None
6	N/A	TDF, FTC, DRV/r	I54V, V82A	K43T, M46I, F53L, I 62V, L63P, H69K, A71V, **T74P,** L90M, I93L	**K65R, D67N, M184V**	None	None	None	None

ART: antiretroviral therapy; PR: protease; NRTI: nucleotide reverse transcriptase inhibitor; NNRTI: non-nucleoside reverse transcriptase inhibitor; INSTI: integrase strand transfer inhibitor; A: alanine; R: arginine; N: asparagine; D: aspartic acid; C: cysteine; Q: glutamine; E: Glutamic acid; G: glycine; H: histidine; I :isoleucine; L: leucine; K: lysine; M: methionine; F: Phenylalanine; S: serine; T: threonine; W: tryptophan; Y: tyrosine; V: valine; N/A: not available.* For a description of all the antiretroviral drug abbreviations, refer to Table 1.1 in Chapter 1: Introduction.

Table 3.4: Phenotypic resistance and resistance scores for HIV-1 virus from the six South African patient samples obtained from the Stanford University HIV-1 Drug Resistance Database version 8.9-1.

Patient	PI'S				NRTI'S							NNRTI's			INSTI's	
	ATV	DRV	SQV	LPV	ABC	ddI	FTC	D4t	3TC	TDF	AZT	EFV	ETR	NVP	RAL	DTG
1	80	70	80	140	20	15	65	-5	65	-5	-5	0	0	0	0	0
2	70	5	75	85	15	10	60	-10	60	-10	-10	225	30	225	10	0
3	90	45	90	60	60	70	90	50	90	50	-25	0	0	0	0	0
4	100	30	135	85	110	145	85	170	85	60	155	110	45	155	70	10
5	0	0	0	0	90	120	85	125	85	60	115	120	30	120	60	10
6	145	5	165	105	65	75	90	65	90	55	-10	0	0	0	0	0

-25 to 9	Susceptible
10 to 14	Potential low-level resistance
15 to 29	Low-level resistance
30 to 59	Intermediate resistance
>= 60	High-level resistance

A detailed analysis of the prevalence of the major mutations against the third line PI DRV/r, showed they were present in 50% (n=3/6) of patient samples, and 67% (n= 4/6) contained accessory mutations against DRV/r (Figure 3.3). The major PI mutations that could have emerged from prior exposure to PI drugs (LPV/r, ATV/r and SQV/r) were prevalent at 67% (n=4/6). TAMs type 1 or type 2 were observed in two patients (n=2/6, 33%), and M184V was present in 100% of patient samples.

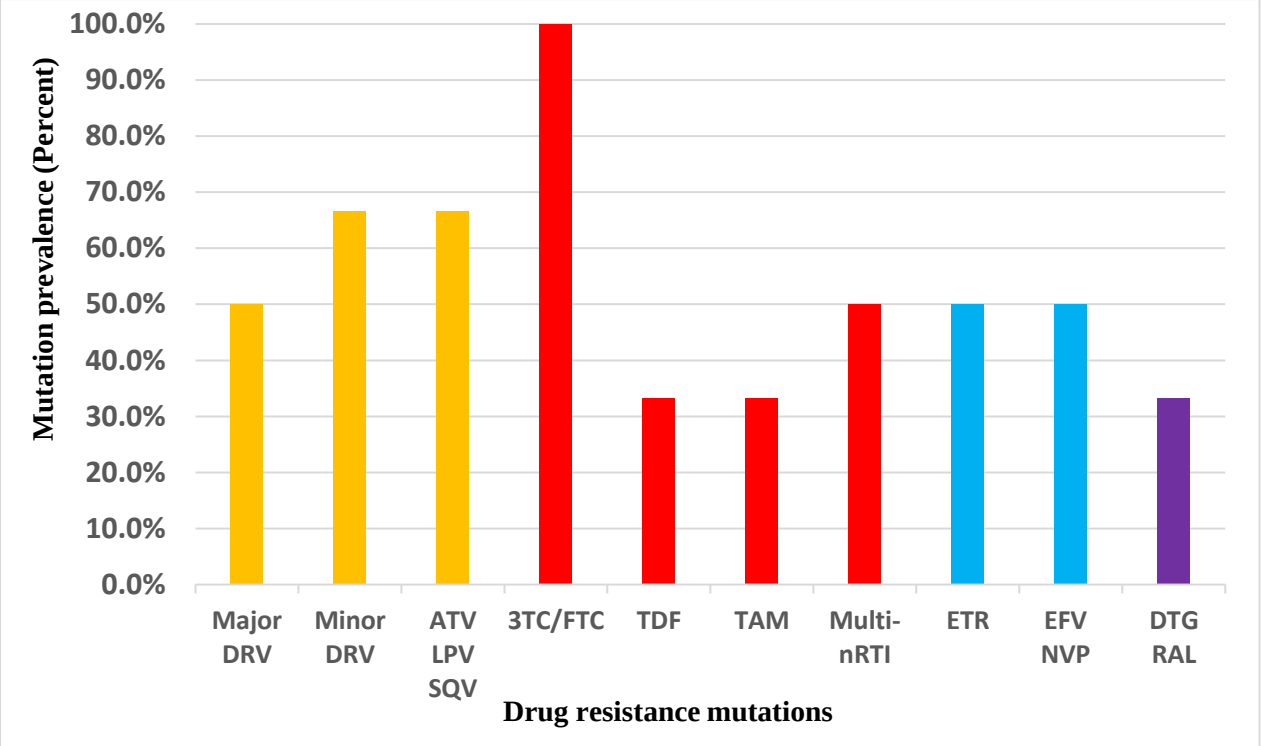

Figure 3.3: Prevalence of antiretroviral (ARV) drug mutations present in patient samples that cause failure to therapy. The prevalence (%) of major, minor/accessory drug resistance mutations against FDA approved inhibitors available for treatment from the different drug classes is shown. The yellow bars show the prevalence of protease inhibitor mutations contributing to resistance, the red bars show the prevalence of NRTI mutations contributing to resistance, the blue bars indicate the prevalence of NNRTI mutations, and the purple bar indicates the INSTI mutations contributing to resistance. The ARV drug abbreviations are defined in Table 1.1 in Chapter 1: Introduction.

The *gag* cleavage sites and PTAP insertions were manually analysed by alignment and comparison to the HXB2 and HIV-1 consensus C reference sequences. The amino acids within 5 positions in the Gag cleavage sites, namely MA/CA, CA/P2, P2/NC, NC/P1, P1/P6 (Table 3.7), as well as PTAP insertions (Figure 3.4) were analysed.

The MA/CA (128-VSQNY/PIVQN-137) and CA/P2 (359-KARVL/AEAMS-368) cleavage sites in HXB2 and the HIV-1 consensus C sequence are identical. For the MA/CA, all patients (n=6/6, 100%) showed an amino acid change from the valine (V) at position 128 to an isoleucine (I), when compared to both the consensus C and HXB2 reference amino acid positions (results not shown). The amino acid positions 129 - 137 were conserved. Assessing the cleavage site CA/P2, no changes in amino acids were observed in the patient samples relative to the consensus C and HXB2 reference sequence (results not shown).

Several amino acid changes and deletions were observed within the remaining three Gag cleavage sites, with the P2/NC showing the most sequence diversity (Table 3.7).

Table 3.7: Alignment of the HIV-1 PR55^{gag} polyprotein P2/NC, NC/P1 and P1/P6 cleavage sites from the six HIV-1 positive South African patient samples with HXB2 and HIV-1 consensus C sequences.

Gag Cleavage Site	P2/NC SATIM/MQRGN										NC/P1 ERQAN/FLGKI										P1/P6 RPGNF/LQSRP									
HXB2 amino acid position	373	374	375	376	377	378	379	380	381	382	428	429	430	431	432	433	434	435	436	437	444	445	446	447	448	449	450	451	452	453
HXB2	S	A	T	I	M	M	Q	R	G	N	E	R	Q	A	N	F	L	G	K	I	R	P	G	N	F	L	Q	S	R	P
Consensus C	T	N	-	I	M	M	Q	R	S	N	E	R	Q	A	N	F	L	G	K	I	R	P	G	N	F	L	Q	S	R	P
Patient 1	T	-	N	I	M	M	Q	R	N	N	D	R	Q	A	N	F	L	G	K	I	R	P	G	N	F	L	Q	S	R	L
Patient 2	Q	A	T	V	M	M	Q	R	S	N	G	R	Q	V	N	F	L	G	K	I	R	P	G	N	F	L	Q	S	R	P
Patient 3	A	T	-	I	M	M	Q	K	S	N	E	R	Q	V	N	F	L	G	K	I	R	P	G	N	F	L	O	N	R	L
Patient 4	-	-	N	I	L	M	Q	R	S	N	E	R	Q	V	N	F	L	G	K	V	R	P	G	N	F	L	Q	S	K	I
Patient 5	V	N	-	V	M	M	Q	R	S	K	E	R	Q	A	N	F	L	G	K	I	R	P	G	N	F	L	Q	N	R	P
Patient 6	V	-	N	I	M	M	Q	K	S	N	E	R	Q	V	N	F	L	G	K	I	R	P	G	N	F	L	Q	N	R	V

"-"Indicates deletions within the P2/NC cleavage site

Shaded areas indicate amino acids that differ from the references.

The PTAP motif in the 3' end of p6 Gag is a key player in viral budding [270]. An intact PTAP motif was observed in all six samples, and virus from patients 3 and 6 had an additional full or partial PTAP motif, respectively (Figure 3.4).

Overall, genotypic sequence analysis of the *Gag-pol* confirmed that the HIV-1 sequences from each of the six patients used in this study were unique, and justified continued work, and their use in setting up HIV-1 subtype C specific *in vitro* phenotypic inhibition assays.

3.2. Setting up the *in vitro* phenotypic inhibition assays

The *in vitro* phenotypic inhibition assay was set up using the wild-type HIV-1 subtype B pNL4-3.Luc.R-E- and its performance tested against a panel of ARV drugs to confirm its versatility in assessing drug susceptibility for different antiretroviral drug classes (PI, RTI, and INSTI).

3.2.1. Gag-Pro *in vitro* phenotypic assay

The concentration of DRV required for full (100%) suppression of viral activity was observed at $\geq 1.4 \times 10^{-2}$ µM , while viral activity reached a uniform level at $\leq 6.1 \times 10^{-5}$ µM. The quantity of DRV needed to inhibit 50% of viral activity (IC_{50}) was 1.0×10^{-3} µM, as seen in Figure 3.5.

Patient viral sample 1

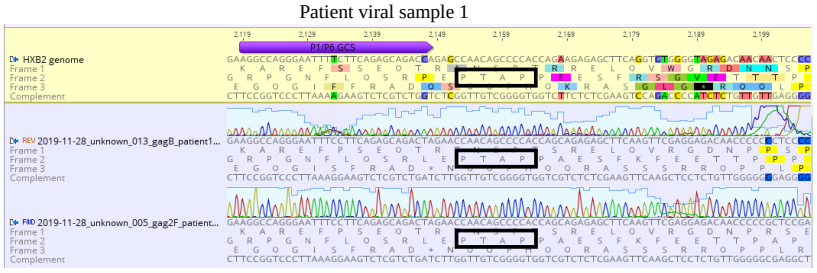

Patient viral sample 2

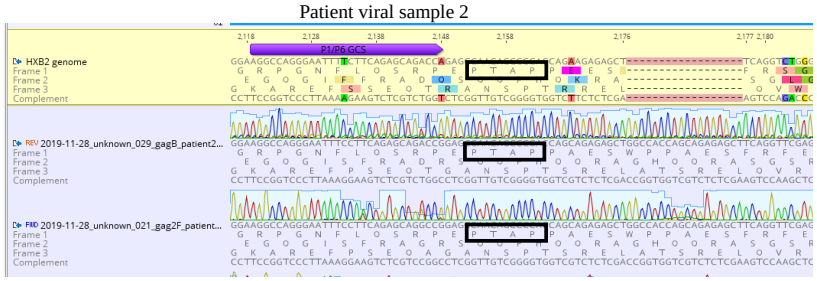

Patient viral sample 3

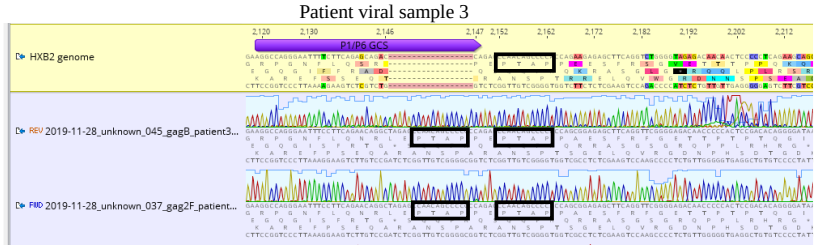

Patient viral sample 4

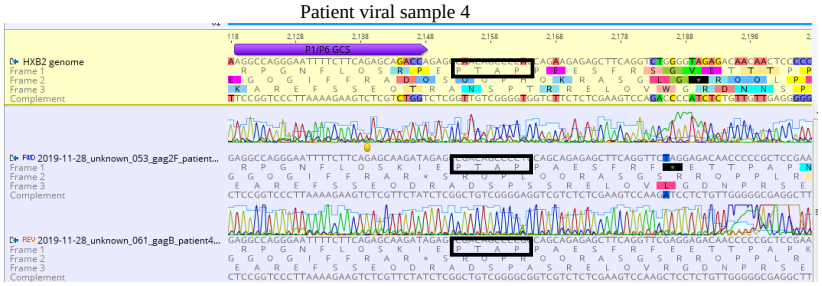

Patient viral sample 5

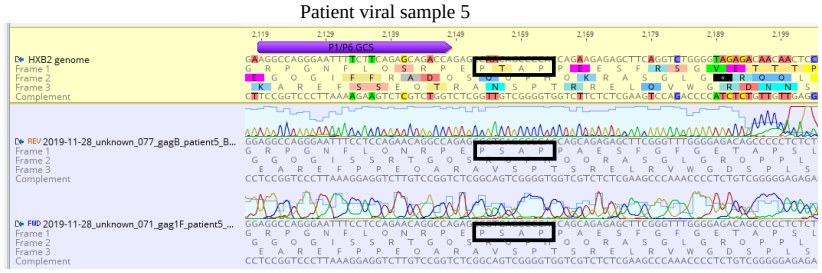

Patient viral sample 6

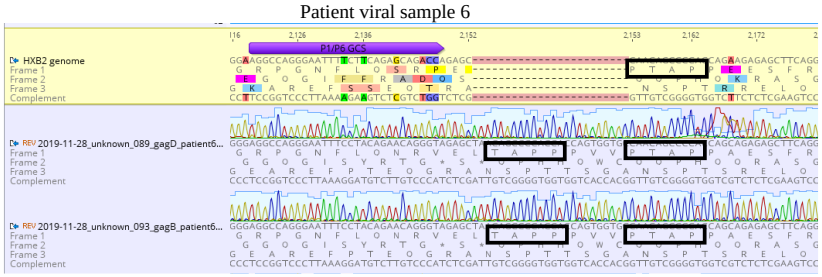

Figure 3.4: Sequencing alignments of the HXB2 p1/p6 region to HIV-1 from patients 1 - 6, with the PTAP regions highlighted in the bold block.

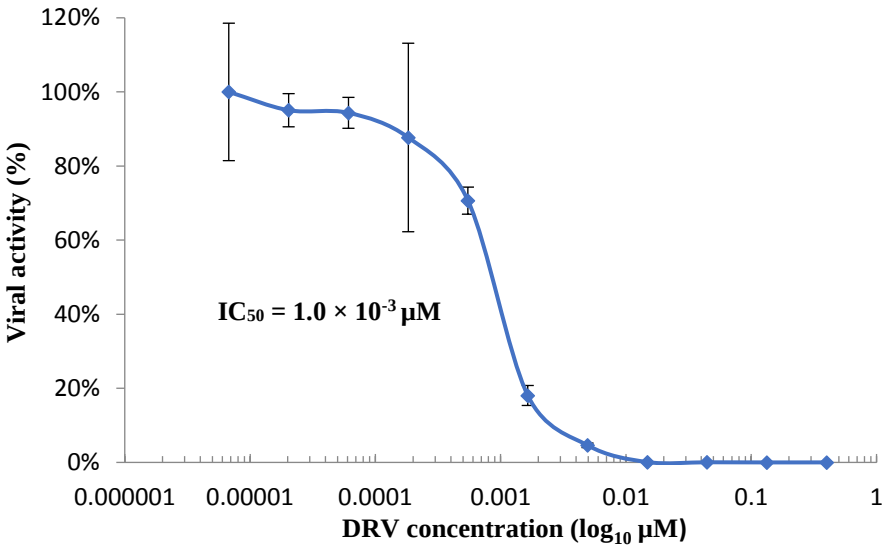

Figure 3.5: Phenotypic inhibition curve of pNL4-3.Luc.R-E- to darunavir (DRV). The inhibition of viral activity of each drug dilution was calculated using the media control as reference. The average percent viral activity was calculated. Error bars represent the standard deviation, which indicate the variability of the data.

3.2.2. RT-IN *in vitro* phenotypic assay

3.2.2.1 Pseudovirus production and titration for RT and IN phenotypic assay

Pseudovirus titration was performed to calculate the amount of pseudovirus needed to produce a standardized bioluminescence of approximately 1 ×as10 ^{6} RLU for the untreated media control. The titration was performed in HEK293T cells averaging 1.5 ×10 ^{5} – 1.6 ×10 ^{7} RLU over a range of dilutions (Figure 3.6) and confirmed that the targeted RLU of 1 ×10 ^{6} RLU would be obtained at a final PSV (pseudovirus) dilution of 40 times.

3.2.2.2. RT and IN Phenotypic assay

The inhibition curves of the dose response to selected NRTIs/NNRTIs and INIs and the corresponding IC_{50} values are shown in Figures 3.7 and 3.8, respectively. The NRTI IC_{50} values ranged between 2.7 ×10 $^{-3}$ µM to 7.9 ×10 $^{-1}$ µM, with TDF showing the greatest potency, at an IC_{50} value of 2.7 ×10 $^{-3}$ µM, followed by AZT (1.1 ×10 $^{-2}$ µM), FTC (1.322 ×10 $^{-1}$ µM), d4T (6.856 ×10 $^{-1}$ µM) and 3TC (7.952 ×10 $^{-1}$ µM). The concentration of ETR needed to inhibit 50% of viral activity (IC_{50}) was 2.1 ×10 $^{-3}$ µM, observed in Figure 3.7E. DTG exhibited the highest potency, 3.0 ×10 $^{-4}$ µM of all the RT/IN drugs tested, followed by RAL at a potency of 3.5 ×10 $^{-3}$ µM (Figure 3.8).

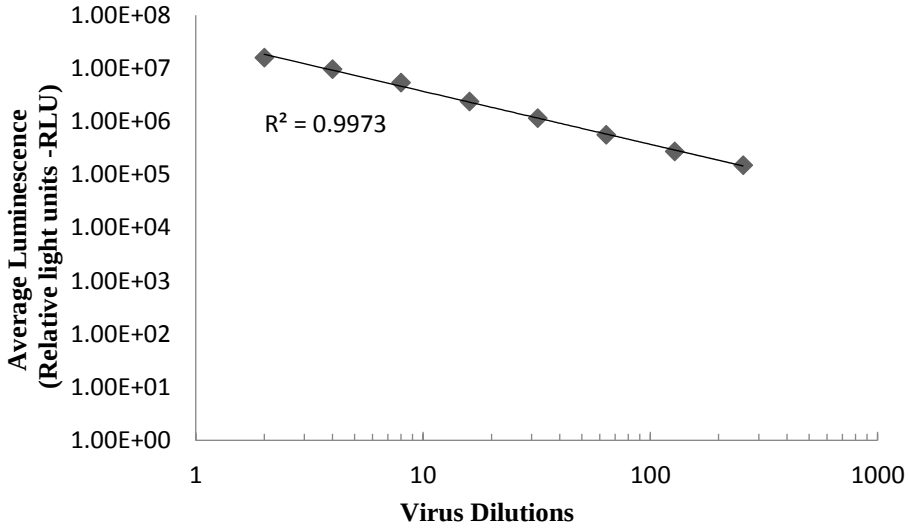

Figure 3.6: Titration of the pNL4-3.Luc.R-E- pseudovirus in HEK293T cells. Two-fold serial dilutions of neat pseudovirus into 50 µl of complete DMEM and cells seeded at 4 ×10 ^{5} cells/ml were prepared in triplicate. Incubation occurred for 48 hours at 37°C where luciferase expression was measured using a bioluminescence GloMax Explorer that expressed mean relative light units (RLU). The average of two replicate curves and standard error bars are shown (r^2= 0.9973).

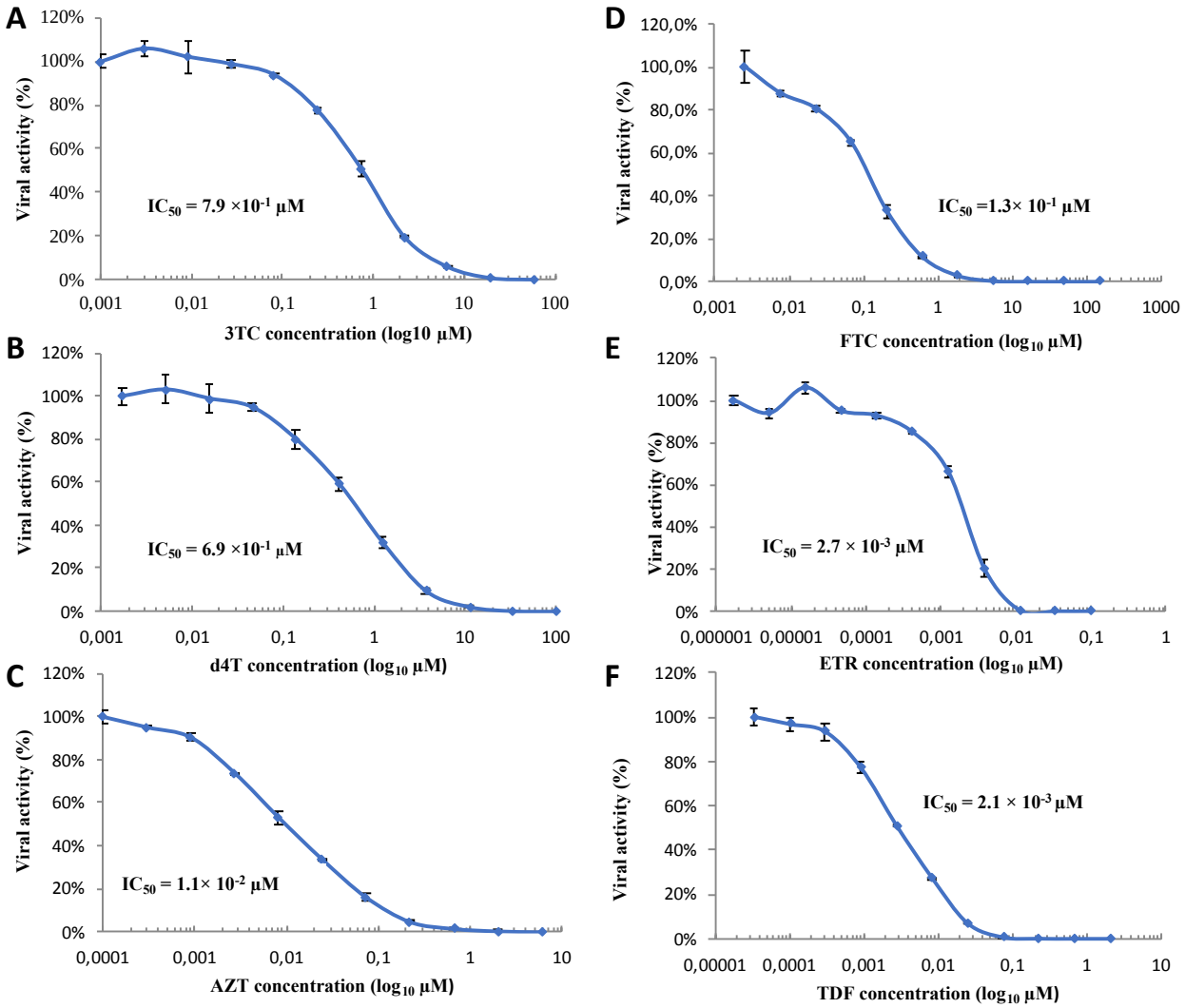

Figure 3.7: Phenotypic inhibition of pNL4-3.Luc.R-E- to (A) lamivudine (3TC), (B) stavudine (d4T), (C) zidovudine (AZT), (D) emtricitabine (FTC), (E) etravirine (ETR), (F) tenofovir disoproxil fumarate (TDF). The percentage viral activity of each ARV dilution was calculated using the media control and the bioluminescence from which the average viral activity percentage was calculated. Error bars were calculated from the standard deviation which indicates the variability of the data.

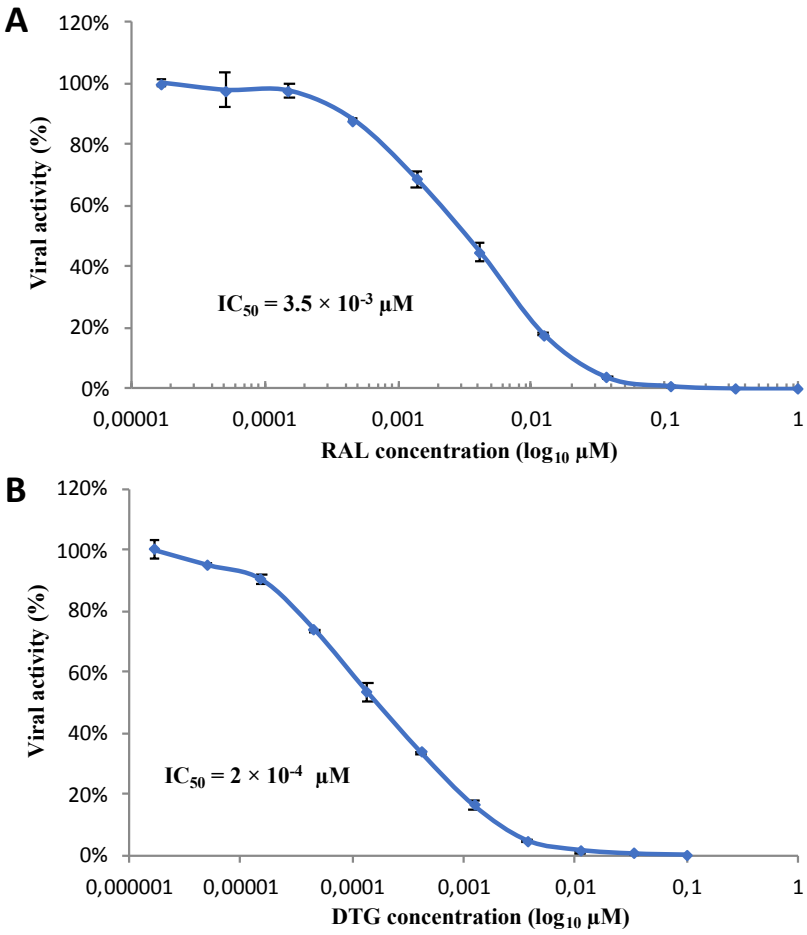

Figure 3.8: Phenotypic inhibition curves of pNL4-3.Luc.R-E- to (A) raltegravir (RAL) and (B) dolutegravir (DTG). The percentage viral activity of each ARV dilution was calculated using the media control and the bioluminescence from which the average viral activity percentage was calculated. Error bars were calculated from the standard deviation which indicates the variability of the data.

Overall, the phenotypic inhibition assays were successfully set up for testing the susceptibility of pNL4-3.Luc.R-E- to RT, PR and IN inhibitors. The next step was to create patient derived *gag-pol* pseudoviruses/expression vectors for substitution of pNL4-3.Luc.R-E- in these assays.

3.3. Constructing patient derived HIV-1 subtype C *gag-pol* expression vectors

Before the preparation of patient-derived HIV-1 subtype C expression vectors, a subtype C wild-type control vector was prepared with the *gag-pol* sequence from pMJ4, using either the psPAX2 or pNL4-3.Luc.R-E- vector backbones for cloning. Two different cloning strategies were followed, namely Gibson assembly (for psPAX2 and pNL4-3.Luc.R-E-) and traditional restriction/ligation (for pNL4-3.Luc.R-E-).

3.3.1. Construction through Gibson assembly

The two vector backbones and pMJ4-derived *gag-pol* were obtained through PCR amplification with primers that contained the corresponding overlaps required for Gibson assembly.

3.3.1.1. Preparation of the psPAX2 vector backbone

The expected product size for the psPAX2 PCR was 6,363 bp. The first optimisation step was the use of different enzyme kits namely CloneAmp™ HiFi PCR Premix (Takara Bio, Mountain View, CA, USA) and Q5® High Fidelity PCR enzyme (New England Biolabs, Ipswich, Massachusetts) at 66°C and gradient annealing temperatures ranging from 54°C-72°C .

Amplification of the vector backbone with CloneAmp™ HiFi PCR Premix at 66°C was successful (Figure 3.9A). The targeted product displayed an intense band at 6,363 bp however, a non-specific product was observed below at position 300 bp. The 6,363 bp product was excised from the gel and purified through agarose gel extraction for use in Gibson assembly. However, amplification of the vector backbone performed with Q5® High Fidelity PCR enzyme at 66°C was unsuccessful (results not shown).

The gradient temperature PCR (Figure 3.9B) performed with the CloneAmp™ HiFi PCR Premix was successful in terms of eliminating nonspecific bands at annealing temperatures greater than 60°C, however, non-specific product was observed at temperatures below 60°C. As the temperature increased the intensity of the targeted 6,363 bp product decreased, since it is expected that at higher temperatures the primers ability to bind decreases. Thus, the optimal annealing temperature chosen to continue with was 65°C.

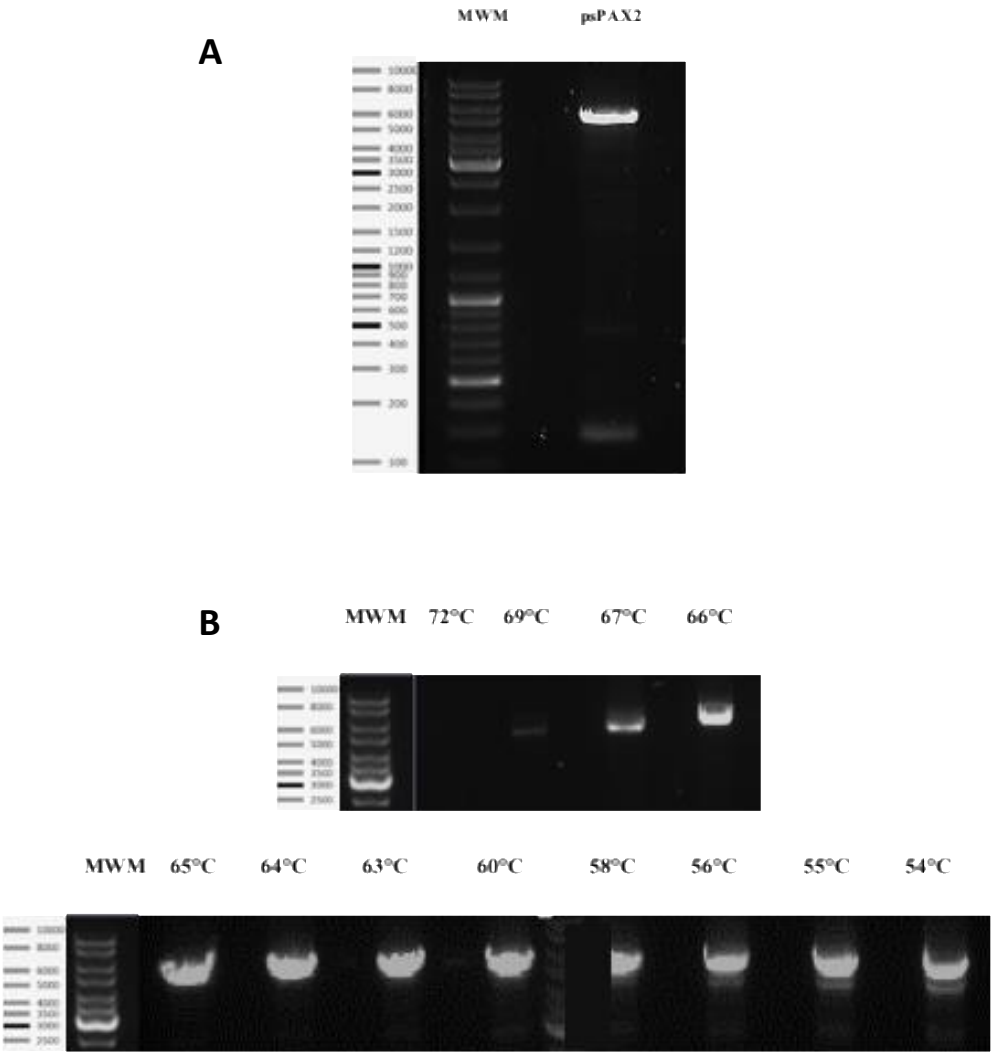

Figure 3.9: Agarose gel electrophoresis of psPAX2 vector backbone PCR performed with CloneAmp™ HiFi PCR Premix at 66°C (A), or at gradient temperatures, 72°C-54°C (B). The vector backbone was resolved on a 1% agarose gel and visualised under UV light. The O' Gene Ruler DNA ladder (Thermo Fisher Scientific, Waltham, MA, USA) was used as a reference molecular weight marker (MWM). The bands are indicated on the left of the image measured in base pairs (bp) at 66°C.

3.3.1.2. Preparation of the pNL4-3.Luc.R-E- vector backbone

The pNL4-3.Luc.E-R- pseudoviral vector backbone was optimised using the CloneAmp™ HiFi PCR Premix kit and Platinum™ Taq DNA Polymerase High Fidelity kit at an annealing temperature of 66°C, as well as gradient annealing temperatures of 54°C to 64°C. A target PCR product of 12,082 bp (Figure 3.10A) was observed using the CloneAmp™ HiFi PCR Premix at a single annealing temperature, as well as a non-specific product at 6,000 bp in the gradient temperature experiments (Figure 3.10B). Amplification with the Platinum™ Taq DNA Polymerase High Fidelity kit proved unsuccessful (results not shown). Thus, the CloneAmp™ HiFi PCR Premix and an annealing temperature at 66°C was used for amplification of the pNL4-3.Luc.R-E- vector backbone PCR, followed by purification and quantification.

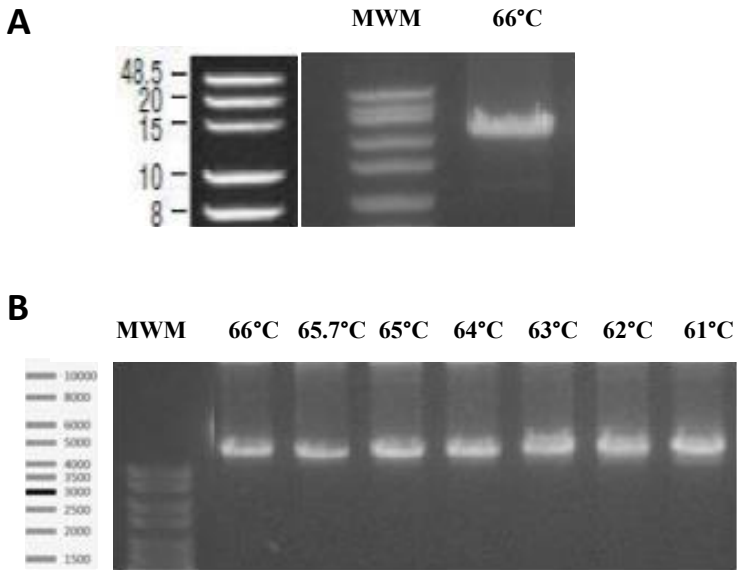

Figure 3.10: Agarose gel electrophoresis of pNL4-3.Luc.R-E- vector backbone PCR performed with CloneAmp™ HiFi PCR Premix at 66°C (A) and at gradient temperatures 61°C to 66°C (B). The vector backbone was resolved on a 1% agarose gel and visualised under UV light. The Quick Load® Purple 1kb Extended DNA Ladder was used as a reference molecular weight marker (MWM) in (A) , and the bands indicated on the left of the image measured in kilobase pairs. The O' Gene Ruler DNA ladder was used as a reference MWM in (B) and the bands are indicated on the left of the image measured in base pairs (bp).

3.3.1.3. Preparation of pMJ4/patient *gag-pol* inserts

Amplification of the pMJ4 *gag-pol* was optimised by testing annealing temperatures of 65°C and gradient annealing temperatures of 54°C to 65°C, using the CloneAmp™ HiFi PCR Premix kit, Platinum™ Taq DNA Polymerase High Fidelity kit, and the Q5® High Fidelity PCR enzyme kit. Amplification with Platinum™ Taq DNA Polymerase High Fidelity kit and Q5® High Fidelity PCR enzyme kit was unsuccessful (results not shown). The single temperature and gradient PCR using the CloneAmp™ HiFi PCR Premix was successful regardless of what temperature was used, with an amplicon of the correct size (4,314 bp) and no non-specific products being amplified (Figure 3.11).

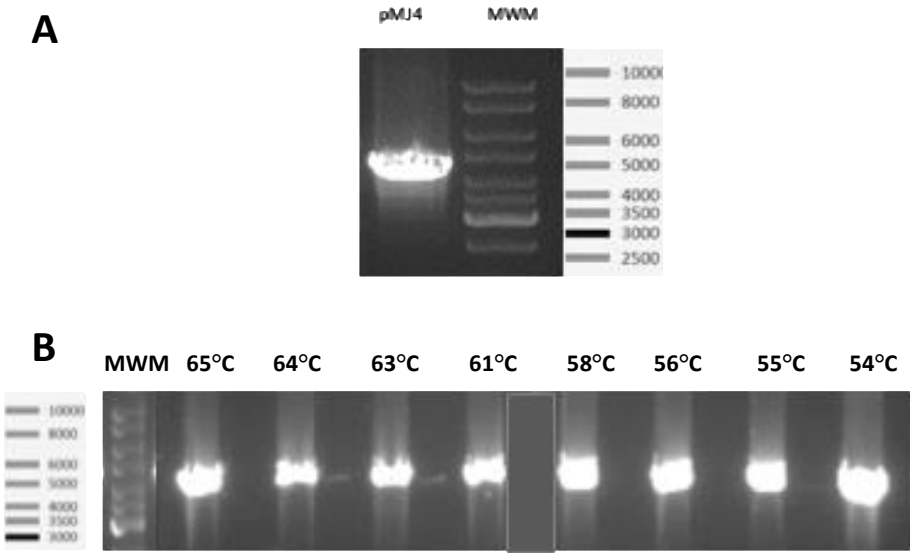

Figure 3.11: Agarose gel electrophoresis of pMJ4 *gag-pol* insert PCR performed with the CloneAmp™ HiFi PCR Premix at 65°C (A) and at gradient temperatures 54°C to 65°C (B). The *gag-pol* insert was resolved on a 1% agarose gel and visualised under UV light. The O' Gene Ruler DNA ladder was used as a reference molecular weight marker (MWM). The bands are indicated on the left of the image measured in base pairs (bp).

3.3.1.4. Gibson Assembly reaction

Gibson assembly was performed with the psPAX2 vector backbone by combining 100 ng (1.47 $\times 10^{10}$ copies) of vector backbone and 132 ng (2.84 $\times 10^{10}$ copies) of *gag-pol* insert at a copy ratio of ±1:2. Approximately 100 - 200 colonies were present on the selective LB agar plates after assembly and transformation, and 8 colonies were selected for validation.

To assess the performance of Gibson assembly in an alternative vector, the procedure was repeated using pMJ4 *gag-pol* and the pNL4-3.Luc.R-E vector backbone. The Gibson Assembly was performed by combining 75 ng (5.79 $\times 10^{9}$ copies) linearized and purified pNL4-3.Luc.R-E-vector with 150 ng (3.23 $\times 10^{10}$ copies) *gag-pol* insert at a copy ratio of ±1:6. Approximately 45 colonies were present on the selective LB agar plate after assembly and transformation, and 20 colonies were selected for validation.

3.3.1.5 Validation of Clones by restriction enzyme digest and Sequence analysis

Single and double restriction enzyme digests using *Nhe*I and *Pvu*I were performed for the validation of the clones produced by Gibson assembly of the psPAX2 vector backbone and pMJ4 *gag-pol*.

As expected, extracted plasmid DNA from clones A-H were cleaved once by *Nhe*I to produce a fragment of >10,000 bp (Figure 3.12A), and twice by *Pvu*I (Figure 3.12B). However, restriction with PvuI shows dissimilar restriction patterns between the plasmid DNA from clones A-H, and psPAX2 (Figure 3.12B). Two restriction fragments were observed for the plasmid DNA from clones at 8,000 bp and 2,500 bp, while only a single fragment >10,000 bp was observed for psPAX2.

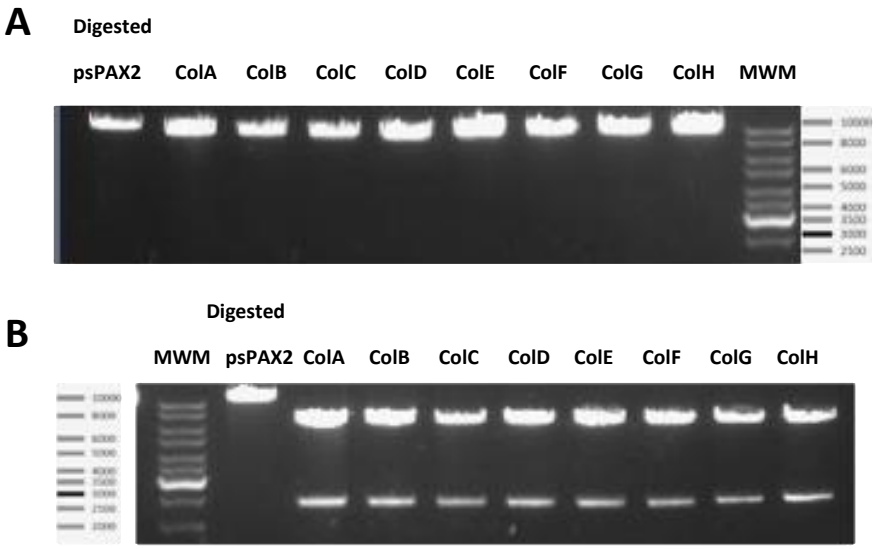

Figure 3.12: Endonuclease restriction of recombinant psPAX2 clones potentially containing the MJ4 gag-pol insert. Plasmid DNA from eight colonies were digested with either *Nhe*I (A) or *Pvu*I (B), resolved on a 1% agarose gel and visualised under UV light. The original psPAX2 was included as a positive control in the digest. The O' Gene Ruler DNA ladder was used as a molecular weight marker (MWM).

To verify the insert *gag-pol* is from pMJ4, DNA from the clones (A to G) were sequenced to confirm the identity of the inserts. Phylogenetic tree analysis confirmed that the sequences of clones A, D, E, F and G clustered with psPAX2 PR/RT (Figure 3.13), however, clones B and C clustered with pMJ4 and the HIV-1 subtype C reference sequences, which indicated that the

cloning procedure was successful in these two clones. The two clones were not further validated.

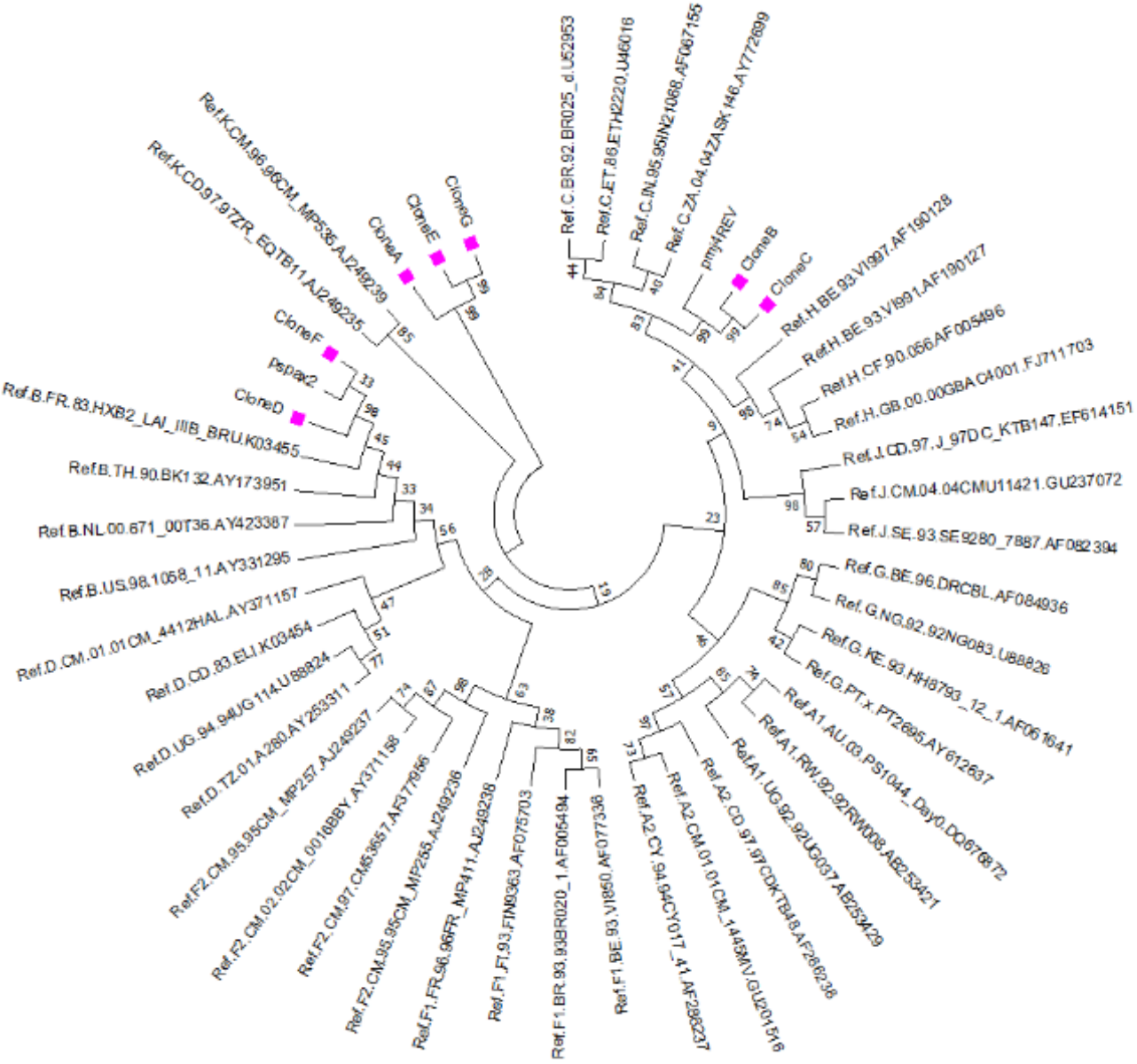

Figure 3.13: A neighbour-joining phylogenetic tree illustrating the association between clones A-G and HIV-1 group M reference subtype sequences. The phylogenetic analysis was performed on *pol* reference sequences and is based on the neighbour joining method [267]. The evolutionary distances were computed using the Maximum Composite Likelihood method [268]. Units indicate the number of base substitutions per site. Evolutionary analyses were conducted in MEGA7 [269] with HIV-1 subtype reference sequences and clones A-G.

Restriction enzyme digests using *Bam*HI were performed for the validation of the clones produced by Gibson assembly with the pNL3-4.Luc.R-E- vector backbone and pMJ4 *gag-pol* as the insert (Figure 3.14). It was expected that *Bam*HI restriction enzyme digest of clones containing the pMJ4 insert would linearize the plasmid, whereas the pNL3-4.Luc.R-E- backbone would be cut twice, resulting in two fragments. Results indicated that 12 of the 20 clones were linearized (Figure 3.14).

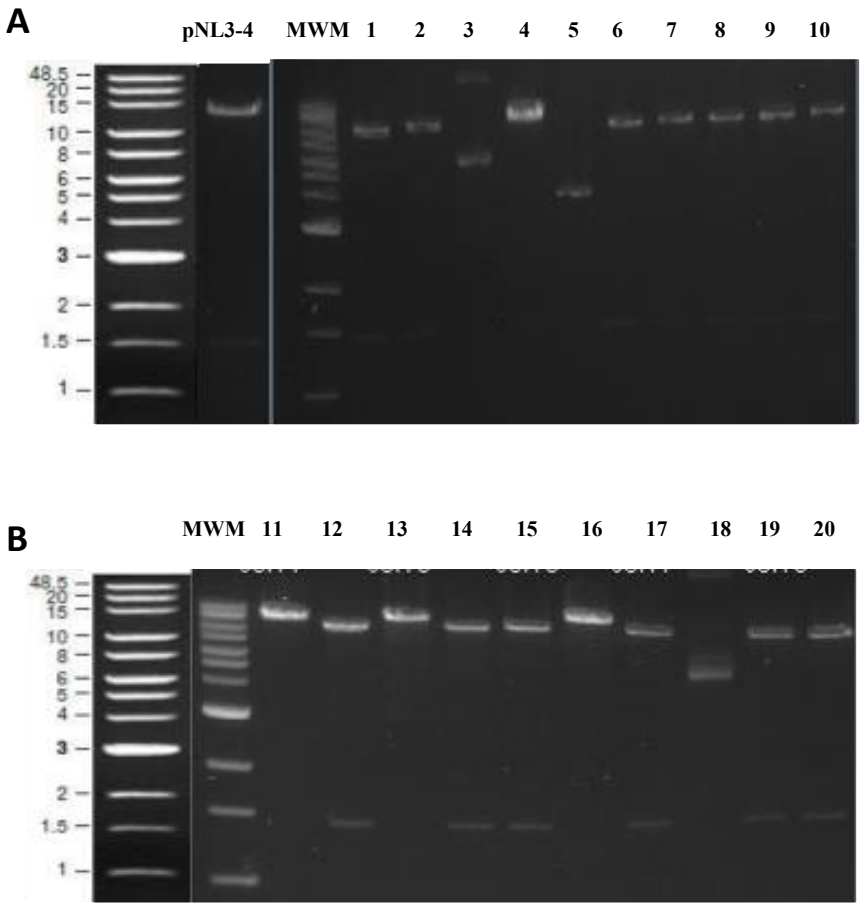

Figure 3.14: Endonuclease restriction of recombinant pNL3-4.Luc.R-E- clones potentially containing the MJ4 *gag-pol* insert. Plasmid DNA from 20 colonies were digested with *Bam*HI, resolved on a 1% agarose gel and visualised under UV light. The parent pNL4-3.Luc.R-E- was also digested, as a positive control. The Quick Load® Purple 1kb Extended DNA Ladder was used as a molecular weight marker (MWM).

To verify the insert *gag-pol* is from pMJ4 plasmid, plasmid DNA from the clones was submitted for population-based Sanger sequencing of RT and PR to confirm the identity of the insert. Phylogenetic tree analysis confirmed that 11 clones (1, 2, 8, 9, 10, 12, 14, 15, 17, 19 and 20)

clustered with HIV-1 subtype C reference sequences while 9 clones (3, 4, 5, 6, 7, 11, 13, 16 and 18) clustered with HIV-1 subtype B reference sequences (Figure 3.15).

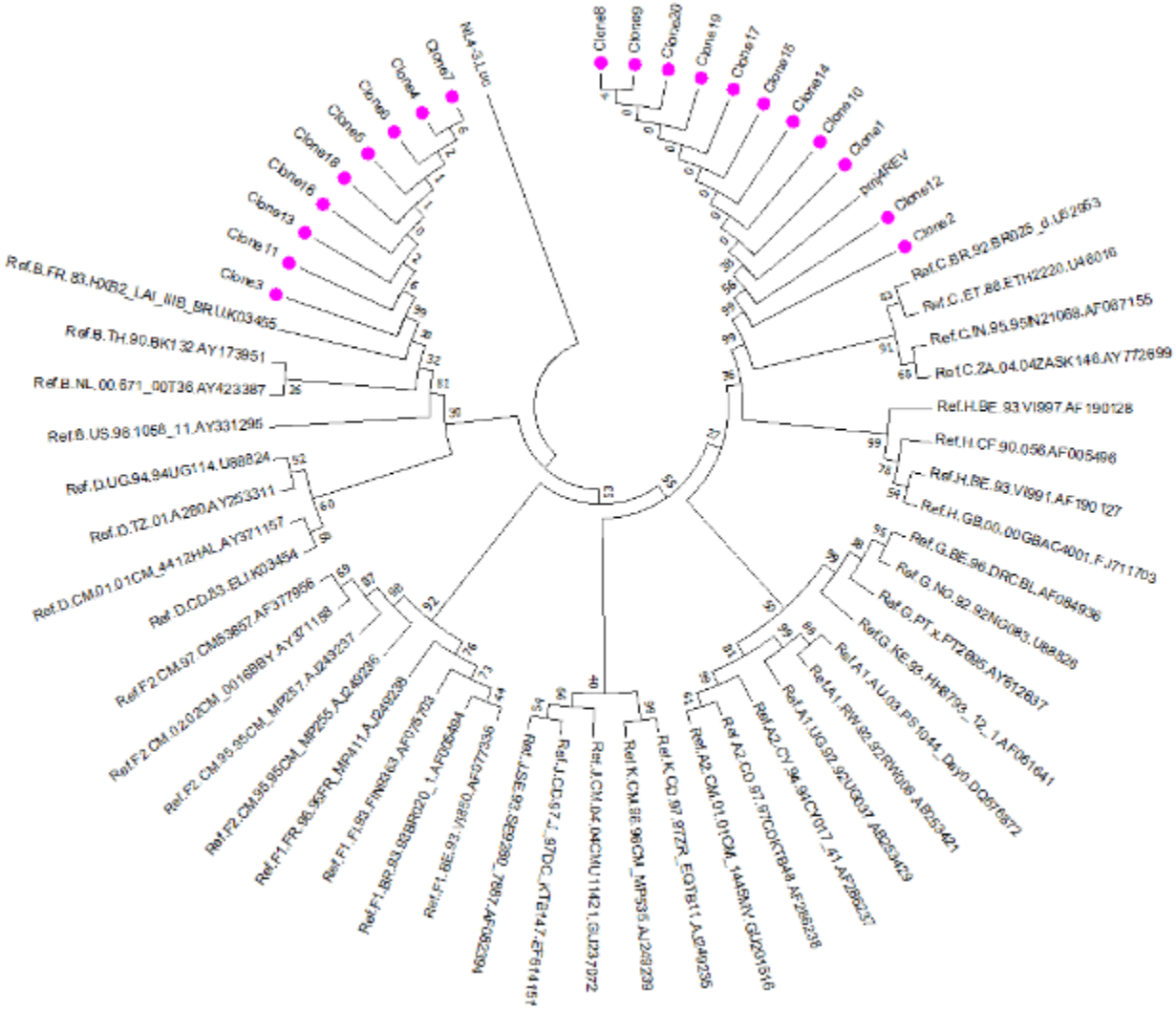

Figure 3.15: A neighbour-joining phylogenetic tree illustrating the association between clones 1-20 and HIV-1 group M reference subtypes. The phylogenetic analysis was performed on *pol* reference sequences and is based on the neighbour joining method [267]. The evolutionary distances were computed using the Maximum Composite Likelihood method [268]. Units indicate the number of base substitutions per site. Evolutionary analyses were conducted in MEGA7 [269] with HIV-1 subtype reference sequences and clones 1-20.

3.3.1.6. *In vitro* performance of patient derived pseudoviruses

The HEK 293T cells were transfected with clones 1, 2, 8, 9, 10, 12, 14, 15, 17, 19, 20 to produce patient derived pseudoviruses. The transfection controls (parent pNL4-3.Luc.R-E- and pMJ4) and patient derived pseudoviruses were tittered, as per the layout in Figure 3.16. Unfortunately, all RLU values were low, except for the controls and clone 11, so it appeared that no functional

virus was produced from the titrations performed for the remainder of the clones. Since Clone 11 appeared to be a subtype B clone as seen in Figure 3.15, no further analysis was completed.

	1	2	3	4	5	6	7	8	9	10	11	12
A	Blank	Blank	Blank	Blank	Blank	Blank	Blank	Blank	Blank	Blank	Blank	Blank
B	Blank	Col 1	Col 2	Col 8	Col 9	Col 10	Col 11	Col 12	Col 15	Col 17	Blank	Blank
C	Blank	Col 1	Col 2	Col 8	Col 9	Col 10	Col 11	Col 12	Col 15	Col 17	Blank	Blank
D	Blank	Col 1	Col 2	Col 8	Col 9	Col 10	Col 11	Col 12	Col 15	Col 17	Blank	Blank
E	Blank	Col 20	pMJ4	pNL4-3	Comb	Col 19	Blank	Blank	Blank	Blank	Blank	Blank
F	Blank	Col 20	pMJ4	pNL4-3	Comb	Col 19	Blank	Blank	Blank	Blank	Blank	Blank
G	Blank	Col 20	pMJ4	pNL4-3	Comb	Col 19	Blank	Blank	Blank	Blank	Blank	Blank
H	Blank	Blank	Blank	Blank	Blank	Blank	Blank	Blank	Blank	Blank	Blank	Blank

	1	2	3	4	5	6	7	8	9	10	11	12
A	2.80E+01	2.00E+01	3.20E+01	2.20E+01	3.20E+01	1.80E+02	3.44E+02	1.56E+02	4.00E+01	3.20E+01	2.20E+1	3.40E+01
B	3.20E+01	2.20E+01	1.40E+01	1.20E+01	2.00E+01	4.38E+02	7.15E+05	3.98E+02	2.20E+01	2.20E+01	2.20E+01	3.00E+01
C	1.40E+01	2.00E+01	2.60E+01	1.40E+01	2.80E+01	4.76E+02	7.62E+05	4.88E+02	1.00E+01	1.40E+01	2.00E+01	3.60E+01
D	2.00E+01	1.80E+02	6.36E+02	9.34E+02	4.22E+02	3.72E+02	6.91E+05	3.94E+02	1.80E+01	1.20E+01	2.60E+01	1.80E+01
E	2.60E+01	3.80E+02	7.81E+05	2.13E+06	1.04E+03	1.32E+02	4.18E+02	1.58E+02	1.40E+01	2.20E+01	2.60E+01	3.60E+01
F	2.00E+01	4.84E+02	6.29E+05	2.12E+06	1.56E+03	2.20E+01	3.40E+01	1.60E+01	3.80E+01	1.80E+01	3.40E+01	3.00E+01
G	1.40E+01	2.54E+02	4.88E+05	1.90E+06	1.15E+03	3.20E+01	3.40E+01	2.80E+01	1.80E+01	1.40E+01	3.40E+01	1.40E+01
H	2.00E+01	1.42E+02	6.46E+02	1.15E+03	6.42E+02	3.40E+01	2.60E+01	2.40E+01	2.00E+01	2.60E+01	2.60E+01	8.00E+00

Figure 3.16: The plate layout of the titrations completed with positive clones formed from pNL4-3.Luc.R-E- and pMJ4 (top). Comb means combined -the vector and insert were combined without going through Gibson assembly. The corresponding titration signal data, measured in relative light units, are shown at the bottom layout.

3.3.2. Construction through traditional restriction enzyme digest/ligation

Traditional restriction/ligation as an alternative approach to cloning of HIV *gag-pol* into the pNL4-3.Luc.R-E- vector was investigated. However, in the absence of available restriction sites at the 5' end of *gag* and 3' end of *pol* in pNL4-3.Luc.R-E-, the Silent Mutator online *in-silico* mutagenesis tool was used to assists with the generation of new restriction sites at these positions. Sites were selected that would require minimal changes in nucleic acid sequence and not modify the encoded amino acid sequence of the protein (Figure 3.17).

The *gag-pol* restriction sites, *Sac*II and *Nru*I, for pMJ4 were located at the 5' *gag* start (MGARA, nucleotide positions 5,461 to 5,590) and the 3' *pol* end (MENRW, nucleotide positions 9,621 to 9,880), respectively (Figure 3.17A and B). The same restriction sites were used for pNL4-3.Luc.R-E-, with the MGARA start site positioned at nucleotides 1,681 to 1,800 and MENRW site between nucleotides 5,881 and 6,000 (Figure 3.17 C and D).

Figure 3.17: Silent mutator software indicating the targeted region and the unique restriction site on the (A) pMJ4 reference plasmid at the 5' gag start site (MGARA); (B) pMJ4 reference plasmid at the Integrase 3' end (MENRW); and (C) the targeted 5' *gag-pol* region and (D) 3' targeted *gag-pol* region and the unique restriction site for the pNL4-3.Luc.R-E- reference plasmid.

PCR primers containing restriction sites were successfully designed to introduce the *Nru*I and *Sac*II sequences during PCR for both the insert pMJ4 and the pNL4-3.Luc.R-E- backbone.

3.3.2.1. Preparation of vector backbone and pMJ4 *gag-pol* inserts

PCR amplification of the pNL4-3.Luc.E-R- vector backbone using the CloneAmp™ HiFi PCR Premix kit and gradient annealing temperatures (50°C to 72°C) as well as the Expand Long Template PCR System, used 3 different buffers with an annealing temperature of 68°C was successful, as evidenced by the approximately 12,1 kb fragment (Figure 3.18 A and B). Figure 3.18A shows a decrease in the non-specific amplification products and amplicon intensity as the primer annealing temperatures increase (65°C-72°C). Therefore, an annealing temperature of 68°C was selected. Non-specific products were evident in PCR reactions using buffers 1 and 2 (Figure 3.18B), hence the CloneAmp™ HiFi PCR Premix kit, at 68°C was subsequently used.

The *gag-pol* insert (4,615 bp) was successfully amplified from pMJ4 using the previously established method, (Figure 3.18C), with the new primers introducing the *Nru*I and *Sac*II restriction enzyme sites. Since additional non-specific products were amplified, the insert was purified through gel extraction and quantified before further *Dpn*I and restriction enzyme digestions were completed.

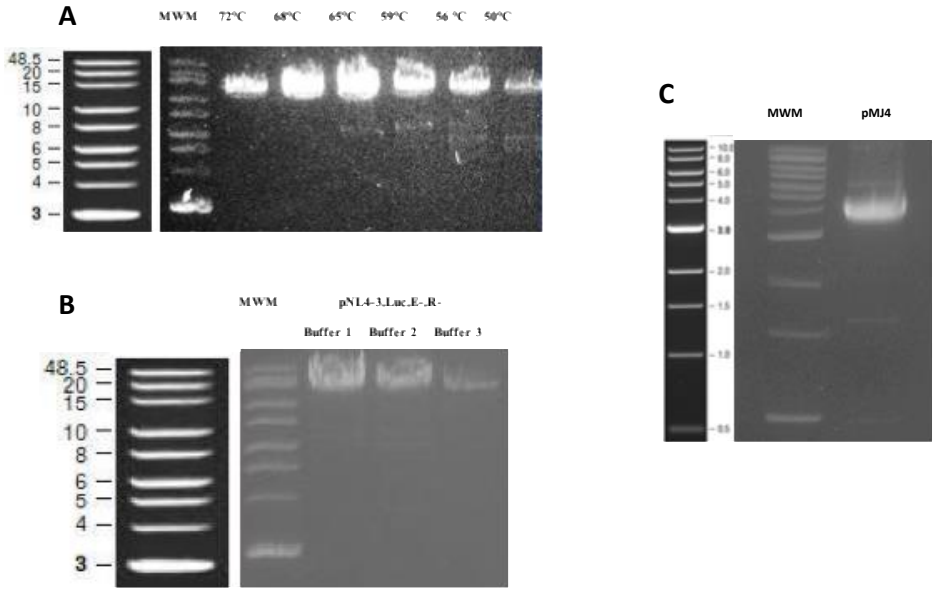

Figure 3.18: Agarose gel electrophoresis of the pNL4-3.Luc.R-E- vector backbone amplicon with CloneAmp™ HiFi PCR Premix (A) and the Expand™ Long Template PCR System (B), and the pMJ4 *gag-pol* insert PCR with a primer annealing temperature of 60°C (C). Amplicons were resolved on a 1% agarose gel and visualised under UV light. The Quick Load® Purple 1kb Extended DNA Ladder was used as a molecular weight marker (MWM), indicated on the left of the image measured in kilobase pairs (kb).

3.3.2.2. Restriction enzyme/ligation reactions

After initial treatment with *Dpn*I to remove the intact parent plasmids, the vector and *gag-pol* amplicons were digested with *Nru*I and *Sac*II in preparation for ligation (Figure 3.19). In addition, the restricted vector backbone amplicon was dephosphorylated to prevent self-ligation.

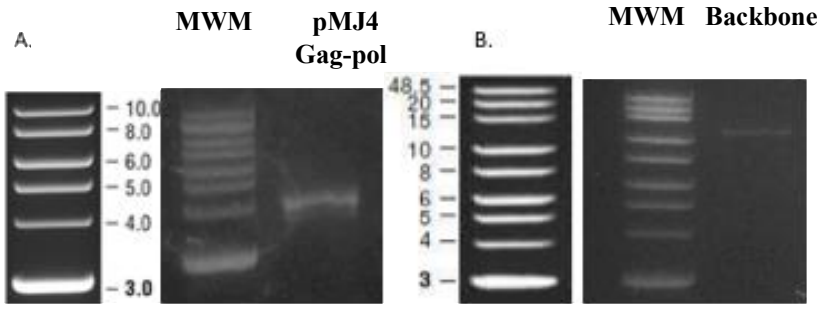

Figure 3.19: Endonuclease restriction of PCR products with SacII and NruI for (A) *gag-pol* pMJ4 and (B) pNL3-4. Luc.R-E- vector backbone. Amplicons were resolved on a 1% agarose gel and visualised under UV light. The Quick Load® Purple 1kb DNA Ladder for (A) and the Quick Load® Purple 1kb Extended DNA Ladder for (B) were used as molecular weight markers (MWM).

The ligation reaction was optimised by testing different ratios of *gag-pol* insert and vector backbone: 3.77 x 10^9 copies vector + 7.72 x 10^9 copies *gag-pol* (1:2) or 18.9 x 10^9 copies *gag-pol* (1:5) and performing ligations at 25°C or 37°C. Two reactions of each were made and incubated at either 25°C or 37°C. Analysis of the ligation reaction through agarose gel electrophoresis showed that all ligation reactions had products with sizes larger than the linear insert and the vector. This implied that ligation was successful (Figure. 3.20). Unfortunately, after transformation, no bacterial colonies were present on the selective LB agar plate. Cloning of MJ4 *gag-pol* into pNL4-3.Luc.R-E- through traditional restriction/ligation was therefore unsuccessful, despite several attempts. Ultimately, due to time constraints, the experiments were terminated.

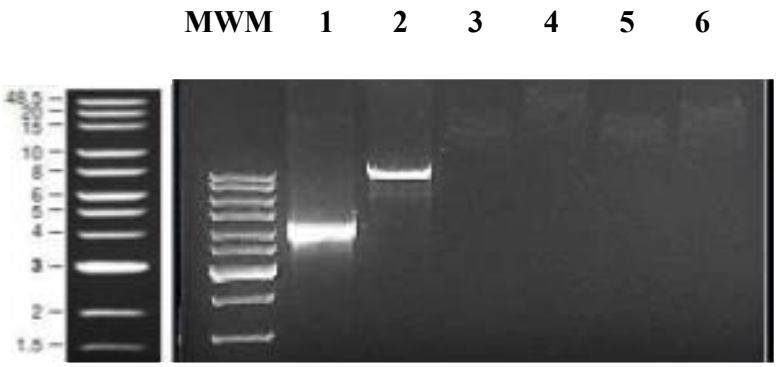

Figure 3.20: Ligation reaction of the restricted pNL4-3.Luc.R-E- backbone and pMJ4 gag-pol insert. The reactions were resolved on a 1% agarose gel, and visualised under UV light. Lanes 1 and 2 depict the restricted *gag-pol* insert (4,615 bp) and the vector backbone (12,151 bp), respectively. Lanes 3 and 5 contain the ligation reactions at 37°C at a ratio of 1:2 and 1:5, respectively. Lanes 4, 6 are the ligation reactions at 25°C, at ratios of 1:2 and 1:5, respectively. The Quick Load® Purple 1kb Extended DNA Ladder was used as a molecular weight marker (MWM), indicated as kilobase pairs (kb).

Chapter 4: Discussion

Eligibility for third-line therapy in South Africa is reserved for patients failing a PI-based ART regimen despite good adherence and displaying a genotypic antiretroviral drug resistance profile that indicates PI resistance [253]. Patients being switched to third-line therapy have RAL, EVG as INSTI options, DRV/r as the only third-line PI, ETR as the NNRTI, and AZT and/or TDF as NRTI third-line drug agents [167]. Currently, there are approximately 1600 patients in South Africa on third line therapy with an estimated 10% failing therapy [253]. Unfortunately, these patients continue to stay on the failing therapy, since there are no further recommendations regarding alternative ARV options or resistance testing [253].

There is an increasing amount of evidence of third line ART failures in developing countries [253, 271, 272] especially amongst patients on RAL and EVG. In South Africa approximately 17-22% of patients on TLART are not supressed [168, 253]. In Uganda it was reported that the prevalence of INSTI resistance in patients on a failing RAL or EVG based therapy is at approximately 47% (n=24/50) [272]. Similarly, in an Argentinian survey 72% of patients on an INSTI salvage ART presented with resistance and 32% presented with intermediate resistance while 29% displayed high level resistance and 2% acquired cross resistance to DTG [271]. Data from Botswana has also displayed that 20% (n=4/20) of patients are failing a DTG based salvage regimen [273]. It can be reasonably anticipated that the emergence of multiclass resistance in low and middle-income country settings with serious limitations such as no firm recommendations for treatment post third line ART failure, limited drug options, and the inability to monitor participants for therapy effectiveness will have a major impact on survival and well-being [274]. Hence, this study aimed to identify the genotypic and phenotypic resistance profiles of HIV-1 from third-line failure patients in South Africa to assess how the known ARV drug resistance profiles, as well as Gag cleavage sites mutations and PTAP insertions contribute to resistance, in addition to determining what future therapy clinicians have available for third line failures.

To achieve this aim, the HIV-1 *gag-pol* regions from six patients failing a third-line regimen were amplified through an optimized PCR, and their genotypic drug resistance profiles assessed through population-based Sanger sequencing. An *in vitro* phenotypic inhibition assay was set up and assessed for determining inhibition to different classes of ARVs, and an attempt was made to clone the patient-derived *gag-pol* amplicons into an HIV-1 expression vector for phenotypic drug inhibition assessment.

Plasma samples from six patients were available for assessment. Five of the six patients were adults, and all six had viral loads >1,000 copies/ml, and were either on a DRV/r- and/or RAL/DTG-based regimen. To optimize the amplification of HIV-1 *gag-pol* from these samples,

we investigated three different annealing temperatures for the RT-PCR (50°C, 53°C and 56°C), and for the nested PCR reaction, a single annealing temperature (66°C) as well as touchdown PCR with decreasing annealing temperatures (68°C, 66°C, 64°C and 62°C) was performed. Overall, a single annealing temperature of 66°C in the nested PCR protocol provided the most optimal amplification of HIV-1 *gag-pol* from patient plasma samples (Figure 3.1B). Subsequent population-based Sanger sequencing and phylogenetic tree analysis of HIV-1 *gag-pol* amplicons confirmed that all six patients were all infected with HIV-1 subtype C, and the lack of cross-contamination between the amplicons during analysis (Figure 3.2). This was as expected, since it is well characterized that the predominant circulating subtype causing the HIV-1 epidemic in South Africa is C [16].

Overall, drug resistance interpretation through the Stanford University HIV Genotypic Resistance Interpretation Algorithm indicated the presence of PI drug resistance mutations that are typically observed in patients failing on a DRV/r containing regimen. Several amino acid deletions and changes were detected in Gag cleavage sites P2/NC, NC/P1 and P1/P6, with changes in MA/CA and CA/P2 being less likely. Cleavage site CA/P2 had one amino acid change from valine to isoleucine at position 128 and the most diverse cleavage site within patients in this study was P2/NC. Virus from patients 4 and 5 showed substantial resistance against either RAL or DTG, and consisted mainly of the N155H major and/or T97A and E157Q minor INSTI mutations. Patient 4, however, contained the N155H and T97A INSTI mutations without documented exposure to either RAL or DTG. We also observed typical NRTI mutations (e.g. M184V, K65R, TAMS) in these patients, as well as PI (e.g. I54V, V82A) and NNRTI (e.g. K103N, Y181C) mutations associated with failing first- and second-line regimens. Taking into consideration both current and previous exposure to inhibitors, patients displayed resistance to all the drug classes, with 83%, 100%, 50% and 33% indicating high level resistance to the PI, NRTI, NNRTI and INSTI drug classes, respectively. The *in vitro* phenotypic inhibitory assay was successfully set up and the IC_{50}'s obtained for NRTIs (3TC, AZT, d4T, TDF), NNRTIs (ETR), PIs (DRV) and INSTIs (RAL, DTG) correlated with the literature. Unfortunately, after several attempts using different HIV-1 expression vectors and two different cloning strategies, we were unable to produce functional patient-derived pseudoviruses (using *gag-pol* from our six patient samples) for assessment in the *in vitro* phenotypic assay.

While all patients received DRV/r, only one patient (Patient 1) was phenotypically predicted to have high-level resistance to this drug due to the presence of DRV-specific resistance mutations (Table 3.3). The remaining patients contained ≤2 major DRV-specific mutations (i.e. I54L, I84V) in the background of ATV/LPV/SQV-related major (e.g. I54V, V82A) and minor (e.g.

M46I/L, A71V, L90M) mutations. These patients were phenotypically predicted to be fully susceptible to, or exhibit potential low-level resistance to DRV. Certain major mutations selected by ATV/LPV/SQV were shown to persist due to the cross resistance between the PI drugs, likely due to the selective pressure of DRV. Clutter et al [275] demonstrated the presence of a large number of PI DRMs, as well as different substitutions at the exact position, have evidently different properties on PI susceptibility and that cross resistance is complex [276] i.e. for drug resistance mutations at positions 50, 54 and 82 [277]. de Meyer et al [278] and Pozniak [279] reported on the effect of drug resistance mutations in response to DRV/r particularly in treatment experienced patients, these patients displayed decreased responses with 3 of the 5 of DRV drug resistance mutations: V11I, V32I, L33F, I47V, I50V, I54L/M, T74P, I84V and L89V.

In addition to drug resistance mutations in PR, the contribution of changes in HIV-1 Gag to PI resistance also needs to be emphasized. Studies have reported the presence of gag mutations in association with mutations in protease-coding regions, these mutations were identified within the P4-P3' regions that interact directly with the PR. Most studies have linked gag mutation accumulation with protease inhibitor experienced patients rather than naïve patients. This therefore suggests mutations are selected under PI selective pressure direct mechanisms of resistance to compensatory mechanisms to increase mutant PR activity [280]. Amino acids substitutions linked with PI resistance have been described at three highly variable gag CSs (p2/NC, NC/P1, P1/P6) [281]. The most commonly occurring substitutions related to PI exposure are at Gag codon 128 in p2/NC, codons 431, 436 and 437 in NC/p1 and at codons 449, 452 and 453 in p1/p6, and are detected regularly *in vitro* and *in vivo* [281]. These changes in Gag were also identified in our six patient samples (Table 3.7). The structural and functional analyses of the processing efficiencies of wild type or mutant substrates displayed an enhanced processing and/or binding affinities for the mutant substrate [282]. The enhanced processing of Gag modifies the equilibrium of PI-Gag substrate with viral PR that favours Gag substrate resulting resistance toward PI's [278].

Mutations in Gag conferring enhanced resistance to patients on DRV/r therapy were found at Gag codon 128 in all patient samples, and have been related to viral rebound in patients on DRV/r [283]. A substitution in Gag codon 452 (observed in patient sample 4) combined with PI mutations I84V, or I84V/L90M is known to reduce susceptibility to all PIs except TPV [284]. Substitutions at position 453, displayed in patient samples 1, 3, 4 and 6, increase PI resistance in combination with PR mutation I50V [284] and I84V [284] and these mutations are selected

by DRV/r, LPV/r and FPV/r and all other PIs, respectively. In addition, mutation E428G, observed in patient sample 2, has been associated with a reduced response to DRV/r in the POWER trials [283]. Since all patients were exposed to DRV/r in their third line therapy, the presence of these Gag mutations could have caused a decrease in resistance or viral rebound to this ARV, particularly in patient 4 that indicated a predicted phenotypic response of an intermediate level resistance for DRV/r with only 1 major resistance mutation, I50V. The Gag cleavage sites exhibited several other acquired mutations however, these mutations are aligned to previous PI exposure with either ATV/LPV/SQV [284, 285]. In comparison to DRV/r selected Gag mutations, these PIs have selected for the more commonly occurring Gag cleavage site mutations, namely A431V [281]. A431V has been observed *in vivo* during PI therapy with RTV, IDV, NFV, SQV, and LPV and it confers resistance to all PIs except DRV [284]. Thus, A431V a Gag mutation that is likely considered similarly to a primary PI resistance mutation since PI resistance is conferred in the absence of known mutations in the viral PR [285].

Interestingly, patient sample 5 was predicted to be phenotypically susceptible to DRV/r due to the absence of major PI mutations, despite being exposed to LPV/r, ATV/r and DRV/r. This patient was shown to harbour virus with three Gag cleavage site substitutions i.e. 373V, 376V and 451N. According to Verheyn et al [286] and Mammano et al [280] these substitutions are selected by PI exposure, however, do not cause resistance , and are thus not associated with treatment failure. The relevance of the p1/p6 substitution at position 451 from arginine to asparagine, has not been fully evaluated, hence this apparent association to PI resistance would need to be established to fully understand treatment failure in patient 5. Moreover, an *in vitro* phenotypic inhibition assay based on patient derived *gag-pol* sequences would be a key indicator of whether treatment failure in patient 5 is associated with PI resistance in the absence of known PI mutations, and if DRV/r resistance is associated with the presence of Gag 451N.

Apart from mutations observed in the Gag cleavages sites of our patients, we also observed partial or full PT/SAP duplications in Gag-p6 in two patients. Duplications in the PTAP motif are frequently observed in viruses that originate from patients on PI therapy [287]. Martin et al. [288] examined the effect of PT/SAP duplication in the context of PI resistance mutations and established that PTAP duplication evidently improves resistance to a panel of PIs. The biological analysis showed that the PTAP duplication reverses a Gag processing defect brought about by the PI resistance mutations.

Patient sample 3 displayed an intermediate resistance to DRV/r due to the two major mutations selected by DRV/r, I54L and I84V, as well as several Gag cleavage site substitutions

that cause DRV/r resistance. A third factor that may have contributed to treatment failure could be the duplication of PT/SAP in the patient's viral genome. In patient sample 6, while no mutations selected by DRV/r were observed, several Gag cleavage site mutations were detected which increase resistance to PIs, as well as a PT/SAP duplication that potentially contributed to increased Gag processing leading to increased replicative capacity [270]. Interestingly, patient 6 had the highest viral load, 143,000 RNA copies/ml, amongst all the patients tested. Thus, future work should evaluate the impact of the PT/SAP duplication on replicative capacity in this context.

Overall, studies have not fully characterized Gag-Pol mutations in third line failure patients exposed to DRV/r, hence this is the first study describing the relationship between DRV/r PI and Gag cleavage site and PT/SAP associations. The interplay between major and accessory/minor mutations as well as compensatory mutations, and their impact on viral replication and ultimately treatment failure, warrants further investigation. Hence, we attempted to set up an *in vitro* phenotypic inhibition assay to evaluate patient derived *gag-pol*, and the impact of these sequences on drug susceptibility or resistance in that particular patient.

Only the N155H major INSTI resistance mutation was seen amongst one of the three patients receiving RAL or DTG (Table 3.3). Although this mutation was predicted by the Stanford University HIV Genotypic Resistance Interpretation Algorithm to cause high-level resistance to RAL, its impact on DTG resistance is minimal. As such, all patients, including patient 3 who was on a DTG containing regimen, were predicted to be susceptible to DTG. Currently, DTG has the highest known genetic barrier to developing resistance amongst the available ARV drugs [289] , and it was made available in the public sector as part of the first line regimen in South Africa in November 2019. An additional option for INSTI is Bictegravir; where *in vitro* studies has shown that it may be effective against strains of HIV-1 that are no longer affected by other HIV antivirals [290, 291, 292, 293, 294].

Of particular interest is the seven-year-old paediatric patient (patient 4) with a major (i.e. N155H) and accessory (i.e. T97A) INSTI resistance mutation despite the lack of documented exposure to either RAL or DTG. There may have been an error in reporting on the patient's previous and/or current ART exposure. Alternatively, since the route of transmission in this patient is unknown, it could be speculated that these mutations were not transmitted through mother-to-child transmission, since the South African third line RAL containing regimen was only implemented in 2013 [270]. It is possible this child developed INSTI resistance by sharing medicine with parents/guardians, or was infected later in life with a drug resistant virus (transmitted/primary drug resistance) [292, 295, 296]. One could also argue that

these were natural occurring viral variants. It has been shown that the presence of the accessory mutation T97A may exist prior to INSTI treatment, however it is rarely found in patients with the major INSTI resistance associated mutations [295, 296, 297]. Although rare, transmission within the INSTI class can occur, and should be monitored in routine surveillance studies of transmitted-drug resistance [292, 295, 296].

Various NRTI resistance mutations were observed in all of the patients, with the most prominent mutation being M184V (Table 3.3) selected for by 3TC and FTC [298] . It is well-know that this mutation not only causes high-level resistance to 3TC and FTC, but also evokes a significant loss in viral replicative fitness [298]. The latter is considered to be particularly advantageous, to some extent, for patients continuing the use of failing regimens. The affected viral fitness decreases the ability of the virus to replicate and can therefore slows viral load accumulation through dissociation of the nucleotide attachments during RT processivity [299]. An additional beneficial trait of M184V is its association with the cellular immune system, thereby suppressing viral replication. A study observed specific CD8+ CTL responses to HIV-1 sequences that included the M184V mutation in one patient and concluded that improved CTL recognition of some mutations could potentially contribute to lower replicative capacity of viruses harbouring this mutation [300]. The final benefit of M184V is the delayed appearance of other resistance associated mutations. The CNAB 3002 study established that the presence of M184V was linked with substantially lower TAMs incidences, particularly mutations D67N, L210W, and T215Y/F; furthermore, this was independent of the HIV-1 RNA levels and duration of prior ARV treatment [301]. Finally, the phenotypic resistance levels to AZT and d4T were decreased in patients carrying the M184V mutation selected as a result of previous exposure to 3TC [301]. This factor has clinical benefits by decreasing RT processivity, improved immune response, improved RT fidelity and reduced replicative fitness, hence patients will develop additional NRTI mutations slower than patients without M184V. Additionally,M184V/I increases susceptibility to AZT, d4T and TDF [302, 303] and slows the emergence of AZT, d4T, and TDF resistance, thus virus is more susceptible to these ARV's than the wild-type virus, termed hyper-susceptibility [302, 304, 305, 306, 307]. In addition to the M184V mutation, some patients also contained the K65R and TAMs that lead to a predicted intermediate/high-level resistance to most of the NRTIs in their current and previous regimens. Future options available for the six patients included a unique investigational nucleoside reverse transcriptase translocation inhibitor (NRTTIs), currently in Phase 2b clinical development – Islatravir, which may also be effective against certain HIV strains that are resistant to other HIV drugs [308].

Although none of the patients' current regimens contained NNRTIs, we observed NNRTI resistance mutations in three of the six patients related to EFV/NVP (K103N, Y181C) and ETR resistance (A98G, L100I). Sarah et al [309] reported the persistence of K103N after halting NNRTI-containing therapy, and mentions that since the K103N mutation appears to have negligible effect on the replicative fitness of HIV-1, the virus seems to allow K103N variants to linger as dominant species after discontinuing of NNRTI therapy. In their study results indicated that acquired drug resistance lingers for ≥5 years after therapy cessation [309]. Another study reported that in extreme cases, the mutant virus evidently remained at nearly 100% for almost 6 years after cessation of efavirenz treatment [309]. Furthermore, studies have reported that if multidrug-resistant viruses are obtained during acute HIV-1 infection, primary drug resistance can linger indeterminately in the absence of antiretroviral therapy [310, 311, 312, 313].

According to a South African study the most expected drug resistance class is NNRTI's at approximately 18.9% of the 200 persons identified for drug resistance. The following resistance mutations accumulated were from the NRTI's which sums to 7.8% and approximately 0.5% of the resistance class is from NNRTI's, NRTI's and PI's [314]. In Barth et al's review [315] the most common mutations that were found were M184V in approximately 65% of patients where in this study 100% of the patients contained it, K103N mutation in 52% of patients and in this study at 50% of patients contained it as well as TAMs (M41L, D67N, K70R, L210W, T215Y/F, and K219Q/E) ranging from 5-20% whereas this study had a higher percentage of about 33% and lastly K65R at 5% and this study at 33%, these mutations appeared in most of the patient resistance profiles which indicates that the expected NNRTI and NRTI mutations identified in South Africa are similar to this study. The small study that focussed mainly on patients receiving PI therapy indicated resistance against SQV/r with L90M and V82A appearing mostly in 16% of patients. In this study patients not only received SQV/r [316] but received LPV/r AND ATV/r hence, many other mutations were also observed, including V82A observed at 50% and L90M present at 33%, which is quite higher than the review focussed on Sub Saharan Africa. These resistance class patterns are expected since the first line of therapy is based mainly targets the RT, hence resistance patterns are at a lower percentage for PI inclusive of the RT class resistance patterns. This coincides with the class resistance patterns seen with these patients, with slight changes to the percentages due to the 6 patients being exposed mostly to NRTI's first and some lingering NRTI resistance patterns.

Newer NNRTIs that could potentially be used in these patients are doravirine and rilpivirine seeing as patients have not been exposed to these. However, if observing the NNRTI

resistance mutations (K103N, Y181C, A98G and L100I) present in the patients rilpivirine would not be an option seeing as a resistance mutation (L100I) already exists within the patient's profile selected by ETR. Additionally, patients should ideally be prescribed therapy **whereby** no associated resistance mutations are present seeing as failure is what is trying to be avoided. Fortunately, The NNRTI doravirine is a newly approved NNRTI and that is potent at low doses against HIV-1 and active against viral strains with common NNRTI-resistance associated substitutions such as K103N, Y181C, G190A, E101K, E138K, and K103N/Y181C [317]. Another alternative is Elsufavirine, which is already approved for use as an oral NNRTI for once daily dosing, but is being investigated as a long acting injectable formulation indicating potential for monthly use both intramuscularly and subcutaneously [318].

From the above results it is clear that virological treatment failure due to the emergence of ARV drug resistance can be attributed to a complex interplay of primary, accessory (polymorphic and non-polymorphic) and compensatory mutations which emerge in the viral genome over time. Moreover, the genotypic prediction of resistance may not fully explain virological failure in some patients. As the HIV pandemic evolves, and newer ARV drugs become available on the market, it is essential to phenotypically characterize mutations and understand their contribution to treatment failure. The *in vitro* phenotypic inhibition assay described in this study can be used to evaluate the impact of single and combination mutations on drug susceptibility or resistance [45], monitor the frequency of transmitted drug-resistant virus [319, 320], characterize baseline variation in susceptibilities to various drugs [320], gain a better understanding of how and why patients fail current treatments [321, 322] and, screen for novel antiviral drugs that are also active against resistant strains of HIV-1. Furthermore, the generated data can be used to improve the interpretation of HIV-1 genotypes with respect to resistance to all ARVs. Genotype-phenotype pairs can be used for identifying complex resistance patterns and for the improvement of various bioinformatics tools that offer phenotype-based resistance predictions.

As a first step, we successfully implemented an *in vitro* phenotypic inhibitory assay which allowed for testing of DRV, 3TC, d4T, AZT, FTC, TDF, ETR, RAL and DTG against the pNL4-3.Luc.R-E- pseudovirus without genotypic resistance to any ARV drugs (Figures 3.5, 3.7 and 3.8). As expected, pNL4-3.Luc.R-E- was susceptible to all ARVs tested, and the determined IC_{50} values were within the expected ranges for each drug [323, 324]. The IC_{50} values can serve as a baseline for subsequent testing of patient derived *gag-pol* pseudoviruses to establish fold changes in resistance. The disadvantages of the phenotypic inhibitory assay stems mainly from the lack of clinical significance of the IC_{50} fluctuations for each ARV. The

fluctuations are highly likely to be different for each ARV and is dependent on the level of ARV in the blood. Another major drawback of phenotyping assay is the lack of detection of minority variants, seeing as single clones are usually tested using the inhibitory phenotypic assay. Therefore, following population-based cloning and screening the impact of minority variants in the assay may not be reflected [235]. Even the newer highly sensitive phenotypic assays cannot quantify the minority variants and are only used to detect low frequency drug resistant virus variants in clinical specimens [325].

The second step was to establish a platform where *gag-pol* sequences derived from patients failing treatment, such as the genotypically characterized samples from the 6 patients described above, are cloned into psPAX2 and pNL4-3.Luc.R-E- backbone and tested for susceptibility to ARVs.

These clones were further verified with the *in vitro* performance testing through titration. From this *in vitro* performance test none of the clones produced functional virus. This could have stemmed from the preparation of the amplicons by either primer sequences being incorrectly synthesised, PCR error through the addition of extra nucleotides which in turn affects the cloning procedure. If the ends of the PCR amplicons are not homologous or have random nucleotide insertions this could potentially create unsuccessful cloning. Another potential reason why cloning would be unsuccessful is if there are potential sites within the genome that could be homologous to the amplicon ends where binding could have occurred at the homologous site leading to incorrect proteins being generated hence no functional clone was produced. Ways in which these errors in cloning and preparation could be avoided is by firstly sequencing the amplicon and vector backbone amplicon with second or third generation strategies to make sure that no errors are introduced during PCR. A factor that could have affected the cloning in terms of the Gibson assembly could potentially be the size of the primers that amplify the vector, this was made exactly the same size as the insert (4.3kb) primers whereas the vector backbone is twice as large as that of the insert. The enzyme for amplification could potentially be introducing additions when amplifying the fragments which decreases the cloning efficiency. A high-fidelity enzyme that could be used is Q5 HS HiFi enzyme. Once these factors are overcome the fragment ratios can be altered beginning with a 1:1 as required by the kit.

The traditional restriction ligation cloning strategy was unsuccessful despite the alterations of DNA copy number ratios for the insert and vector backbone, as well as cloning temperature changes. Several factors could have been the reason behind the unsuccessful cloning however the most probable point of failure could have been during the large vector

backbone preparation. Restriction enzymes could have not fully restricted the amplicons hence no ligation, or parental strands could have filtered their way through to the transformation step. The ligation seemed to be the main issue seeing as the sizes of the fragments were correct from the agarose gels. If ligation is the issue it is due to 2 issues namely that the DNA fragment ends are not compatible, the DNA is damaged from the UV treatment (vector and insert preparation) or there is a chemical inhibitor within the reaction. Beginning with the latter, this could be avoided by using water as an elution buffer after purification from the PCR steps, with regard to the first issue one would have to test that the restriction enzymes are working correctly by doing test cuts, if unexpected bands appear a sequencing would be the next option to make sure what is being restricted. Another option is using a different ligation enzyme, T4 Ligase which seems to be the enzyme that is recommended by scientists in the laboratory. Speculations as to why the limiting step within this study, cloning, did not produce clones could be due to not being able to determine the structural differences at the PCR product ends [347]. A way in which this could have been improved is through the use of fluorescent primers that can directly confirm restriction enzyme cleavage of PCR products. It has also been reported that the newer polymerase enzymes used in the preparation steps (PCR) in this study might be more accurate, processive and thermostable, nevertheless could be less compatible with cloning [326, 327]. The polymerases could have obstructed the DNA ends from being digested by endonucleases or are able to add nucleotides, completely altering the overhangs. A second factor that could decrease the cloning efficiency is the thermostability of PCR polymerases [328], that generally correlates with better structural stability in organic solvents [329, 330] and chaotropic salts [331],which increase the difficultly of purification of PCR products from the polymerase. Guanidine hydrochloride concentrations in marketable PCR purification kits are insufficient (<4.5 M) to denature the polymerase [332, 333].

With regards to the restriction enzymes, these are inhibited by complex DNA substrates, simply stating that if the DNA is quite lengthy more of the target restriction site will be present and this is seen as an enzyme inhibitor or different substrates at suitably high concentrations [334]. Partial restriction enzyme digests can also ultimately lead to unnecessary parental plasmid colonies as background populations from which the ideal recombinant plasmids must be identified through costly high-throughput screens [335, 336]. This could be avoided by using smaller vector plasmids and subcloning with the smaller vectors.

All of the abovementioned strategies can be tested in future studies to optimize cloning and successfully set up the modified *in vitro* phenotypic inhibition assay for testing locally relevant *gag-pol* sequences.

In conclusion, genotypic testing of HIV-1 *gag-pol* from six South African patients failing a third line regimen identified expected and novel combinations of ARV drug mutations, as well as the absence of mutations associated with treatment failure on their current regimen. Therefore, we need to continuously predict the effectiveness of newly introduced ARV drugs amongst the large number of ART-experienced South Africans. Results highlight the importance of correlating genotypic data to phenotypic characterization of these sequences, to establish viral susceptibility to the ARVs used in various combinations. Thus, the successful set up and application of this modified *in vitro* phenotypic inhibition assay is critical to help predict ARV drug resistance as a guideline for clinicians to obtain a combined interpretation among genotypic resistance, phenotypic inhibition for the optimal future treatment of difficult to treat patients with treatment failure.

References:

Introduction

1. Hirsch VM, Dapolito GA, Goldstein S, McClure H, Emau P, Fultz PN, et al. A distinct African lentivirus from Sykes' monkeys. J Virol. 1993 Mar;67(3):1517–28.

2. Hahn BH, Shaw GM, De Cock KM, Sharp PM. AIDS as a zoonosis: scientific and public health implications. Science. 2000 Jan 28;287(5453):607–14.

3. Vahlne A. A historical reflection on the discovery of human retroviruses. Retrovirology. 2009 May 1;6:40.

4. Clavel F, Guétard D, Brun-Vézinet F, Chamaret S, Rey MA, Santos-Ferreira MO, et al. Isolation of a new human retrovirus from West African patients with AIDS. Science. 1986 Jul 18;233(4761):343–6.

5. Chakrabarti L, Guyader M, Alizon M, Daniel MD, Desrosiers RC, Tiollais P, et al. Sequence of simian immunodeficiency virus from macaque and its relationship to other human and simian retroviruses. Nature. 1987 Aug;328(6130):543–7.

6. Guyader M, Emerman M, Sonigo P, Clavel F, Montagnier L, Alizon M. Genome organization and transactivation of the human immunodeficiency virus type 2. Nature. 1987 Apr;326(6114):662–9.

7. Sharp PM, Hahn BH. Origins of HIV and the AIDS Pandemic. Cold Spring Harb Perspect Med. 2011 Sep;1(1).

8. Guindon S, Gascuel O. A Simple, Fast, and Accurate Algorithm to Estimate Large Phylogenies by Maximum Likelihood. Syst Biol. 2003 Oct 1;52(5):696–704.

9. Roser M, Ritchie H. HIV / AIDS. Our World in Data [Internet]. 2018 Apr 3 [cited 2020 Mar 9]; Available from: https://ourworldindata.org/hiv-aids

10. Global HIV and AIDS statistics [Internet]. Avert. 2015 [cited 2020 Mar 9]. Available from: https://www.avert.org/global-hiv-and-aids-statistics

11. UNAIDS 'AIDSinfo' (accessed August 2019) http://aidsinfo.unaids.org/

12. Bendavid E. Past and Future Performance: PEPFAR in the Landscape of Foreign Aid for Health. Curr HIV/AIDS Rep. 2016 Oct;13(5):256–62.

13. Luciw PA, Pratt-Lowe E, Shaw KE, Levy JA, Cheng-Mayer C. Persistent infection of rhesus macaques with T-cell-line-tropic and macrophage-tropic clones of simian/human immunodeficiency viruses (SHIV). Proc Natl Acad Sci U S A. 1995 Aug 1;92(16):7490–4.

14. Orloff GM, Kennedy MS, Dawson C, McDougal JS. HIV-1 binding to CD4 T cells does not induce a Ca2+ influx or lead to activation of protein kinases. AIDS Res Hum Retroviruses. 1991 Jul;7(7):587–93.

15. Wilen CB, Tilton JC, Doms RW. HIV: Cell Binding and Entry. Cold Spring Harb Perspect Med. 2012 Aug;2(8).

16. Hemelaar J. The origin and diversity of the HIV-1 pandemic. Trends in Molecular Medicine. 2012 Mar 1;18(3):182–92.

17. German Advisory Committee Blood (Arbeitskreis Blut), Subgroup 'Assessment of Pathogens Transmissible by Blood'. Human Immunodeficiency Virus (HIV). *Transfus Med Hemother*. 2016;43(3):203-222.

18. Takehisa J, Kraus MH, Ayouba A, et al. Origin and biology of simian immunodeficiency virus in wild-living western gorillas. *J Virol*. 2009;83(4):1635-1648.

19. Carr JK, Torimiro JN, Wolfe ND, Eitel MN, Kim B, Sanders-Buell E, et al. The AG recombinant IbNG and novel strains of group M HIV-1 are common in Cameroon. Virology. 2001 Jul 20;286(1):168–81.

20. Lau KA, Wong JJL. Current Trends of HIV Recombination Worldwide. Infect Dis Rep. 2013 Jun ;5(Suppl 1).

21. Checkley MA, Luttge BG, Freed EO. HIV-1 Envelope Glycoprotein Biosynthesis, Trafficking, and Incorporation. J Mol Biol. 2011 Jul 22;410(4):582–608.

22. Fanales-Belasio E, Raimondo M, Suligoi B, Buttò S. HIV virology and pathogenetic mechanisms of infection: a brief overview. Ann Ist Super Sanita. 2010;46(1):5–14.

23. Saphire EO, Parren PW, Pantophlet R, Zwick MB, Morris GM, Rudd PM, et al. Crystal structure of a neutralizing human IGG against HIV-1: a template for vaccine design. Science. 2001 Aug 10;293(5532):1155–9.

24. Arthos J, Cicala C, Martinelli E, Macleod K, Van Ryk D, Wei D, et al. HIV-1 envelope protein binds to and signals through integrin alpha4beta7, the gut mucosal homing receptor for peripheral T cells. Nat Immunol. 2008 Mar;9(3):301–9.

25. Joseph SB, Arrildt KT, Swanstrom AE, Schnell G, Lee B, Hoxie JA, et al. Quantification of entry phenotypes of macrophage-tropic HIV-1 across a wide range of CD4 densities. J Virol. 2014 Feb;88(4):1858–69.

26. Orloff GM, Kennedy MS, Dawson C, McDougal JS. HIV-1 binding to CD4 T cells does not induce a Ca2+ influx or lead to activation of protein kinases. AIDS Res Hum Retroviruses. 1991 Jul;7(7):587–93.

27. Wilen CB, Tilton JC, Doms RW. HIV: Cell Binding and Entry. Cold Spring Harb Perspect Med. 2012 Aug;2(8).

28. Maddon PJ, Dalgleish AG, McDougal JS, Clapham PR, Weiss RA, Axel R. The T4 gene encodes the AIDS virus receptor and is expressed in the immune system and the brain. Cell. 1986 Nov 7;47(3):333–48.

29. Pritchard LK, Vasiljevic S, Ozorowski G, Seabright GE, Cupo A, Ringe R, et al. Structural constraints determine the glycosylation of HIV-1 envelope trimers. Cell Rep. 2015 Jun 16;11(10):1604–13.

30. Liu H, Chao D, Nakayama EE, Taguchi H, Goto M, Xin X, et al. Polymorphism in RANTES chemokine promoter affects HIV-1 disease progression. Proc Natl Acad Sci U S A. 1999 Apr 13;96(8):4581–5.

31.. Berger EA, Doms RW, Fenyö E-M, Korber BTM, Littman DR, Moore JP, et al. A new classification for HIV-1. Nature. 1998 Jan;391(6664):240–240.

32. PR Clapham PR, McKnight Á. HIV-1 receptors and cell tropism. British Medical Bulletin. 2001 September;58(1):43–59.

33. Kwong PD, Wyatt R, Robinson J, Sweet RW, Sodroski J, Hendrickson WA. Structure of an HIV gp120 envelope glycoprotein in complex with the CD4 receptor and a neutralizing human antibody. Nature. 1998 Jun 18;393(6686):648–59.

34. da Silva ES, Mulinge M, Bercoff DP. The frantic play of the concealed HIV envelope cytoplasmic tail. Retrovirology. 2013 May 24;10:54.

35. Moore JP, Trkola A, Dragic T. Co-receptors for HIV-1 entry. Curr Opin Immunol. 1997 Aug;9(4):551–62.

36. Chan DC, Fass D, Berger JM, Kim PS. Core structure of gp41 from the HIV envelope glycoprotein. Cell. 1997 Apr 18;89(2):263–73.

37. Melikyan GB. Common principles and intermediates of viral protein-mediated fusion: the HIV-1 paradigm. Retrovirology. 2008 Dec 10;5:111.

38. Miyauchi K, Kim Y, Latinovic O, Morozov V, Melikyan GB. HIV enters cells via endocytosis and dynamin-dependent fusion with endosomes. Cell. 2009 May 1;137(3):433–44.

39.. Goto T, Nakai M, Ikuta K. The life-cycle of human immunodeficiency virus type 1. Micron. 1998 Jun;29(2–3):123–38.

40. Sarafianos SG, Marchand B, Das K, Himmel D, Parniak MA, Hughes SH, et al. Structure and function of HIV-1 reverse transcriptase: molecular mechanisms of polymerization and inhibition. J Mol Biol. 2009 Jan 23;385(3):693–713.

41. Hu W-S, Hughes SH. HIV-1 reverse transcription. Cold Spring Harb Perspect Med. 2012 Oct 1;2(10).

42. Alberts B, Johnson A, Lewis J, Raff M, Roberts K, Walter P. DNA Replication Mechanisms. Molecular Biology of the Cell 4th edition [Internet]. 2002 [cited 2020 Mar 9]; Available from: https://www.ncbi.nlm.nih.gov/books/NBK26850/

43. Jayappa KD, Ao Z, Yao X. The HIV-1 passage from cytoplasm to nucleus: the process involving a complex exchange between the components of HIV-1 and cellular machinery to access nucleus and successful integration. Int J Biochem Mol Biol. 2012 Feb 25;3(1):70–85.

44. Varmus HE, Brown PO, Berg DE, Howe MM 1989. Retroviruses in Mobile DNA. American Society for Microbiology. 1989;53–108.

45. Corboy JR, Buzy JM, Zink MC, Clements JE: Expression directed from HIV long terminal repeats in the central nervous system of transgenic mice. Science 1992, 258: 1804-1808.

46. Sundquist WI, Kräusslich H-G. HIV-1 assembly, budding, and maturation. Cold Spring Harb Perspect Med. 2012 Jul;2(7):a006924.

47. Maartens G, Celum C, Lewin SR. HIV infection: epidemiology, pathogenesis, treatment, and prevention. Lancet. 2014 Jul 19;384(9939):258–71.

48. Wells TN, Power CA, Lusti-Narasimhan M, Hoogewerf AJ, Cooke RM, Chung CW, et al. Selectivity and antagonism of chemokine receptors. J Leukoc Biol. 1996 Jan;59(1):53–60.

49. Arthos J, Rubbert A, Rabin RL, Cicala C, Machado E, Wildt K, et al. CCR5 Signal Transduction in Macrophages by Human Immunodeficiency Virus and Simian Immunodeficiency Virus Envelopes. J Virol. 2000 Jul;74(14):6418–24.

50. Clapham PR, McKnight Á. Cell surface receptors, virus entry and tropism of primate lentiviruses. J Gen Virol. 2002 Aug;83(Pt 8):1809–29.

51. Pustylnikov S, Sagar D, Jain P, Khan ZK. Targeting the C-type Lectins-Mediated Host-Pathogen Interactions with Dextran. J Pharm Pharm Sci. 2014;17(3):371–92.

52. Geijtenbeek TB, Torensma R, van Vliet SJ, van Duijnhoven GC, Adema GJ, van Kooyk Y, et al. Identification of DC-SIGN, a novel dendritic cell-specific ICAM-3 receptor that supports primary immune responses. Cell. 2000 Mar 3;100(5):575–85.

53. Liu C, Perilla JR, Ning J, Lu M, Hou G, Ramalho R, et al. Cyclophilin A stabilizes the HIV-1 capsid through a novel non-canonical binding site. Nat Commun. 2016 Apr;7(1):10714.

54. Forshey BM, von Schwedler U, Sundquist WI, Aiken C. Formation of a Human Immunodeficiency Virus Type 1 Core of Optimal Stability Is Crucial for Viral Replication. J Virol. 2002 Jun;76(11):5667–77.

55. Brass AL, Dykxhoorn DM, Benita Y, Yan N, Engelman A, Xavier RJ, et al. Identification of Host Proteins Required for HIV Infection Through a Functional Genomic Screen. Science. 2008 Feb 15;319(5865):921–6.

56. Cen S, Khorchid A, Javanbakht H, Gabor J, Stello T, Shiba K, et al. Incorporation of lysyl-tRNA synthetase into human immunodeficiency virus type 1. J Virol. 2001 Jun;75(11):5043–8.

57. Shehu-Xhilaga M, Lee J-Y, Campbell S, Marshall JA, Crowe SM, Mak J. Overexpression and incorporation of GagPol precursor does not impede packaging of HIV-1 tRNA (Lys3) but promotes intracellular budding of virus-like particles. J Biomed Sci. 2002 Dec;9(6 Pt 2):697–705.

58. König R, Zhou Y, Elleder D, Diamond TL, Bonamy GMC, Irelan JT, et al. Global analysis of host-pathogen interactions that regulate early-stage HIV-1 replication. Cell. 2008 Oct 3;135(1):49–60.

59. Valle-Casuso JC, Di Nunzio F, Yang Y, Reszka N, Lienlaf M, Arhel N, et al. TNPO3 is required for HIV-1 replication after nuclear import but prior to integration and binds the HIV-1 core. J Virol. 2012 May;86(10):5931–6.

60. Ao Z, Huang G, Yao H, Xu Z, Labine M, Cochrane AW, et al. Interaction of Human Immunodeficiency Virus Type 1 Integrase with Cellular Nuclear Import Receptor Importin 7 and Its Impact on Viral Replication. J Biol Chem. 2007 May 4;282(18):13456–67.

61. Ciuffi A, Llano M, Poeschla E, Hoffmann C, Leipzig J, Shinn P, et al. A role for LEDGF/p75 in targeting HIV DNA integration. Nat Med. 2005 Dec;11(12):1287–9.

62. Kalpana GV, Marmon S, Wang W, Crabtree GR, Goff SP. Binding and stimulation of HIV-1 integrase by a human homolog of yeast transcription factor SNF5. Science. 1994 Dec 23;266(5193):2002–6.

63. Sorin M, Cano J, Das S, Mathew S, Wu X, Davies KP, et al. Recruitment of a SAP18-HDAC1 Complex into HIV-1 Virions and Its Requirement for Viral Replication. PLoS Pathog. 2009 Jun 5;5(6).

64. Hamamoto S, Nishitsuji H, Amagasa T, Kannagi M, Masuda T. Identification of a Novel Human Immunodeficiency Virus Type 1 Integrase Interactor, Gemin2, That Facilitates Efficient Viral cDNA Synthesis In Vivo. J Virol. 2006 Jun;80(12):5670–7.

65. Wang W, Côté J, Xue Y, Zhou S, Khavari PA, Biggar SR, et al. Purification and biochemical heterogeneity of the mammalian SWI-SNF complex. EMBO J. 1996 Oct 1;15(19):5370–82.

66. Clerzius G, Gélinas J-F, Daher A, Bonnet M, Meurs EF, Gatignol A. ADAR1 Interacts with PKR during Human Immunodeficiency Virus Infection of Lymphocytes and Contributes to Viral Replication. Journal of Virology. 2009 Oct 1;83(19):10119–28.

67. Clerzius G, Shaw E, Daher A, Burugu S, Gélinas J-F, Ear T, et al. The PKR activator, PACT, becomes a PKR inhibitor during HIV-1 replication. Retrovirology. 2013 Sep 11;10:96.

68. Mogensen TH. Pathogen recognition and inflammatory signalling in innate immune defenses. Clin Microbiol Rev. 2009 Apr;22(2):240-73.

69. Diebold SS. Innate Antiviral Responses by Means of TLR7-Mediated Recognition of Single-Stranded RNA. Science. 2004 Mar 5;303(5663):1529–31.

70. Kadowaki N, Ho S, Antonenko S, de Waal Malefyt R, Kastelein RA, Bazan F, et al. Subsets of Human Dendritic Cell Precursors Express Different Toll-like Receptors and Respond to Different Microbial Antigens. The Journal of Experimental Medicine. 2001 Sep 17;194(6):863–70.

71. Meier A, Alter G, Frahm N, Sidhu H, Li B, Bagchi A, et al. MyD88-Dependent Immune Activation Mediated by Human Immunodeficiency Virus Type 1-Encoded Toll-Like Receptor Ligands. Journal of Virology. 2007 Aug 1;81(15):8180–91.

72. Stacey AR, Norris PJ, Qin L, Haygreen EA, Taylor E, Heitman J, et al. Induction of a Striking Systemic Cytokine Cascade prior to Peak Viremia in Acute Human Immunodeficiency Virus Type 1 Infection, in Contrast to More Modest and Delayed Responses in Acute Hepatitis B and C Virus Infections. Journal of Virology. 2009 Apr 15;83(8):3719–33.

73. Lapenta C, Santini SM, Proietti E, Rizza P, Logozzi M, Spada M, Parlato S, Fais S, Pitha PM, Belardelli F. Type I interferon is a powerful inhibitor of in vivo HIV-1 infection and preserves human CD4(+) T cells from virus-induced depletion in SCID mice transplanted with human cells. Virology. 1999 Oct 10;263(1):78-88.

74. Alter G, Teigen N, Ahern R, Streeck H, Meier A, Rosenberg ES, et al. Evolution of Innate and Adaptive Effector Cell Functions during Acute HIV-1 Infection. J Infect Dis. 2007 May 15;195(10):1452–60.

75. Fausther-Bovendo H, Sol-Foulon N, Candotti D, et al. HIV escape from natural killer cytotoxicity: nef inhibits NKp44L expression on CD4+ T cells. AIDS. 2009;23:1077–87.

76. McMichael AJ, Borrow P, Tomaras GD, Goonetilleke N, Haynes BF. The immune response during acute HIV-1 infection: clues for vaccine development. Nat Rev Immunol. 2010 Jan;10(1):11–23.

77. Borrow P, Lewicki H, Hahn BH, Shaw GM, Oldstone MB. Virus-specific CD8+ cytotoxic T-lymphocyte activity associated with control of viremia in primary human immunodeficiency virus type 1 infection. J Virol. 1994 Sep;68(9):6103–10.

78. Euler Z, Schuitemaker H. Cross-reactive broadly neutralizing antibodies: timing is everything. Front Immunol. 2012;3:215.

79. Boasso A, Shearer GM, Chougnet C. Immune dysregulation in human immunodeficiency virus infection: know it, fix it, prevent it? Journal of Internal Medicine. 2009 Jan;265(1):78–96.

80. InformedHealth.org [Internet]. Cologne, Germany: Institute for Quality and Efficiency in Health Care (IQWiG); 2006-. The defense mechanisms of the adaptive immune system. 2010 Dec 14 [Updated 2016 Aug 4]. Available from: https://www.ncbi.nlm.nih.gov/books/NBK279397/

81. Tomaras GD, Yates NL, Liu P, Qin L, Fouda GG, Chavez LL, et al. Initial B-cell responses to transmitted human immunodeficiency virus type 1: virion-binding immunoglobulin M (IgM) and IgG antibodies followed by plasma anti-gp41 antibodies with ineffective control of initial viremia. J Virol. 2008 Dec;82(24):12449–63.

82. Richman DD, Wrin T, Little SJ, Petropoulos CJ. Rapid evolution of the neutralizing antibody response to HIV type 1 infection. Proc N86, atl Acad Sci USA. 2003 Apr 1;100(7):4144–9.

83. Klein E, Ho RJY. Challenges in the development of an effective HIV vaccine: Current approaches and future directions. Clinical Therapeutics. 2000 Mar 1;22(3):295–314.

84. Forthal DN. Functions of Antibodies. Microbiol Spectr. 2014 Aug 15;2(4):1–17.

85. Forthal DN, Landucci G, Haubrich R, Keenan B, Kuppermann BD, Tilles JG, et al. Antibody-dependent cellular cytotoxicity independently predicts survival in severely immunocompromised human immunodeficiency virus-infected patients. J Infect Dis. 1999 Oct;180(4):1338–41.

86. de Vries W, Haasnoot J, van der Velden J, van Montfort T, Zorgdrager F, Paxton W, et al. Increased virus replication in mammalian cells by blocking intracellular innate defense responses. Gene Therapy. 2008 Apr;15(7):545–52.

87. Alter G, Martin MP, Teigen N, Carr WH, Suscovich TJ, Schneidewind A, et al. Differential natural killer cell–mediated inhibition of HIV-1 replication based on distinct KIR/HLA subtypes. Journal of Experimental Medicine. 2007 Nov 26;204(12):3027–36.

88. Favoreel HW, Van de Walle GR, Nauwynck HJ, Pensaert MB. Virus complement evasion strategies. J Gen Virol. 2003 Jan;84(Pt 1):1–15.

89. Goto T, Kennel SJ, Abe M, Takishita M, Kosaka M, Solomon A, et al. A novel membrane antigen selectively expressed on terminally differentiated human B cells. Blood. 1994 Sep 15;84(6):1922–30.

90. Serra-Moreno R, Jia B, Breed M, Alvarez X, Evans DT. Compensatory changes in the cytoplasmic tail of gp41 confer resistance to tetherin/BST-2 in a pathogenic nef-deleted SIV. Cell Host Microbe. 2011 Jan 20;9(1):46–57.

91. Reitter JN, Means RE, Desrosiers RC. A role for carbohydrates in immune evasion in AIDS. Nat Med. 1998 Jun;4(6):679–84.

92. Piguet V, Trono D. Living in oblivion: HIV immune evasion. Semin Immunol. 2001 Feb;13(1):51–7.

93. Stevenson M. HIV-1 pathogenesis. Nature Medicine. 2003 Jul;9(7):853–60.

94. Keckesova Z, Ylinen LMJ, Towers GJ. The human and African green monkey TRIM5alpha genes encode Ref1 and Lv1 retroviral restriction factor activities. Proceedings of the National Academy of Sciences of the United States of America 2004;101:10780–5.

95. Asaoka K, Ikeda K, Hishinuma T, Horie-Inoue K, Takeda S, Inoue S. A retrovirus restriction factor TRIM5alpha is transcriptionally regulated by interferons. Biochemical and Biophysical Research Communications 2005;338:1950–6.

96. Tissot C, Mechti N. Molecular cloning of a new interferon-induced factor that represses human immunodeficiency virus type 1 long terminal repeat expression. J Biol Chem. 1995 Jun 23;270(25):14891–8.

97. Kajaste-Rudnitski A, Marelli SS, Pultrone C, Pertel T, Uchil PD, Mechti N, et al. TRIM22 inhibits HIV-1 transcription independently of its E3 ubiquitin ligase activity, Tat, and NF-kappaB-responsive long terminal repeat elements. J Virol. 2011 May;85(10):5183–96.

98. Li M, Kao E, Gao X, Sandig H, Limmer K, Pavon-Eternod M, et al. Codon-usage-based inhibition of HIV protein synthesis by human schlafen 11. Nature. 2012 Nov 1;491(7422):125–8.

99. Neil SJD, Zang T, Bieniasz PD. Tetherin inhibits retrovirus release and is antagonized by HIV-1 Vpu. Nature. 2008 Jan 24;451(7177):425–30.

100. Perez-Caballero D, Zang T, Ebrahimi A, McNatt MW, Gregory DA, Johnson MC, et al. Tetherin inhibits HIV-1 release by directly tethering virions to cells. Cell. 2009 Oct 30;139(3):499–511.

101. Langford SE, Ananworanich J, Cooper DA. Predictors of disease progression in HIV infection: a review. AIDS Res Ther. 2007 May 14;4:11.

102. Fauci AS, Pantaleo G, Stanley S, Weissman D. Immunopathogenic Mechanisms of HIV Infection. Ann Intern Med. 1996;124:654–663.

103. Imami N, Westrop SJ, Grageda N, Herasimtschuk AA. Long-Term Non-Progression and Broad HIV-1-Specific Proliferative T-Cell Responses. Front Immunol [Internet]. 2013 Mar 1 [cited 2020 Apr 1];4. Available from: https://www.ncbi.nlm.nih.gov/pmc/articles/PMC3585435/

104. Pandhi D, Ailawadi P. Initiation of antiretroviral therapy. Indian Journal of Sexually Transmitted Diseases and AIDS. 2014 Jan 1;35(1):1.

105. Keiser O, Chi BH, Gsponer T, Boulle A, Orrell C, Phiri S, et al. Outcomes of antiretroviral treatment in programmes with and without routine viral load monitoring in southern Africa: AIDS. 2011 Sep;25(14):1761–9.

106. Zhang N, Huang T, Kang D, Wang N. Increase Access to Timely and Periodic Viral Load Testing to Achieve the 90-90-90 Targets for Human Immunodeficiency Virus in China. Clin Infect Dis. 2018 Aug 16;67(5):808–9.

107. Sigaloff KC1, Hamers RL, Wallis CL, Kityo C, Siwale M, Ive P, Botes ME, Mandaliya K, Wellington M, Osibogun A, Stevens WS, van Vugt M, de Wit TF; PharmAccess African Studies to Evaluate Resistance (PASER). Unnecessary antiretroviral treatment switches and accumulation of HIV resistance mutations; two arguments for viral load monitoring in Africa. J Acquir Immune Defic Syndr. 2011 Sep 1;58(1):23–31.

108. Haas AD, Keiser O, Balestre E, Brown S, Bissagnene E, Chimbetete C, et al. Monitoring and Switching of First-line Antiretroviral Therapy in sub-Saharan Africa: Collaborative Analysis of Adult Treatment Cohorts. Lancet HIV. 2015 Jul 1;2(7):e271–8.

109. Hankins CA, de Zalduondo BO. Combination prevention: a deeper understanding of effective HIV prevention. AIDS. 2010 Oct;24 Suppl 4:S70-80.

110. Auvert B, Taljaard D, Lagarde E, Sobngwi-Tambekou J, Sitta R, Puren A. Randomized, Controlled Intervention Trial of Male Circumcision for Reduction of HIV Infection Risk: The ANRS 1265 Trial. PLOS Medicine. 2005 Oct 25;2(11):e298.

111. Krishnaratne S, Hensen B, Cordes J, Enstone J, Hargreaves JR. Interventions to strengthen the HIV prevention cascade: a systematic review of reviews. The Lancet HIV. 2016 Jul 1;3(7):e307–17.

112. Wilton J, Senn H, Sharma M, Tan DH. Pre-exposure prophylaxis for sexually acquired HIV risk management: a review. HIiV AIDS (Auckl). 2015 Apr 28;7:125–36.

113. World Health Organization. Consolidated Guidelines on HIV Prevention, Diagnosis, Treatment and Care for Key Populations. Geneva, Switzerland: World Health Organization; 2014. http://apps.who.int/iris/bitstream/10665/128048/1/9789241507431_eng.pdf?ua=1&ua=1.).

114. PrEP | HIV Basics | HIV/AIDS | CDC [Internet]. 2019 [cited 2020 Mar 9]. Available from: https://www.cdc.gov/hiv/basics/prep.html.

115. Sultan B, Benn P, Waters L. Current perspectives in HIV post-exposure prophylaxis. HIV AIDS (Auckl). 2014 Oct 24;6:147–58.

116. Meintjes G, Moorhouse MA, Carmona S, Davies N, Dlamini S, van Vuuren C, et al. Adult antiretroviral guidelines 2017. South Afr J HIV Med [Internet]. 2017 Jul 15 [cited 2020 Apr 3];18(1). Available from: https://www.ncbi.nlm.nih.gov/pmc/articles/PMC5843236/

117. ART Guidelines 15052015.pdf [Internet]. [cited 2020 Mar 9]. Available from: https://sahivsoc.org/Files/ART%20Guidelines%2015052015.pdf

118. Ministry of Health/National AIDS Council Zimbabwe (2018) 'Global AIDS Monitoring Zimbabwe Country Report', p.14 [pdf[).

119. Arts EJ, Hazuda DJ. HIV-1 Antiretroviral Drug Therapy. Cold Spring Harb Perspect Med. 2012 Apr;2(4).

120. Collier DA, Stöber G, Li T, Heils A, Catalano M, Di Bella D, et al. A novel functional polymorphism within the promoter of the serotonin transporter gene: possible role in susceptibility to affective disorders. Mol Psychiatry. 1996 Dec;1(6):453–60.

121. Autran B, Carcelain G, Li TS, Blanc C, Mathez D, Tubiana R, et al. Positive effects of combined antiretroviral therapy on CD4+ T cell homeostasis and function in advanced HIV disease. Science. 1997 Jul 4;277(5322):112–6.

122. Dragic T, Trkola A, Thompson DA, Cormier EG, Kajumo FA, Maxwell E, et al. A binding pocket for a small molecule inhibitor of HIV-1 entry within the transmembrane helices of CCR5. Proc Natl Acad Sci USA. 2000 May 9;97(10):5639–44.

123. Dorr P, Westby M, Dobbs S, Griffin P, Irvine B, Macartney M, et al. Maraviroc (UK-427,857), a potent, orally bioavailable, and selective small-molecule inhibitor of chemokine receptor CCR5 with broad-spectrum anti-human immunodeficiency virus type 1 activity. Antimicrob Agents Chemother. 2005 Nov;49(11):4721–32.

124.. Hendrix CW, Collier AC, Lederman MM, Schols D, Pollard RB, Brown S, et al. Safety, Pharmacokinetics, and Antiviral Activity of AMD3100, a Selective CXCR4 Receptor Inhibitor, in HIV-1 Infection. JAIDS Journal of Acquired Immune Deficiency Syndromes. 2004 Oct 1;37(2):1253–1262.

125. Wild C, Greenwell T, Matthews T. A synthetic peptide from HIV-1 gp41 is a potent inhibitor of virus-mediated cell-cell fusion. AIDS Res Hum Retroviruses. 1993 Nov;9(11):1051–3.

126. Kilby JM, Hopkins S, Venetta TM, DiMassimo B, Cloud GA, Lee JY, et al. Potent suppression of HIV-1 replication in humans by T-20, a peptide inhibitor of gp41-mediated virus entry. Nat Med. 1998 Nov;4(11):1302–7.

127. Yuan W, Craig S, Si Z, Farzan M, Sodroski J. CD4-Induced T-20 Binding to Human Immunodeficiency Virus Type 1 gp120 Blocks Interaction with the CXCR4 Coreceptor. Journal of Virology. 2004 May 15;78(10):5448–57.

128. Rimsky LT, Shugars DC, Matthews TJ. Determinants of Human Immunodeficiency Virus Type 1 Resistance to gp41-Derived Inhibitory Peptides. J Virol. 1998 Feb;72(2):986–93.

129. Wei X, Decker JM, Liu H, Zhang Z, Arani RB, Kilby JM, et al. Emergence of Resistant Human Immunodeficiency Virus Type 1 in Patients Receiving Fusion Inhibitor (T-20) Monotherapy. Antimicrob Agents Chemother. 2002 Jun;46(6):1896–905.

130. Reeves JD, Hibbitts S, Simmons G, McKnight Á, Azevedo-Pereira JM, Moniz-Pereira J, et al. Primary Human Immunodeficiency Virus Type 2 (HIV-2) Isolates Infect CD4-Negative Cells via CCR5 and CXCR4: Comparison with HIV-1 and Simian Immunodeficiency Virus and Relevance to Cell Tropism In Vivo. J Virol. 1999 Sep;73(9):7795–804.

131. Ray PE, Soler-García AA, Xu L, Soderland C, Blumenthal R, Puri A. Fusion of HIV-1 envelope-expressing cells to human glomerular endothelial cells through an CXCR4-mediated mechanism. Pediatr Nephrol. 2005 Oct;20(10):1401–9.

132. Baldwin CE, Sanders RW, Deng Y, Jurriaans S, Lange JM, Lu M, et al. Emergence of a Drug-Dependent Human Immunodeficiency Virus Type 1 Variant during Therapy with the T20 Fusion Inhibitor. J Virol. 2004 Nov;78(22):12428–37.

133. Mitsuya H, Weinhold KJ, Furman PA, Clair MHS, Lehrman SN, Gallo RC, et al. 3'-Azido-3'-deoxythymidine (BW A509U): an antiviral agent that inhibits the infectivity and cytopathic effect of human T-lymphotropic virus type III/lymphadenopathy-associated virus in vitro. PNAS. 1985 Oct 1;82(20):7096–100.

134. Lavie A, Schlichting I, Vetter IR, Konrads M, Reinstein J, Goody RS. The bottleneck in AZT activation. Nature Medicine. 1997 Aug;3(8):922–4.

135. Richman DM, Wacker DP, Cooper-Brown LJ, Kayser K, Crosland K, Stephens TJ, et al. Stimulus Characteristics Within Directives: Effects on Accuracy of Task Completion. Journal of Applied Behavior Analysis. 2001;34(3):289–312.

136 155. Young FE. The role of the FDA in the effort against AIDS. Public Health Rep. 1988;103: 242–245.

137. Nakashima H, Matsui T, Harada S, Kobayashi N, Matsuda A, Ueda T, et al. Inhibition of replication and cytopathic effect of human T cell lymphotropic virus type III/lymphadenopathy-associated virus by 3'-azido-3'-deoxythymidine in vitro. Antimicrob Agents Chemother. 1986 Dec;30(6):933–7.

138. Hooker DJ, Tachedjian G, Solomon AE, Gurusinghe AD, Land S, Birch C, et al. An in vivo mutation from leucine to tryptophan at position 210 in human immunodeficiency virus type 1 reverse transcriptase contributes to high-level resistance to 3'-azido-3'-deoxythymidine. J Virol. 1996 Nov;70(11):8010–8.

139. De Clercq E. The history of antiretrovirals: key discoveries over the past 25 years. Rev Med Virol. 2009 Sep;19(5):287–99.

140. Prokofjeva MM, Kochetkov SN, Prassolov VS. Therapy of HIV Infection: Current Approaches and Prospects. Acta Naturae. 2016;8(4):23–32.

141. Doong SL, Tsai CH, Schinazi RF, Liotta DC, Cheng YC. Inhibition of the replication of hepatitis B virus in vitro by 2',3'-dideoxy-3'-thiacytidine and related analogues. Proc Natl Acad Sci U S A. 1991 Oct 1;88(19):8495–9.

142. Cihlar T, Ray AS. Nucleoside and nucleotide HIV reverse transcriptase inhibitors: 25 years after zidovudine. Antiviral Res. 2010 Jan;85(1):39–58.

143. Cruchaga C, Ansó E, Rouzaut A, Martínez-Irujo JJ. Selective Excision of Chain-terminating Nucleotides by HIV-1 Reverse Transcriptase with Phosphonoformate as Substrate. J Biol Chem. 2006 Sep 22;281(38):27744–52.

144. Kohlstaedt LA, Wang J, Friedman JM, Rice PA, Steitz TA. Crystal structure at 3.5 A resolution of HIV-1 reverse transcriptase complexed with an inhibitor. Science. 1992 Jun 26;256(5065):1783–90.

145. DeGruttola V, Dix L, D'Aquila R, Holder D, Phillips A, Ait-Khaled M, et al. The relation between baseline HIV drug resistance and response to antiretroviral therapy: re-analysis of retrospective and prospective studies using a standardized data analysis plan. Antivir Ther (Lond). 2000 Mar;5(1):41–8.

146. Hsiou Y, Ding J, Das K, Clark AD, Hughes SH, Arnold E. Structure of unliganded HIV-1 reverse transcriptase at 2.7 A resolution: implications of conformational changes for polymerization and inhibition mechanisms. Structure. 1996 Jul 15;4(7):853–60.

147. de Béthune M-P. Non-nucleoside reverse transcriptase inhibitors (NNRTIs), their discovery, development, and use in the treatment of HIV-1 infection: a review of the last 20 years (1989-2009). Antiviral Res. 2010 Jan;85(1):75–90.

148. Grob PM, Wu JC, Cohen KA, Ingraham RH, Shih CK, Hargrave KD, et al. Nonnucleoside inhibitors of HIV-1 reverse transcriptase: nevirapine as a prototyp1e drug. AIDS Res Hum Retroviruses. 1992 Feb;8(2):145–52.

149. Tsibris AMN, Hirsch MS. 130 - Antiretroviral Therapy for Human Immunodeficiency Virus Infection. In: Bennett JE, Dolin R, Blaser MJ, editors. Mandell, Douglas, and Bennett's Principles and Practice of Infectious Diseases (Eighth Edition) [Internet]. Philadelphia: Content Repository Only; 2015:1622-1641.e6.

150. Debyser Z, Pauwels R, Andries K, Desmyter J, Kukla M, Janssen PA, et al. An antiviral target on reverse transcriptase of human immunodeficiency virus type 1 revealed by tetrahydroimidazo-[4,5,1-jk] [1,4] benzodiazepin-2 (1H)-one and -thione derivatives. Proc Natl Acad Sci U S A. 1991 Feb 15;88(4):1451–5.

151. Fletcher RS, Syed K, Mithani S, Dmitrienko GI, Parniak MA. Carboxanilide derivative non-nucleoside inhibitors of HIV-1 reverse transcriptase interact with different mechanistic forms of the enzyme. Biochemistry. 1995 Apr 4;34(13):4346–53.

152. Rittinger K, Divita G, Goody RS. Human immunodeficiency virus reverse transcriptase substrate-induced conformational changes and the mechanism of inhibition by nonnucleoside inhibitors. Proc Natl Acad Sci U S A. 1995 Aug 15;92(17):8046–9.

153. Hang JQ, Li Y, Yang Y, Cammack N, Mirzadegan T, Klumpp K. Substrate-dependent inhibition or stimulation of HIV RNase H activity by non-nucleoside reverse transcriptase inhibitors (NNRTIs). Biochem Biophys Res Commun. 2007 Jan 12;352(2):341–50.

154. Park J, Morrow CD. Mutations in the Protease Gene of Human Immunodeficiency Virus Type 1 Affect Release and Stability of Virus Particles. Virology. 1993 Jun 1;194(2):843–50.

155. Madruga JV, Cahn P, Grinsztejn B, Haubrich R, Lalezari J, Mills A, et al. Efficacy and safety of TMC125 (etravirine) in treatment-experienced HIV-1-infected patients in DUET-1: 24-week results from a randomised, double-blind, placebo-controlled trial. Lancet. 2007 Jul 7;370(9581):29–38.

156. Roberts NA, Martin JA, Kinchington D, Broadhurst AV, Craig JC, Duncan IB, et al. Rational design of peptide-based HIV proteinase inhibitors. Science. 1990 Apr 20;248(4953):358–61.

157. Shafer RW, Dupnik K, Winters MA, Eshleman SH. A Guide to HIV-1 Reverse Transcriptase and Protease Sequencing for Drug Resistance Studies. HIV Seq Compend. 2001; 2001:1–51.

158. Clavel F, Hance AJ. HIV Drug Resistance. New England Journal of Medicine. 2004 Mar 4;350(10):1023–35.

159 . Wensing AMJ, van Maarseveen NM, Nijhuis M. Fifteen years of HIV Protease Inhibitors: raising the barrier to resistance. Antiviral Res. 2010 Jan;85(1):59–74.

160. Espeseth AS, Felock P, Wolfe A, Witmer M, Grobler J, Anthony N, et al. HIV-1 integrase inhibitors that compete with the target DNA substrate define a unique strand transfer conformation for integrase. Proc Natl Acad Sci U S A. 2000 Oct 10;97(21):11244–9.

161. Hazuda DJ, Felock P, Witmer M, Wolfe A, Stillmock K, Grobler JA, et al. Inhibitors of Strand Transfer That Prevent Integration and Inhibit HIV-1 Replication in Cells. Science. 2000 Jan 28;287(5453):646–50.

162. Grobler JA, Stillmock K, Hu B, Witmer M, Felock P, Espeseth AS, et al. Diketo acid inhibitor mechanism and HIV-1 integrase: Implications for metal binding in the active site of phosphotransferase enzymes. Proc Natl Acad Sci U S A. 2002 May 14;99(10):6661–6.

163. Grinsztejn B, Nguyen B-Y, Katlama C, Gatell JM, Lazzarin A, Vittecoq D, et al. Safety and efficacy of the HIV-1 integrase inhibitor raltegravir (MK-0518) in treatment-experienced patients with multidrug-resistant virus: a phase II randomised controlled trial. Lancet. 2007 Apr 14;369(9569):1261–9.

164. Hare S, Vos AM, Clayton RF, Thuring JW, Cummings MD, Cherepanov P. Molecular mechanisms of retroviral integrase inhibition and the evolution of viral resistance. Proc Natl Acad Sci U S A. 2010 Nov 16;107(46):20057–62.

165. Palella FJ, Delaney KM, Moorman AC, Loveless MO, Fuhrer J, Satten GA, et al. Declining morbidity and mortality among patients with advanced human immunodeficiency virus infection. HIV Outpatient Study Investigators. N Engl J Med. 1998 Mar 26;338(13):853–60.

166. DeGruttola V, Dix L, D'Aquila R, Holder D, Phillips A, Ait-Khaled M, et al. The relation between baseline HIV drug resistance and response to antiretroviral therapy: re-analysis of retrospective and prospective studies using a standardized data analysis plan. Antivir Ther (Lond). 2000 Mar;5(1):41–8.

167. Iacob SA, Iacob DG, Jugulete G. Improving the Adherence to Antiretroviral Therapy, a Difficult but Essential Task for a Successful HIV Treatment—Clinical Points of View and Practical Considerations. Front Pharmacol. 2017 Nov 23;8.

168. Gardner EM, Burman WJ, Steiner JF, Anderson PL, Bangsberg DR. Antiretroviral medication adherence and the development of class-specific antiretroviral resistance. AIDS. 2009 Jun 1;23(9):1035–46.

169. Kumar S, Rao P, Earla R, Kumar A. Drug–drug interactions between anti-retroviral therapies and drugs of abuse in HIV systems. Expert Opin Drug Metab Toxicol. 2015 Mar;11(3):343–55.

170. Haase AT. Population biology of HIV-1 infection: viral and CD4+ T cell demographics and dynamics in lymphatic tissues. Annu Rev Immunol. 1999; 17:625–56.

171. Ho DD, Neumann AU, Perelson AS, Chen W, Leonard JM, Markowitz M. Rapid turnover of plasma virions and CD4 lymphocytes in HIV-1 infection. Nature. 1995 Jan12;373(6510):123–6.

172. RM, Mellors JW, Havlir D, Eron JJ, Gonzalez C, McMahon D, et al. Treatment with indinavir, zidovudine, and lamivudine in adults with human immunodeficiency virus infection and prior antiretroviral therapy. N Engl J Med. 1997 Sep 11;337(11):734–9.

173. Coffin JM. HIV Population Dynamics in Vivo: Implications for Genetic Variation, Pathogenesis, and Therapy. Science. 1995; 267:483–489.

174. De Luca A, Zazzi M. Interplay Between Transmitted and Acquired HIV Type 1 Drug Resistance: Reasons for a Disconnect. J Infect Dis. 2015 Jul 1;212(1):5–7.

175. Thierry E, Deprez E, Delelis O. Different Pathways Leading to Integrase Inhibitors Resistance. Front Microbiol [Internet]. 2017 Jan 11 [cited 2020 Apr 1];7. Available from: https://www.ncbi.nlm.nih.gov/pmc/articles/PMC5225119/

176. Oliveira M, Mesplède T, Quashie PK, Moïsi D, Wainberg MA. Resistance mutations against dolutegravir in HIV integrase impair the emergence of resistance against reverse transcriptase inhibitors: AIDS. 2014 Mar;28(6):813–9.

177. Li JZ, Paredes R, Ribaudo H, Svarovskaia ES, Metzner KJ, Kozal MJ, et al. Minority HIV-1 Drug Resistance Mutations and the Risk of NNRTI-based Antiretroviral Treatment Failure: A Systematic Review and Pooled Analysis. JAMA. 2011 Apr 6;305(13):1327–35.

178. Harrigan PR, Larder BA. Extent of Cross-Resistance between Agents Used To Treat Human Immunodeficiency Virus Type 1 Infection in Clinically Derived Isolates. Antimicrobial Agents and Chemotherapy. 2002 Mar 1;46(3):909–12.

179. Shafer RW, Kantor R, Gonzales MJ. The Genetic Basis of HIV-1 Resistance to Reverse Transcriptase and Protease Inhibitors. 2008;31.

180. Dulioust A, Paulous S, Guillemot L, Delavalle A-M, Boué F, Clavel F. Constrained Evolution of Human Immunodeficiency Virus Type 1 Protease during Sequential Therapy with Two Distinct Protease Inhibitors. J Virol. 1999 Jan;73(1):850–4.

181. Lobritz MA, Ratcliff AN, Arts EJ. HIV-1 Entry, Inhibitors, and Resistance. Viruses. 2010 Apr 29;2(5):1069–105.

182. Cilliers T, Nhlapo J, Coetzer M, Orlovic D, Ketas T, Olson WC, et al. The CCR5 and CXCR4 Coreceptors Are Both Used by Human Immunodeficiency Virus Type 1 Primary Isolates from Subtype C. Journal of Virology. 2003 Apr 1;77(7):4449–56.

183. Trkola A, Kuhmann SE, Strizki JM, Maxwell E, Ketas T, Morgan T, et al. HIV-1 escape from a small molecule, CCR5-specific entry inhibitor does not involve CXCR4 use. Proc Natl Acad Sci U S A. 2002 Jan 8;99(1):395–400.

184. Westby M, Lewis M, Whitcomb J, Youle M, Pozniak AL, James IT, et al. Emergence of CXCR4-Using Human Immunodeficiency Virus Type 1 (HIV-1) Variants in a Minority of HIV-1-Infected Patients following Treatment with the CCR5 Antagonist Maraviroc Is from a Pretreatment CXCR4-Using Virus Reservoir. J Virol. 2006 May;80(10):4909–20.

185. Derdeyn CA, Decker JM, Sfakianos JN, Zhang Z, O'Brien WA, Ratner L, et al. Sensitivity of human immunodeficiency virus type 1 to fusion inhibitors targeted to the gp41 first heptad repeat involves distinct regions of gp41 and is consistently modulated by gp120 interactions with the coreceptor. J Virol. 2001 Sep;75(18):8605–14.

186. Iyidogan P, Anderson KS. Recent findings on the mechanisms involved in tenofovir resistance. Antivir Chem Chemother. 2014 Dec 16;23(6):217–22.

187. Sarafianos SG, Das K, Ding J, Boyer PL, Hughes SH, Arnold E. Touching the heart of HIV-1 drug resistance: the fingers close down on the dNTP at the polymerase active site. Chem Biol. 1999 May;6(5): R137-146.

188. Descamps D, Flandre P, Calvez V, Peytavin G, Meiffredy V, Collin G, et al. Mechanisms of Virologic Failure in Previously Untreated HIV-Infected Patients from a Trial of Induction-Maintenance Therapy. JAMA. 2000 Jan 12;283(2):205–11.

189. Iversen AK, Shafer RW, Wehrly K, Winters MA, Mullins JI, Chesebro B, et al. Multidrug-resistant human immunodeficiency virus type 1 strains resulting from combination antiretroviral therapy. J Virol. 1996 Feb;70(2):1086–90.

190. Smit E, White E, Clark D, Churchill D, Zhang H, Collins S, et al. An association between K65R and HIV-1 subtype C viruses in patients treated with multiple NRTIs. J Antimicrob Chemother. 2017 Jul;72(7):2075–82.

191. Larder BA, Darby G, Richman DD. HIV with reduced sensitivity to zidovudine (AZT) isolated during prolonged therapy. Science. 1989 Mar 31;243(4899):1731–4.

192. Boucher CA, O'Sullivan E, Mulder JW, Ramautarsing C, Kellam P, Darby G, et al. Ordered appearance of zidovudine resistance mutations during treatment of 18 human immunodeficiency virus-positive subjects. J Infect Dis. 1992 Jan;165(1):105–10.

193. Picard V, Angelini E, Maillard A, Race E, Clavel F, Chêne G, et al. Comparison of genotypic and phenotypic resistance patterns of human immunodeficiency virus type 1 isolates from patients treated with stavudine and didanosine or zidovudine and lamivudine. J Infect Dis. 2001 Sep 15;184(6):781–4.

194. Esnouf RM, Ren J, Hopkins AL, Ross CK, Jones EY, Stammers DK, et al. Unique features in the structure of the complex between HIV-1 reverse transcriptase and the bis(heteroaryl)piperazine (BHAP) U-90152 explain resistance mutations for this nonnucleoside inhibitor. Proc Natl Acad Sci USA. 1997 Apr 15;94(8):3984–9.

195. Wainberg MA. The Need for Development of New HIV-1 Reverse Transcriptase and Integrase Inhibitors in the Aftermath of Antiviral Drug Resistance. Scientifica. 2012; 2012:1–28.

196. Richman DD, Havlir D, Corbeil J, Looney D, Ignacio C, Spector SA, et al. Nevirapine resistance mutations of human immunodeficiency virus type 1 selected during therapy. J Virol. 1994 Mar;68(3):1660–6.

197. Wei X, Ghosh SK, Taylor ME, Johnson VA, Emini EA, Deutsch P, et al. Viral dynamics in human immunodeficiency virus type 1 infection. Nature. 1995 Jan 12;373(6510):117–22.

198. Condra JH, Schleif WA, Blahy OM, Gabryelski LJ, Graham DJ, Quintero JC, et al. In vivo emergence of HIV-1 variants resistant to multiple protease inhibitors. Nature. 1995 Apr 6;374(6522):569–71.

199. Kaplan AH, Michael SF, Wehbie RS, Knigge MF, Paul DA, Everitt L, et al. Selection of multiple human immunodeficiency virus type 1 variants that encode viral proteases with decreased sensitivity to an inhibitor of the viral protease. Proc Natl Acad Sci USA. 1994 Jun 7;91(12):5597–601.

200. Hertogs K, Bloor S, Kemp SD, Van den Eynde C, Alcorn TM, Pauwels R, et al. Phenotypic and genotypic analysis of clinical HIV-1 isolates reveals extensive protease inhibitor cross-resistance: a survey of over 6000 samples. AIDS. 2000 Jun 16;14(9):1203–10.

201. Codoñer FM, Peña R, Blanch-Lombarte O, Jimenez-Moyano E, Pino M, Vollbrecht T, et al. Gag-protease coevolution analyses define novel structural surfaces in the HIV-1 matrix and capsid involved in resistance to Protease Inhibitors. Sci Rep. 2017 Jun 16;7.

202. Clavel F, Mammano F. Role of Gag in HIV Resistance to Protease Inhibitors. Viruses. 2010 Jul 5;2(7):1411–26.

203. Mammano F, Trouplin V, Zennou V, Clavel F. Retracing the Evolutionary Pathways of Human Immunodeficiency Virus Type 1 Resistance to Protease Inhibitors: Virus Fitness in the Absence and in the Presence of Drug. J Virol. 2000 Sep;74(18):8524–31.

204. Diamond TL, Bushman FD. Role of metal ions in catalysis by HIV integrase analyzed using a quantitative PCR disintegration assay. Nucleic Acids Res. 2006 Dec;34(21):6116–25.

205. Marinello J, Marchand C, Mott B, Bain A, Thomas CJ, Pommier Y. Comparison of Raltegravir and Elvitagravir on HIV-1 Integrase Catalytic Reactions and on a Series of Drug-Resistant Integrase Mutants. Biochemistry. 2008 Sep 9;47(36):9345–54.

206. Fransen S, Karmochkine M, Huang W, Weiss L, Petropoulos CJ, Charpentier C. Longitudinal analysis of raltegravir susceptibility and integrase replication capacity of human immunodeficiency virus type 1 during virologic failure. Antimicrob Agents Chemother. 2009 Oct;53(10):4522–4.

207. Hazuda DJ, Anthony NJ, Gomez RP, Jolly SM, Wai JS, Zhuang L, et al. A naphthyridine carboxamide provides evidence for discordant resistance between mechanistically identical inhibitors of HIV-1 integrase. Proc Natl Acad Sci U S A. 2004 Aug 3;101(31):11233–8.

208. Métifiot M, Marchand C, Pommier Y. Chapter Three - HIV Integrase Inhibitors: 20-Year Landmark and Challenges. In: De Clercq E, editor. Advances in Pharmacology. Academic Press; 2013; 67:75–105.

209. Thierry E, Deprez E, Delelis O. Different Pathways Leading to Integrase Inhibitors Resistance. Front Microbiol. 2017 Jan 11 ;7.

210. Hightower KE, Wang R, DeAnda F, Johns BA, Weaver K, Shen Y, et al. Dolutegravir (S/GSK1349572) Exhibits Significantly Slower Dissociation than Raltegravir and Elvitegravir from Wild-Type and Integrase Inhibitor-Resistant HIV-1 Integrase-DNA Complexes. Antimicrob Agents Chemother. 2011 Oct;55(10):4552–9.

211. Kobayashi M, Yoshinaga T, Seki T, Wakasa-Morimoto C, Brown KW, Ferris R, et al. In Vitro Antiretroviral Properties of S/GSK1349572, a Next-Generation HIV Integrase Inhibitor. Antimicrob Agents Chemother. 2011 Feb;55(2):813–21.

212. Oliveira M, Mesplède T, Quashie PK, Moïsi D, Wainberg MA. Resistance mutations against dolutegravir in HIV integrase impair the emergence of resistance against reverse transcriptase inhibitors: AIDS. 2014 Mar;28(6):813–9.

213. Tsiang M, Jones GS, Goldsmith J, Mulato A, Hansen D, Kan E, et al. Antiviral Activity of Bictegravir (GS-9883), a Novel Potent HIV-1 Integrase Strand Transfer Inhibitor with an Improved Resistance Profile. Antimicrobial Agents and Chemotherapy. 2016 Dec 1;60(12):7086–97.

214. Anstett K, Brenner B, Mesplede T, Wainberg MA. HIV drug resistance against strand transfer integrase inhibitors. Retrovirology. 2017 Jun 5;14(1).

215. Dybul, M. et al. Guidelines for using antiretroviral agents among HIV-infected adults and adolescents: Ann. Intern. Med.2002; 137:381–433.

216. Sax, P. E. et al. Should resistance testing be performed for treatment-naive HIV-infected patients? A cost-effectiveness analysis: Clin. Infect. Dis. 2005; 41:1316–1323.

217. Johnson VA, Calvez V, Günthard HF, Paredes R, Pillay D, Shafer RW, et al. Update of the Drug Resistance Mutations in HIV-1: March 2013. Top Antivir Med. 2016 Nov 28;21(1):6–7.

218. Paredes R, Marconi VC, Campbell TB, Kuritzkes DR. Systematic Evaluation of Allele-Specific Real Time PCR for the Detection of Minor HIV-1 Variants with pol and env Resistance Mutations. J Virol Methods. 2007 Dec;146(0):136–46.

219. Wilson RC, Wei JQ, Cheng KC, Mercado AB, New MI. Rapid deoxyribonucleic acid analysis by allele-specific polymerase chain reaction for detection of mutations in the steroid 21-hydroxylase gene. J Clin Endocrinol Metab. (1995) 80:1635–40.

220. Tobe VO, Taylor SL, Nickerson DA. Single-well genotyping of diallelic sequence variations by a two-color ELISA-based oligonucleotide ligation assay. Nucleic Acids Res. 1996 Oct 1;24(19):3728–32.

221. Edelstein RE, Nickerson DA, Tobe VO, Manns-Arcuino LA, Frenkel LM. Oligonucleotide Ligation Assay for Detecting Mutations in the Human Immunodeficiency Virus Type 1 pol Gene That Are Associated with Resistance to Zidovudine, Didanosine, and Lamivudine. J Clin Microbiol. 1998 Feb;36(2):569–72.

222. Sanger F, Nicklen S, Coulson AR. DNA sequencing with chain-terminating inhibitors. Proc Natl Acad Sci U S A. 1977 Dec;74(12):5463–7.

223. Hert DG, Fredlake CP, Barron AE. Advantages and limitations of next-generation sequencing technologies: a comparison of electrophoresis and non-electrophoresis methods. Electrophoresis. 2008 Dec;29(23):4618–26.

224. Zhang J, Chiodini R, Badr A, Zhang G. The impact of next-generation sequencing on genomics. J Genet Genomics. 2011 Mar 20;38(3):95–109.

225. Schadt EE, Turner S, Kasarskis A. A window into third-generation sequencing. Human Molecular Genetics. 2010 Oct 15;19(R2): R227–40.

226. Jose Antonio Garrido-Cardenas, Federico Garcia-Maroto, Francisco Manzano-Agugliaro, Jose Antonio Alvarez-Bermejo. DNA Sequencing Sensors: An Overview. Sensors (Basel). 2017 Mar;17(3):588.

227. Harris TD, Buzby PR, Babcock H, Beer E, Bowers J, Braslavsky I, et al. Single-molecule DNA sequencing of a viral genome. Science. 2008 Apr 4;320(5872):106–9.

228. Fatih Ozsolak. Third-generation sequencing techniques and applications to drug discovery. 2012;7(3):231–43.

229. Levene MJ, Korlach J, Turner SW, Foquet M, Craighead HG, Webb WW. Zero-Mode Waveguides for Single-Molecule Analysis at High Concentrations. Science. 2003 Jan 31;299(5607):682–6.

230. Travers KJ, Chin C-S, Rank DR, Eid JS, Turner SW. A flexible and efficient template format for circular consensus sequencing and SNP detection. Nucleic Acids Res. 2010 Aug;38(15): e159.

231. Pacific Biosciences. Media Kit, <http://www.pacb.com/company/news-events/media-resources/page/3/> (May 19, 2018, date last accessed).

232. Eid J, Fehr A, Gray J, Luong K, Lyle J, Otto G, et al. Real-time DNA sequencing from single polymerase molecules. Science. 2009 Jan 2;323(5910):133–8.

233. Eastman PS, Boyer E, Mole L, Kolberg J, Urdea M, Holodniy M. Nonisotopic hybridization assay for determination of relative amounts of genotypic human immunodeficiency virus type 1 zidovudine resistance. J Clin Microbiol. 1995 Oct;33(10):2777–80.

234. Stuyver L, Wyseur A, Rombout A, Louwagie J, Scarcez T, Verhofstede C, et al. Line probe assay for rapid detection of drug-selected mutations in the human immunodeficiency virus type 1 reverse transcriptase gene. Antimicrob Agents Chemother. 1997 Feb;41(2):284–91.

235. Petropoulos CJ, Parkin NT, Limoli KL, Lie YS, Wrin T, Huang W, et al. A Novel Phenotypic Drug Susceptibility Assay for Human Immunodeficiency Virus Type 1. Antimicrob Agents Chemother. 2000 Apr;44(4):920–8.

236. Japour AJ, Mayers DL, Johnson VA, et al. Standardized peripheral blood mononuclear cell culture assay for determination of drug susceptibilities of clinical human immunodeficiency virus type 1 isolates. The RV-43 Study Group, the AIDS Clinical Trials Group Virology Committee Resistance Working Group. Antimicrob Agents Chemother 1993; 37:1095–101

237. Daar ES, Moudgil T, Meyer RD, Ho DD. Transient high levels of viremia in patients with primary human immunodeficiency virus type 1 infection. N Engl J Med. 1991 Apr;324(14):961-4.

238. Kozal MJ, Shafer RW, Winters MA, Katzenstein DA, Merigan TC. A mutation in human immunodeficiency virus reverse transcriptase and decline in CD4 lymphocyte numbers in long-term zidovudine recipients. J Infect Dis 1993; 167:526–32. 3.

239. Koch N, Yahi N, Ariasi F, Fantini J, Tamalet C. Comparison of human immunodeficiency virus type 1 (HIV-1) protease mutations in HIV-1 genomes detected in plasma and in peripheral blood mononuclear cells from patients receiving combination drug therapy. J Clin Microbiol 1999; 37:1595–7.

240. Young B, Johnson S, Bahktiari M, et al. Resistance mutations in protease and reverse transcriptase genes of human immunodeficiency virus type 1 isolates from patients with combination antiretroviral therapy failure. J Infect Dis 1998; 178:1497–501. 5.

241. Bacheler L, Cordova B, Hanna G, et al. Resistance of HIV-1 clinical isolates to efavirenz and other NNRTIs [abstract 316]. Clin Infect Dis 1999; 29:1017.

242. McMahon MA, Shen L, Siliciano RF. New approaches for quantitating the inhibition of HIV-1 replication by antiviral drugs in vitro and in vivo. Curr Opin Infect Dis. 2009 Dec;22(6):574-82.

243. Hertogs K, de Béthune MP, Miller V, Ivens T, Schel P, Van Cauwenberge A, Van Den Eynde C, Van Gerwen V, Azijn H, Van Houtte M, Peeters F, Staszewski S, Conant M, Bloor S, Kemp S, Larder B, Pauwels R. A rapid method for simultaneous detection of phenotypic resistance to inhibitors of protease and reverse transcriptase in recombinant human immunodeficiency virus type 1 isolates from patients treated with antiretroviral drugs. Antimicrob Agents Chemother. 1998 Feb;42(2):269-76.

244. Miller V, Sabin C, Hertogs K, et al. Virological and immunological effects of treatment interruptions in HIV-1 infected patients with treatment failure. AIDS. 2000;14(18):2857-2867.

245. Benson CA, Vaida F, Havlir DV, et al. A randomized trial of treatment interruption before optimized antiretroviral therapy for persons with drug-resistant HIV: 48-week virologic results of ACTG A5086. J Infect Dis. 2006;194(9):1309- 1318.

246. National consolidated guidelines: for the prevention of mother-to child transmission of HIV (PMTCT) in children, adolescents and adults. The Department of Health; 2015.

247. Republic of South Africa National Department of Health. 2019 ART Clinical Guidelines for the Management of HIV in Adults, Pregnancy, Adolescents, Children, Infants and Neonates [Internet]. 2019.

248. Mesplède T, Quashie PK, Hassounah S, Osman N, Han Y, Liang J, Singhroy DN, Wainberg MA. The R263K substitution in HIV-1 subtype C is more deleterious for integrase enzymatic function and viral replication than in subtype B. AIDS. 2015 Jul 31;29(12):1459–66.

249. Kantor R, Shafer RW, Follansbee S, et al. Evolution of resistance to drugs in HIV-1- infected patients failing antiretroviral therapy. AIDS 2004;18(11):1503-1511.

250. World Health Organization (WHO). HIV Resistance Report, 2012. Geneva: WHO, 2012. http://www.who.int/hiv/pub/drugresistance/report2012/en/index.html

251. Williams I, Churchill D, Anderson J, et al. British HIV Association guidelines for the treatment of HIV-1-positive adults with antiretroviral therapy 2012. HIV Med 2012; 13:1-85.

252. Thompson MA, Aberg JA, Hoy JF, et al. Antiretroviral treatment of adult HIV infection: 2012 recommendations of the International Antiviral Society – USA Panel. JAMA 2012;308(4):387-402.

253. Steegen K, Van Zyl G, Letsoalo E, Claassen M, Hans L, Carmona S. Resistance in Patients Failing Integrase Strand Transfer Inhibitors: A Call to Replace Raltegravir With Dolutegravir in Third-Line Treatment in South Africa. Open Forum Infect Dis. 2019 Oct 1;6(10).

Methods:

254. Connor RI, Chen BK, Choe S, Landau NR. Vpr is required for efficient replication of human immunodeficiency virus type-1 in mononuclear phagocytes. Virology. 1995 Feb 1;206(2):935–44.

255. He J, Choe S, Walker R, Di Marzio P, Morgan DO, Landau NR. Human immunodeficiency virus type 1 viral protein R (Vpr) arrests cells in the G2 phase of the cell cycle by inhibiting p34cdc2 activity. J Virol. 1995 Nov;69(11):6705–11.

256. Chen BK, Saksela K, Andino R, Baltimore D. Distinct modes of human immunodeficiency virus type 1 proviral latency revealed by superinfection of nonproductively infected cell lines with recombinant luciferase-encoding viruses. J Virol. 1994 Feb;68(2):654–60.

257. Ndung'u T, Renjifo B, Essex M. Construction and analysis of an infectious human Immunodeficiency virus type 1 subtype C molecular clone. J Virol. 2001 Jun;75(11):4964–72.

258. Chang L-J, Urlacher V, Iwakuma T, Cui Y, Zucali J. Efficacy and safety analyses of a recombinant human immunodeficiency virus type 1 derived vector system. Gene Ther. 1999 May;6(5):715–28.

259. Carnell GW, Ferrara F, Grehan K, Thompson CP, Temperton NJ. Pseudotype-based neutralization assays for influenza: a systematic analysis. Front Immunol. 2015;6:161.

260. Zufferey R, Dull T, Mandel RJ, Bukovsky A, Quiroz D, Naldini L, et al. Self-inactivating lentivirus vector for safe and efficient in vivo gene delivery. J Virol. 1998 Dec;72(12):9873–80.

261. Aiken, C. Pseudotyping HIV-1 by the glycoprotein of VSV targets HIV-1 entry to an endocytic pathway and suppresses both the requirement for Nef and the sensitivity to cyclosporin A. J. Virol. 71, 5871−5877.

262. Hastie, E., Cataldi, M., Marriott, I., & Grdzelishvili, V. Z. (2013). Understanding and altering cell tropism of vesicular stomatitis virus. *Virus research*, *176*(1-2), 16–32.

263. Rhee, S. Y., M. J. Gonzales, R. Kantor, B. J. Betts, J. Ravela, and R. W. Shafer. 2003. Human immunodeficiency virus reverse transcriptase and protease sequence database. Nucleic Acids Res. 31:298-303.

Results

264. Wensing AM, Calvez V, Ceccherini-Silberstein F, Charpentier C, Günthard H.F, Paredes R, Shafer RW, Richman DD. 2019 Update of the Drug Resistance Mutations in HIV. Topics in Antiviral Medicine. July/August 2019;27(3):1-11.

265. Tamura K, Peterson D, Peterson N, Stecher G, Nei M, Kumar S. MEGA5: molecular evolutionary genetics analysis using maximum likelihood, evolutionary distance, and maximum parsimony methods. Mol Biol Evol. 2011:28: 2731-2739.

266. Young B, Fransen S, Greenberg KS, Thomas A, Martens S, St Clair M, et al. Transmission of integrase strand-transfer inhibitor multidrug-resistant HIV-1: case report and response to raltegravir-containing antiretroviral therapy. Antivir Ther. 2011;16(2):253–6.

267. Saitou N, Nei M. The neighbor-joining method: a new method for reconstructing phylogenetic trees. Mol Biol Evol. 1987 Jul 1;4(4):406–25.

268. Felsenstein J. Confidence Limits on Phylogenies: An Approach Using the Bootstrap. Evolution. 195;39(4):783–91.

269. Kumar S, Stecher G, Tamura K. MEGA7: Molecular Evolutionary Genetics Analysis Version 7.0 for Bigger Datasets. Mol Biol Evol. 2016 Jul 1;33(7):1870–4.

270. Sharma S, Aralaguppe SG, Abrahams M-R, Williamson C, Gray C, Balakrishnan P, et al. The PTAP sequence duplication in HIV-1 subtype C Gag p6 in drug-naive subjects of India and South Africa. BMC Infectious Diseases. 2017 Jan 24;17(1):95.

Discussion

271. Cecchini DM, Castillo S, Copertari G, Lacal V, Rodriguez CG, Cassetti I. Resistance to HIV integrase strand transfer inhibitors in Argentina: first interim survey. Rev Esp Quimioter. 2019 Jun;32(3):263–7.

272. Ndashimye E, Avino M, Kyeyune F, Nankya I, Gibson RM, Nabulime E, et al. Absence of HIV-1 Drug Resistance Mutations Supports the Use of Dolutegravir in Uganda. AIDS Res Hum Retroviruses. 2018;34(5):404–14.

273. Seatla KK, Avalos A, 2018 …Seatla KK, Avalos A, Mphoyakgosi T, et al. Preliminary virologic outcomes and prevalence of integrase strand transfer inhibitor resistance mutations among highly treatment experienced patients receiving dolutegravir in Botswana. In: 22nd International AIDS Conference; 23–27 July 2018; Amsterdam, The Netherlands.

274. Boender TS, Hamers RL, Ondoa P, Wellington M, Chimbetete C, Siwale M, et al. Protease Inhibitor Resistance in the First 3 Years of Second-Line Antiretroviral Therapy for HIV-1 in Sub-Saharan Africa. J Infect Dis. 2016 Sep 15;214(6):873–83.

275. Clutter DS, Jordan MR, Bertagnolio S, Shafer RW. HIV-1 drug resistance and resistance testing. Infection, Genetics and Evolution. 2016 Dec;46:292–307.

276. Tang MW, Shafer RW. HIV-1 Antiretroviral Resistance. Drugs. 2012;72(9):e1–25.

277. Rhee S-Y, Taylor J, Fessel WJ, Kaufman D, Towner W, Troia P, et al. HIV-1 Protease Mutations and Protease Inhibitor Cross-Resistance. Antimicrob Agents Chemother. 2010 Oct;54(10):4253–61.

278. de Meyer S, Vangeneugden T, van Baelen B, de Paepe E, van Marck H, Picchio G, et al. Resistance profile of darunavir: combined 24-week results from the POWER trials. AIDS Res Hum Retroviruses. 2008 Mar;24(3):379–88.

279. Pozniak A, Arasteh K, Molina J, Grinsztejn B, De Meyer S, Casteele TVD, et al. POWER 3 analysis: 144-week efficacy and safety results for darunavir/ritonavir (DRV/r) 600/100 mg BID in treatment-experienced HIV patients. JIAS. 2008 Nov 10;11(1):P24.

280. Mammano 1998 Mammano F, Petit C, Clavel F. Resistance-Associated Loss of Viral Fitness in Human Immunodeficiency Virus Type 1: Phenotypic Analysis of Protease and gag Coevolution in Protease Inhibitor-Treated Patients. J Virol. 1998 Sep;72(9):7632–7.

281. Fun A, Wensing AM, Verheyen J, Nijhuis M. Human Immunodeficiency Virus gag and protease: partners in resistance. Retrovirology. 2012 Aug 6;9(1):63.

282. Maguire MF, Guinea R, Griffin P, Macmanus S, Elston RC, Wolfram J, Richards N, Hanlon MH, Porter DJ, Wrin T, Parkin N, Tisdale M, Furfine E, Petropoulos C, Snowden BW, Kleim JP: Changes in human immunodeficiency virus type 1 Gag at positions L449 and P453 are linked to I50V protease mutants in vivo and cause reduction of sensitivity to amprenavir and improved viral fitness in vitro. J Virol. 2002, 76: 7398-7406.

283. Dierynck I, De Meyer S, C-V K, Van Marck H, Lathouwers E, Thys K, Maes B, de Bethune MP. Impact of Gag cleavage site mutations on the virological response to darunavir/ritonavir in treatment-experienced patients in POWER 1, 2 and 3. Antivir Ther. 2007;12:S23.

284. Kolli M, Stawiski E, Chappey C, Schiffer CA. Human Immunodeficiency Virus Type 1 Protease-Correlated Cleavage Site Mutations Enhance Inhibitor Resistance. J Virol. 2009 Nov;83(21):11027–42.

285. Nijhuis M, van Maarseveen NM, Lastere S, Schipper P, Coakley E, Glass B, et al. A Novel Substrate-Based HIV-1 Protease Inhibitor Drug Resistance Mechanism. 2007 Jan;4(1).

286. Verheyn 2010 Verheyen J, Verhofstede C, Knops E, Vandekerckhove L, Fun A, Brunen D, Dauwe K, Wensing AM, Pfister H, Kaiser R, Nijhuis M. High prevalence of bevirimat resistance mutations in protease inhibitor-resistant HIV isolates. AIDS. 2010; 24:669–673.

287. Martins AN, Waheed AA, Ablan SD, Huang W, Newton A, Petropoulos CJ, et al. Elucidation of the Molecular Mechanism Driving Duplication of the HIV-1 PTAP Late Domain. J Virol. 2016 15;90(2):768–79.

288. Martins AN, Arruda MB, Pires AF, Tanuri A, Brindeiro RM. Accumulation of P(T/S)AP late domain duplications in HIV type 1 subtypes B, C, and F derived from individuals failing ARV therapy and ARV drug-naive patients. AIDS Res Hum Retroviruses. 2011 Jun;27(6):687–92.

289. Fantauzzi A, Mezzaroma I. Dolutegravir: clinical efficacy and role in HIV therapy. Ther Adv Chronic Dis. 2014 Jul;5(4):164-17.

290. White K, Cihlar T, Miller MD. Potent activity of bictegravir (BIC; GS-9883), a novel unboosted HIV-1 integrase strand transfer inhibitor (INSTI), against patient isolates with INSTI-resistance. American Society for Microbiology (ASM) Microbe; June 16-20, 2016; Boston, MA. http://www.natap.org/2016/HIV/062316_02.htm.

291. Jones G, Goldsmith J, Mulato A, et al. Bictegravir (GS-9883), a novel HIV-1 integrase strand transfer inhibitor (INSTI) with optimized in vitro resistance profile. American Society for Microbiology (ASM) Microbe; June 16-20, 2016.

292. Boston, MA. Levin: Bictegravir (GS-9883), a novel HIV-1 integrase strand transfer inhibitor (INSTI) with optimized in vitro resistance profile; National AIDS Treatment Advocacy Project (NATAP); HIV Articles; 2016. http://www.natap.org/2016/HIV/062016_03.htm.

293. Lazerwith S, Cai R, Chen X, et al. Discovery of GS-9883, an HIV-1 integrase strand transfer inhibitor (INSTI) with improved pharmacokinetics and in vitro resistance profile. American Society for Microbiology (ASM) Microbe; June 16-20, 2016.

294. Boston, MA. Levin: Discovery of bictegravir (GS-9883), a novel, unboosted, once-daily HIV-1 integrase strand transfer inhibitor (INSTI) with improved pharmacokinetics and in vitro resistance profile; National AIDS Treatment Advocacy Project (NATAP); HIV Articles; 2016. http://www.natap.org/2016/HIV/062016_05.htm.

295. Hurt CB. Transmitted resistance to HIV integrase strand-transfer inhibitors: right on schedule. Antivir Ther. 2011;16(2):137–40.

296. Boyd SD, Maldarelli F, Sereti I, Ouedraogo GL, Rehm CA, Boltz V, et al. Transmitted raltegravir resistance in an HIV-1 CRF_AG-infected patient. Antivir Ther. 2011;16(2):257–61.

297. Abram ME, Ram RR, Margot NA, Barnes TL, White KL, Callebaut C, et al. Lack of impact of pre-existing T97A HIV-1 integrase mutation on integrase strand transfer inhibitor resistance and treatment outcome. 2017 Feb;12(2):e0172206

298. Marcelin A-G. Resistance to nucleoside reverse transcriptase inhibitors. In: Geretti AM, editor. Antiretroviral Resistance in Clinical Practice. London: Mediscript; 2006.

299. Petrella M, Wainberg MA. Might the M184V substitution in HIV-1 RT confer clinical benefit? AIDS Rev. 2002 Dec;4(4):224–32.

300. Schmitt M, Harrer E, Goldwich A, Bäuerle M, Graedner I, Kalden JR, et al. Specific recognition of lamivudine-resistant HIV-1 by cytotoxic T lymphocytes. AIDS. 2000 Apr 14;14(6):653–8.

301. Ait-Khaled M, Stone C, Amphlett G, Clotet B, Staszewski S, Katlama C, et al. M184V is associated with a low incidence of thymidine analogue mutations and low phenotypic resistance to zidovudine and stavudine. AIDS. 2002 Aug 16;16(12):1686–9.

302. Larder BA, Kemp SD, Harrigan PR. Potential mechanism for sustained antiretroviral efficacy of AZT-3TC combination therapy. Science. 1995 Aug 4;269(5224):696–9.

303. Masquelier B, Descamps D, Carrière I, Ferchal F, Collin G, Denayrolles M, et al. Zidovudine resensitization and dual HIV-1 resistance to zidovudine and lamivudine in the delta lamivudine roll-over study. Antivir Ther (Lond). 1999;4(2):69–77.

304. Whitcomb JM, Parkin NT, Chappey C, Hellmann NS, Petropoulos CJ. Broad nucleoside reverse-transcriptase inhibitor cross-resistance in human immunodeficiency virus type 1 clinical isolates. J Infect Dis. 2003 Oct 1;188(7):992–1000.

305. Götte M, Arion D, Parniak MA, Wainberg MA. The M184V mutation in the reverse transcriptase of human immunodeficiency virus type 1 impairs rescue of chain-terminated DNA synthesis. J Virol. 2000 Apr;74(8):3579–85.

306. Boyer PL, Sarafianos SG, Arnold E, Hughes SH. The M184V mutation reduces the selective excision of zidovudine 5'-monophosphate (AZTMP) by the reverse transcriptase of human immunodeficiency virus type 1. J Virol. 2002 Apr;76(7):3248–56.

307. Ross L, Parkin N, Chappey C, Fisher R, Clair MS, Bates M, et al. Phenotypic impact of HIV reverse transcriptase M184I/V mutations in combination with single thymidine analog mutations on nucleoside reverse transcriptase inhibitor resistance. AIDS. 2004 Aug 20;18(12):1691–6.

308. Grobler J. Efficacy of MK-8591 against diverse HIV-1 subtypes and NRTI-resistant clinical isolates. Webcast presented at: International Congress of Drug Therapy in HIV Infection (HIV Glasgow); October 28-31, 2018; Glasgow, United Kingdom. https://vimeo.com/298576925.

309. Palmer S, Boltz V, Martinson N, Maldarelli F, Gray G, McIntyre J, et al. Persistence of nevirapine-resistant HIV-1 in women after single-dose nevirapine therapy for prevention of maternal-to-fetal HIV-1 transmission. Proceedings of the National Academy of Sciences. 2006 May 2;103(18):7094–9.

310. Brenner B, Routy JP, Quan Y, Moisi D, Oliveira M, Turner D, *et al*. Persistence of multidrug-resistant HIV-1 in primary infection leading to superinfection. AIDS 2004; 18:1653–1660.

311. Salomon H, Wainberg MA, Brenner B, Quan Y, Rouleau D, Cote P, *et al*. Prevalence of HIV-1 resistant to antiretroviral drugs in 81 individuals newly infected by sexual contact or injecting drug use. Investigators of the Quebec Primary Infection Study. AIDS 2000; 14:F17–F23.

312. Barbour JD, Hecht FM, Wrin T, Liegler TJ, Ramstead CA, Busch MP, *et al*. Persistence of primary drug resistance among recently HIV-1 infected adults. AIDS 2004; 18:1683–1689.

313. Pao D, Andrady U, Clarke J, Dean G, Drake S, Fisher M, *et al*. Long-term persistence of primary genotypic resistance after HIV-1 seroconversion. J Acquir Immune Defic Syndr 2004; 37:1570–1573.

314. Moyo S et al. HIV drug resistance in South Africa: results from a population-based household survey. Conference on Retroviruses and Opportunistic Infections, Seattle, abstract 152, 2019

315. Virological follow-up of adult patients in antiretroviral treatment programmes in sub-Saharan Africa: a systematic review. Barth RE, van der Loeff MF, Schuurman R, Hoepelman AI, Wensing AM Lancet Infect Dis. 2010 Mar; 10(3):155-66.

316. Sow PS, Otieno LF, Bissagnene E, et al. Implementation of an antiretroviral access program for HIV-1-infected individuals in resource-limited settings: clinical results from 4 African countries. Journal of Acquired Immune Deficiency Syndromes (1999). 2007 Mar;44(3):262-267.

317. Lai M-T, Feng M, Falgueyret J-P, Tawa P, Witmer M, DiStefano D, et al. In vitro characterization of MK-1439, a novel HIV-1 nonnucleoside reverse transcriptase inhibitor. Antimicrob Agents Chemother. 2014;58(3):1652–63.

318. Bichko V et al. Pre-clinical pharmacokinetics of elsulfavirine/VM1500A long acting injectable formulations. IAS 2017, 23-26 July, Paris. Poster abstract WEPEA0190. http://programme.ias2017.org/Abstract/Abstract/1515.

319. Hecht FM, Grant RM, Petropoulos CJ, Dillon B, Chesney MA, Tian H, et al. Sexual transmission of an HIV-1 variant resistant to multiple reverse-transcriptase and protease inhibitors. N Engl J Med. 1998 Jul 30;339(5):307–11.

320. Little SJ. Reduced Antiretroviral Drug Susceptibility Among Patients with Primary HIV Infection. JAMA. 1999 Sep 22;282(12):1142.

321. Havlir DV, Hellmann NS, Petropoulos CJ, Whitcomb JM, Collier AC, Hirsch MS, et al. Drug susceptibility in HIV infection after viral rebound in patients receiving indinavir-containing regimens. JAMA. 2000 Jan 12;283(2):229–34.

322. Parkin NT, Lie YS, Hellmann N, Markowitz M, Bonhoeffer S, Ho D, Petropoulos CJ. Phenotypic changes in drug susceptibility associated with failure of human immunodeficiency virus type 1 (HIV-1) triple combination therapy. J. Infect. Dis.1998: 180:865–870.

323. Parkin NT, Hellmann NS, Whitcomb JM, Kiss L, Chappey C, Petropoulos CJ. Natural variation of drug susceptibilities in wild-type Human Immunodeficiency Virus type 1. Antimicrob Agents Chemother. 2004 Jan;48(2):437-443.

324. Acosta EP, Limoli KL, Trinh L, Parkin NT, King JR, Weidler JM, Ofotokun I, Petropoulos CJ. Novel method to assess antiretroviral target trough concentrations using in vitro susceptibility data. Antimicrob Agents Chemother. 2012 Nov; 56(11): 5938–5945.

325. Louvel S, Battegay M, Vernazza P, Bregenzer T, Klimkait T, Hamy F; Swiss HIV Cohort Study. Detection of drug-resistant HIV minorities in clinical specimens and therapy failure. HIV Med. 2008 Mar;9(3):133-41.

326. Wang Y, Prosen DE, Mei L, Sullivan JC, Finney M, Vander Horn PB. A novel strategy to engineer DNA polymerases for enhanced processivity and improved performance in vitro. Nucleic Acids Res. 2004;32(3):1197–207.

327. Carballeira N, Nazabal M, Brito J, Garcia O. Purification of a thermostable DNA polymerase from Thermus thermophilus HB8, useful in the polymerase chain reaction. BioTechniques. 1990 Sep;9(3):276–81.

328. Terpe K. Overview of thermostable DNA polymerases for classical PCR applications: from molecular and biochemical fundamentals to commercial systems. Appl Microbiol Biotechnol. 2013 Dec;97(24):10243–54.

329. Moore JC, Arnold FH. Directed evolution of a para-nitrobenzyl esterase for aqueous-organic solvents. Nat Biotechnol. 1996 Apr;14(4):458–67.

330. Giver L, Gershenson A, Freskgard P-O, Arnold FH. Directed evolution of a thermostable esterase. PNAS. 1998 Oct 27;95(22):12809–13.

331. Sirotkin VA, Winter R. Volume Changes Associated with Guanidine Hydrochloride, Temperature, and Ethanol Induced Unfolding of Lysozyme. J Phys Chem B. 2010 Dec 23;114(50):16881–6.

332. Hitti YS, Bertino AM. Proteinase K and T4 DNA polymerase facilitate the blunt-end subcloning of PCR products. BioTechniques. 1994 May;16(5):802–5.

333. Wybranietz WA, Lauer U . Distinct combination of purification methods dramatically improves cohesive-end subcloning of PCR products *BioTechniques* 1998 24: 578–580.

334. Robinson CR, Sligar SG. Molecular recognition mediated by bound water. A mechanism for star activity of the restriction endonuclease EcoRI. J Mol Biol. 1993 Nov 20;234(2):302–6.

335. Dallas-Yang Q, Jiang G, Sladek FM. Avoiding false positives in colony PCR. BioTechniques. 1998 Apr;24(4):580–2.

336. Campbell TN, Choy FY. Large-scale colony screening and insert orientation determination using PCR. BioTechniques. 2001 Jan;30(1):32–4.

Appendix A

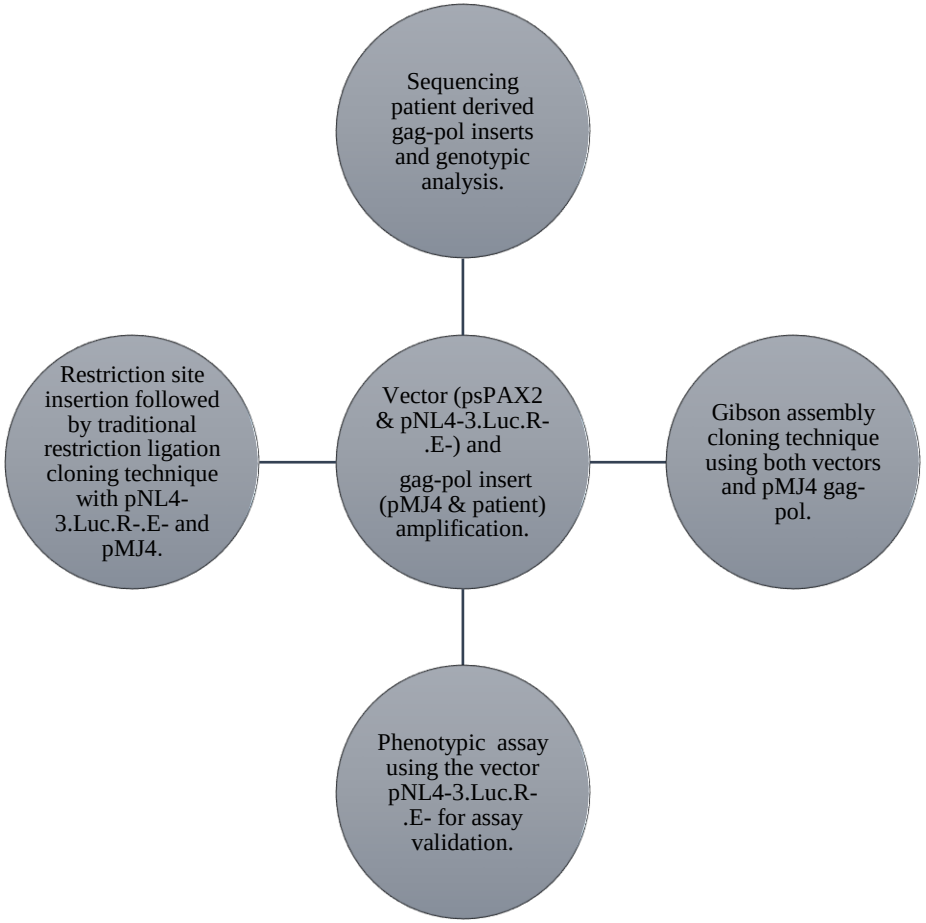

Figure A1: Flow chart describing the laboratory objectives utilised to achieve the specified aim.

Appendix B

Figure B1: Ethical clearance certificate No: M180658 from the Human Research Ethics Committee (HREC: Medical) at the University of Witwatersrand.

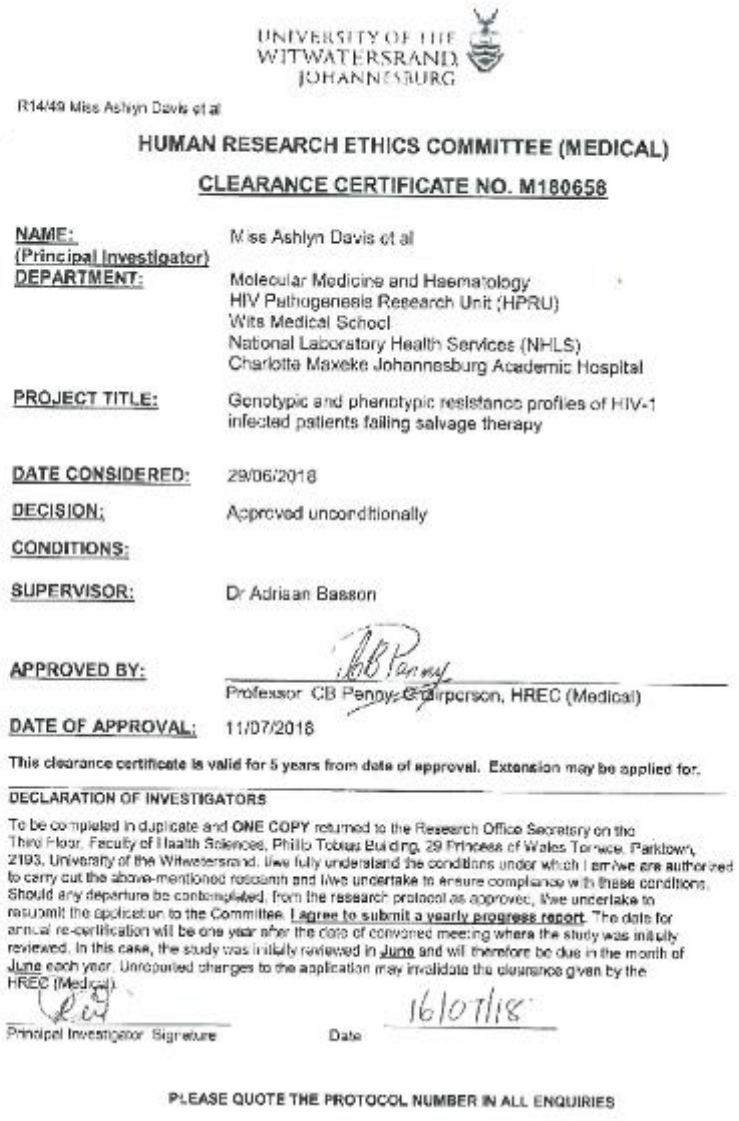

UNIVERSITY OF THE WITWATERSRAND JOHANNESBURG

R14/49 Miss Ashlyn Davis et al

HUMAN RESEARCH ETHICS COMMITTEE (MEDICAL)

CLEARANCE CERTIFICATE NO. M180658

NAME: (Principal Investigator)	Miss Ashlyn Davis et al
DEPARTMENT:	Molecular Medicine and Haematology HIV Pathogenesis Research Unit (HPRU) Wits Medical School National Laboratory Health Services (NHLS) Charlotte Maxeke Johannesburg Academic Hospital
PROJECT TITLE:	Genotypic and phenotypic resistance profiles of HIV-1 infected patients failing salvage therapy
DATE CONSIDERED:	29/06/2018
DECISION:	Approved unconditionally
CONDITIONS:	
SUPERVISOR:	Dr Adrian Basson
APPROVED BY:	Professor CB Penny, Chairperson, HREC (Medical)
DATE OF APPROVAL:	11/07/2018

This clearance certificate is valid for 5 years from date of approval. Extension may be applied for.

DECLARATION OF INVESTIGATORS

To be completed in duplicate and **ONE COPY** returned to the Research Office Secretary on the Third Floor, Faculty of Health Sciences, Phillip Tobias Building, 29 Princess of Wales Terrace, Parktown, 2193, University of the Witwatersrand. I/we fully understand the conditions under which I am/we are authorized to carry out the above-mentioned research and I/we undertake to ensure compliance with these conditions. Should any departure be contemplated from the research protocol as approved, I/we undertake to resubmit the application to the Committee. **I agree to submit a yearly progress report.** The date for annual re-certification will be one year after the date of convened meeting where the study was initially reviewed. In this case, the study was initially reviewed in June and will therefore be due in the month of June each year. Unreported changes to the application may invalidate the clearance given by the HREC (Medical).

Principal Investigator Signature

Date 16/07/18

PLEASE QUOTE THE PROTOCOL NUMBER IN ALL ENQUIRIES

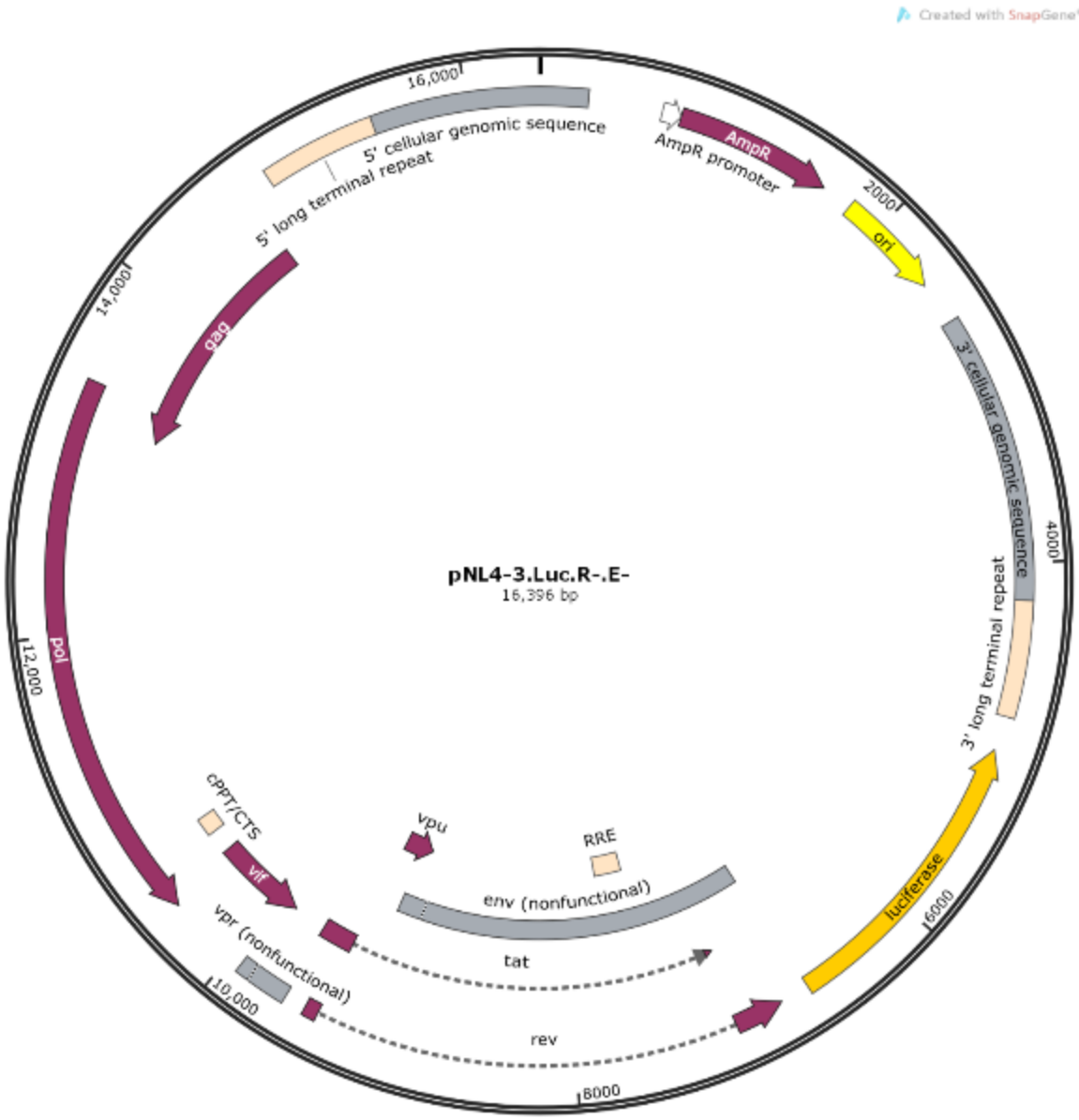

Figure B2: A plasmid map of HIV-1 pNL4-3 luciferase reporter vector that contains defective Nef, Env and Vpr.

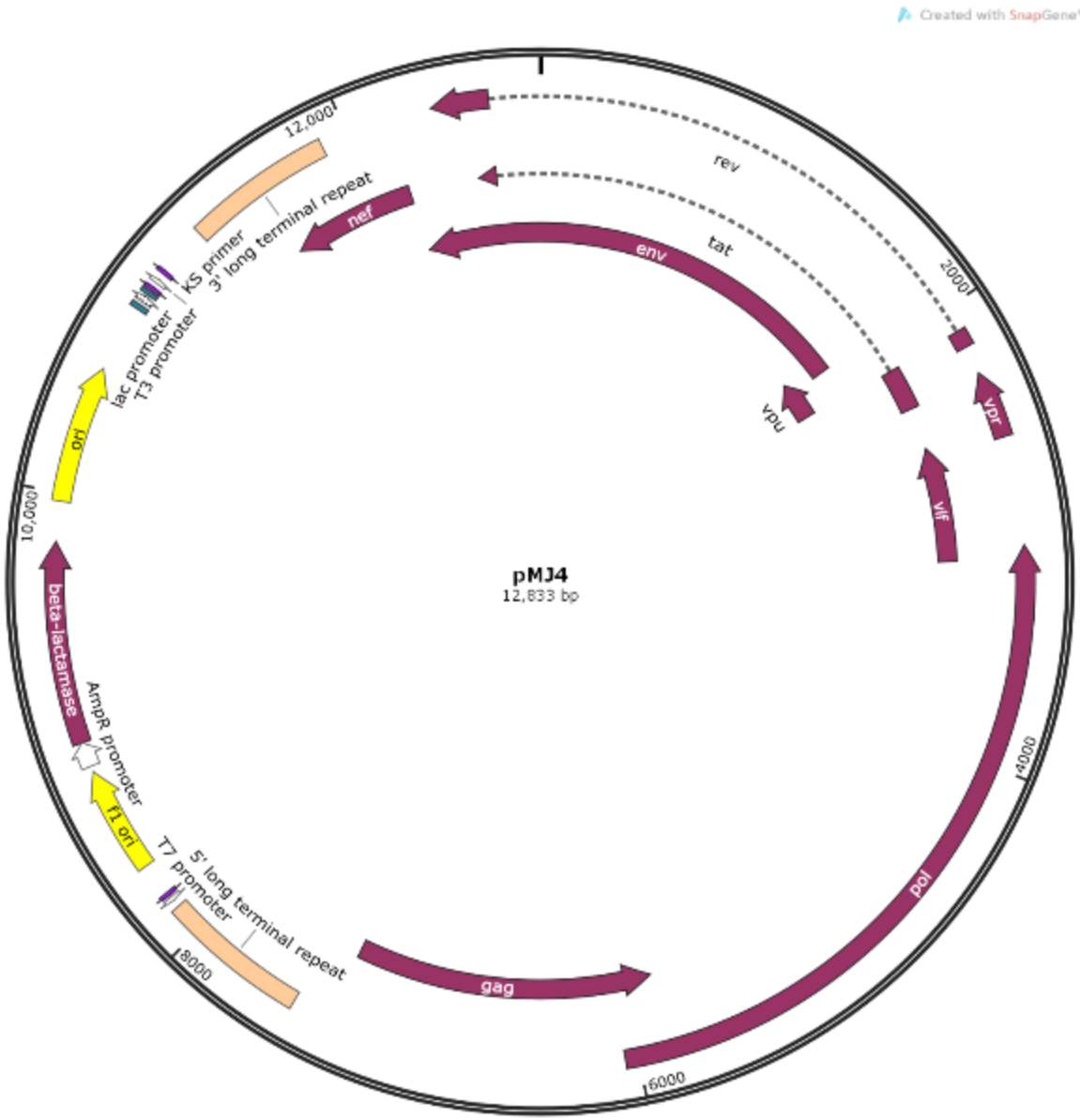

Figure B3: The plasmid map of pMJ4, an infectious HIV-1 subtype C molecular clone, isolated from Southern Africa (Botswana).

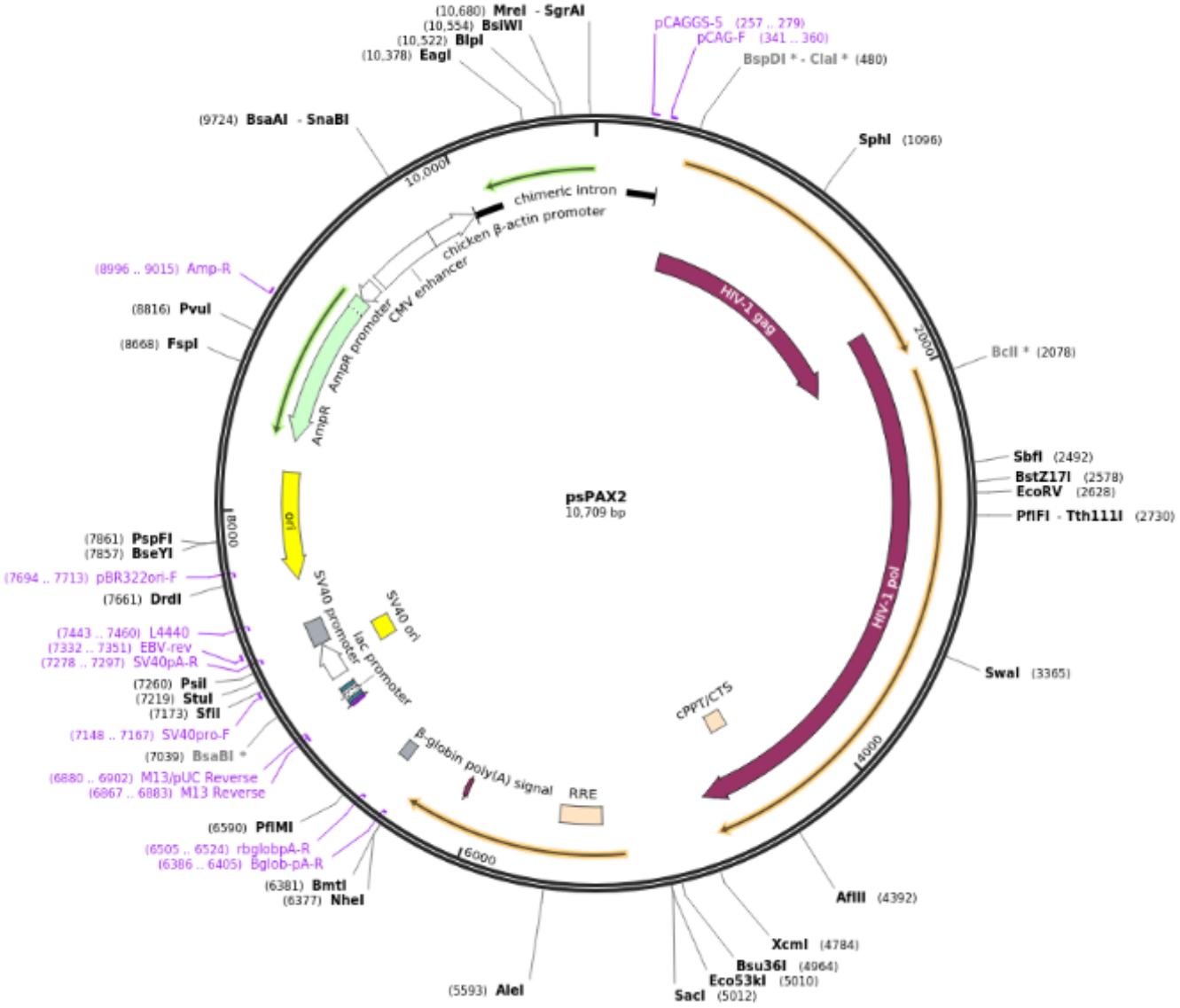

Figure B4: The packaging HIV-1 construct pSPAX2 a second-generation plasmid used to produce HIV-1 lentivectors.

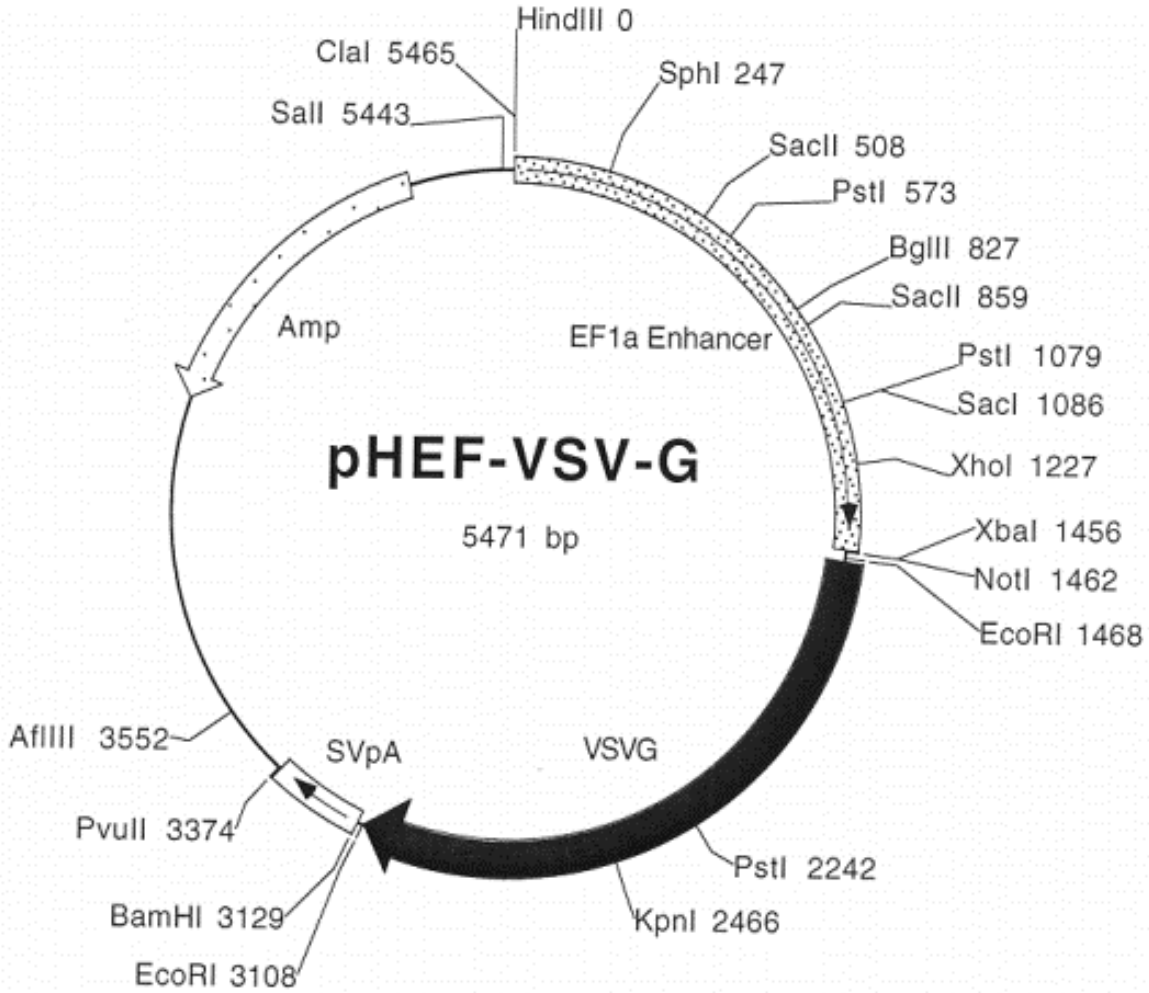

Figure B5: The packaging construct, pHEF-VSVG encodes the vesicular stomatitis virus G gene.

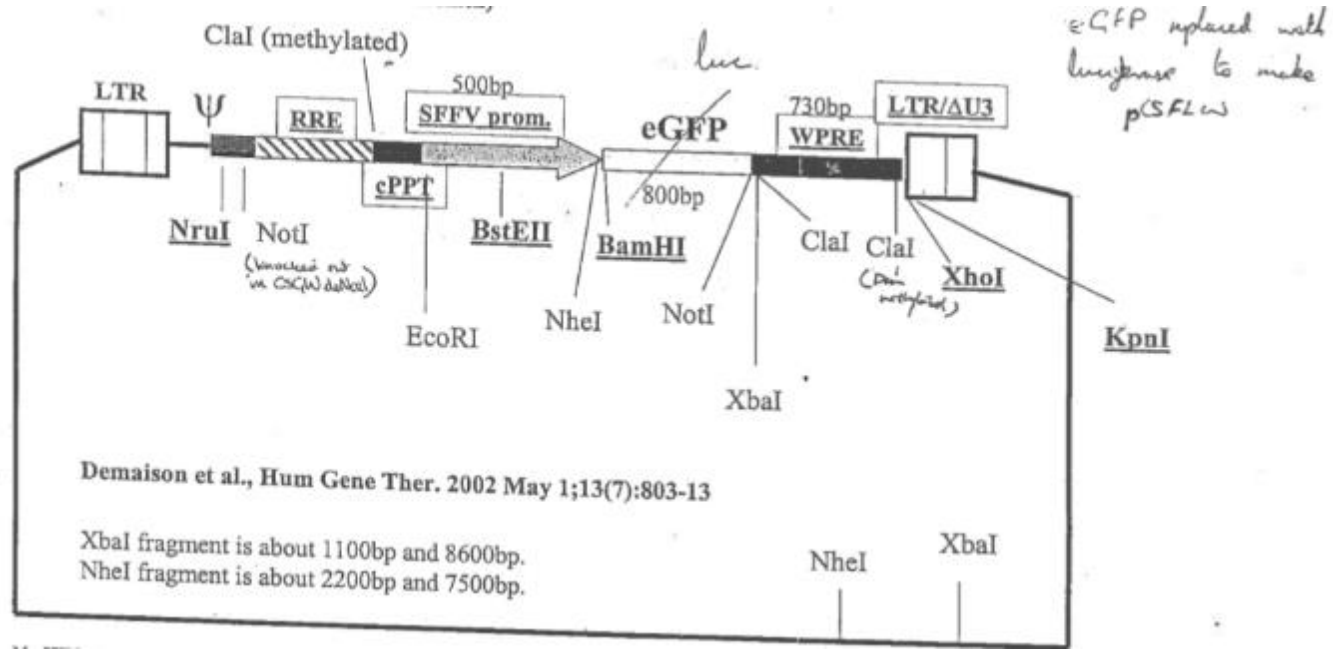

Figure B6: The pCSFLW reporter construct, derived from pHR-SIN-CSGW, that expresses firefly (*Photinus pyralis*) luciferase under the Spleen Focus Forming Virus promoter.

1)

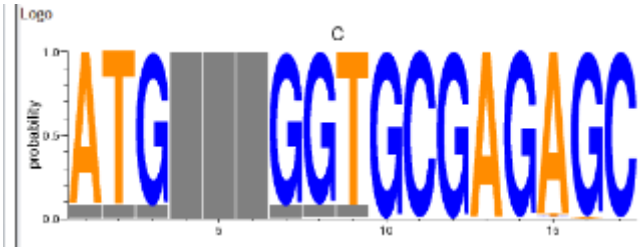

2)

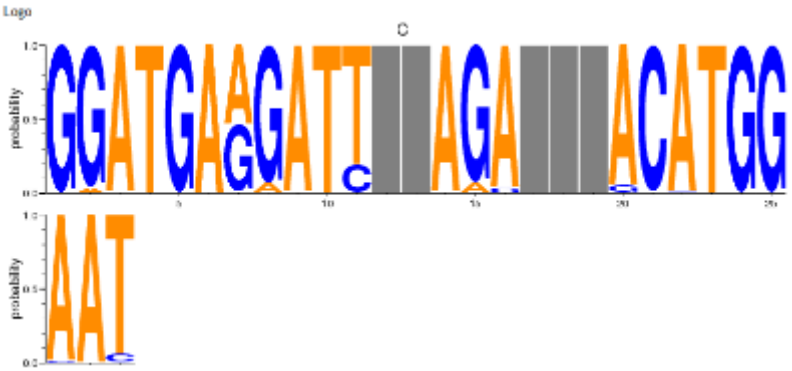

Figure B7: The specific HIV-1 subtype C changes made with regards to the 1) Gp_1st_Fwd and 2) Gp_1st_Rev primers, respectively. Sequence 1 represents the *gag-pol* forward primer. There are 14 conserved nucleotides (orange and blue) and 3 nucleotides that were removed (grey bars) due to them not occurring within subtype C sequences (from 719 sequences). Sequence 2 represents the *gag-pol* reverse primer. There are 15 conserved nucleotides without

mixes. The mixes are indicated by nucleotides below the original sequence (smaller in size or similar in size but below). There are approximately 8 nucleotide mixture sites.

3)

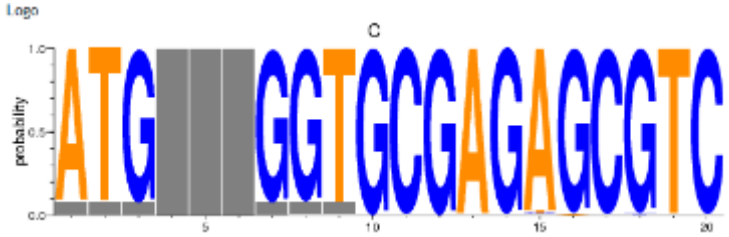

4)

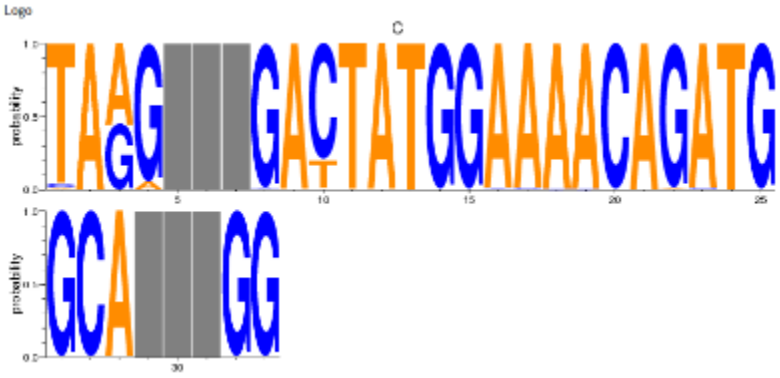

Figure B8: The specific subtype HIV-1 C changes made with regards to the Gp_2nd_Fwd and Gp_2nd_Rev primers, respectively. Sequence 3 represents the forward second *gag-pol* primer. There are 17 conserved nucleotide sites (orange and blue) seen and 3 nucleotides have been removed (grey bars). Sequence 4 is the second reverse primer for *gag-pol*. There are 23 conserved nucleotide sites (orange and blue) and 4 mixtures. The mixtures indicate the subtype C changes (from719 sequences) that are to be incorporated in the sequence.

Appendix C

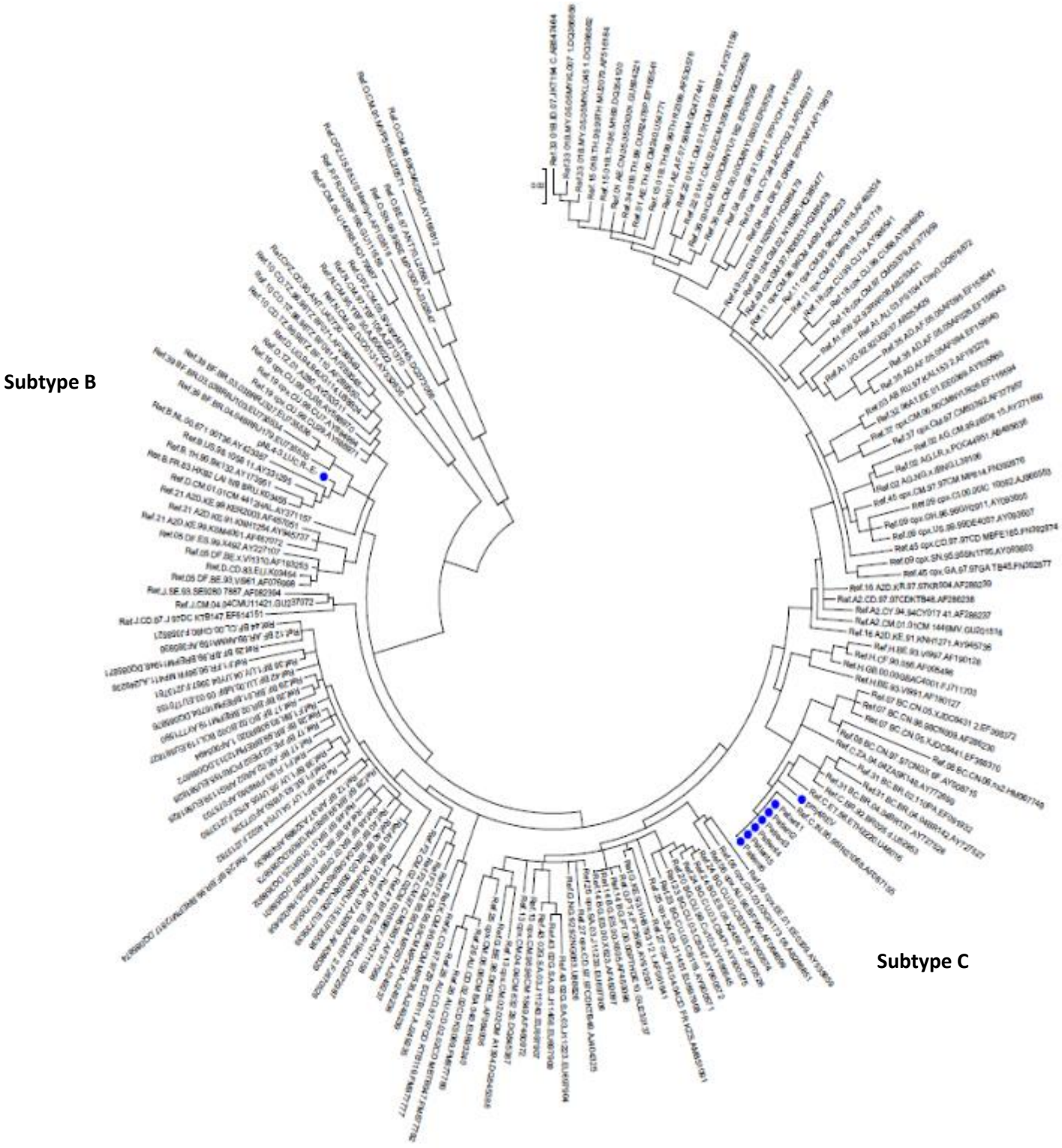

Figure C1: A neighbour-joining tree illustrating the association between patient sequences and HIV-1 group M subtypes. The phylogenetic analysis based on the neighbour joining method was performed on *protease* Subtype reference and third line failure patient (●) sequences [267], and evolutionary distances conducted with MEGA7 were computed using the Maximum Composite Likelihood method [268, 269].

Appendix D

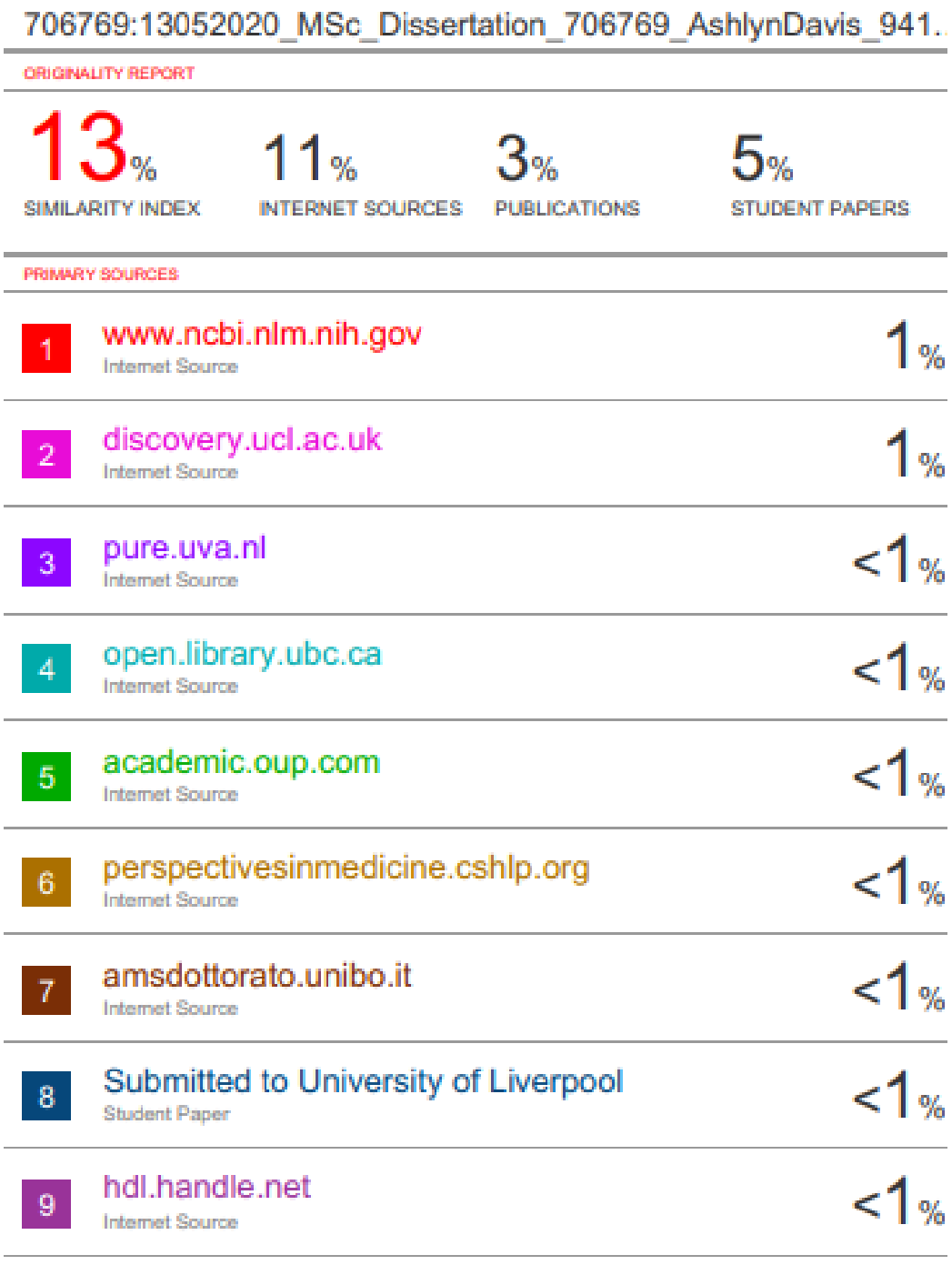

706769:13052020_MSc_Dissertation_706769_AshlynDavis_941.

ORIGINALITY REPORT

13%	11%	3%	5%
SIMILARITY INDEX	INTERNET SOURCES	PUBLICATIONS	STUDENT PAPERS

PRIMARY SOURCES

1	www.ncbi.nlm.nih.gov Internet Source	1%
2	discovery.ucl.ac.uk Internet Source	1%
3	pure.uva.nl Internet Source	<1%
4	open.library.ubc.ca Internet Source	<1%
5	academic.oup.com Internet Source	<1%
6	perspectivesinmedicine.cshlp.org Internet Source	<1%
7	amsdottorato.unibo.it Internet Source	<1%
8	Submitted to University of Liverpool Student Paper	<1%
9	hdl.handle.net Internet Source	<1%

Figure D1: Plagiarism report generated from the Turnitin software for the above dissertation.